UNIVERSIDAD COMPLUTENSE DE MADRID

FACULTAD DE CIENCIAS QUÍMICAS

TESIS DOCTORAL

Development of new type 2 Lysophosphatidic acid receptor LPA2 antagonists

Desarrollo de nuevos antagonistas del receptor de ácido Lisofosfatídico LPA2

MEMORIA PARA OPTAR AL GRADO DE DOCTOR

PRESENTADA POR

Román Foronda Sainz

DIRIGIDA POR

Silvia Ortega Gutiérrez

María del Henar Vázquez Villa

UNIVERSIDAD COMPLUTENSE DE MADRID

FACULTAD DE CIENCIAS QUÍMICAS

Programa de Doctorado en Química Orgánica

DEVELOPMENT OF NEW TYPE 2 LYSOPHOSPHATIDIC ACID RECEPTOR LPA_2 ANTAGONISTS

DESARROLLO DE NUEVOS ANTAGONISTAS DEL RECEPTOR DE ÁCIDO LISOFOSFATÍDICO LPA_2

Memoria para optar al Grado de Doctor presentada por

Román Foronda Sainz

Directores:

Silvia Ortega Gutiérrez

María del Henar Vázquez Villa

A mis padres y a mis hermanos

El presente trabajo ha sido realizado en el Laboratorio de Química Médica del Departamento de Química Orgánica de la Facultad de Ciencias Químicas de la Universidad Complutense de Madrid, bajo la supervisión de la ***Catedrática Silvia Ortega Gutiérrez*** *y la* ***Prof. María del Henar Vázquez Villa*** *a quienes deseo agradecer de corazón la oportunidad que me dieron para la realización de este proyecto y la confianza depositada en mí, así como sus numerosas enseñanzas a lo largo de estos tres años, la paciencia que han tenido y lo a gusto que me han hecho sentir.*

Asimismo, quiero expresar mi agradecimiento:

A la Catedrática María Luz López Rodríguez y las Prof. Bellinda Benhamú Salama, Mar Martín-Fontecha Corrales y Ángeles Canales Mayordomo por su simpatía y su constante ayuda e interés.

A la Prof. Isabel Rozas y al Dr. Marco Minneci por acogerme durante mi estancia predoctoral en el Trinity Collage Dublin y hacer de ello una experiencia maravillosa y enriquecedora.

Al Dr. Rubèn López Vales, de la Universidad Autónoma de Barcelona, en cuyo laboratorio se han llevado a cabo los experimentos in vivo.

A Elena, Marga, Ángel y Lola del Centro de Apoyo a la Investigación (CAI) de Resonancia Magnética Nuclear de la UCM, por su atenta ayuda y cercanía, a pesar de los muchos tubos mal rotulados.

A todos mis compañeros de laboratorio durante estos años, especialmente a Verónica, Iván, Jon, Anabel, Andrea, Paola, Daniel, Patri y Marcelino; durante el tiempo que he pasado a vuestro lado me habéis inculcado diferentes valores que han hecho de mí el científico y la persona que soy hoy en día. Verónica, con su increíble perseverancia y esfuerzo, gracias por tu cariño y complicidad, por tu humor (no)inteligente, y por escuchar mis locas reflexiones y contribuir a que lo sean aún más. Iván, de los mejores químicos de Europa, gracias por enseñarme tanto y por hacer que me duela la tripa de la risa. Jon, vecino provinciano, gracias por decirme los fallos y errores a la cara y por hacer que me cuestione más las cosas, por demostrarme que la ciencia está hecha para salsear y divertirse, gracias por la música. Anabel, compañera de vitrina, gracias por aguantarme, que sé que no ha sido tarea fácil, por tu ética de trabajo y por tu honestidad. Andrea, Paola, Daniel, Patri y Marcelino, gracias por transmitirme vuestra pasión y amor por la ciencia, por hacerme reír y por enseñarme. Gracias a Alegría, por supervisar su proyecto de grado.

A todos los compañeros y amigos de los diferentes grupos de investigación del departamento de química orgánica, con los que he compartido muy buenos momentos, especialmente a los Nazarios.

A todos mis amigos de Logroño, en concreto a la "24 KCLAIS", la mejor cuadrilla que uno puede tener, por hacerme sentir tan feliz y orgulloso durante tantos años y ser un refugio en los buenos y malos momentos. Mención especial a Alfonso, por enseñarme a pensar y a ser una persona con criterio, por demostrarme su amor y apoyarme en todo.

A Alicia, mi compañera de vida, por llenar mi mundo de felicidad y quererme tan bien. Porque a tu lado río, lloro, crezco como persona y aprendo. Gracias por regalarme tu sonrisa y por ser el remanso de paz y tranquilidad que a mi tanto me gusta llamar hogar.

A las dos personas que más admiro, mi padre y mi madre, por criarme en un hogar lleno de cariño y rock and roll, por educarme tan bien, porque nunca me faltara de nada y por su apoyo incondicional, el cual me ha dado alas para volar. A mi hermana Ángela y mi hermano Ernesto, quienes irrumpieron en mi privilegiada vida de hijo único hace 25 años y resultaron ser el mayor regalo que un niño pude tener. Gracias por aguantarme durante toda la vida, por estar siempre que os he necesitado, por recibirme con una sonrisa y mil preguntas siempre que vuelvo a casa y por hacerme ver que siempre estaremos juntos. Espero que algún día lleguen a estar tan orgullosos de mí como yo lo estoy de ellos.

A mis abuelos Pepe y Gloria, por regalarme un lugar donde pude descubrir la naturaleza y dar mis primeros pasos como científico durante mi infancia. A mi yaya Tita, por demostrarme su cariño y ayudarme a cumplir mis sueños. Al resto de mi familia, por preocuparse por mí y apoyarme, especialmente a mi tía Rocío, mi tío José Manuel y mi prima Rocío, por darme un hogar en Madrid. Sin vuestro apoyo incondicional jamás habría logrado estar aquí. GRACIAS

TABLE OF CONTENTS

ABBREVIATIONS AND ACRONYMS

Throughout this manuscript, abbreviations and acronyms recommended by the American Chemical Society in the Organic Chemistry and Medicinal Chemistry areas have been employed (revised in the *Journal of Organic Chemistry* and *Journal of Medicinal Chemistry* in May 2024); In addition, those indicated below have been used:

AC	Adenylyl cyclase
ACN	Acetonitrile
AGPAT	Acylglycerophosphate acyltransferase
Akt	Protein kinase B
ATX	Autotaxin
CAI	Centro de apoyo a la investigación
cAMP	Cyclic adenosine monophosphate
DAG	Diacylglycerol
DGK	Diacylglycerol kinase
DMADMA	*N,N*-dimethylacetamide dimethyl acetal
DMEM	Dulbecco's modified eagle medium
ECL	Extracellular loop
EDC	*N*-(3-Dimethylaminopropyl)-*N*'-ethylcarbodiimide
Edg	Endothelial differentiation gene
E_{max}	Maximum blockade effect
E.R.	Endoplasmic reticulum
FA	Fatty acyl
FBS	Fetal bovine serum
FDG	Fluorescein-di-β-galactopyranoside
GL	Glycerolipid
GP	Glycerophospholipid
G3P	Glycerol-3-phosphate
GPAT	Glycerophosphate acyltranferase
GPCR	G protein-coupled receptor
GRK	GPCR kinase

HLM	Human liver microsome
ICL	Intracellular loop
IP3	Inositol trisphosphate
K_d	Dissociation constant
LCAT	Lecithin-cholesterol acyltranferase
LDL	Low-density lipoprotein
LPA	Lysophosphatidic acid
LPAR	Lysophosphatidic acid receptor
LPC	Lysophosphatidylcholine
LPE	Lysophosphatidylethanolamine
LPP	Lipid phosphate phosphohydrolase
LPs	Lysophospholipids
LPS	Lysophosphatidylserine
MAG	Monoacylglycerol
MAGK	Monoacylglycerol kinase
MLM	Mouse liver microsome
MTT	3-(4,5-Dimethyl-2-thiazolyl)-2,5-diphenyl-2*H*-tetrazolium bromide
MW	Microwave
NE	No effect
P	Permeability
PA	Phosphatidic acid
PC	Phosphatidylcholine
PE	Phosphatidylethanolamine
PI3K	Phosphatidylinositol 3-kinase
PKC	Protein kinase C
PLA	Phospholipase A
PLC	Phospholipase C
PLD	Phospholipase D
PPARγ	Peroxisome proliferator-activated receptor γ
PR	Prenol lipid
PS	Phosphatidylserine

P2Y	Purinergic receptor family
SP	Sphingolipid
SRF	Serum response factor
ST	Sterol lipid
TM	Transmembrane domain
tPSA	Topological polar surface area
UCM	Universidad Complutense de Madrid

RESUMEN

DESARROLLO DE NUEVOS ANTAGONISTAS DEL RECEPTOR DE ÁCIDO LISOFOSFATÍDICO LPA_2

Los lípidos son un conjunto muy heterogéneo de biomoléculas presentes en nuestras células, tejidos y fluidos, con importantes funciones estructurales, señalizadoras y de almacenamiento de energía. La función de los lípidos como moléculas de señalización ha quedado consolidada en las tres últimas décadas, con numerosos ejemplos descritos a lo largo de la literatura. En el contexto de moléculas lipídicas con funcion señalizadora, destaca el ácido lisofosfatídico (LPA). El LPA ejerce su acción a través de la interacción con sus receptores (LPA_{1-6}), mediando importantes procesos fisiológicos celulares. De entre todos los receptores del ácido lisofosfatídico, este trabajo se centra en el receptor LPA_2 debido a su relevancia biológica poco explorada y a la falta de moduladores potentes y selectivos con eficacia *in vivo* probada. Algunos de los ligandos más representativos se muestran en la Figura 1.

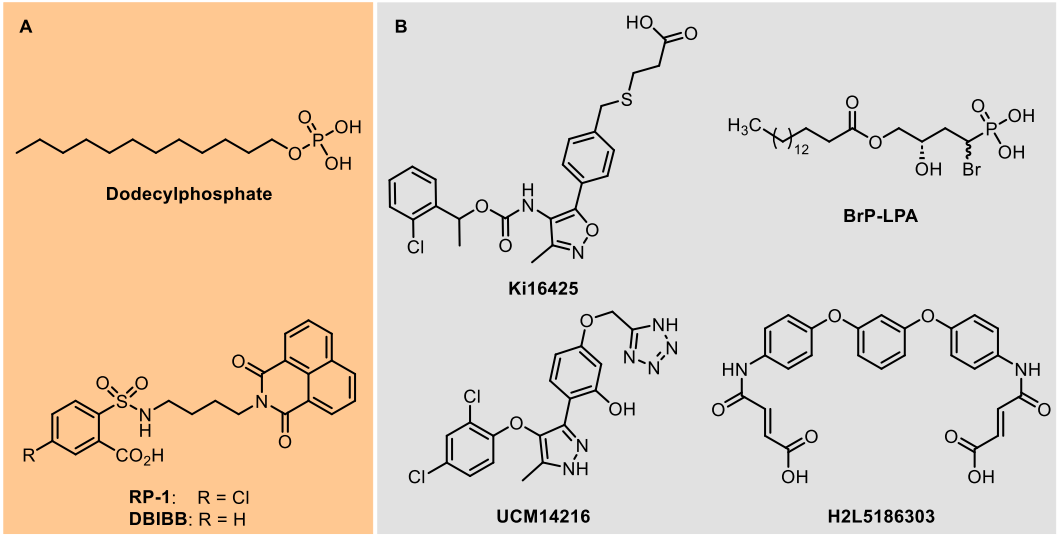

Figura 1. Estructura de los ligandos más representativos del receptor LPA_2: agonistas (A) and antagonistas (B).

Recientemente, nuestro grupo de investigación ha identificado una nueva familia de derivados de pirazol, entre los que destaca el compuesto **UCM-14216** (Figura 1) como el antagonista más potente y selectivo del receptor LPA_2 (E_{max}=90±2%; CI_{50}=1.9 µM; K_d=1.3 nM; inactivo en $LPA_{1,3-6}$) descrito hasta la fecha, con eficacia *in vivo* demostrada en un modelo de ratón con lesión de médula espinal. Sin embargo, sus propiedades farmacocinéticas limitan su biodisponibilidad. Por ello, el objetivo principal del presente trabajo ha sido el desarrollo de nuevos antagonistas potentes y selectivos del receptor LPA_2 con un perfil farmacocinético y una actividad *in vivo* mejorados, para así validar este receptor como diana terapéutica de interés en procesos (neuro)inflamatorios. Con este objetivo, hemos seleccionado como punto de partida el compuesto **UCM-14250** (E_{max}=57±9%; IC_{50}≈10 µM; Figura 2), previamente caracterizado en nuestro grupo de investigación, y hemos desarrollado un programa de química médica en el que se han modificado sistemáticamente los diferentes elementos estructurales de este *hit* (Figura 2). Para la evaluación de la actividad antagonista y la selectividad de los compuestos sintetizados, se ha utilizado un ensayo funcional para detectar la movilización de calcio en células transfectadas de forma estable con los receptores LPA_{1-3}. Entre todos los compuestos caracterizados, el derivado **65** (UCM-22018, Figura 3) ha mostrado un excelente perfil *in vitro* (E_{max}=92.0±0.2%; IC_{50}=0.2±0.1 µM; K_d=0.96 nM; inactivo en $LPA_{1,3}$), superior al compuesto **UCM-14216** descrito previamente.

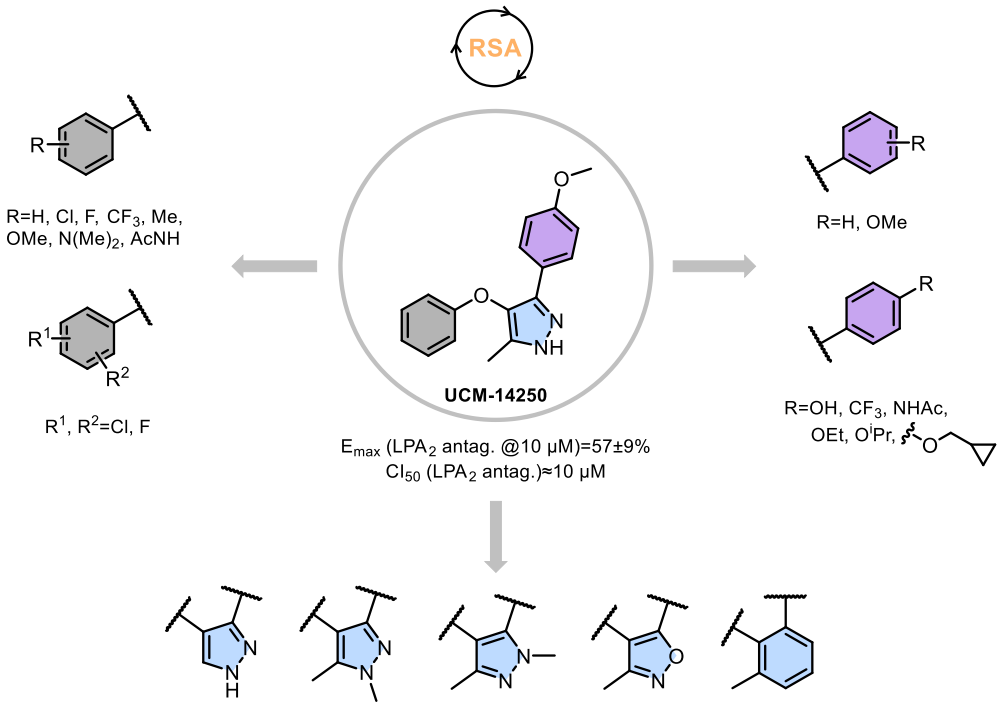

Figura 2. Estudio de la relación estructura actividad del compuesto de partida **UCM-14250**.

La caracterización farmacológica en profundidad del compuesto **65** (UCM-22018) ha revelado buenos valores para las distintas propiedades ADME estudiadas, como la estabilidad en suero y microsomas de ratón y humano, la permeabilidad, la unión a la albúmina de suero humano y la toxicidad celular (Figura 3). Además, en un estudio farmacocinético *in vivo* se confirmó la capacidad del compuesto para atravesar la barrera hematoencefálica y alcanzar el sistema nervioso central. Estos resultados mostraron que se alcanzaron niveles significativos del compuesto **65** tanto en el cerebro como en la médula espinal de los ratones tratados durante las dos primeras horas tras la administración, y que aún se detectaban niveles más bajos del compuesto después de 6 horas. Por último, evaluamos la eficacia *in vivo* del compuesto **65** en el modelo de dolor inducido por adyuvante completo de Freund, en el que el compuesto **65** indujo efectos antiinflamatorios significativos en comparación con los animales no tratados.

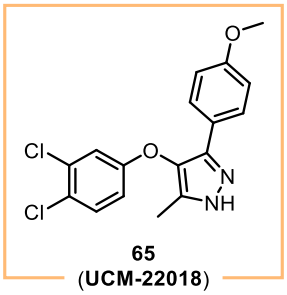

65
(**UCM-22018**)

E_{max} (LPA_2)=92.0±0.2%
CI_{50}(LPA_2)=0.2±0.1 μM
K_d(LPA_2)=0.96 nM; Inactivo en $LPA_{1,3}$

P=7.0·10^{-6} cm/s
$t_{1/2}$(suero) > 24 h
$t_{1/2}$(microsomas) > 2.8 h
K_d(HSA)=1.8·10^{-5} M; F_b(HSA)=97%
No citotóxico a 25 μM

Figura 3. Estructura y perfil farmacológico del antagonista del receptor LPA_2 **65** (UCM-22018).

SUMMARY

DEVELOPMENT OF NEW TYPE 2 LYSOPHOSPHATIDIC ACID RECEPTOR LPA_2 ANTAGONISTS

Lipids are an extremely heterogeneous set of biomolecules present in our cells, tissues, and fluids, which have important structural, signaling and energy storage functions. The role of lipids as signaling molecules has been well established in the last three decades with numerous examples described along the literature. In the context of lipid molecules with signaling functions, lysophosphatidic acid (LPA) stands out. LPA exerts its extracellular signaling through the interaction with its receptors (LPA_{1-6}), mediating important cellular physiological processes. Among all the lysophosphatidic acid receptors, this work is focused on the LPA_2 due to its underexplored biological relevance and the lack of potent and selective modulators with probed *in vivo* efficacy. Some of the most representative ligands are shown in Figure 1.

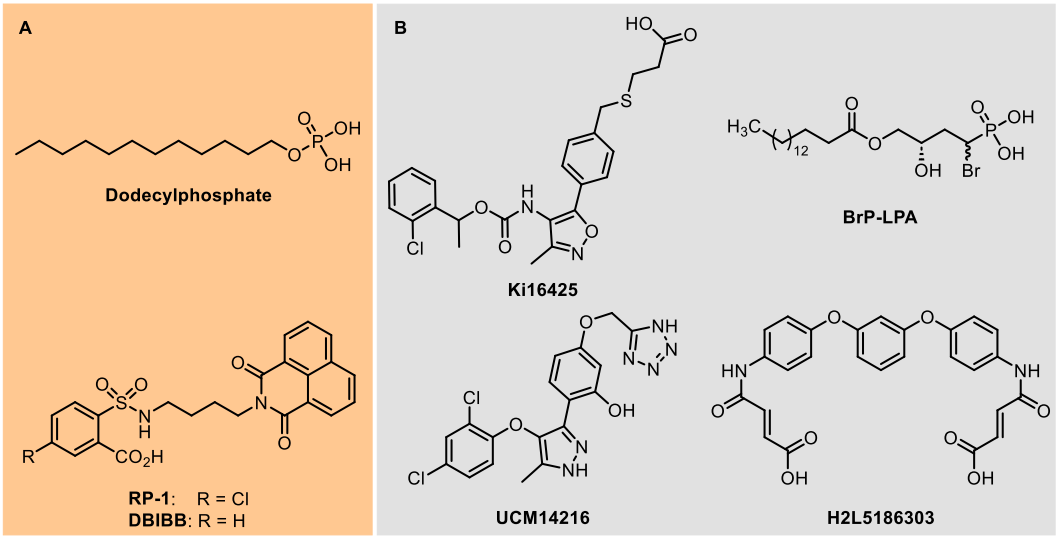

Figure 1. Structure of the most representative LPA_2 receptor ligands: agonists (A) and antagonists (B).

Recently, our research group has identified a new family of pyrazole-based derivatives, among which compound **UCM-14216** (Figure 1) stands out as the most potent and selective LPA_2 receptor antagonist (E_{max}=90±2%; IC_{50}=1.9 µM; K_d=1.3 nM; inactive at $LPA_{1,3-6}$) described so far with *in vivo* efficacy in a spinal cord injury mouse model. However, its pharmacokinetic (PK) properties limit its bioavailability. Therefore, the main objective of the present work has been to develop new potent and selective LPA_2 antagonists with an improved PK profile and *in vivo* activity, to validate this receptor as a

therapeutic target of interest in (neuro)inflammatory processes. Towards this aim, we have selected as starting point compound **UCM-14250** (E_{max}=57±9%; IC_{50}≈10 μM; Figure 2), previously characterized in our research group, and we have developed a medicinal chemistry program in which the different structural elements of this hit were systematically modified (Figure 2). For the evaluation of the antagonist activity and selectivity of the synthesized compounds, a functional assay has been used to detect calcium mobilization in cells stably transfected with LPA_{1-3} receptors. Among all the characterized compounds, derivative **65** (UCM-22018, Figure 3) has shown an excellent *in vitro* profile (E_{max}=92.0±0.2%; IC_{50}=0.2±0.1 μM; K_d=0.96 nM; inactive at $LPA_{1,3}$), superior to previously described compound **UCM-14216**.

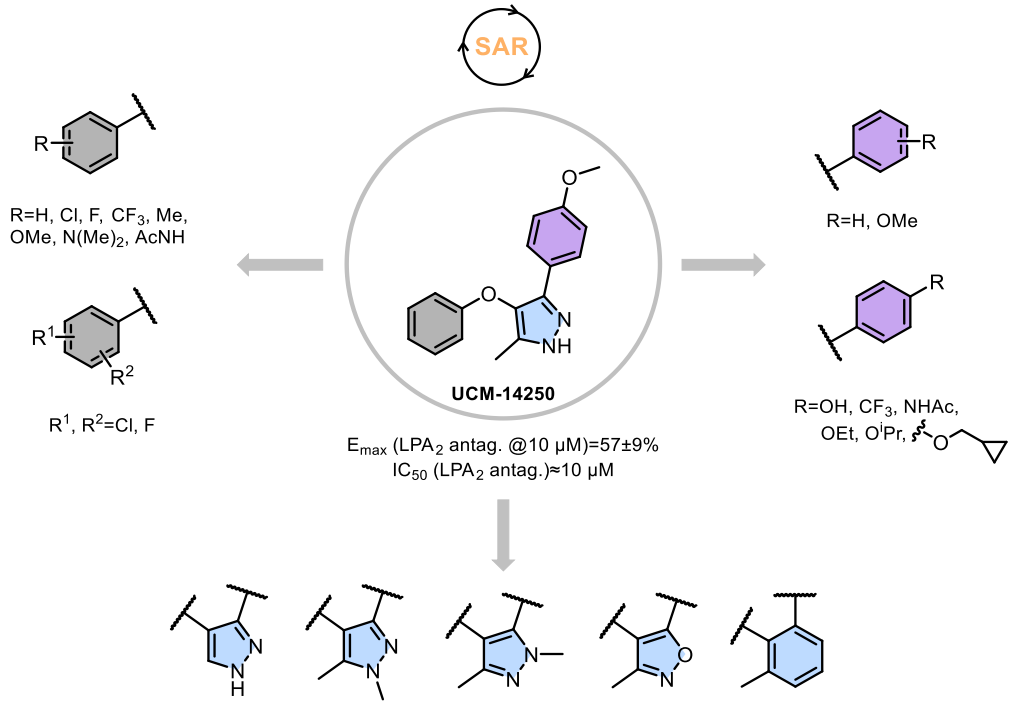

Figure 2. Structure-activity relationship study of hit **UCM-14250**.

The in-depth pharmacological characterization of compound **65** (UCM-22018) has revealed good values for the different ADME (absorption, distribution, metabolism, and excretion) properties studied, such as stability in mouse and human serum and microsomes, permeability, binding to human serum albumin and cell toxicity (Figure 3). In addition, the ability of the compound to cross the blood-brain barrier and reach the central nervous system was confirmed in an *in vivo* PK study. The results showed that significant levels of compound **65** were reached in both brain and spinal cord of treated mice during the first two hours post-administration, and lower levels of compound were

still detectable after 6 hours. Finally, we assessed the *in vivo* efficacy of compound **65** in the complete Freund's adjuvant pain mouse model, in which compound **65** induced significant antiinflammatory effects compared to non-treated animals.

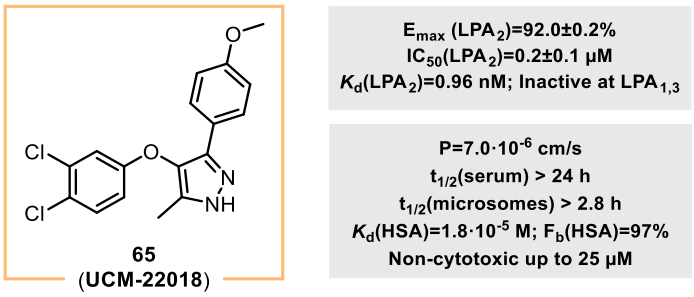

Figure 3. Structure and pharmacological profile of the LPA_2 antagonist **65** (UCM-22018).

1. INTRODUCTION AND OBJECTIVES

1. INTRODUCTION AND OBJECTIVES

Lipids are an extremely heterogeneous set of biomolecules present in our cells, tissues, and fluids,[1] which have important structural,[2-4] signaling[5-7] and energy storage functions.[8,9] The role of lipids as signaling molecules has been well established in the last three decades, and there are numerous examples described along in the literature.[10-12] As representative examples, we can mention stearic, oleic or linoleic acids (Figure 1), members of the fatty acid family which control a wide range of cellular processes and physiological functions related to fatty acid uptake at the plasma membrane, their utilization and metabolic actions;[13] or prostaglandin D_2 and leukotriene B_4 (Figure 1), both belonging to the eicosanoid subfamily, which are a pivotal part of the machinery that initiates and governs the inflammatory network in eukaryotes.[14] Other relevant examples include *N*-arachidonoyl ethanolamine and 2-arachidonoylglycerol (Figure 1), the most prominent members of the endocannabinoid subfamily. These two molecules, along with the cannabinoid receptors, transporters and enzymes regulating their synthesis and degradation, constitute the endocannabinoid system (ECS), which support and control multiple physiological processes both in the central nervous system (CNS) and the periphery.[15]

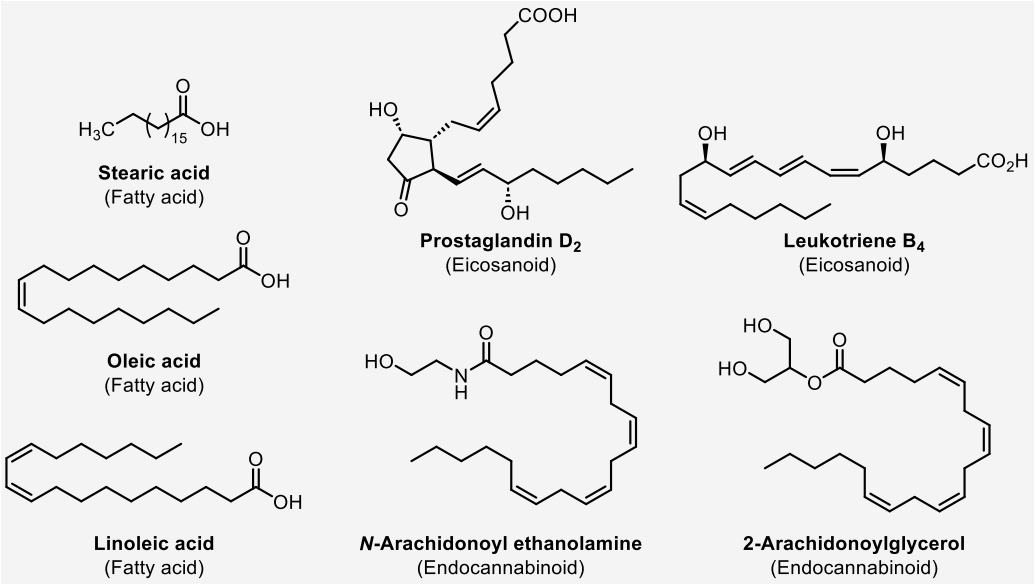

Figure 1. Structures of representative signaling lipids.

In the context of lipid molecules with signaling functions, lysophospholipids (LPs) are receiving an increased attention in the last years.[16,17] LPs derive from phospholipids that have undergone enzymatic hydrolysis to remove one of the two acyl groups and can be classified into two groups of molecules, namely lysosphingolipids and lysoglycerophospholipids, being sphingosine-1-phosphate (S1P)[18] and lysophosphatidic acid (LPA)[19] the most well-studied species of each of these classes, respectively (Figure 2).

The role of S1P has been well studied and different S1P receptor modulators are approved for the treatment of multiple sclerosis, such us Fingolimod (Gilenya®) or Siponimod (Mayzent®).[18] In contrast, LPA has been less studied despite its biological relevance, being the association of its receptors for specific therapeutic indications a current objective of biomedical research.

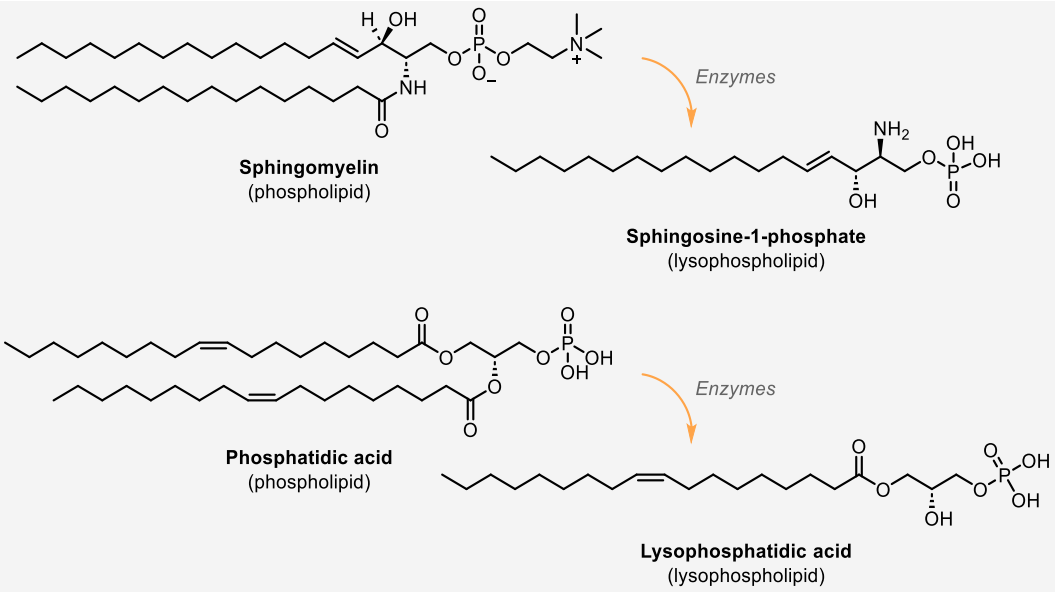

Figure 2. Structures of sphingosine-1-phosphate (S1P) and lysophosphatidic acid (LPA), and their corresponding phospholipid precursors.

The generic term LPA refers to a family of structural analogues containing a phosphate head group and a central glycerol backbone linked at *sn*-1 or *sn*-2 position by an ester linkage to a fatty acid chain with different length and degree of unsaturation (1-acyl or 2-acyl-LPA species, respectively; Figure 3), being the most abundant LPA species the one acylated at the *sn*-1 position.[20] In addition, *sn*-1 alkyl and alkenyl ether-linked LPA species also exist. The most abundant forms of LPA in human plasma are arachidonoyl LPA (20:4), linoleoyl LPA (18:2), oleoyl LPA (18:1), stearoyl LPA (18:0) and palmitoyl LPA (16:0) (Figure 3).[21] Among these species, the 18:1 form, 1-oleoyl-2-hydroxy-*sn*-glycerol-3-phosphate (Figure 2), is the most abundant and relevant LPA isoform from the point of view of its signaling properties, since it shows activity at all LPA receptors (LPARs), so it is the one we will refer to as LPA throughout this work.

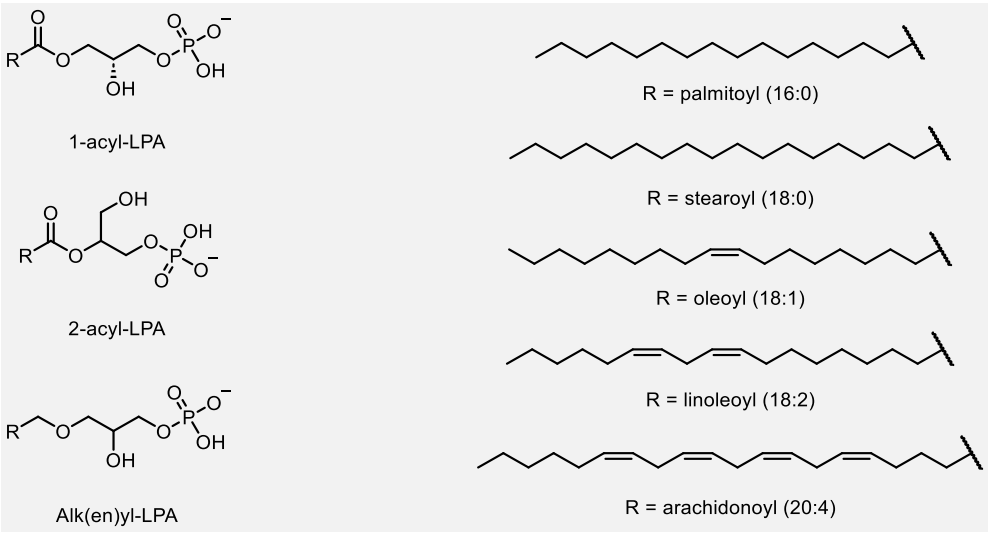

Figure 3. LPA general structures and major species.

LPA is produced during the synthesis of cell membranes, either under physiological or pathophysiological conditions in all eukaryotic tissues and blood plasma,[22-24] notably within the developing and adult nervous system.[25] LPA exerts its extracellular signaling through its interaction with its receptors,[26] mediating important responses such as cell proliferation and migration, cytoskeletal reorganization, platelet aggregation and cytokine and chemokine secretion, among others.[27-30] In the CNS, LPA mediates a wide range of effects, including neural progenitor cell physiology, astrocyte and microglia activation, neuronal cell death, axonal retraction, and neuroinflammation.[31,32] Therefore, deregulation of LPA is linked to certain kinds of diseases such as cancer,[33,34] angiogenesis,[35] fibrosis,[36] hypertension,[37] atherosclerosis,[38] and neurological, metabolic and cardiovascular disorders. [39-41]

1.1. Endogenous LPA system

The LPA, together with the enzymes responsible of its biosynthesis and degradation, and its receptors, comprise the endogenous LPA system. All these elements will be described through the following sections.

1.1.1. LPA metabolism: biosynthesis and degradation pathways

There are two mayor synthetic pathways involving LPA production (Figure 4). The first pathway is responsible for the extracellular LPA production, which is thought to

mediate cellular responses through LPARs (especially in serum and plasma).[42] The second pathway involves both extra and intracellular LPA production, mainly devoted to the *de novo* biosynthesis of complex glycerolipids, including mono-, di-, and triglycerides, as well as phospholipids.[43]

In the first pathway, membrane phospholipids such as phosphatidylcholine (PC), phosphatidylserine (PS), and phosphatidylethanolamine (PE) are converted into their corresponding LPs lysophosphatidylcholine (LPC), lysophosphatidylserine (LPS), and lysophosphatidylethanolamine (LPE), respectively. In activated platelets, this occurs by the action of phosphatidylserine-specific phospholipase A_1 (PS-PLA_1) or secretory phospholipase A_2 (sPLA_2) activity. In plasma, LPC is produced via lecithin-cholesterol acyltransferase (LCAT) and PLA_1 activity. In both cases, the resulting LPs are converted to LPA via autotaxin (ATX) activity. The second pathway involves the synthesis of phosphatidic acid (PA) from membrane phospholipids via phospholipase D (PLD_1 and PLD_2 isoforms) or from intracellular diacylglycerol (DAG) through diacylglycerol kinase (DGK) action, and subsequent conversion to LPA by the actions of either PLA_1 or PLA_2.[44]

In addition, intracellular LPA can be generated through the acylation of glycerol-3-phosphate (G3P) by glycerophosphate acyltransferase (GPAT), the phosphorylation of monoacylglycerol by monoacylglycerol kinase (MAGK), and oxidative modification of low-density lipoprotein (LDL) (Figure 4). Inverse steps of three of the fourth intracellular mechanisms of LPA production are the main routes for LPA degradation: G3P production by lysophosphatases and lysophospholipases, generation of MAG by lipid phosphate phosphatases (LPPs) and conversion into PA by acylglycerophosphate acyltransferase (AGPAT).[24]

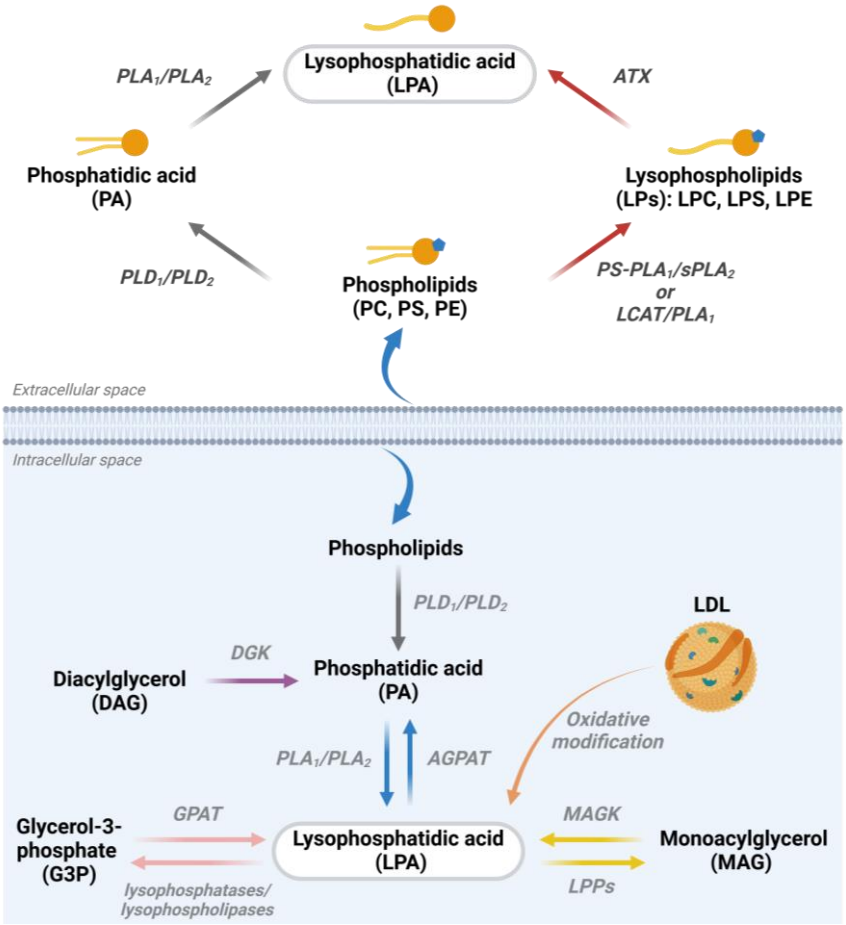

Figure 4. Intra and extracellular LPA biosynthesis and degradation pathways. Abbreviations: AGPAT: acylglycerophosphate acyltransferase; ATX: autotaxin; DGK: diacylglycerol kinase; GPAT: glycerophosphate acyltransferase; LCAT: lecithin-cholesterol acyltransferase; LDL: low-density lipoprotein; LPPs: lipid phosphate phosphohydrolases; MAGK: monoacylglycerol kinase; PL: phospholipase (Adapted from reference[24]).

1.1.2. Signaling through LPA receptors

The diverse and numerous physiological effects of LPA are mediated by signaling through its receptors. There are six different receptors (LPA_{1-6}),[26,45-47] which belong to the G-protein coupled receptors (GPCRs) superfamily, the largest class of drug targets which have more than 800 members encoded by the human genome.[48] GPCRs comprise at least five structurally distinct subfamilies based on sequence conservation, where class A (rhodopsin-like)[49] is the major and most studied, and where LPA_{1-6} receptors belong to. By coupling with one or more intracellular heterotrimeric guanine nucleotide-binding proteins (G proteins), GPCRs can transform extracellular stimulus into intracellular responses.

G proteins are composed of Gα, Gβ, and Gγ subunits (Figure 5), and are located inside the plasma membrane, to which they are bound by their α and γ subunits via hydrophobic structures (the β-subunit is bound by association to the γ-subunit). The extensive array of G proteins can be classified into four subfamilies based on the homology of the Gα subunits ($G\alpha_s$, $G\alpha_i$, $G\alpha_{q/11}$, and $G\alpha_{12/13}$).[50] Activation of $G\alpha_s$ leads to the elevation of the adenylyl cyclase (AC) activity, resulting in an increase in cyclic adenosine monophosphate (cAMP) and activation of protein kinase A (PKA) downstream signaling cascades. In contrast, $G\alpha_i$ activation leads to AC inhibition and decreased cAMP levels. $G\alpha_{q/11}$ activates phospholipase C (PLC), resulting in the production of two different second messengers, diacylglycerol (DAG) and inositol trisphosphate (IP_3), which activates protein kinase C (PKC) and induces Ca^{2+} release into the cytoplasm, respectively. Finally, $G\alpha_{12/13}$ subfamily members activate small GTPases and promotes the Rho/ROCK (Rho-associated protein kinase) and Rho/SRF (serum response factor) pathways.

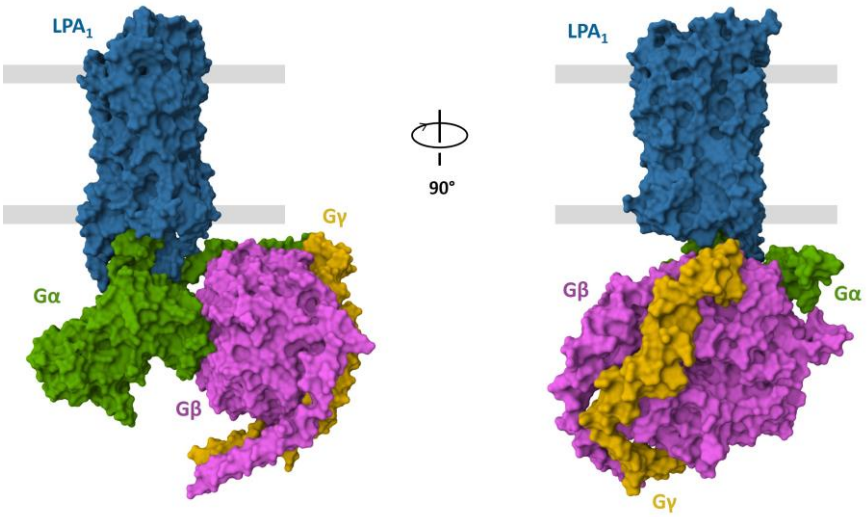

Figure 5. Molecular surface representation of LPA_1-$G\alpha_i$ complex bound to LPA. Blue: LPA_1 receptor; green, pink and yellow: heterotrimeric G-protein $G\alpha_i$. Source: PDB (Protein ID: 7TD0).

LPARs have been extensively studied over the last 30 years, when the first member, the LPA_1 receptor, was identified.[51] LPARs are divided in two subfamilies according to their primary structure homology.[20,24,45] LPA_{1-3} receptors belong to the endothelial differentiation gene (EDG) family, which share 45-56% similarity in the amino acid sequence, while LPA_{4-6} receptors comprise the second subgroup, belonging to the P2Y purinergic receptors family, which share~35% amino acid identity with each other (Table 1).[24] Among the six receptors identified so far, only the LPA_1 and LPA_6 have been crystallized and their 3D structures published.[52,53]

Table 1. Molecular characteristics of LPARs.

Receptor	Other names	G protein	Number of amino acids	MW (KDa)	Signaling pathways
EDG family					
LPA_1	Edg2	$G\alpha_i$, $G\alpha_{q/11}$, $G\alpha_{12/13}$	364	~41	MAPK, PLC, Akt, Rho, Ca^{2+} and YAP/Taz activation, AC inhibition
LPA_2	Edg4	$G\alpha_i$, $G\alpha_{q/11}$, $G\alpha_{12/13}$	348	~39	MAPK, PLC, Akt, Ca^{2+} and Rho activation, AC inhibition
LPA_3	Egd7	$G\alpha_i$, $G\alpha_{q/11}$	353	~40	MAPK, PKC, PLC, Ca^{2+}, and YAP/Taz activation
P2Y family					
LPA_4	P2Y9/ GPR23	$G\alpha_s$, $G\alpha_i$, $G\alpha_{q/11}$, $G\alpha_{12/13}$	370	~42	MAPK, PLC, Akt, Ca^{2+} and Rho/ROCK activation, AC inhibition
LPA_5	GPR92/ GPR93	$G\alpha_{q/11}$, $G\alpha_{12/13}$	372	~41	PLC and Ca^{2+} activation
LPA_6	P2Y5	$G\alpha_s$, $G\alpha_i$, $G\alpha_{12/13}$	344	~39	Rho activation

Abbreviations: MAPK: mitogen-activated protein kinase; PLC: phospholipase C; Akt: protein kinase B; Rho: rho protein; YAP: yes-associated protein; Taz: transcriptional co-activator with PDZ-binding motif; AC: adenylyl cyclase; ROCK: Rho-associated protein kinase.

When LPA binds to $LPA_{1\text{-}6}$ receptors, it activates different Gα proteins ($G\alpha_s$, $G\alpha_i$, $G\alpha_{q/11}$, and $G\alpha_{12/13}$), initiating a variety of complex downstream signaling pathways that regulate various physiological functions (Figure 6)[54,55] such as cell morphology, growth, motility, migration and survival, cytoskeletal changes, Ca^{2+} mobilization, immune response, and cognitive functions.[20]

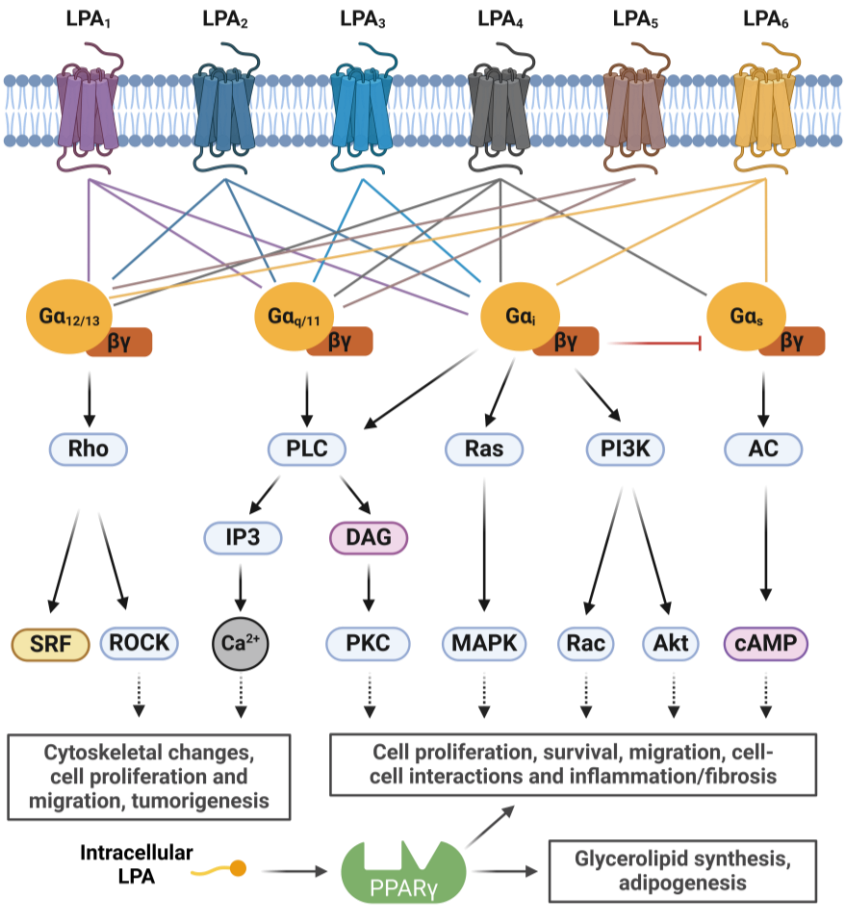

Figure 6. LPARs and signaling pathways. Abbreviations: DAG: diacylglycerol; Rho: rho protein; PLC: phospholipase C; Ras: ras protein; PI3K: phosphatidylinositol 3-kinase; AC: adenylyl cyclase; SRF: serum response factor; ROCK: Rho-associated protein kinase; PKC: protein kinase C; MAPK: mitogen-activated protein kinase; cAMP: cyclic adenosine 3,5-monophosphate (Adapted from reference[24]).

LPA_1 is the best studied of the six LPARs, whit several agonists and antagonists described,[56,57] and it is widely expressed in various tissues and organs of human body such as brain, uterus, testis, lung, heart, stomach, kidney, and skeletal muscle.[58] LPA mediates a great diversity of physiological functions through LPA_1 coupled to the G protein ($G\alpha_i$, $G\alpha_{q/11}$ and $G\alpha_{12/13}$), including cell survival, cell proliferation, cell adhesion, cell migration, cytoskeletal changes, Ca^{2+} mobilization, immune function, and myelination.[59] In the nervous system, LPA promotes astrocyte proliferation and neuronal differentiation, proliferation of oligodendrocytes and smooth muscle cells, migration, and anti-apoptosis of Schwann cells.[60-62]

LPA_2 was identified four years after the discovery of LPA_1,[63] and couples to the same G proteins as the LPA_1 receptor. During development, LPA_2 receptor is highly expressed in

the CNS,[64] and LPA_2 activation is associated with cell survival and migration. In addition, LPA mediates anti-apoptosis of cells through LPA_2 receptor, and the damage repair effect of LPA_2 receptor on DNA can protect cells from radiation.[65]

LPA_3 was discovered from a gene library homology search of orphan GPCR genes.[66,67] It is distributed through heart, testis, prostate, pancreas, lung, ovary and brain,[68] and appears to be involved in reproduction[69-72] and in determining vertebrate left-right patterning during embryogenesis, a crucial process for proper organ formation and function.[73]

In 2003, LPA_4 was discovered by ligand screening and was the first LPA receptor identified showing a dissimilar amino acid sequence from the other LPARs, LPA_{1-3}, sharing only ~20% amino acid identity with LPA_1.[74] This receptor is present in ovary, thymus, pancreas, brain, heart, small intestine, testis, prostate, colon, and spleen. LPA_4 receptor regulates the differentiation of adipogenesis of mesenchymal progenitor cells and bone formation,[75] induces neurite retraction and stress fiber formation,[76,77] promotes angiogenesis and vascular development,[78] and also influence the differentiation of immortalized hippocampal progenitor cells.[79] Interestingly, activation of LPA_4 inhibits LPA-induced cell migration and invasion.[80,81]

LPA_5 was identified in 2006 as a member of the LPA receptor family.[82,83] It is highly expressed in the spleen, mast cells, small intestine, colon, spinal cord and dorsal root ganglia. LPA_5 activation is related with stress fiber formation and neurite contraction,[82] pain signaling in the spinal cord,[84] promotion of Na^+-dependent water absorption,[85,86] and inhibition of T-cell activation.[87] In melanoma cells, LPA inhibits migration through LPA_5, similar to its LPA_4-mediated effect.[88]

LPA_6 was recognized in 2008 as an LPA receptor, being the most recent addition to the LPA receptor family.[89] LPA_6 is highly expressed in hair cells and leukocytes, and it is implicated in hair growth regulation and alopecia.[89,90] Moreover, the binding of LPA to the LPA_6 receptor regulates vascular permeability[91,92] and facilitate lymphocytes transmigration.[93]

Apart from the LPA_{1-6} receptors, other receptors such as GPR87,[94] P2Y10,[95] the transient receptor potential vanilloid 1 (TRPV1) ion channel,[96] and the transcription factor peroxisome proliferator activated receptor-gamma (PPARγ) nuclear receptor,[97] have been reported to respond to LPA.

Among all LPARs, we will focus on the LPA_2 receptor due to its underexplored biological relevance and the lack of potent and selective modulators with probed *in vivo* efficacy.

1.2. LPA_2 Receptor

Type 2 lysophosphatidic acid receptor (LPA_2) was identified from a genetic library of orphan GPCR genes,[63] and shares approximately 53% and 47% amino acid similarity with the LPA_1 and LPA_3 receptors, respectively (Figure 7). It is constituted by 348 amino acids and has a molecular weight around 39 kDa. Nowadays, there is no structural information regarding LPA_2. However, computational homology models and mutagenesis experiments have revealed three key residues that, when altered, decrease LPA binding affinity: arginine 3.28, glutamine 3.29 and lysine/arginine 7.36 (Figure 7).[65,98]

Figure 7. Sequence alignment of LPA_{1-3} receptors. The residues marked with asterisk (*) are identical, residues marked with a colon (:) represents 80% similarity, and residues marked with a dot (.) indicates 50% similarity. Red: key residues involved in LPA binding. Figure made with the align tool of UniProt.

In terms of structure (Figure 8), LPA_2 receptor is constituted by an extracellular *N*-terminus, followed by seven transmembrane (TM) α-helical domains connected by three loops facing the intracellular environment (ICLs) and three loops facing the extracellular environment (ECLs), and an intracellular *C*-terminus. The extracellular region modulates ligand access, whereas the TM region binds ligands and transduces signals to the intracellular region, which is the interface for interaction with intracellular signaling proteins. A remarkable feature of LPA_2 structure is its unique carboxyl-terminal tail (amino acids 296-348), in which it contains two distinct protein-protein interaction domains that

allows the formation of specific intracellular macromolecular complexes with various PDZ scaffold proteins (such as NHERF-2 or MAGI-3) and zinc-finger proteins (such as Siva-1 or TRIP6), respectively.[65,99-101]

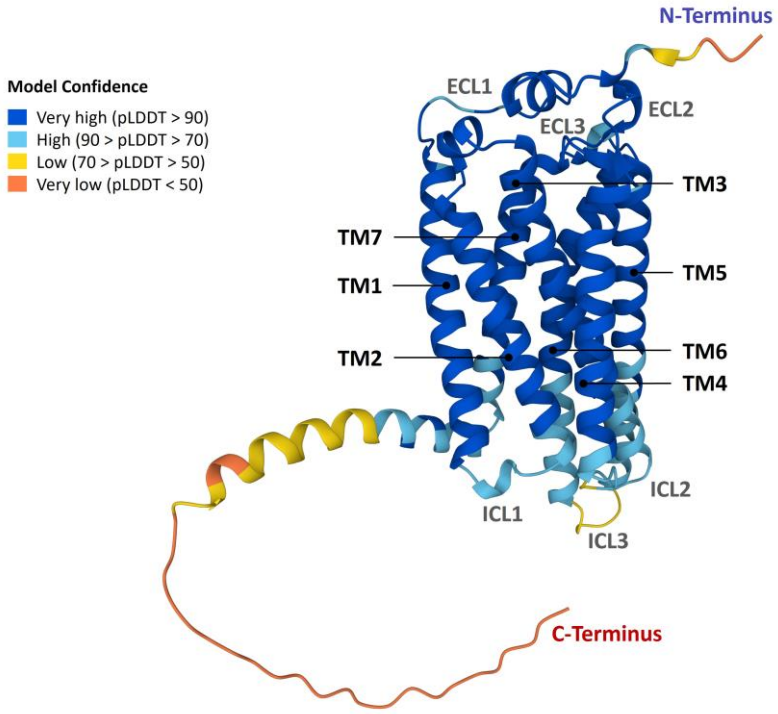

Figure 8. AlphaFold[102] structure prediction of LPA_2 and its domains (UniProt accession: Q9HBW0). pLDDT corresponds to the model's prediction of its score on the local distance difference test (between 0 and 100). ECL: extracellular loop; ICL: intracellular loop; TM: transmembrane region.

In the inactive state, the LPA_2 receptor is bound to a heterotrimeric G protein complex (G_i, $G_{q/11}$ or $G_{12/13}$). Binding of an agonist to the receptor results in a conformational change that is transmitted to the bound Gα subunit of the heterotrimeric G protein via protein domain dynamics (Figure 9A). The activated Gα subunit exchanges guanosine trisphosphate (GTP) in place of guanosine diphosphate (GDP) which in turn triggers the dissociation of Gα subunit from the Gβγ dimer and from the receptor. The dissociated Gα and Gβγ subunits interact with other intracellular proteins (effectors) initiating downstream signaling pathways through proteins such as Ras, MAPK, PI3K, Rac, PLC and Rho, producing another signaling molecules that mediate diverse cellular responses which are involved in cell survival and migration, immune function, lymphocytes transmigration, and several aspects of nervous system development and function. [46,103,104]

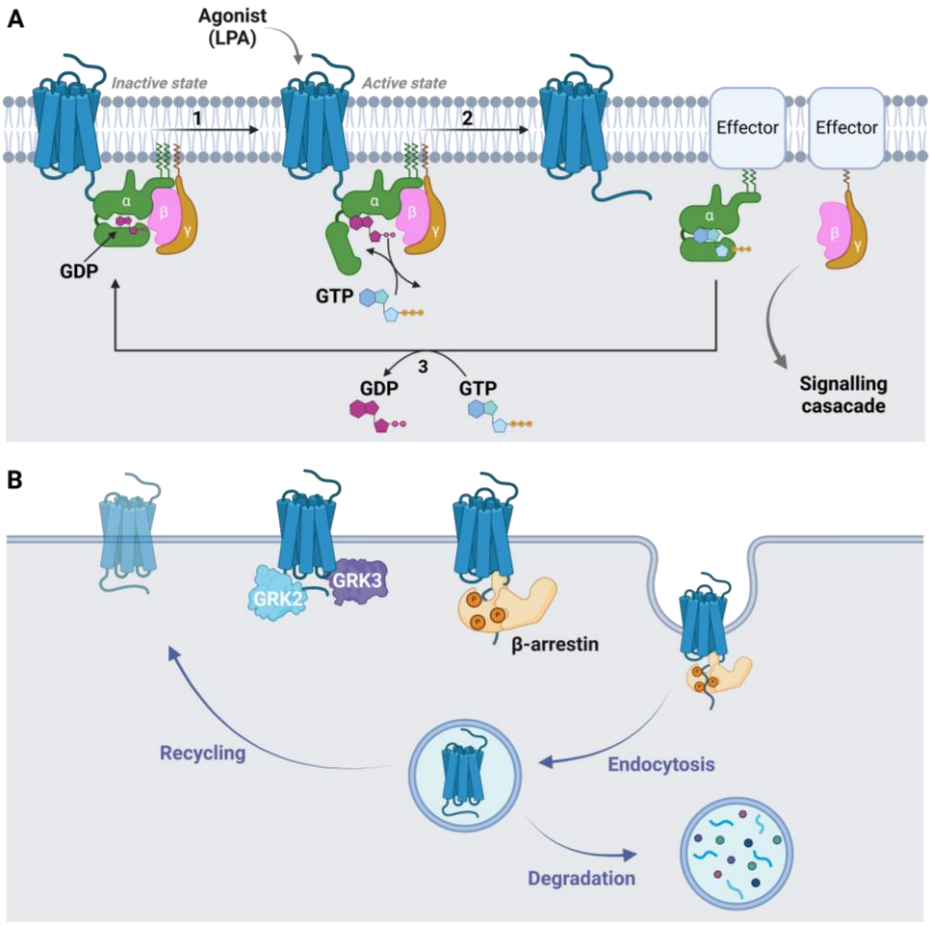

Figure 9. (A) G protein activation/deactivation cycle; (B) LPA_2 desensitization and internalization mechanism. GDP: guanosine diphosphate; GTP: guanosine trisphosphate; GRK: GPCR kinase (Adapted from reference[105]).

Upon activation, the LPA_2 receptor, like other class A GPCRs, can recruit GPCR kinases (GRK) that mediate phosphorylation of the receptor (Figure 9B), causing β-arrestin binding, desensitization, and ultimately receptor internalization. Thus, the freed GPCR can rebind to another heterotrimeric G protein to form a new complex that is ready to initiate another round of signal transduction. In addition, the α subunit of G protein has a GTPase activity, and once it hydrolyzes GTP to GDP, it becomes inactive.[106]

1.3. Expression of LPA_2 receptor and therapeutic applications

LPA_2 receptor is widely expressed in leukocytes, testis, prostate, spleen, thymus, pancreas, and in almost all cells of the CNS and peripheral tissues, with a remarkable expression during embryonic development.[46,64] Thus, this receptor is involved in the

regulation of numerous cellular physiological processes and implicated in the development and progression of numerous pathologies and diseases (Figure 10).[24,26,46,47] Among all the processes in which LPA_2 is involved, three stand out: cancer, fibrosis and neuroinflammation.

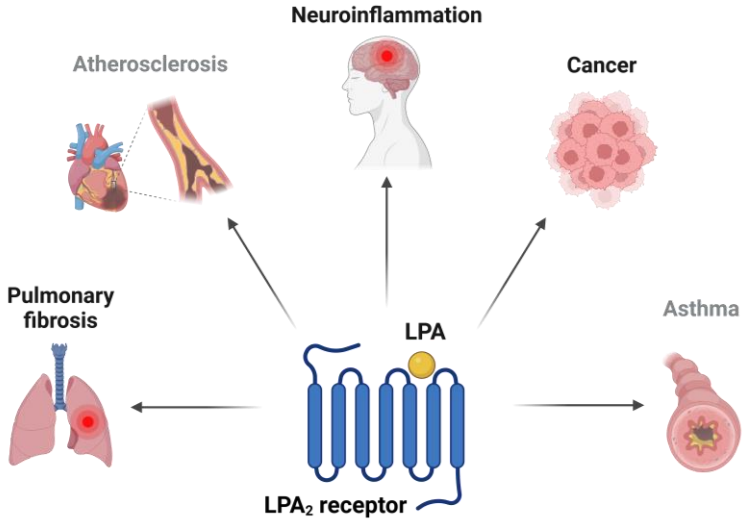

Figure 10. Different pathologies and diseases in which LPA_2 receptor is implicated.

Several studies have linked increased LPA signaling with the biological events associated with cancer development and tumor progression.[36,107] These processes include malignant cell transformation, elevated proliferation of cancer stem cells, enhanced invasion and metastasis and alteration of tumor environments.[108] In particular, LPA_2 receptor activation and/or overexpression has been shown to associate with stimulation of cell survival and apoptosis inhibition. In colon cancer, LPA enhances cell proliferation and angiogenesis factor production via LPA_2 receptor signaling.[26] In ovarian cancer, overexpression of LPA_2 (along with LPA_3) stimulate proliferation and migration of cancer cells via Rho/Rac signaling pathway.[109,110] In breast cancer, LPA_2 can also promote breast cancer proliferation, migration, and invasion.[111] Interestingly, LPA_2 is implicated in protecting cancer cells against apoptotic stress after irradiation and chemotherapy by augmenting DNA damage repair response and inhibiting the mitochondrial apoptosis cascade.[112]

LPA_2 signaling has also been linked to fibrosis, a pathological condition in which an excess of fibrous connective tissue replaces normal tissue producing scars in a wide range of organ systems, being closely associated with end-stage organ failure. It has been demonstrated that, after kidney injury, LPA induces TGF-β activation mainly through the LPA_2-Gαq-Rho/ROCK pathway, thereby promoting the development of renal fibrosis.[113] In

lung injury, fibrosis and death can be alleviated by knocking out the LPA_2 receptor, highlighting the importance of this receptor in the process of pulmonary fibrosis.[114]

Neuroinflammation is a localized form of inflammation in the peripheral nervous system (PNS) and CNS. Characteristic features of neuroinflammation are vasculature changes that result in increased vascular permeability, infiltration of immune cells, activation of glial cells and production of inflammatory mediators including cytokines and chemokines. Additionally, neuroinflammation is a major feature of several neurological and neuropsychiatric diseases such as Alzheimer's disease,[115] Parkinson disease,[116] amyotrophic lateral sclerosis,[117] neuropathic pain,[118] chronic pain[119,120] and rheumatoid arthritis.[121] Accumulating evidence suggests that LPA_2 signaling is implicated in the regulation of numerous neuroinflammatory processes since LPA_2 receptor is expressed in neurons and glial cells (mainly in oligodendrocytes, astrocytes, and microglia). In the spinal cord injury (SCI), recent advances have shown that activation of the LPA_2 receptor contributes to secondary damage after trauma.[31]

In this regard, inhibition of LPA_2 receptor signaling has recently emerged as a new therapeutic option to limit the neuroinflammation. However, the lack of potent and selective LPA_2 receptor antagonists, with good oral bioavailability, has limited the validation of this receptor as a therapeutic target. At the present time, there are no drugs targeting this receptor that have been approved by the FDA, and current compounds under clinical development only comprise LPA_1 antagonists (Table 2). This fact highlights the need of the development of new LPA_2 ligands with global safety and good efficacy profiles that enable the therapeutic validation of LPA_2 receptor.

Table 2. Clinical trials targeting LPARs[a].

Compound	Mechanism of action	Phase	Indication	ClinicalTrials.gov Identifier
BMS-986020	LPA_1 antagonist	2	Idiopathic pulmonary fibrosis	NCT01766817
BMS-986278	LPA_1 antagonist	2	Idiopathic pulmonary fibrosis	NCT04308681
^{18}F-BMS-986327	LPA_1 antagonist	1	Idiopathic pulmonary fibrosis	NCT04069143
SAR100842	LPA_1 antagonist	2	Systemic sclerosis	NCT01651143

[a]Data extracted from www.clinicaltrials.gov (accessed in February 2024).

1.4. LPA_2 ligands: agonists and antagonists

As a general classification, there are two types of ligands according to their binding to the target protein: orthosteric ligands, which bind to the endogenous ligand binding site, and allosteric modulators, that bind to a different region of the protein than the endogenous ligand does. In turn, orthosteric ligands are divided into three subclasses depending on their activity (Figure 11A): those that act as agonists, mimicking the response of the endogenous ligand by activating the receptor; neutral antagonists, which bind to the protein and block the action of the endogenous ligand, thus preventing receptor activation; and inverse agonists, a third class of ligands that can reduce the constitutive activity of a receptor below that of the basal state, producing the opposite effect of an agonist.[122] Agonist ligands can be further divided into full or partial agonists depending on their capacity to induce a full or partial stimulation of the receptor. In addition, some agonists can stabilize distinct receptor conformations linked to diverse functional outcomes. This phenomenon has been termed biased agonism (Figure 11B).[123,124]

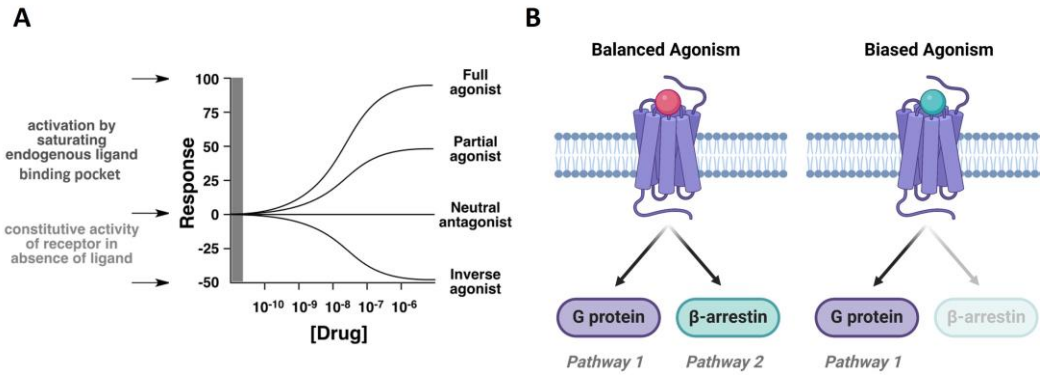

Figure 11. (A) Representative dose-response curves of a full agonist, partial agonist, neutral antagonist, and inverse agonist. (B) Schematic representation of biased agonism, where two different ligands stabilize distinct receptor conformations that will each promote distinct functional outcomes at two signaling pathways.

Regarding LPA_2 receptor, no allosteric modulators have been described but some orthosteric ligands (agonists and antagonists) have been developed.[47,125]

LPA_2 receptor agonists described so far can be classified into two different groups depending on their lipid or non-lipid nature. Among the most representative LPA_2 agonists of lipid nature (Table 3), we can find dodecylphosphate **C1**, with a half-maximal effective concentration (EC_{50}) of 700 nM,[126] and oleoyl-thiophosphate **C2** (EC_{50}=244 nM).[127] The latter shows potency improvements respect compound **C1**, although it also has partial

agonist activity towards LPA_1 and LPA_3 receptors. *N*-acyl ethanolamide phosphate **C3** (EC_{50}=30 nM)[128] and *sn*-2-OH alkoxymethylene phosphonate LPA analogue **C4** (EC_{50}=258 nM)[129] have been described more recently, showing higher potency and selectivity than compounds **C1** and **C2**.

Table 3. Structure and EC_{50} value of representative LPA_2 receptor agonists of lipid nature.

Compound	Structure	EC_{50} (nM)[a]		
		LPA_1	LPA_2	LPA_3
C1	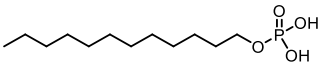	N.D.[b]	700	N.D.
C2	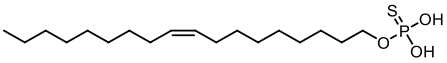	193	244	546
C3	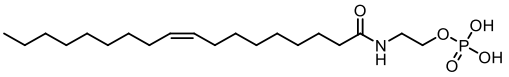	197	30	>5000
C4	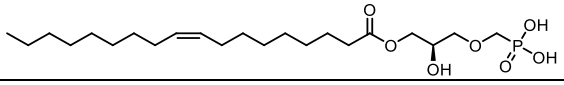	>4000	258	1360
LPA (18:1)	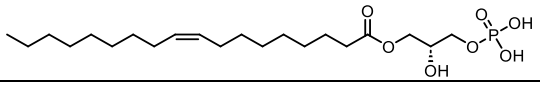	5-12	7-10	253

[a]Activity data from functional calcium mobilization assay.[126-129] [b]N.D., no data.

With respect to LPA_2 agonists of non-lipid nature (Figure 12), the most representative ligands are carbamoyl benzoic acid derivatives **NSC12404** (EC_{50}=9.5 μM), **H2L5547924** (EC_{50}=2.8 μM), **H2L5828102** (EC_{50}=3.3 μM) and thiobenzoic acid derivative **GRI977143** (EC_{50}=3.3 μM).[130,131] However, all of them show antagonist activity towards either LPA_1 or LPA_3 receptors. Based on the last compound, two sulfamoyl benzoic acid analogues have been developed, **RP-1** (EC_{50}=0.005 nM), the first non-lipid agonist of LPA_2 with picomolar activity, and compound **DBIBB** (EC_{50}=1420 nM).[132]

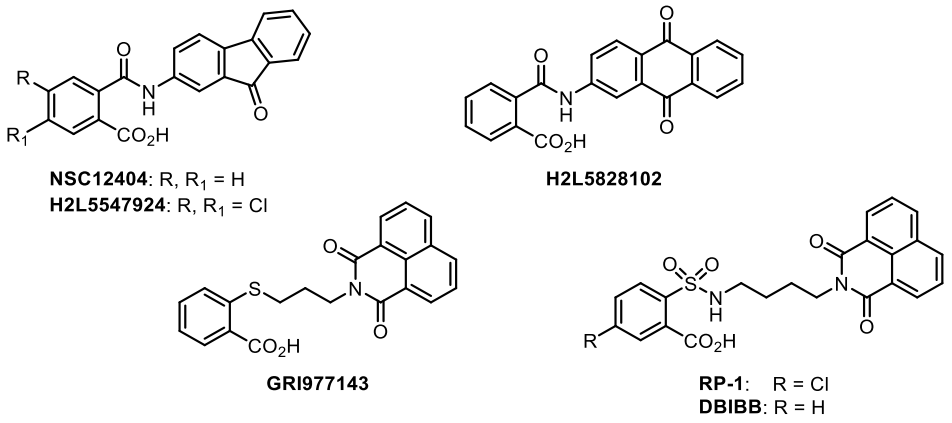

Figure 12. Representative LPA_2 receptor agonists of non-lipid nature.

The first reported LPA_2 antagonist of lipid nature (Figure 13) was tetradecyl phosphonate **C5**, whit a half-maximal inhibitory concentration (IC_{50}) of 5.5 μM,[127] followed by oleoyl α-bromo analog **BrP-LPA** [IC_{50} (LPA_2)=0.47 μM].[133] Although both compounds display moderate potency at LPA_2 receptor, they are not selective since they also show antagonist activity at LPA_1 and/or LPA_3 receptors.

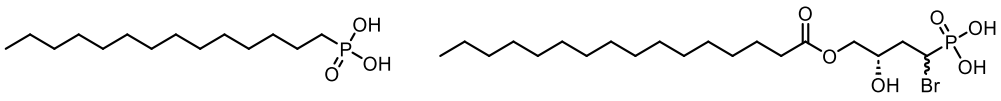

C5

IC_{50} (LPA_1) > 30 μM
IC_{50} (LPA_2)= 5.5 μM
IC_{50} (LPA_3)= 3.1 μM

BrP-LPA

IC_{50} (LPA_1)=0.6-2.0 μM
IC_{50} (LPA_2)=0.47 μM
IC_{50} (LPA_3)=2.1-4.4 μM

Figure 13. LPA_2 receptor antagonists of lipid nature. Reported IC_{50} data were obtained using the functional calcium mobilization assay. [127,133]

Different LPA_2 antagonists of non-lipid nature with high potency have been synthesized during the last years (Figure 14). Among the most representative ones, isoxazole derivative **Ki16425** [IC_{50} (LPA_2)=6.5 μM], developed by Ohta *et al*. in 2003,[134] stands out as the first potent LPA_2 receptor antagonist reported although it shows higher affinity for LPA_1 and LPA_3 receptors. Thienopyrimidine derivatives **AMG19** [IC_{50} (LPA_2)=0.26 μM] and **AMG35** [IC_{50} (LPA_2)=0.017 μM] were discovered by high-throughput screening, both showing potent LPA_2 antagonists with high selectivity *vs* LPA_1 and LPA_3 receptors.[135] Although **AMG35** has been tested *in vitro* and showed an inhibitory effect on ERK phosphorylation and cell proliferation induced by LPA in the HCT-116 colon cancer cell line, there is no information regarding its pharmacokinetic (PK) profile or *in vivo* activity. Compound **H2L5186303** was obtained by structure-based virtual screening using a three-point pharmacophore, being the first potent and selective LPA_2 antagonist described with nanomolar activity [IC_{50} (LPA_2)=9 nM], but no PK or *in vivo* characterization has been reported so far.[136,137] More recently, our research group has identified a new family of pyrazole-based derivatives, among which compound **UCM14216** stands out as a potent and selective LPA_2 receptor antagonist [IC_{50} (LPA_2)=1.9 μM; K_d (LPA_2)=1.3 nM] with *in vivo* efficacy in a spinal cord injury (SCI) mouse model.[138] Finally, **C58** has been the latest addition to the LPA_2 receptor antagonist family.[139] Although this compound shows high potency and selectivity against LPA_1 receptor, and has a good PK profile, there is no data regarding its selectivity for the other members of the LPARs or its ability to cross the blood-brain barrier (BBB) and reach the CNS.

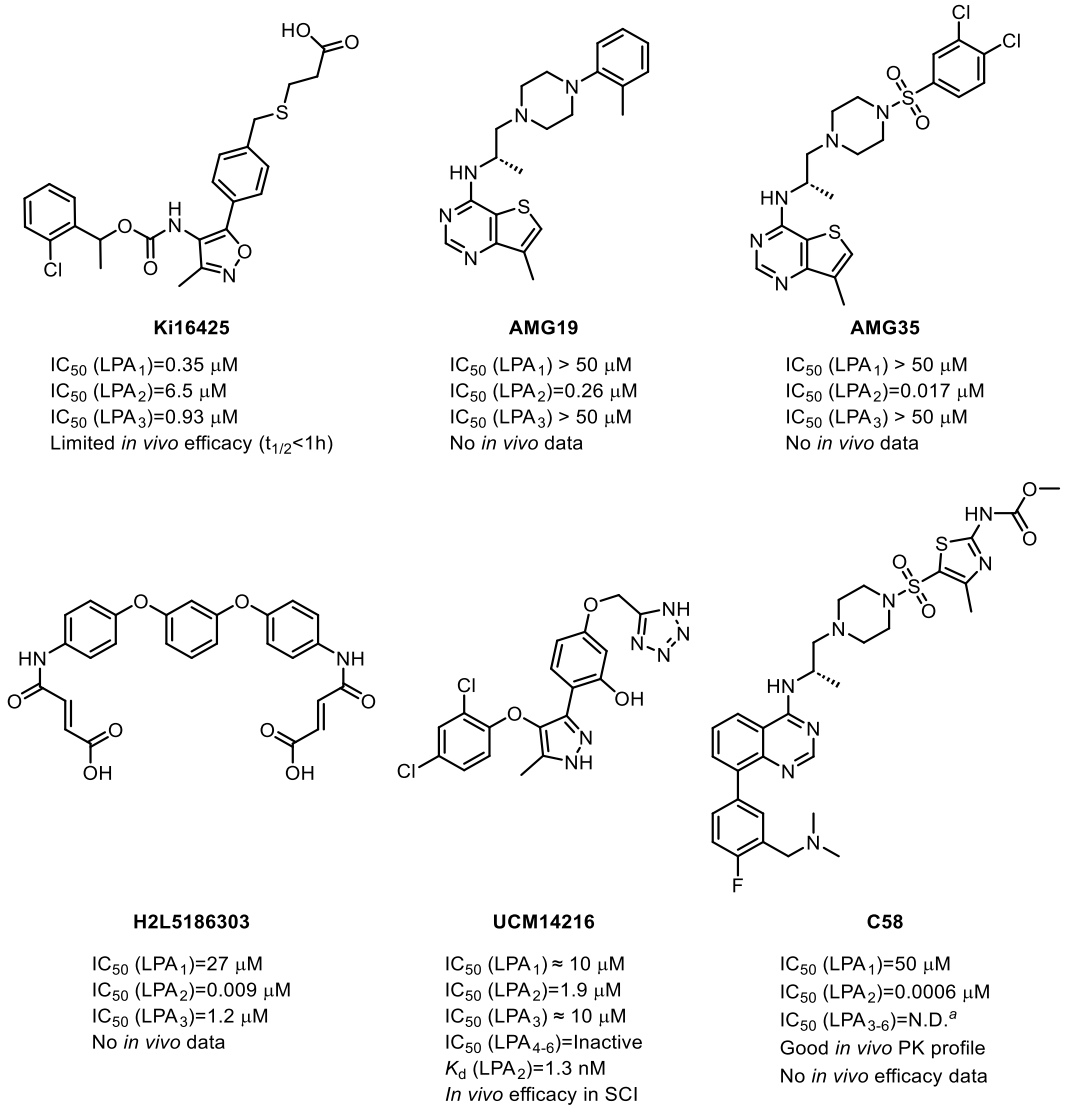

Figure 14. LPA_2 receptor antagonists of non-lipid nature. Reported IC_{50} data were obtained using the functional calcium mobilization assay.[134-139] [a]N.D., no data reported.

In view of the lack of potent and selective LPA_2 receptor antagonists targeting the CNS with good PK profiles, it is clear the need of developing new LPA_2 antagonists that overcome the current limitations in order to validate the suitability of this receptor to become a new therapeutic target for the treatment of (neuro)inflammation.

1.5. Objectives

The main objective of the present work is the design and synthesis of new potent and selective LPA_2 antagonists, with a good PK profile and *in vivo* activity, to validate this receptor as a therapeutic target of interest in (neuro)inflammatory processes. This goal includes the following specific objectives:

1) Design and synthesis of new compounds with antagonist activity at LPA_2 receptor.
2) Assessment of LPA_2 receptor antagonism activity and study of the selectivity *vs* LPA_1 and LPA_3 receptors.
3) Pharmacological characterization of selected compound(s).
4) Study of the *in vivo* efficacy of selected compound(s).

2. RESULTS AND DISCUSSION

2. RESULTS AND DISCUSSION

Previous results obtained in our research group identified compound **UCM-14216** (Figure 15) as the most potent and selective LPA_2 antagonist described to date.[138] Although this compound has shown good *in vivo* activity, being effective in an animal model of SCI, it has a relatively moderate stability that limits its bioavailability. Therefore, in the present project we have addressed the development of new potent and selective LPA_2 antagonists with improved biological and PK profiles. Towards this aim, we selected as starting point a previously characterized antagonist, **UCM-14250** (Figure 15), which was synthesized during the development of **UCM-14216**.[138] Although this compound exhibits a moderate activity value, with a maximum blockade effect of the activation induced by LPA (E_{max}) of 57±9%, it represents an interesting scaffold for optimization considering its selectivity, lower molecular weight (MW=280.3 g/mol) and reduced topological polar surface area (tPSA=47.1 Å) compared to **UCM-14216** (MW=433.3 g/mol; tPSA=121.8 Å). Thus, we initiated a medicinal chemistry project around compound **UCM-14250**.

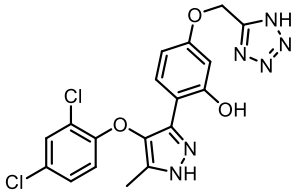

UCM-14216

E_{max} (LPA_2 antag. @10 μM)=90±2%
IC_{50} (LPA_2 antag.)=1.9±0.2 μM
Inactive at $LPA_{1,3-6}$
K_d (LPA_2)=1.3 nM
MW=433.3 g/mol; tPSA=121.8 Å

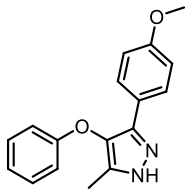

UCM-14250

E_{max} (LPA_2 antag. @10 μM)=57±9%
Inactive at $LPA_{1,3-6}$
MW=280.3 g/mol; tPSA=47.1 Å

Figure 15. LPA_2 antagonists previously developed in our research group.

2.1. Structure-activity relationship study

Before initiating a systematic structural exploration around **UCM-14250**, we evaluated the importance of the different parts of the molecule for the antagonist activity at the LPA_2 receptor. Thus, we studied the influence of the phenoxy and *p*-methoxyphenyl moieties with commercially available 3-(4-methoxyphenyl)-5-methyl-1*H*-pyrazole and compound **1**, respectively (Figure 16).

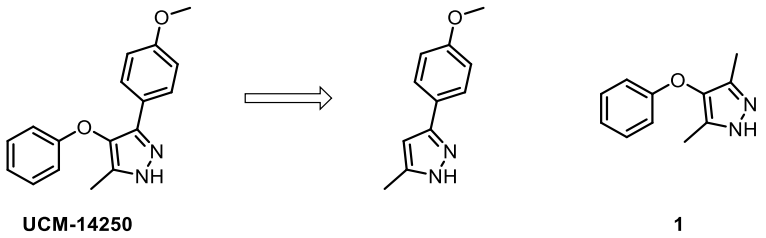

Figure 16. Exploration of the influence of the phenyl rings of **UCM-14250**.

The synthesis of compound **1** was planned through a Chan-Lam coupling reaction between phenylboronic acid and *N*-protected 4-hydroxypyrazole **4** (Scheme 1). In a first approach to selectively protect the NH, we used *tert*-butoxycarbonyl (Boc) group, but the reaction took place in the OH rather than in the NH, making necessary the initial protection of the hydroxy group. For this purpose, different sets of orthogonal protecting groups were tested, including trimethylsilyl (TMS)/triphenylmethyl (Tr), *tert*-butyldimethylsilyl (TBDMS)/Tr, Boc/9-fluorenylmethyloxycarbonyl (Fmoc), and Boc/benzyl (Bn) pairs. Among them, Boc/Bn pair allowed the selective protection of the hydroxy and NH groups, respectively. Thus, 4-hydroxypyrazole was *O*-protected using di-*tert*-butyl dicarbonate followed by reaction with benzyl chloride to obtain intermediate **3** (Scheme 1). Treatment with trifluoroacetic acid afforded *N*-benzylpyrazole **4** which reacted via Chan-Lam coupling with phenylboronic acid to yield ether **5**, that was transformed in target compound **1** by removal of the benzyl group by hydrogenation.

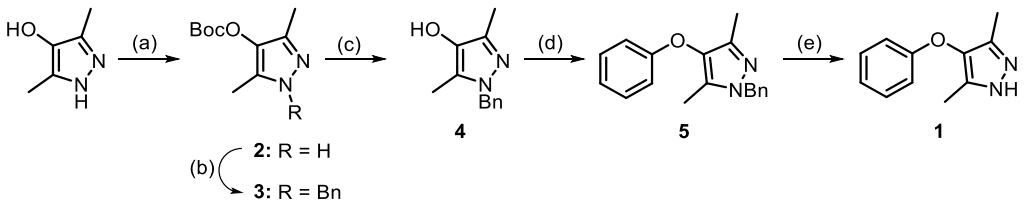

Scheme 1. Reagents and conditions: (a) Di-*tert*-butyl dicarbonate, Et_3N, DCM, rt, 1 h, 84%; (b) i. KOH, DMSO, 80 °C, 1 h; ii. Benzyl chloride, rt, 2 h, 55%; (c) TFA, DCM, rt, 1.5 h, quant.; (d) Phenylboronic acid, $Cu(OAc)_2$, Et_3N, 4 Å MS, DCM, rt, 16 h, 33%; (e) 10% Pd/C, H_2, DMF, 70 °C, 67%.

Evaluation of the activity of the two compounds at the LPA_2 receptor was performed using a calcium mobilization assay in B103 cells stably transfected with the LPA_2 receptor. This fluorescence assay (Figure 17) is based on the quantification of the amount of calcium released into the intracellular medium after stimulation with the endogenous agonist (LPA) using Fluo-4 NW, a calcium-sensitive fluorescent probe (λ_{exc}=494 nm, λ_{em}=516 nm). Thus, after loading the cells with the probe, the compounds under study are added at a concentration of 10 µM and the cells are subsequently stimulated with LPA at the same concentration. The antagonist activity (E_{max}) is determined as the capacity of the compound to reduce the LPA-mediated calcium response. To evaluate selectivity against LPA_1 and LPA_3 receptors (the other members of the EDG-type receptor subfamily), RH7777 and B103 cells stably transfected with LPA_1 or LPA_3 receptors, respectively, were used in an analogous functional assay. Those compounds that showed values of E_{max} < 50% were considered inactive (IC_{50} > 10 µM). For compounds with E_{max} values > 85%, dose-response experiments were carried out to determine their IC_{50} value.

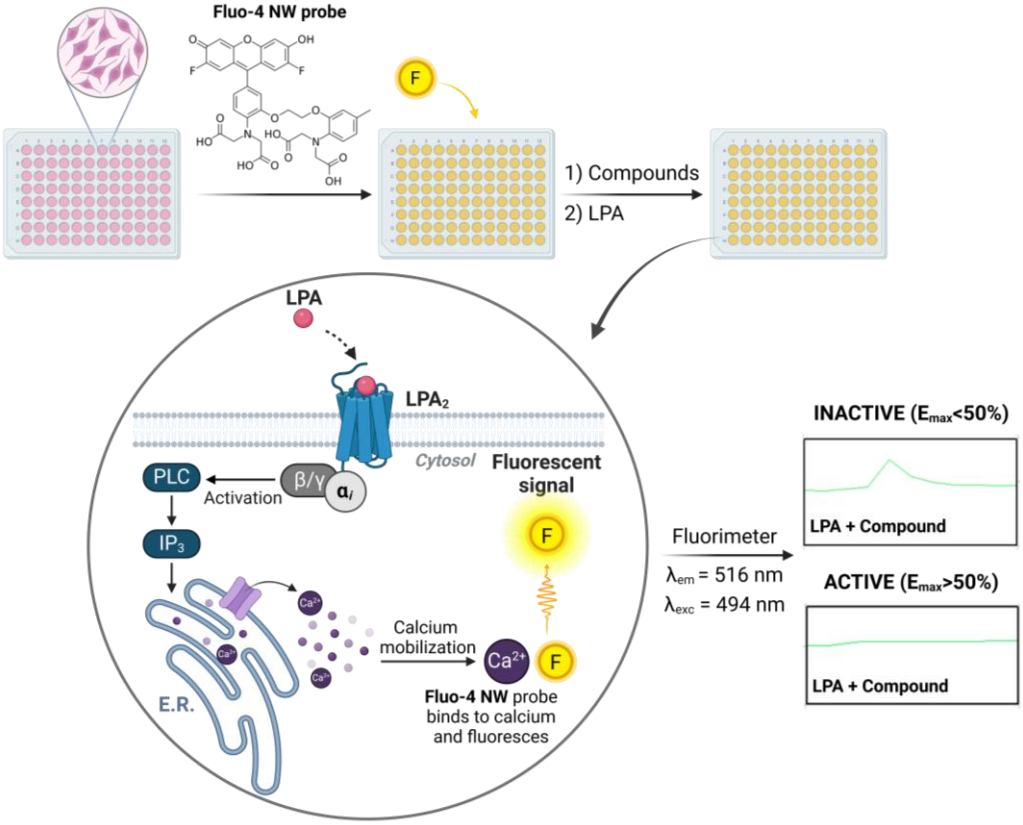

Figure 17. Schematic representation of the calcium mobilization assay for assessment of the activity at the LPA_2 receptor. F: Fluo-4 NW fluorescent probe; α, β/γ: heterotrimeric G-protein subunits; PLC: phospholipase C; IP_3: inositol trisphosphate.

Biological evaluation of compound **1** and 3-(4-methoxyphenyl)-5-methyl-1*H*-pyrazole revealed that both compounds had lower antagonist activity at LPA_2 receptor (E_{max}=25±9%, E_{max}=46±7%, respectively) than **UCM-14250** (E_{max}=57±9%), highlighting the need of both aromatic rings to keep the antagonist activity.

Based on these initial results, we started a thorough exploration around **UCM-14250**. For this purpose, a series of systematic modifications in the phenoxy system, the *p*-methoxyphenyl moiety, and the central heterocycle were made (Figure 18). The synthesis and biological evaluation on the LPA_{1-3} receptors were done iteratively, so that the biological results guide the design and synthesis of the new compounds.

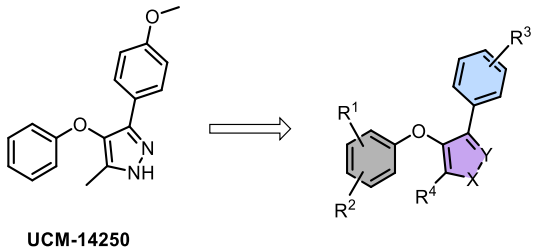

Figure 18. Systematic structural modifications carried out around hit **UCM-14250**.

2.1.1. Structural exploration around the phenoxy system

We initiated the structural exploration of **UCM-14250** by modifying the phenoxy moiety. Hence, we synthesized analogues **6**-**24** that have one substituent with different electronic and steric properties at *o*-, *m*-, and *p*- positions of the phenoxy ring (Figure 19).

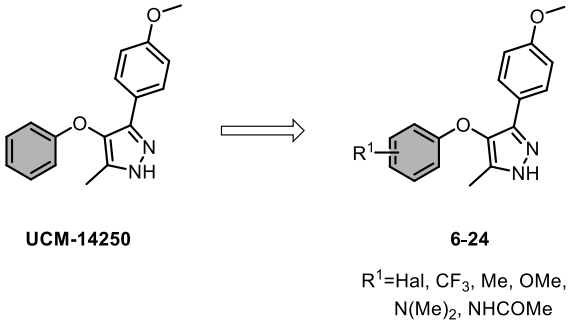

Figure 19. Exploration around the phenoxy system of **UCM-14250**.

The synthesis of compounds **6**-**24** was planned through a three-step route (Scheme 2). Thus, a Williamson reaction between 2-bromo-4-methoxyacetophenone and the adequately substituted phenol was carried out to form intermediate ketones **25**-**43** which were transformed into the corresponding enaminones **44**-**62** by reaction with *N,N*-

dimethylacetamide dimethyl acetal (DMADMA). Final cyclocondensation of the enaminones with hydrazine yielded desired pyrazoles **6**-**24**. This synthetic route allowed us to obtain target compounds with low to moderate yields. In the case of the initial Williamson reaction, the yields were rather moderate, except for the reaction with the *o*-NHCOMe and *p*-OMe substituted phenols, which gave the highest yields, consistent with the favorable effect of electron donating groups in this transformation.

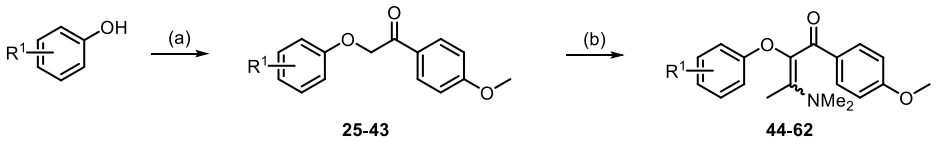

25-27: R^1=*o*, *m*, *p*-Cl **37-39:** R^1=*o*, *m*, *p*-OCH_3
28-30: R^1=*o*, *m*, *p*-F **40,41:** R^1=*m*, *p*-$N(CH_3)_2$
31-33: R^1=*o*, *m*, *p*-CF_3 **42,43:** R^1=*o*, *m*-$NHCOCH_3$
34-36: R^1=*o*, *m*, *p*-CH_3

44-46: R^1=*o*, *m*, *p*-Cl **56-58:** R^1=*o*, *m*, *p*-OCH_3
47-49: R^1=*o*, *m*, *p*-F **59,60:** R^1=*m*, *p*-$N(CH_3)_2$
50-52: R^1=*o*, *m*, *p*-CF_3 **61,62:** R^1=*o*, *m*-$NHCOCH_3$
53-55: R^1=*o*, *m*, *p*-CH_3

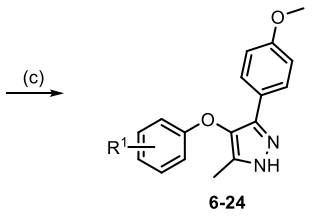

6-8: R^1=*o*, *m*, *p*-Cl **18-20:** R^1=*o*, *m*, *p*-OCH_3
9-11: R^1=*o*, *m*, *p*-F **21,22:** R^1=*m*, *p*-$N(CH_3)_2$
12-14: R^1=*o*, *m*, *p*-CF_3 **23,24:** R^1=*o*, *m*-$NHCOCH_3$
15-17: R^1=*o*, *m*, *p*-CH_3

Scheme 2. Reagents and conditions: (a) 2-Bromo-4-methoxyacetophenone, DBU, DMF, MW, 140 °C, 45 min, 30-81%; (b) DMADMA, toluene, 90 °C, 6-16 h; (c) $N_2H_4 \cdot H_2O$, ethanol, reflux, 30 min, 10-72%.

Another step that affects negatively to the overall yield is the enaminone formation. This intermediate is usually obtained impurified with significant amounts of methyl 4-methoxybenzoate (compound A, Scheme 3) together with two biphenyl derivatives (compounds B and C, Scheme 3). Attempts to purify the enaminone by column chromatography were unsuccessful, leading to partial decomposition. To try to improve this step, efforts were made to optimize the enaminone synthesis. Initial reaction conditions employed an excess of DMADMA (4 eq.), 90 °C, reaction times between 16-24 h and no solvent. Under these conditions, and according to the results described in the literature,[140] a significant amount of methyl 4-methoxybenzoate (compound A, Scheme 3) is formed by nucleophilic attack of a methoxide (generated from DMADMA) to the ketone group. Moreover, the progression of the reaction favors the formation of the two extra biphenyl by-products (compounds B and C, Scheme 3) through the addition of a

second molecule of DMADMA to target enaminone to generate a polysubstituted butadiene that evolves to the biphenyl by-products. Therefore, a reduction in the reaction times and in the amount of DMADMA employed, could minimize the formation of these secondary products. Thus, we decreased the equivalents of DMADMA to 1.5 eq., reduced the reaction times (6-16 h), and used toluene as a solvent, keeping the reaction temperature at 90 °C. Under these conditions we observed a decrease in the amount of methyl 4-methoxybenzoate formed, and the disappearance of the biphenyl by-products B and C, thus leading to an increase in the conversion of the desired enaminone. Hence, the overall yields of the pyrazoles synthesized from the enaminones obtained under these conditions increased considerably (40-72% *vs* 10-40% obtained with the non-optimized initial reaction conditions).

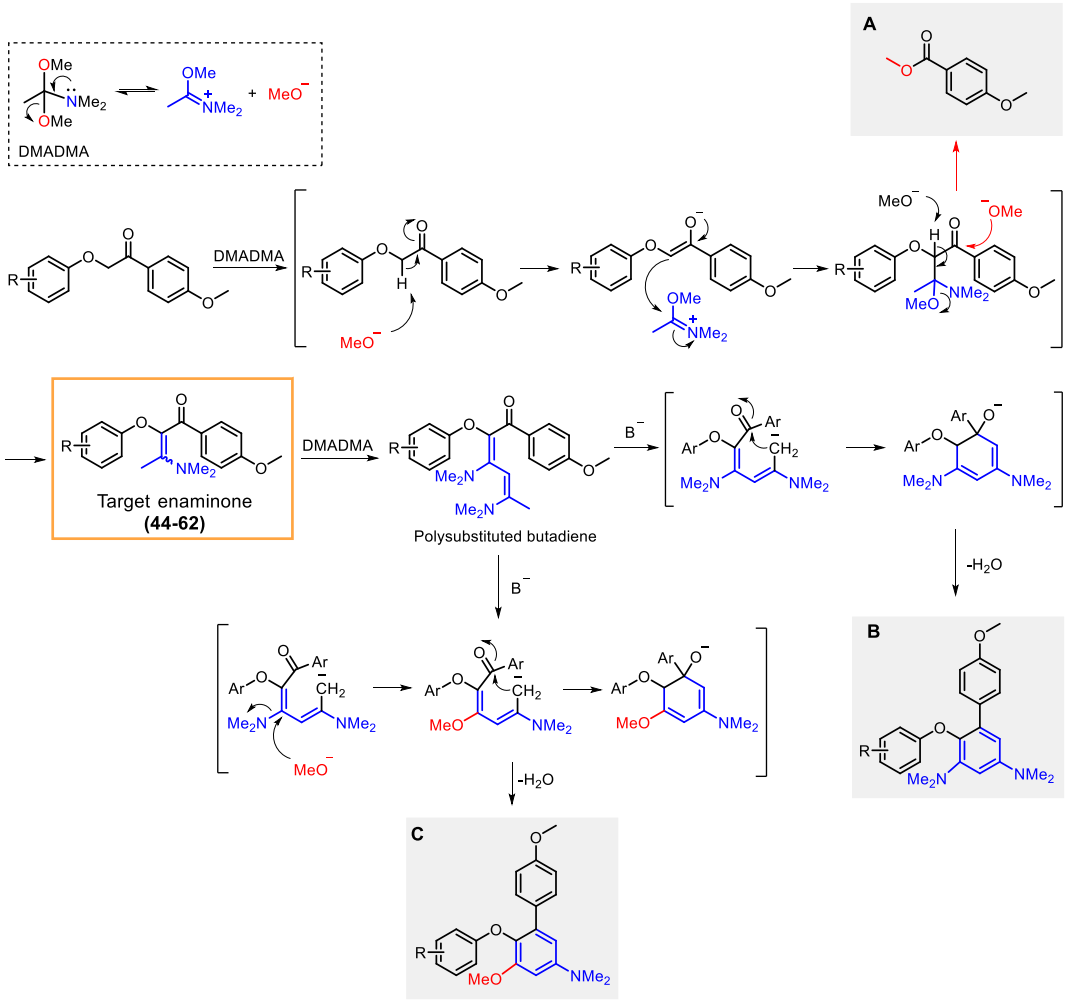

Scheme 3. Reported proposed reaction mechanism[140] for the synthesis of enaminones from *N,N*-dimethylacetamide dimethyl acetal (DMADMA) and the corresponding ketone. The main by-products obtained are methyl ester derivative (A), diaminobiphenyl derivative (B), and aminomethoxybiphenyl derivative (C).

Once compounds **6**-**24** were synthesized, they were tested for their antagonist activity at the LPA_2 receptor, and their selectivity against LPA_1 and LPA_3 receptors (Table 4). The results revealed that the presence of at least one substituent in the phenoxy system was in general favorable for the activity, as most of the new compounds exhibited higher antagonist activity than **UCM-14250** (E_{max}=57±9%). Although no obvious trends regarding steric or electronic effects of the substituents could be drawn from the activity results, they suggest that the presence of a chlorine or fluorine atom or trifluoromethyl group are favorable for activity, since compounds **6**, **9**, **13** and **14** exhibit E_{max} values between 76% and 87%, higher than the E_{max} value of 57% shown by **UCM-14250**.

Regarding selectivity, most of the compounds were considered inactive at LPA_1 receptor, whereas they showed different activities at LPA_3 receptor, ranging from an E_{max} value of 83% for compound **10**, to the inactivity (E_{max} < 50%) of derivatives **6**, **12**, **14**, **15** and **22**.

Table 4. Antagonist activity of **UCM-14250** and compounds **6**-**24** at LPA_{1-3} receptors.

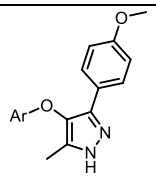

Comp.	Ar	E_{max} (%)[a] [IC_{50} (μM)][b]			Comp.	Ar	E_{max} (%)[a] [IC_{50} (μM)][b]		
		LPA_1R	LPA_2R	LPA_3R			LPA_1R	LPA_2R	LPA_3R
UCM-14250		Inact.[c]	57±9	Inact.	**15**		Inact.	74±2	Inact.
6		Inact.	76±1	Inact.	**16**		Inact.	9±1	82±5
7	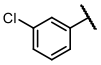	Inact.	50±2	73±1	**17**		Inact.	74±3	56±4
8	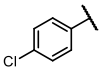	Inact.	46±5	69±9	**18**		51±3	60 ±3	63±6
9		68±9	76±1	68±2	**19**	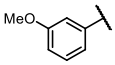	Inact.	69±4	79±1
10		54±0	68±8	83±8	**20**	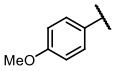	Inact.	62 ±7	70±3
11		68±1	68±7	71±1	**21**	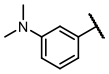	53±1	64±1	61±8
12		Inact.	50±5	Inact.	**22**	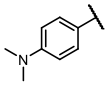	Inact.	70±6	Inact.
13	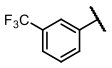	Inact.	87±4 [5±1]	70±1	**23**	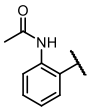	Inact.	57±8	53±5
14	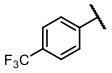	Inact.	76±3	Inact.	**24**	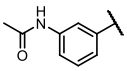	Inact.	60±1	70±6

[a] E_{max}=maximum blockade effect of the activation induced by 10 μM of LPA (18:1, 1-oleoyl-*sn*-glycerol-3-phosphate) at a concentration of the compound under study of 10 μM. Values shown are the mean±s.e.m. of 2-4 independent experiments performed in triplicate. [b] For E_{max} > 85%, IC_{50} values are expressed as mean±s.e.m, from a minimum of two independent experiments, performed in triplicate. [c] Inact., compounds that show an E_{max} < 50% at the highest concentration tested (10 μM) are considered inactive (IC_{50} > 5 μM).

Taken into account the influence of the position of the substituents (for example *o*-chloro derivative **6** was highly active with an E_{max} value of 76% whereas its *meta* isomer **7** was considerably less active, with an E_{max} value of 50%; *m*-trifluoromethyl derivative **13** showed an E_{max} value of 87% while its *ortho* isomer **12** exhibited an E_{max} value of 50%; *o*-methyl derivative **15** exhibited an E_{max} value of 74% whereas its *meta* isomer **16** was inactive, with an E_{max} value of 9%), we explored the possibility that the introduction of a second substituent might improve the activity of the compounds at the LPA_2 receptor.

Considering that the best results from the previous compounds have been obtained for halogen-containing derivatives **6**, **9**, **13** and **14** (with an E_{max} between 76 and 87%), we started to study the influence of introducing a second chlorine atom in different positions (Scheme 4, compounds **63**-**66**). These new derivatives were synthesized through Williamson reaction between 2-bromo-4-methoxyacetophenone and the corresponding dichlorophenol to obtain intermediates **69**-**72**. Then, treatment with DMADMA yielded enaminones **75**-**78**, which were finally transformed into the target pyrazoles **63**-**66** by reaction with hydrazine. Biological evaluation of the compounds at LPA_2 receptor (Table 5) revealed that 2,5- and 3,4-dichloro substitution increased the antagonist activity, with derivatives **65** and **66** as the best ligands identified so far, with E_{max} values higher than 90%.

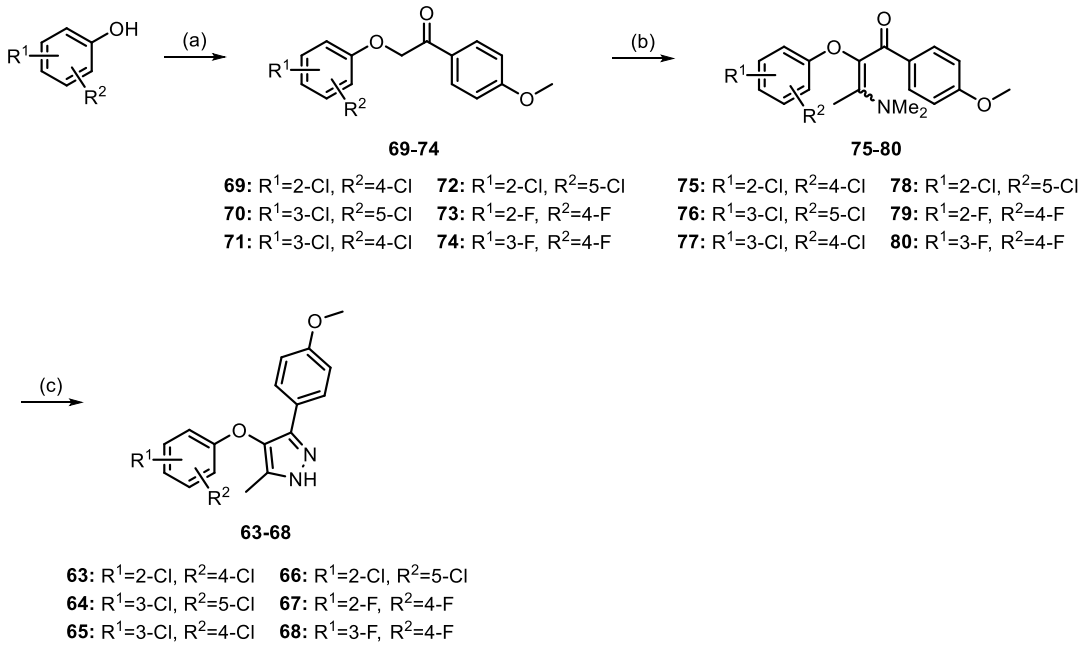

Scheme 4. Reagents and conditions: (a) 2-Bromo-4-methoxyacetophenone, DBU, DMF, MW, 140 °C, 45 min, 58-68%; (b) DMADMA, toluene, 90 °C, 6-16 h; (c) $N_2H_4 \cdot H_2O$, ethanol, reflux, 30 min, 17-54%.

Then, we addressed whether the replacement of the chlorine atom by fluorine could lead to an improvement of its potency, as the positive effects of this change in biological activity and physicochemical properties has been well stablished for a number of different ligands.[141] Hence, we synthesized the fluorinated analogs of derivatives **63** and **65** (Scheme 4) but no improvement in terms of activity was observed for compounds **67** and **68** (Table 5). As such, fluorinated derivative **67** showed an activity similar to compound **63** (E_{max} values of 66% and 67%, respectively) and its isomer **68** exhibited less activity that its

chlorinated counterpart **65** (E_{max} values of 78% and 92%, respectively) and also decreased selectivity against LPA_1 and LPA_3 receptors (E_{max} value < 50% for compound **65** at LPA_1 and LPA_3 receptors *vs* 55% for derivative **68** at LPA_1 and 82% at LPA_3).

Table 5. Antagonist activity of **UCM-14250** and compounds **63-68** at LPA_{1-3} receptors.

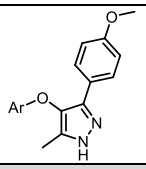

Comp.	Ar	E_{max} (%)[a] [IC_{50} (μM)][b]		
		LPA_1R	**LPA_2R**	**LPA_3R**
63	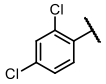	Inact.[c]	67±7	Inact.
64	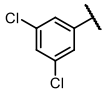	Inact.	79±1	79±1
65	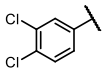	Inact.	92.0±0.2 [0.2±0.1]	Inact.
66	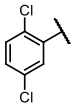	Inact.	91.0±0.4 [1.0±0.2]	71±4
67		Inact.	66±4	Inact.
68	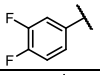	55±2	78±6	82±1
UCM-14250		Inact.	57±9	Inact.

[a]E_{max}=maximum blockade effect of the activation induced by 10 μM of LPA (18:1, 1-oleoyl-*sn*-glycerol-3-phosphate) at a concentration of the compound under study of 10 μM. Values shown are the mean±s.e.m. of 2-4 independent experiments performed in triplicate. [b]For E_{max} > 85%, IC_{50} values are expressed as mean±s.e.m, from a minimum of two independent experiments, performed in triplicate. [c] Inact., compounds that show an E_{max} < 50% at the highest concentration tested (10 μM) are considered inactive (IC_{50} > 5 μM).

At this point, we confirmed the dose-response behavior of those antagonists with E_{max} values higher than 85% and we determined their IC_{50} values. Figure 20 shows the corresponding curves obtained for compounds **13**, **65** and **66**, revealing excellent IC_{50} values in the low micromolar range (IC_{50}=5, 0.2, 1 μM, respectively). In sum, the results obtained up to this moment indicate that derivative **65** is the most potent LPA_2 receptor antagonist described so far, with a maximal efficacy at 10 μM of 92% and an IC_{50} value of 230 nM at LPA_2 receptor and selectivity *vs* LPA_1 and LPA_3 receptors (IC_{50} > 5 μM, more than 20-fold selectivity). Hence, the 3,4-dichlorophenoxy system was selected for continuing with the SAR study.

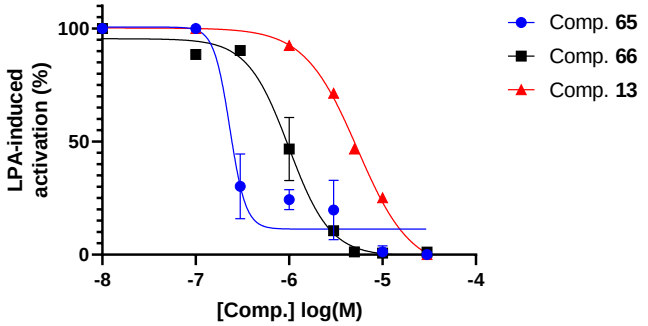

Figure 20. Dose-response curves of compounds **13** (red), **65** (blue) and **66** (black) at LPA_2 receptor. Values shown are the mean±s.e.m. of 2 independent experiments performed in triplicate.

2.1.2. Structural exploration around the *p*-methoxyphenyl system

At this point, we explored the influence of the *p*-methoxyphenyl system of compound **65** in the antagonist efficacy. First, knowing that the aromatic moiety is required for LPA_2 antagonism, as shown by compound **1** (Figure 16) which was inactive, we studied the importance of the methoxy group as well as the influence of its position with the synthesis of compounds **81** (lacking the methoxy group) and **82** and **83**, *ortho*- and *meta*-methoxy isomers of **65**, respectively (Figure 21).

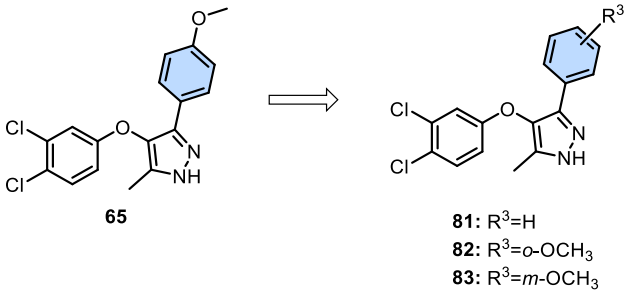

Figure 21. Modifications in the substitution pattern of the *p*-methoxyphenyl moiety.

The synthesis of compounds **81**-**83** was accomplished starting with a Williamson reaction between 3,4-dichlorophenol and the appropriate 2-bromoacetophenone (Scheme 5). The resulting ketones **84**-**86** were treated with DMADMA to obtain the corresponding enaminones **87**-**89** which were transformed into the desired pyrazoles **81**-**83** by reaction with hydrazine.

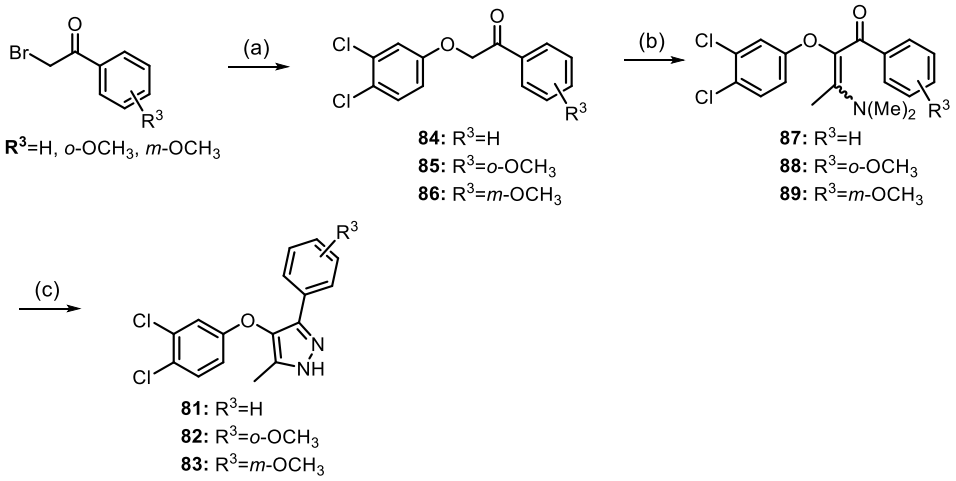

Scheme 5. Reagents and conditions: (a) 3,4-dichlorophenol, DBU, DMF, MW, 140 °C, 45 min, 37-53%; (b) DMADMA, toluene, 90 °C, 6-16 h; (c) $N_2H_4 \cdot H_2O$, ethanol, reflux, 30 min, 10-55%.

Determination of the LPA_2 antagonist character of compounds **81**-**83** revealed that none of them was able to improve the activity and selectivity values of compound **65** (Table 6), suggesting that the presence of the methoxy group at the *para* position was the most favorable for LPA_2 antagonism.

Table 6. Antagonist activity of compounds **65** and **81**-**83** at LPA_{1-3} receptors.

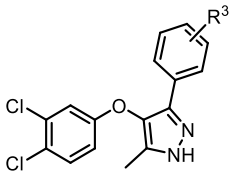

Compound	R^3	E_{max} (%)[a] [IC_{50} (μM)][b]		
		LPA_1R	**LPA_2R**	**LPA_3R**
81	H	Inact.[c]	70±6	56±1
82	*o*-OCH_3	62±6	75±8	Inact.
83	*m*-OCH_3	65±1	59±8	56±2
65	*p*-OCH_3	Inact.	92.0±0.2 [0.2±0.1]	Inact.

[a] E_{max}=maximum blockade effect of the activation induced by 10 μM of LPA (18:1, 1-oleoyl-*sn*-glycerol-3-phosphate) at a concentration of the compound under study of 10 μM. Values shown are the mean±s.e.m. of 2-4 independent experiments performed in triplicate. [b] For E_{max} > 85%, IC_{50} values are expressed as mean±s.e.m, from a minimum of two independent experiments, performed in triplicate. [c] Inact., compounds that show an E_{max} < 50% at the highest concentration tested (10 μM) are considered inactive (IC_{50} > 5 μM).

We next decided to study the effect of the replacement of the methoxy group of compound **65** by other substituents with different electronic and steric effects on the antagonist activity, keeping constant the *para* position of the group (Figure 22). Towards this aim, we synthesized derivatives **90**-**95** in which the methoxy group was replaced by other alkoxy derivatives, as well as by hydroxy, trifluoromethyl and acetamide groups.

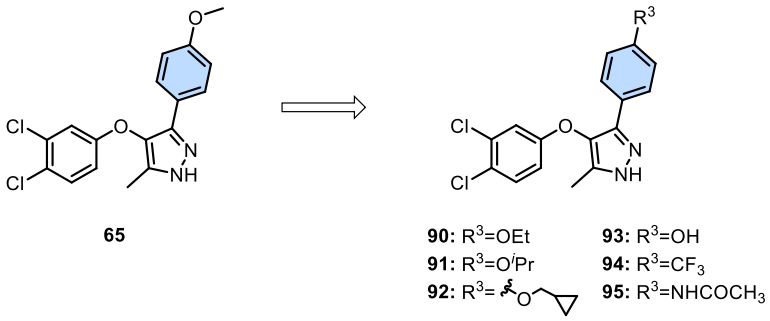

65

90: R^3=OEt
91: R^3=O^{i}Pr
92: R^3=
93: R^3=OH
94: R^3=CF_3
95: R^3=$NHCOCH_3$

Figure 22. Study of the effect of the replacement of the methoxy group by other substituents.

For the synthesis of alkoxy derivatives **90**-**92**, 2-bromo-4-hydroxyacetophenone was employed as starting material (Scheme 6). Thus, the hydroxy group was protected as tetrahydropyranyl (THP) ether followed by Williamson reaction of protected intermediate **96** with 3,4-dichlorophenol and subsequent deprotection under acidic conditions. The resulting phenolic intermediate **98** was reacted with the appropriate haloalkane to form alkoxy derivatives **99**-**101**. Next, transformation into the corresponding enaminones **102**-**104** and final reaction with hydrazine afforded desired pyrazoles **90**-**92**.

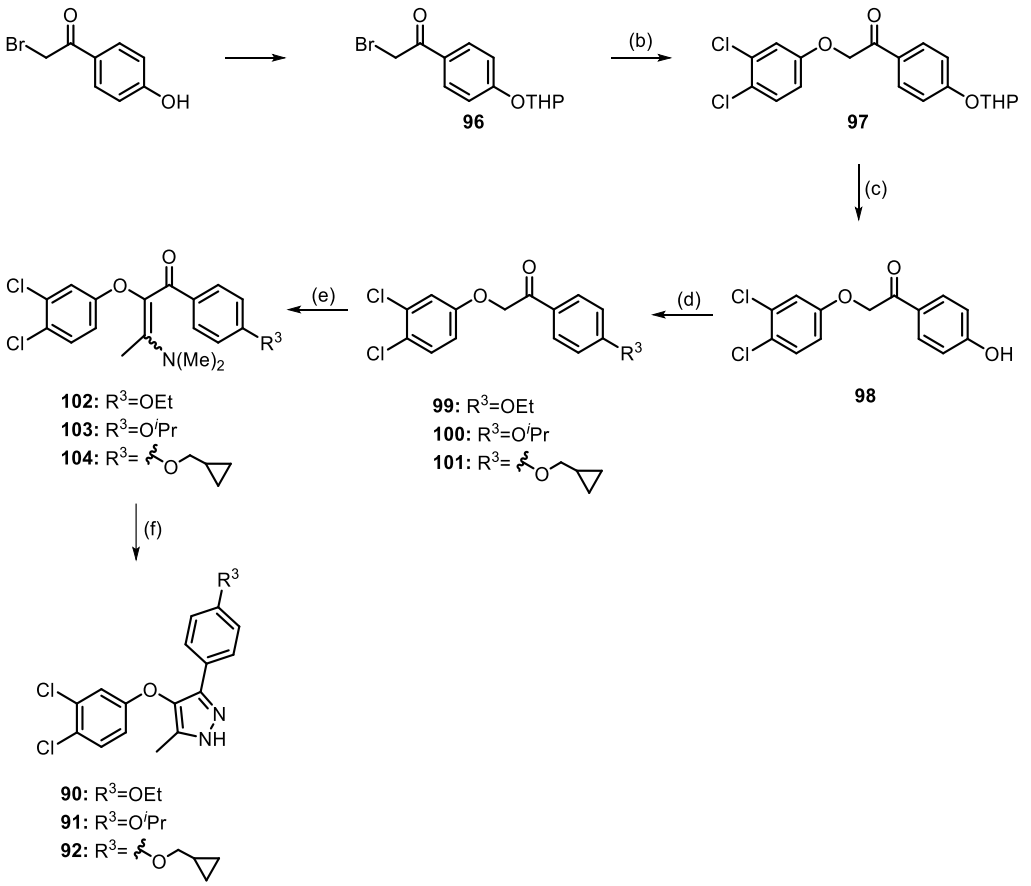

Scheme 6. Reagents and conditions: (a) Dihydropyran, pyridinium *p*-toluenesulfonate, DCM, rt, 3 h, 88%; (b) 3,4-dichlorophenol, K_2CO_3, DMF, MW, 80 °C, 30 min, 50-60%; (c) 3 M aq. HCl, THF, rt, 1 h, 99%; (d) R^3-I or R^3-Br, K_2CO_3, DMF, MW, 130 °C, 14 min, 84-87%; (e) DMADMA, toluene, 90 °C, 6-16 h; (f) $N_2H_4 \cdot H_2O$, ethanol, reflux, 30 min, 20-31%.

Pyrazole **93**, bearing a hydroxy group, was prepared from intermediate **97** (Scheme 7), which was transformed into enaminone **105** followed by cyclization with hydrazine to generate the pyrazole ring. Acidic hydrolysis of the THP group yielded final compound **93**.

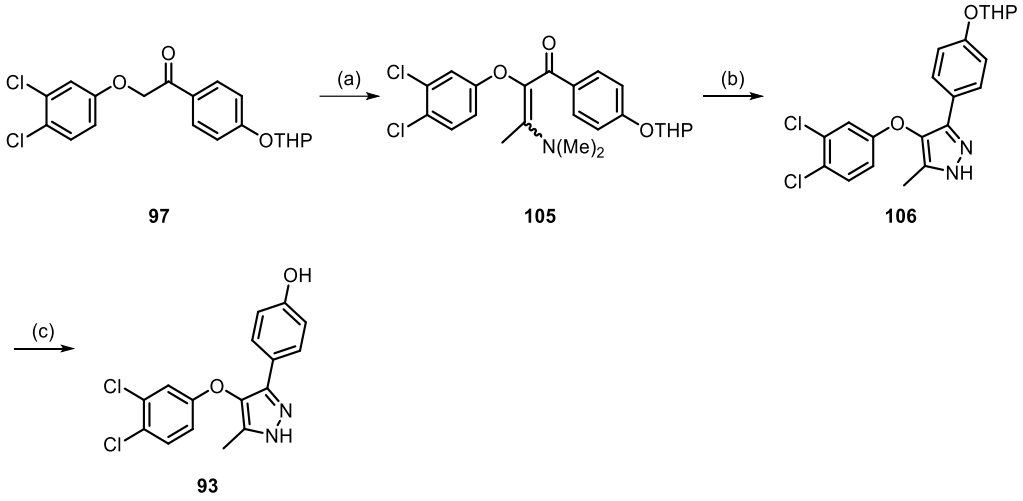

97 105 106 93

Scheme 7. Reagents and conditions: (a) DMADMA, toluene, 90 °C, 2 h; (b) $N_2H_4 \cdot H_2O$, ethanol, reflux, 30 min, 17%; (c) 3 M aq. HCl, THF, rt, 1 h, 60%.

For the synthesis of the trifluoromethyl-containing derivative **94**, we planned a route analogous to the one used for the previous pyrazoles, starting with a Williamson reaction between 3,4-dichlorophenol and 2-bromo-4-(trifluoromethyl)acetophenone (Scheme 8). In this case, the corresponding intermediate ketone **107** was formed almost immediately at rt due to the strong electron withdrawing effect of the CF_3 group. Next, reaction of **107** with DMADMA at lower temperature than usual to avoid decomposition (60 °C instead of 90 °C), and subsequent cyclocondensation with hydrazine yielded pyrazole **94**.

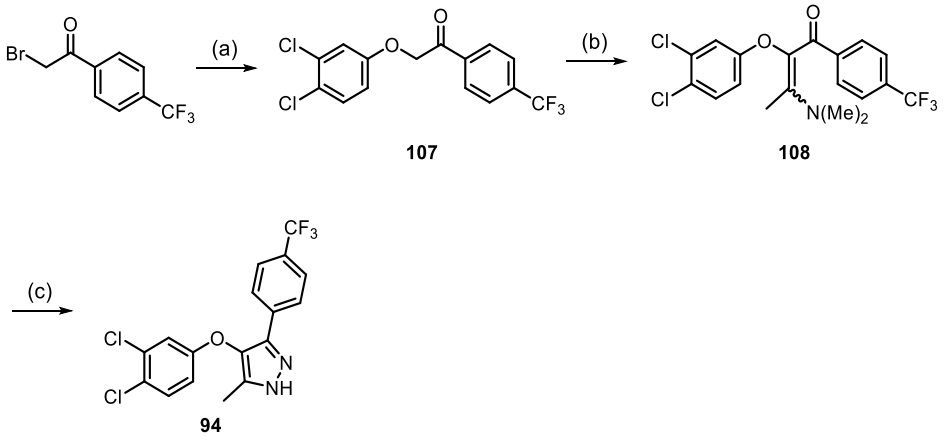

107 108 94

Scheme 8. Reagents and conditions: (a) 3,4-dichlorophenol, DBU, DMF, rt, 1 min, 58%; (b) DMADMA, toluene, 60 °C, 16 h; (c) $N_2H_4 \cdot H_2O$, ethanol, reflux, 30 min, 17%.

Finally, compound **95** was prepared from pyrazole **111**, which was synthesized using 2-bromo-4-nitroacetophenone as starting material (Scheme 9), according to the three-

step route described for previous pyrazoles. In this case, due to the high reactivity of the nitro intermediate, the Williamson reaction with 3,4-dichlorophenol was carried out at rt using potassium carbonate as base and the cyclization with hydrazine was also conducted at rt. Then, reduction of the nitro group of **111** by Pd-catalyzed hydrogenation afforded amino pyrazole **112**, which was acetylated under standard conditions. In this reaction, acetylation of the nitrogen of the pyrazole also occurred and a final hydrolysis step in basic media was necessary to obtain mono acetyl derivative **95**.

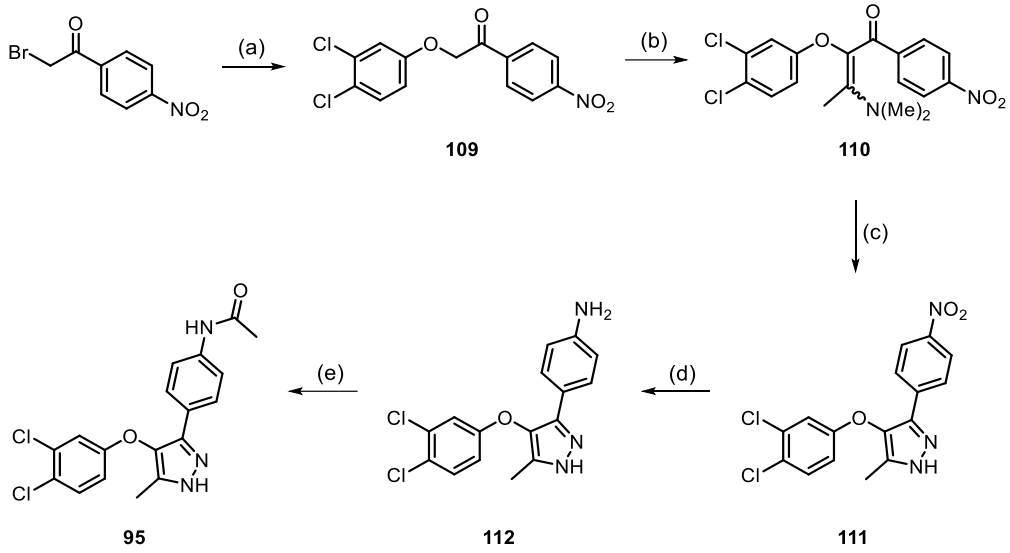

Scheme 9. Reagents and conditions: (a) 3,4-dichlorophenol, K_2CO_3, DMF, rt, 16 h, 49%; (b) DMADMA, toluene, 50 °C, 16 h; (c) $N_2H_4 \cdot H_2O$, ethanol, rt, 1 h, 33%; (d) 10% Pd/C, H_2, DCM, rt, 93%; (e) i. Ac_2O, DCM/pyridine, rt, 4 h; ii. 10% aq. NaOH, THF/MeOH 3:2, rt, 1 h, 23%.

Biological evaluation of compounds **90**-**95** at LPA_2 receptor revealed that none of them exhibited better activity than compound **65** (Table 7), showing similar values of antagonist activity, with E_{max} between 52% and 74% and different degrees of selectivity *vs* LPA_1 and LPA_3 receptors.

Table 7. Antagonist activity of compounds **65** and **90**-**95** at LPA_{1-3} receptors.

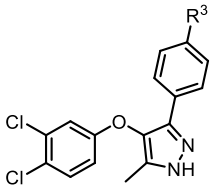

Compound	R^3	E_{max} (%)[a] [IC_{50} (μM)][b]		
		LPA_1R	**LPA_2R**	**LPA_3R**
90	OEt	Inact.[c]	72±9	85±4
91	O^{i}Pr	Inact.	64±8	61±5
92	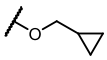	61±5	74±5	64±3
93	OH	Inact.	71±7	Inact.
94	CF_3	84±1	52±6	54±13
95	$NHCOCH_3$	Inact.	69±4	67±4
65	OMe	Inact.	92.0±0.2 [0.2±0.1]	Inact.

[a] E_{max}=maximum blockade effect of the activation induced by 10 μM of LPA (18:1, 1-oleoyl-*sn*-glycerol-3-phosphate) at a concentration of the compound under study of 10 μM. Values shown are the mean±s.e.m. of 2-4 independent experiments performed in triplicate. [b] For E_{max} > 85%, IC_{50} values are expressed as mean±s.e.m, from a minimum of two independent experiments, performed in triplicate. [c] Inact., compounds that show an E_{max} < 50% at the highest concentration tested (10 μM) are considered inactive (IC_{50} > 5 μM).

2.1.3. Structural exploration around central core

The results obtained in the structural exploration carried out so far, have allowed us to select 3,4-dichlorophenoxy and 4-methoxyphenyl moieties as the most favorable substituents of the central pyrazole for antagonism at LPA_2 receptor.

Hence, we next addressed the modification of the central heterocycle (Figure 23). Specifically, we studied the effect of the *N*-methylation of the pyrazole (compounds **113** and **114**), the removal of the methyl group at *C*-5 (compound **115**) and the replacement of the pyrazole by isoxazole and benzene (compounds **116** and **117**, respectively).

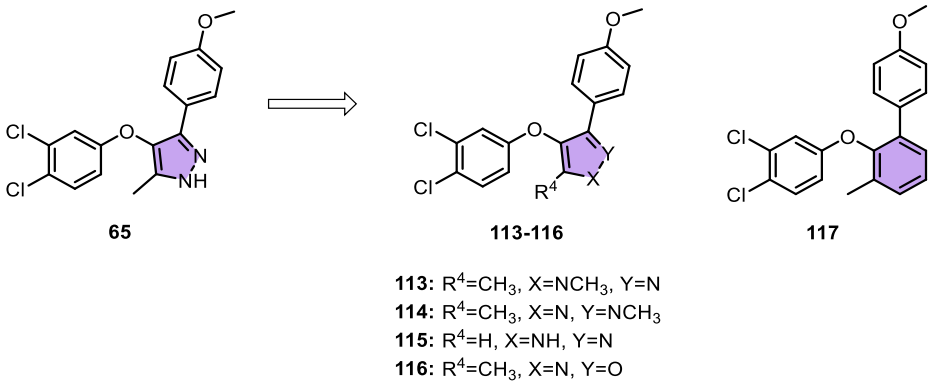

Figure 23. Study of the effect of changes in the pyrazole ring.

N-methyl pyrazoles **113** and **114** were obtained by direct methylation of compound **65**. Thus, reaction with methyl iodide at rt afforded a 2:1 mixture of **113** (1,5-dimethyl) and **114** (1,3-dimethyl) regioisomers (Scheme 10), which were separated by column chromatography. Structural characterization and unequivocal assignment were achieved through heteronuclear multiple bond correlation (HMBC) NMR experiments. In this way, we could detect correlation between the protons of the methyl group attached to the nitrogen and the corresponding carbon at 5 position: C_5-methyl for compound **113** (Figure 24), and C_5-aryl for compound **114** (Figure 25).

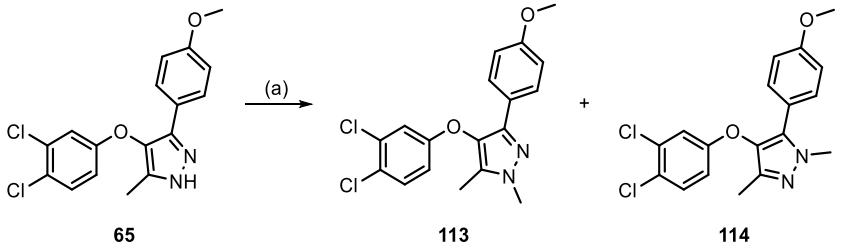

Scheme 10. Reagents and conditions: (a) MeI, NaH, DMF, rt, 16 h, 28% for compound **113** and 13% for compound **114**.

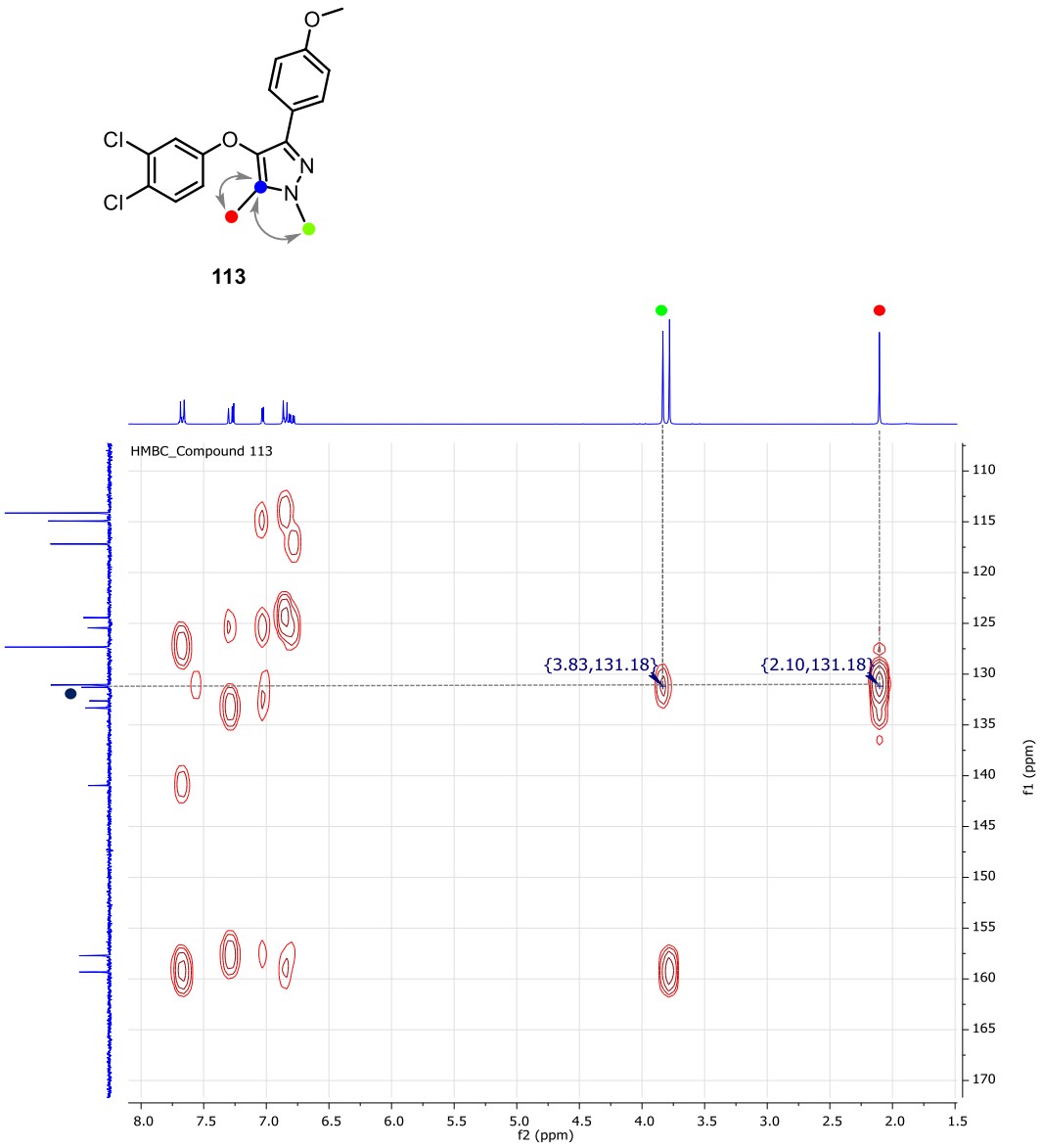

Figure 24. HMBC spectrum of compound **113** in $CDCl_3$ shows the three bonds correlation between the protons of the methyl group attached to the nitrogen (green) and *C*-5 (blue), as shown by the cross peak at 3.83 and 131.18 ppm. *C*-5 (blue) also correlates with the protons of its *C*-methyl group (red) as indicated by the cross peak at 2.10 and 131.18 ppm.

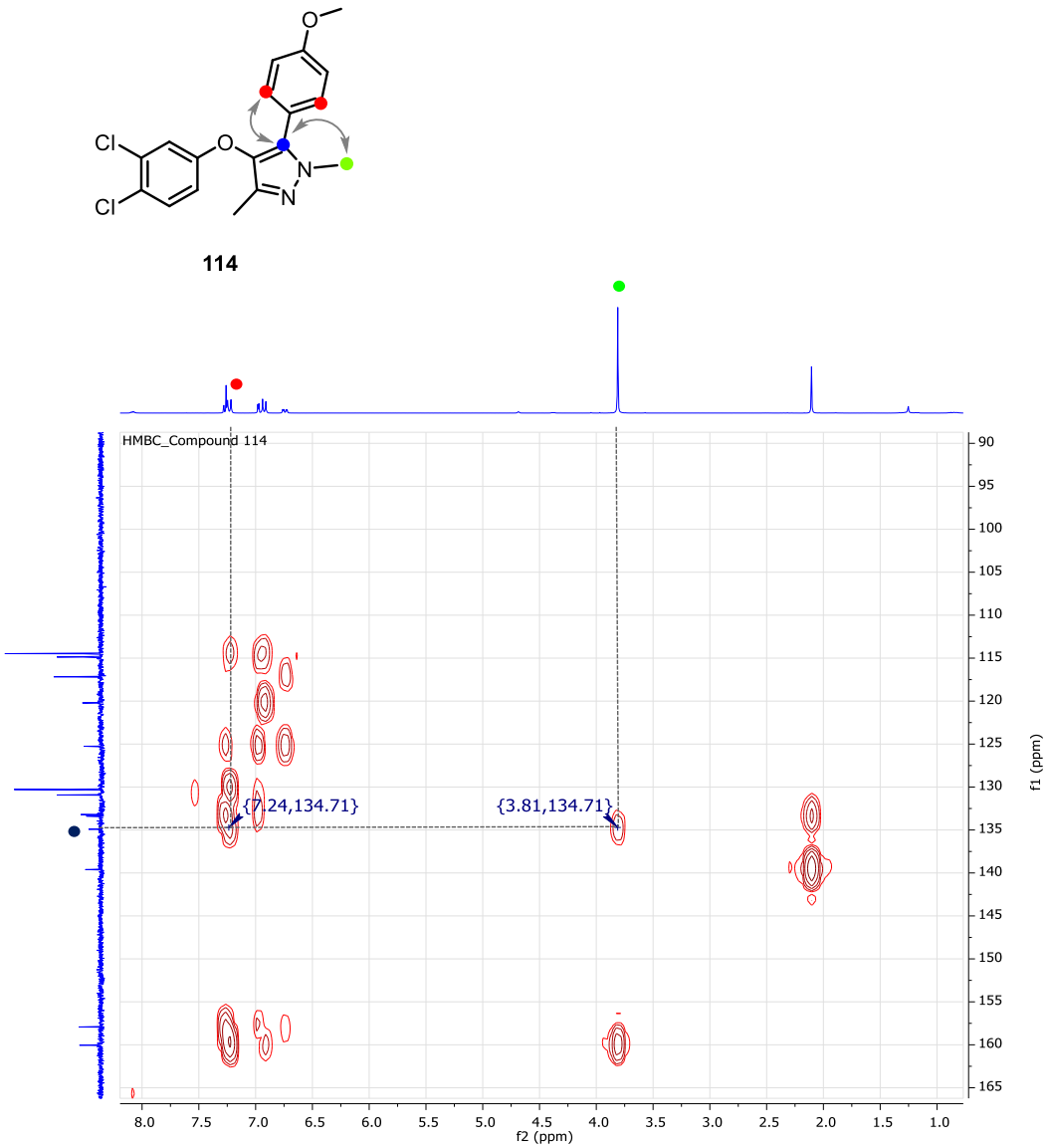

Figure 25. HMBC spectrum of compound **114** in $CDCl_3$ shows the three bonds correlation between the protons of the methyl group attached to the nitrogen (green) and *C*-5 (blue), as shown by the cross peak at 3.81 and 134.71 ppm. *C*-5 (blue) also correlates with two aromatic protons from the *p*-methoxyphenyl moiety (red), as indicated by the cross peak at 7.24 and 134.71 ppm.

The synthesis of pyrazole **115**, lacking the 5-methyl substituent, was addressed starting from intermediate ketone **71** (Scheme 11), which was treated with *N*,*N*-dimethylformamide dimethyl acetal (DMFDMA) under MW irradiation to afford enaminone **118**. Next, the cyclocondesation reaction with hydrazine under acidic conditions allowed us to obtain the desired 3,4-disubstituted pyrazole **115**.

Isoxazole derivative **116** was also synthesized from ketone **71** by reaction of DMADMA to obtain enaminone **77** and subsequent condensation with hydroxylamine to form target isoxazole **116** (Scheme 11).

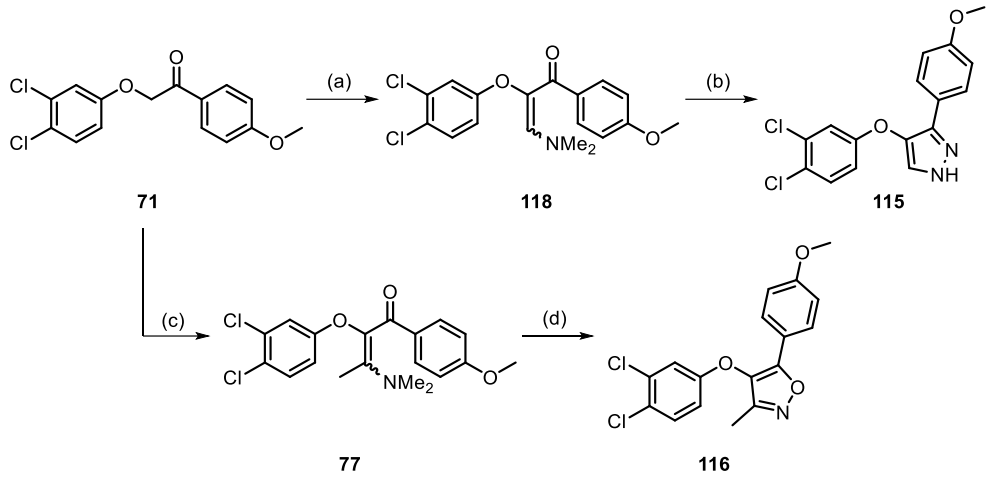

Scheme 11. Reagents and conditions: (a) DMFDMA, DMF, MW, 80 °C, 1 h, 94%; (b) $N_2H_4 \cdot H_2O$, 4 M aq. HCl, ethanol, 65°C, 1 h, 64%; (c) DMADMA, toluene, 90 °C, 16 h; (d) $NH_2OH \cdot HCl$, DME/H_2O, 60 °C, 24 h, 23%.

Finally, for the synthesis of biphenyl derivative **117** (Scheme 12) we proposed a Suzuki coupling reaction between 2-bromo-6-methylphenol and 4-methoxyphenylboronic acid to obtain intermediate **119**, followed by Chan-Lam reaction with 3,4-dichlorophenylboronic acid. Initially, Suzuki coupling was performed using standard MW conditions previously applied in our laboratory, obtaining biphenyl intermediate **119** in low yield (entry 1, Table 8). Thus, we decided to optimize the reaction by changing the catalyst to $Pd(PPh_3)_4$, due to its widespread use,[142] and testing different solvent, base, temperature and time conditions. The use of potassium phosphate in a two-phase system at 160 °C gave the best results, providing target compound in 52% yield (entry 5, Table 8). Finally, Chan-Lam reaction of **119** with 3,4-dichlorophenylboronic acid afforded compound **117**. The low yield of the reaction could be explained by the presence of the two substituents in the *ortho* position with respect to the OH group of derivative **119**, as this reaction is known to be very sensitive to steric effects.[143] However, we did not optimized the Chan-Lam coupling reaction as the amount of the desired compound was enough to carry out the structural characterization and the biological experiments.

Table 8. Experimental conditions to obtain biphenyl intermediate **119.**

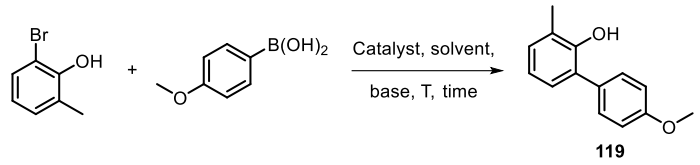

119

Entry	Catalyst	Solvent	Base	T (°C)	Time (min)	Yield (%)
1	$PdCl_2(dppf)\cdot DCM$	DME	Na_2CO_3	140	30	39
2	$Pd(PPh_3)_4$	THF/H_2O	Na_2CO_3	120	70	N.D.[a]
3	$Pd(PPh_3)_4$	THF/H_2O	Na_2CO_3	130	35	26
4	$Pd(PPh_3)_4$	$Toluene/EtOH/H_2O$	K_2CO_3	160	40	44
5	$Pd(PPh_3)_4$	$Toluene/EtOH/H_2O$	K_3PO_4	160	40	52

All the reactions were done under MW irradiation. [a]N.D., not detected.

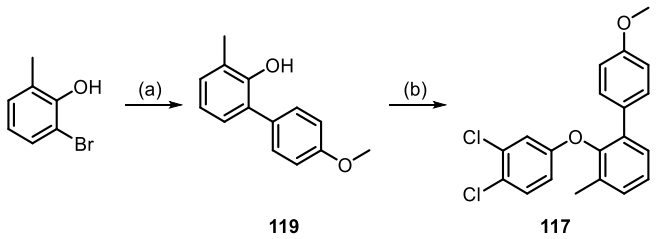

119 117

Scheme 12. Reagents and conditions: (a) 4-Methoxyphenylboronic acid, 5 % mol $Pd(PPh_3)_4$, K_3PO_4, $toluene/EtOH/H_2O$, MW, 160 °C, 40 min, 52%; (b) 3,4-Dichlorophenylboronic acid, $Cu(OAc)_2$, pyridine, DCM, 40 °C, 24 h, 16%.

After biological evaluation of compounds **113**-**117** at the LPA_{1-3} receptors (Table 9), the results showed that none of the modifications made in the pyrazole ring improved the activity of compound **65**. Both *N*-methylation of the pyrazole ring (compounds **113** and **114**) and removal of the methyl group at the *C*-5 (compound **115**) led to a reduction in the antagonist activity at the LPA_2 receptor. A similar effect was observed for the replacement of pyrazole by isoxazole or benzene (derivatives **116** and **117**, respectively), changes that decreased the antagonist activity significantly. Overall, we can conclude that the presence of an NH-pyrazole central core is key for the LPA_2 antagonist activity of compound **65**.

In addition, these modifications conducted to a loss of selectivity, and compounds **113**-**117** showed different degrees of activity at LPA_1 and LPA_3 receptors, with E_{max} values ranging from 56% to 71%.

Table 9. Antagonist activity of compounds **65** and **113**-**117** at LPA_{1-3} receptors.

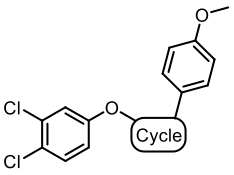

Compound	Cycle	E_{max} (%)[a] [IC_{50} (μM)][b]		
		LPA_1R	**LPA_2R**	**LPA_3R**
113	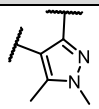	58±6	70±4	56±6
114	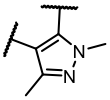	62±9	48±7	56±9
115	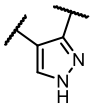	Inact.[c]	75±4	65±3
116	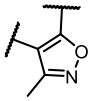	70±5	56±5	Inact.
117		71±3	64±7	Inact.
65	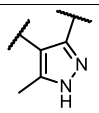	Inact.	92.0±0.2 [0.2±0.1]	Inact.

[a] E_{max}=maximum blockade effect of the activation induced by 10 μM of LPA (18:1, 1-oleoyl-*sn*-glycerol-3-phosphate) at a concentration of the compound under study of 10 μM. Values shown are the mean±s.e.m. of 2-4 independent experiments performed in triplicate. [b] For E_{max} > 85%, IC_{50} values are expressed as mean±s.e.m, from a minimum of two independent experiments, performed in triplicate. [c] Inact., compounds that show an E_{max} < 50% at the highest concentration tested (10 μM) are considered inactive (IC_{50} > 5 μM).

Overall, the results obtained up to this moment indicated that compound **65** was the most potent LPA_2 antagonist identified so far with improved IC_{50} value compared to previously described **UCM-14216**[138] (230 nM *vs* 1.9 μM, respectively) and selectivity against LPA_1 and LPA_3 receptors. Hence, it was an excellent candidate to assess its *in vivo* efficacy in an inflammatory pain model. Before proceeding to study the *in vivo* efficacy, we performed an in-depth pharmacological characterization of this compound.

2.2. Pharmacological characterization of compound 65

In order to complete the pharmacological characterization of compound **65**, we determined its binding affinity to LPA_2 receptor and *in vitro* ADME (absorption, distribution, metabolism and excretion) properties such as cell permeability, stability in human and mouse serum and microsomes, binding to human serum albumin (HSA), and cell toxicity. In addition, to confirm whether it was able to reach the CNS, *in vivo* PK assays were performed.

2.2.1. Binding affinity of compound 65 for LPA_2 receptor

The biological response produced by a drug is related to both the activity and the affinity for its molecular target. Therefore, in collaboration with Prof. Jerold Chun from Sanford Burnham Prebys Institute (La Jolla, California, USA), we determined the binding affinity of compound **65** for the LPA_2 receptor using the recently reported free solution assay-compensated interferometric reader (FSA-CIR) technique (Figure 26).[144,145]

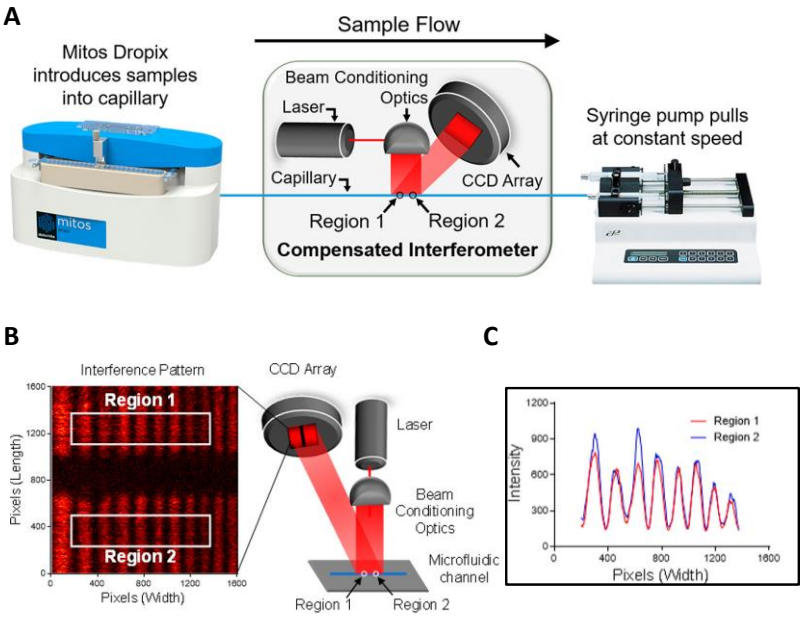

Figure 26. (A) Reader consists of a droplet generator for sample introduction (Mitos Dropix), a compensated interferometer (diode laser, capillary cell, and CCD camera) and a syringe pump. The Mitos Dropix introduces sample droplet trains into the capillary while the syringe pump maintains a constant sample flow through the capillary. Sample and reference pairs flow through regions 1 and 2 where they are simultaneously interrogated by the diode laser. Resultant images of the fringe patterns and their phase shifts under binding/non-binding conditions (B) are converted to a line profile (C) where selected fringes are fast Fourier transformed for analyses (Adapted from reference[144]).

The advantages of FSA-CIR to measure binding interactions between receptor and ligand over backscattering interferometry (BSI), which can be considered its precursor, include the simultaneous measurement of the test and reference samples, increased throughput, and significant decrease of temperature sensitivity.[145] The FSA-CIR technique monitors changes in refractive index (RI) to detect molecular interactions in a free-solution manner. This shift in RI is a result of changes in molecular structure, dipole moment, polarizability, conformation, and solvation that occur during the interaction of the proteins with their ligands.[146] Thus, FSA-CIR can be used to quantify binding affinities by detecting changes in the RI of mixtures of free nanovesicles and ligand that have been incubated to achieve equilibrium. In this case, ligand binding to nanovesicles containing LPA_2 receptor was accomplished by incubating a solution of a fixed nanovesicle concentration with varying concentrations of compound **65** (Figure 27).

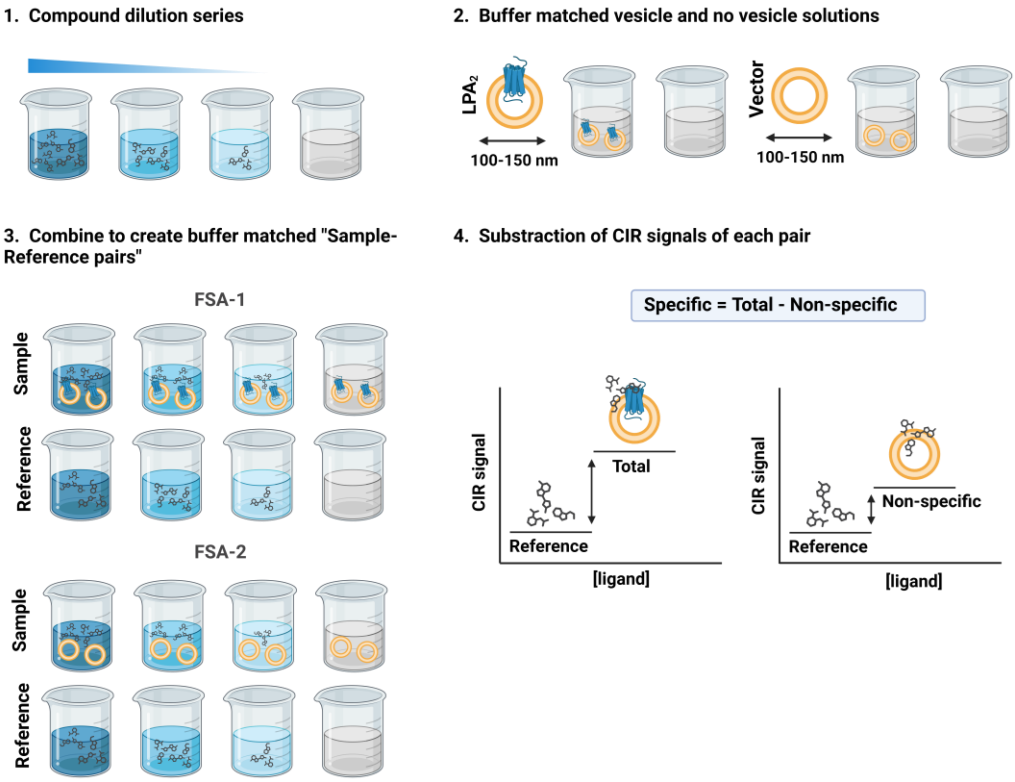

Figure 27. Schematic representation of the free-solution assay (FSA) workflow (Adapted from reference[145]).

The difference between the signals of nanovesicle-ligand complex and free nanovesicle solutions was plotted versus ligand concentration to obtain a saturation binding isotherm (Figure 28), which was fitted to a square hyperbolic function using GraphPad Prism software to determine the dissociation constant (K_d) value (Table 10).

Binding affinity of LPA to nanovesicles containing LPA_2 receptor was measured as positive control, whereas the nanovesicle without any receptor was used to determine the non-specific binding. The obtained K_d value indicated a high binding affinity of compound **65** for LPA_2 receptor (K_d=0.96 nM), higher to that obtained for the endogenous ligand LPA (K_d=6.7 nM) and **UCM-14216** (K_d=1.3 nM) (Table 10).

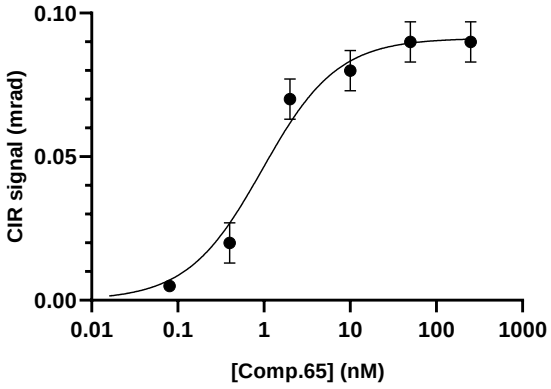

Figure 28. Specific binding signal for compound **65**. CIR signal refers to changes in refractive index (ΔRI in radians) from LPA_2-containing vesicles (total) to which only vector-containing vesicles (non-specific) values have been subtracted after compound binding**.**

Table 10. Binding affinity of compounds **65**, **UCM-14216** and LPA (18:1) for LPA_2 receptor determined by FSA-CIR.

Compound	K_d (nM)[a]	R^2 (%)[b]
65	0.96	99
UCM-14216	1.3[c]	95[c]
LPA (18:1)	6.7[c]	96[c]

[a]K_d values are the means from two or three independent experiments performed in triplicate. The s.e.m. is within a 10% of the mean value. [b]A goodness of fit (R^2) greater than 90% is considered adequate. [c]Value from reference.[138]

2.2.2. *In vitro* ADME properties of compound 65

Assessment of cell permeability was done using the parallel artificial membrane permeability assay (PAMPA), an *in vitro* model of passive transcellular permeation which determines the capacity of compounds to cross through a lipid-infused artificial membrane. In this assay (Figure 29), a solution of the compound is added to a 96-well donor plate and passive diffusion through the membrane can be calculated by measuring the amount of the compound that reaches the acceptor plate, using high pressure liquid chromatography coupled to mass spectrometry (HPLC-MS). Evaluation of the

permeability of compound **65** in the PAMPA assay showed an acceptable permeability value (P) of $7.0 \cdot 10^{-6}$ cm/s (Table 11), considering as reference values $P \leq 10^{-7}$cm/s for low permeable compounds and $P \geq 10^{-5}$ cm/s for highly permeable molecules.

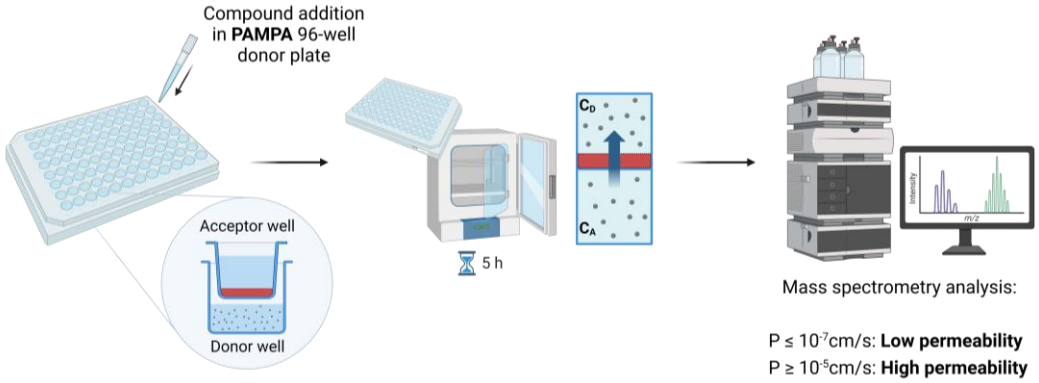

Figure 29. Schematic representation of PAMPA assay.

Metabolic stability in liver microsomes is another important aspect for drug development that was determined as an *in vitro* estimation of first-pass metabolism. It was measured by incubation of compound **65** with human and mouse liver microsomes (HLM and MLM, respectively) and the degradation of the compound over the time was quantified by HPLC-MS (Figure 30). Resulting half-life times ($t_{1/2}$) are shown in Table 11, with values of 2.8±0.2 h for HLM and 1.4±0.1 h for MLM, indicating a good metabolic stability.

Stability of compound **65** in human and mouse serum was also determined by incubating the compound in the corresponding biological media and extracting aliquots at different times (Figure 30). The amount of remaining compound was quantified by HPLC-MS, and $t_{1/2}$ higher than 24 h were obtained for both human and mouse serum (Table 11), which indicates an excellent stability of compound **65** in both biological media.

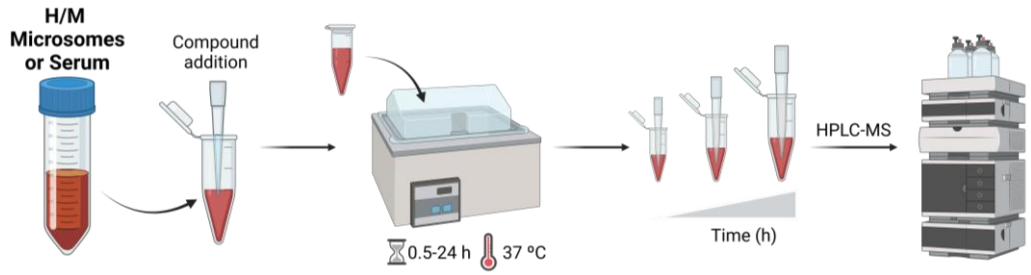

Figure 30. Schematic representation of the stability assays in human (H) and mouse (M) serum and liver microsomes.

HSA is the most abundant plasma protein in blood, whose main function is the transport of hormones, fatty acids, and exogenous substances such as pharmacological drugs through the blood stream. To estimate the ability of compound **65** to be distributed from plasma to the cells, we measured its binding to HSA. For this purpose, we incubated the compound in the presence of increasing concentrations of HSA, extracted samples and quantified the unbound fraction by HPLC-MS (Figure 31). The obtained results (Table 11) suggest higher affinity for HSA than **UCM-14216** (bound fractions of 97.0% and 84.9% and K_d values of 18 and 100 µM, respectively). These parameters could be related with the increase in microsomal stability observed for compound **65** compared to **UCM-14216**, since binding to proteins could shield the compound from the action of microsomal hydrolases.

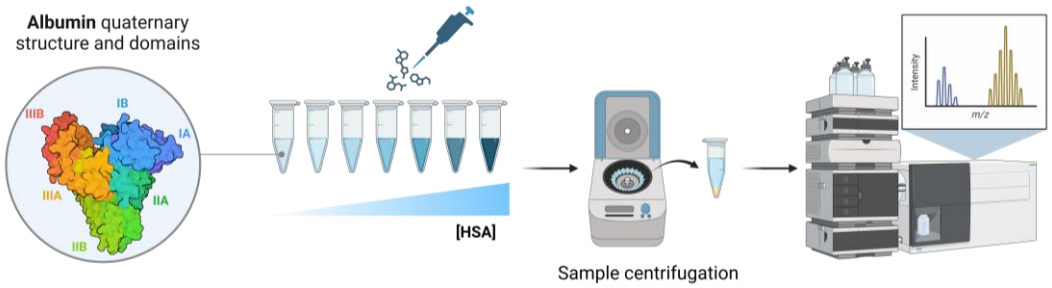

Figure 31. Schematic representation of the human serum albumin (HAS) binding assay.

Table 11. *In vitro* ADME properties of compound **65** and the LPA_2 receptor antagonist **UCM-14216**.

Compound	P (cm/s)[a]	Microsomal stability[b] ($t_{1/2}$, h)		Serum stability[b] ($t_{1/2}$, h)		HSA binding F_b (%), K_d (M)[c]
		HLM	MLM	Human serum	Mouse serum	
65	$7.0 \cdot 10^{-6}$	2.8±0.2	1.4±0.1	>24	>24	97.0±0.1 $1.8 \cdot 10^{-5}$
UCM-14216	$6.0 \cdot 10^{-6}$ [d]	1.6±0.3 [d]	0.8±0.1 [d]	>24	>24	84.9±0.1 $1.1 \cdot 10^{-4}$

[a]Permeability value, considering as reference values P≤10^{-7} cm/s for low permeable compounds and P≥10^{-5} cm/s for highly permeable molecules. [b]Data for stability in mouse and human liver microsomes (MLMs and HLMs, respectively) and serum are expressed as the mean±s.e.m. of at least two experiments performed in duplicate [c]Binding to human serum albumin (HAS) is expressed as the bound fraction (F_b) and the dissociation constant (K_d). [d]Value from reference.[138]

2.2.3. Cellular toxicity of compound 65

To assess cytotoxicity of compound **65** we employed a colorimetric assay in AF3 mouse fibroblasts and in IMR-90 human lung fibroblasts. This assay is based on the metabolic reduction of yellow 3-(4,5-dimethyl-2-thiazolyl)-2,5-diphenyl-2*H*-tetrazolium

bromide (MTT) by viable cells to purple formazan crystals, which are quantified by measuring their absorbance at 570 nm (Figure 32). Cytotoxicity is indicated as the percentage of viability determined in compound-treated cells relative to that in vehicle-treated cells. We consider a compound to be non-cytotoxic if cell viability exceeds 80% after incubation during a certain period of time at a specific concentration. Thus, cells were incubated in the presence of compound **65**, as well as hit **UCM-14250** and the previous characterized LPA_2 receptor antagonist **UCM-14216** for comparative purposes, for 24 h and 48 h at concentrations between 1-25 µM. Obtained results (Figure 33) showed a cell viability of both AF3 and IMR-90 cells treated with each compound around 90%, indicating that neither of the compounds are cytotoxic well above their IC_{50} values (230 nM, 10 µM and 1.9 µM, respectively). This represents a therapeutic window (dosage range between the minimum effective therapeutic concentration and the minimum toxic concentration) for compound **65** of at least 100-fold.

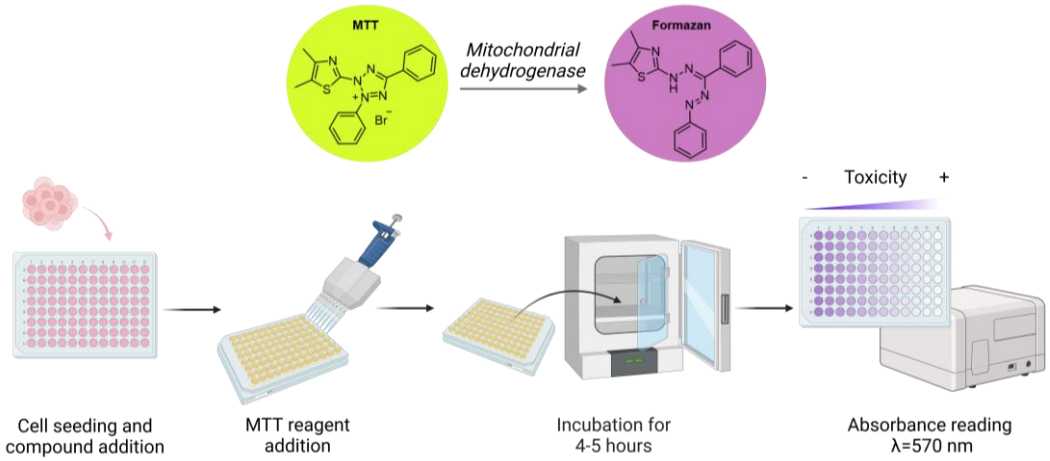

Figure 32. Schematic representation of colorimetric MMT assay used to evaluate the cytotoxicity of tested compounds.

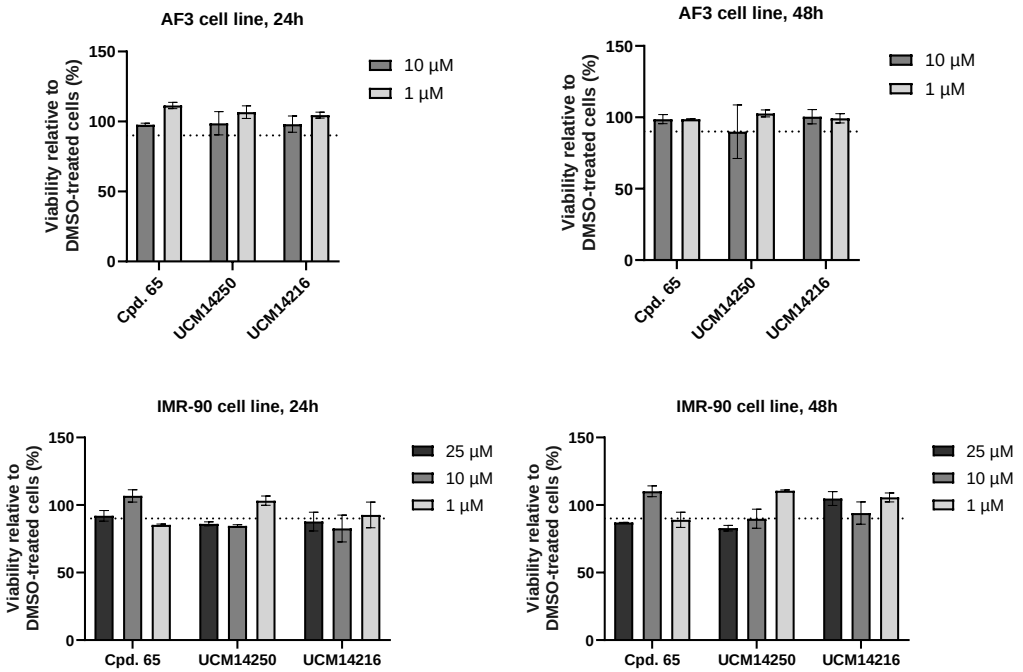

Figure 33. Cell viability of AF3 and IMR-90 cells treated with compounds **65**, **UCM-14250** and **UCM-14216** for 24 and 48 h. Viability is expressed as the percentage relative to cells treated with vehicle (0.1% DMSO) which are considered 100% viable. Error bars represent the means±s.e.m for two independent experiments carried out in triplicate.

2.2.4. *In vivo* pharmacokinetic profile of compound 65

Overall, compound **65** is the most potent and selective LPA_2 receptor antagonist described so far (E_{max}=92%; IC_{50} LPA_2=230 nM; K_d LPA_2=0.96 nM; inactive at LPA_1 and LPA_3 receptors), with good *in vitro* ADME properties. In view of the good results for compound **65** and before carrying out efficacy studies in an *in vivo* model of inflammation, we move on to assess its *in vivo* ability to pass through the BBB and reach the CNS, where the compound is expected to carry out its therapeutic action. For that, healthy mice received a single intraperitoneal (i.p.) injection of compound **65** (25 mg/kg). Samples of plasma, spinal cord and brain were taken at different post-injection times from 30 minutes to 6 hours, and the levels of the compound were quantified by HPLC-MS.

The data obtained (Table 12) indicate that the compound is able to cross the BBB and reach the CNS after 30 minutes of its administration, reaching maximum levels of 2.1 µM in spinal cord and 3.1 µM in brain during the first two hours. Moreover, compound **65** remains in the CNS even 6 hours after its administration, with levels in spinal cord and brain of 0.3 µM and 0.5 µM, respectively, highlighting the good *in vivo* PK profile of compound **65**.

Table 12. *In vivo* levels of compound **65** at different post-injection times.

Time (h)	[65] (μM) after the indicated post-injection times (h)		
	Plasma	Spinal cord	Brain
0.5	0.2	0.3	0.8
1	0.9	1.2	3.1
2	N.D.[b]	2.1	2.4
4	N.D.	0.2	1.9
6	N.D.	0.3	0.5

[a]Mice received a single injection of compound **65** (25 mg/kg, i.p.) and samples were taken at different times, frozen, and the levels of compound quantified by HPLC-MS. Data are the means±s.e.m. from, at least, two independent samples. [b]ND, not detected.

2.2.5. *In vivo* efficacy of compound 65 in a pain mouse model

Since LPA_2 activation plays harmful actions in the beginning and progression of neuroinflammatory processes, we finally assessed whether compound **65** reduces the inflammatory pain response in a peripheral inflammation mouse model, in collaboration with Professor Rubèn López Vales from Universidad Autónoma de Barcelona. For this purpose, complete Freund's adjuvant was administered to the paw of the mice, causing severe paw inflammation, and mechanical and thermal hypersensitivity. Then, mice were treated daily with compound **65** (25 mg/kg, i.p.) starting at 1 h following lesion and for 14 consecutive days, and inflammation was assessed. As shown in Figure 34, mice treated with compound **65** displayed a significant improvement as evidenced by a significant decrease in paw inflammation after treatment for 7 days and sustained in time during the whole duration of the experiment.

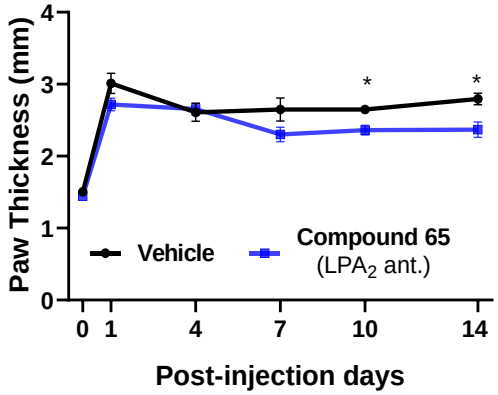

Figure 34. Effect of compound **65** (25 mg/kg daily, i.p.) or vehicle on paw thickness in the complete Freund's adjuvant induced pain model. Data are expressed as mean±s.e.m. and correspond to 7 animals per group. *p < 0.05 compared with vehicle-treated group (two-way repeated measures ANOVA with post hoc test for multiple comparisons).

As a summary, obtained results indicate that compound **65** (UCM-22018) is the most potent and selective LPA_2 receptor antagonist described so far with an optimum PK profile, being able to reach the CNS and reduce the inflammatory response in the complete Freund's adjuvant mouse model. Further *in vivo* efficacy experiments are ongoing in our group with this compound in order to fully validate the LPA_2 receptor therapeutic potential in (neuro)inflammation.

3. CONCLUSIONS

3. CONCLUSIONS

In the present work, we have carried out a medicinal chemistry program where we have performed a series of structural modifications in the initial compound **UCM-14250**, and we have studied their antagonist effect at the LPA_2 receptor and its selectivity *vs* $LPA_{1,3}$ receptors. Thus, we have developed a new series of LPA_2 receptor antagonists, in which compound **65** (UCM-22018) stands out as the most potent and selective compound with good *in vitro* ADME properties and an optimum *in vivo* PK profile. Compound **65** blocks almost fully the signaling through LPA_2, with E_{max} and IC_{50} values of 92% and 230 nM, respectively. In addition, the in-depth pharmacological study of the *in vitro* ADME properties of compound **65** revealed a cell permeability of $7.0 \cdot 10^{-6}$, a human and mouse serum stability > 24 h, a stability in human and mouse microsomes of 2.8 h and 1.4 h, respectively, and a 97% of binding to human serum albumin (K_d=$1.8 \cdot 10^{-5}$). Cell toxicity of compound **65** was also evaluated in human (IMR-90) and non-human (AF3) cells, indicating that this compound is non-cytotoxic well above its IC_{50} value. Furthermore, the assessment of the *in vivo* PK profile of compound **65** showed that it reaches the CNS during the first 2 h after its administration and remains for up to 6 h. Finally, efficacy of compound **65** was demonstrated in a pain mouse model of peripheral inflammation, in which the administration of the compound significantly improved the inflammatory response to pain.

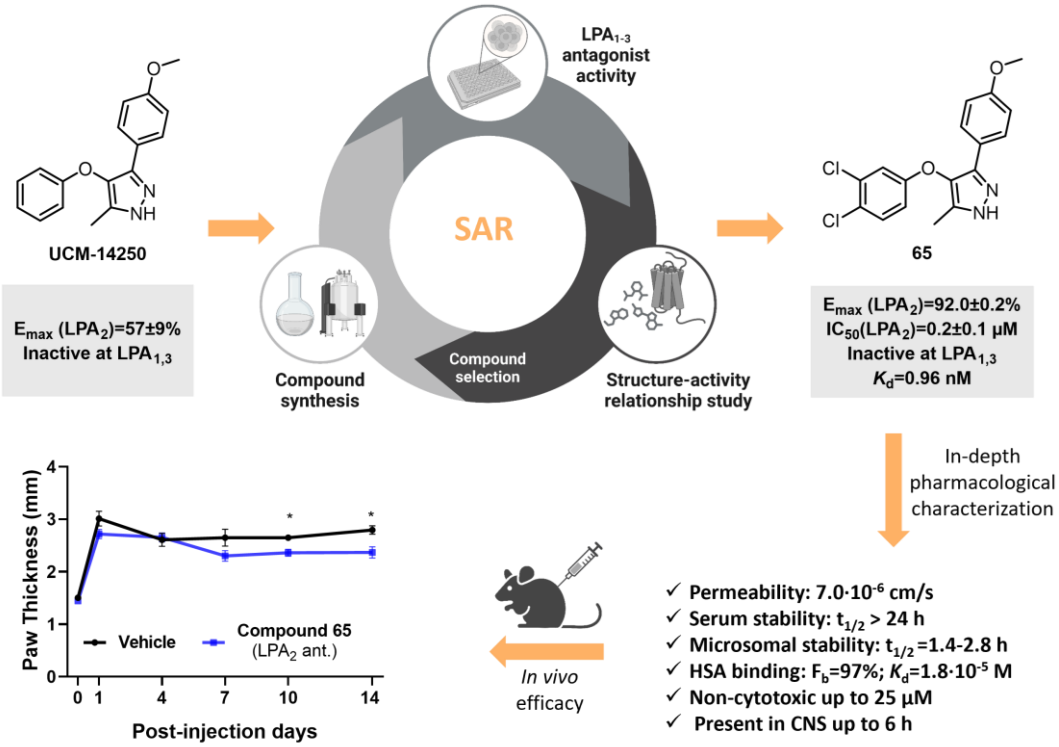
UCM-14250
E_{max} (LPA_2)=57±9%
Inactive at $LPA_{1,3}$
LPA_{1-3} antagonist activity
SAR
Compound synthesis
Compound selection
Structure-activity relationship study
65
E_{max} (LPA_2)=92.0±0.2%
IC_{50}(LPA_2)=0.2±0.1 μM
Inactive at $LPA_{1,3}$
K_d=0.96 nM
In-depth pharmacological characterization
Paw Thickness (mm)
Vehicle
Compound 65 (LPA_2 ant.)
Post-injection days
In vivo efficacy
✓ Permeability: 7.0·10⁻⁶ cm/s
✓ Serum stability: $t_{1/2}$ > 24 h
✓ Microsomal stability: $t_{1/2}$=1.4-2.8 h
✓ HSA binding: F_b=97%; K_d=1.8·10⁻⁵ M
✓ Non-cytotoxic up to 25 μM
✓ Present in CNS up to 6 h

4. EXPERIMENTAL SECTION

4. EXPERIMENTAL SECTION

4.1. Synthetic procedures and compound characterization

The starting materials, reagents, and solvents were purchased as high-grade commercial products from Sigma-Aldrich (Merck), Acros, ABCR, Fluorochem, Scharlab, or Panreac. Dichloromethane (DCM), tetrahydrofuran (THF) and diethyl ether were dried using a Pure Solv^{TM} Micro 100 Liter solvent purification system. Reactions were performed under an argon atmosphere in oven-dried glassware unless otherwise stated. MW irradiation reactions were carried out on a Biotage Initiator 2.5 reactor, using Biotage vials sealed with aluminium caps with septum. Hydrogenation reactions were performed in a Thales Nano H-Cube flow reactor using CatCarts® catalyst cartridges.

Analytical thin-layer chromatography (TLC) was run on Merck silica gel plates (Kieselgel 60 F254), with detection by UV light (λ=254 nm), 5% ninhydrin solution in EtOH, or 10% vanillin solution in EtOH. Unless otherwise stated, products were purified by flash chromatography using a Biotage Selekt system with silica gel cartridges (Biotage Sfär, size particle 60 μM).

Melting points (mp) were determined on a Stuart Scientific electrothermal apparatus. Infrared (IR) spectra were measured on a Bruker Tensor 27 instrument equipped with a Specac ATR accessory of 4000-600 cm^{-1} transmission range; frequencies (ν) are expressed in cm^{-1}.

^{1}H- and ^{13}C-NMR spectra were recorded on a Bruker Avance III 700 MHz (^{1}H, 700 MHz; ^{13}C, 175 MHz), Bruker NEO 500 MHz (^{1}H, 500 MHz; ^{13}C, 125 MHz) or Bruker DPX 300 MHz (^{1}H, 300 MHz; ^{13}C, 75 MHz) instrument at rt at the Universidad Complutense de Madrid (UCM) NMR core facility. Chemical shifts (δ) are expressed in parts per million (ppm), relative to the residual solvent peak for ^{1}H and ^{13}C nuclei ($CDCl_3$: δ_H=7.26, δ_C=77.16; acetone-d_6: δ_H=2.05, δ_C=29.84, 206.26; methanol-d_4: δ_H=3.31, δ_C=49.00; DMSO-d_6: δ_H=2.50, δ_C=39.50); coupling constants (*J*) are in hertz (Hz). The following abbreviations

are used to describe peak patterns when appropriate: s (singlet), d (doublet), t (triplet), q (quadruplet), quint (quintuplet), hept (heptuplet), m (multiplet) and br (broad). 2D NMR experiments –homonuclear correlation spectroscopy (H,H-COSY), heteronuclear multiple quantum correlation (HMQC), and heteronuclear multiple bond correlation (HMBC)– of representative compounds were acquired to assign protons and carbons of structures. The following abbreviations have been used for the peak assignment: Ar (aryl), Ph (phenyl), pyr (pyrazole), cyclop (cyclopropane). If necessary, the relative configuration of the compounds was confirmed by 1D ^{1}H-NMR nuclear Overhauser effect (NOE) experiments, in which the signal of interest was irradiated with a selective pulse and NOE interactions were observed.

For all final compounds, a purity of at least 95% was determined by HPLC-MS using an Agilent 1200LC-MSD VL instrument. LC separation was achieved with an Eclipse XDB-C18 column (5 µm, 4.6 mm x 150 mm), together with a guard column (5 µm, 4.6 mm x 12.5 mm). The mobile phase consisted of water and acetonitrile (ACN) with 0.1% formic acid as solvent modifier, using the gradient indicated in Table 13. MS analysis was performed using an electrospray ionization (ESI) source. The capillary voltage was set to 3.0 kV and the fragmentor voltage to 72 eV. The drying gas temperature was 350 °C, the drying gas flow was 10 L/min, and the nebulizer pressure was 20 psi. Spectra were acquired in positive or negative ionization mode from 100 to 1200 *m/z* and in UV-mode at four different wavelengths (210, 230, 254, and 280 nm). High resolution mass spectrometry (HRMS) was carried out on a FTMS Bruker APEX Q IV spectrometer in ESI or matrix-assisted laser desorption ionization (MALDI) mode at UCM's mass spectrometry facilities.

Table 13. HPLC gradient for compound characterization.

t (min)	% ACN
0	0
2	0
8	80
10	100
18	100
22	0
25	0

4.1.1. General synthetic procedures

General procedure A: Chan-Lam coupling reaction. To a solution of the appropriate arylboronic acid (1.0 eq) in anhydrous DCM (0.07 M), the corresponding hydroxy (hetero)aromatic derivative (1.2 eq), copper acetate (1.7 eq), triethylamine (2.0 eq) or pyridine (6.0 eq) and previously activated 4 Å molecular sieves were added. The reaction was stirred under air at rt or 40 °C until consumption of starting material. Then, the reaction mixture was filtered through celite and the filtrate was washed with a $NaHCO_3$ saturated solution and brine, dried over Na_2SO_4, filtered and concentrated under reduced pressure. The residue was purified by flash chromatography to obtain the corresponding (hetero)aryl ether.

General procedure B: alkylation reaction with 2-bromo-1-arylethanone derivatives. To a solution of the appropriate phenol derivative (1.0 eq) and 1,8-diazabicyclo[5.4.0]undec-7-ene (DBU) (1.2 eq) in anhydrous DMF (0.38 M), the corresponding 2-bromo-1-arylethanone (1.0 eq) was added and the mixture was heated at 140 °C for 45 min under MW irradiation. After cooling to rt, the reaction mixture was diluted with ethyl acetate and washed (3x) with a 1:1 mixture of water/brine. The organic layer was dried over Na_2SO_4, filtered and concentrated under reduced pressure. The residue was purified by flash chromatography to obtain the corresponding ether.

General procedure C: enaminone formation. To a solution of the appropriate 2-aryloxy-1-arylethanone (1.0 eq) in anhydrous toluene (0.50 M), *N,N*-dimethylacetamide dimethyl acetal (DMADMA) (1.5 eq) was added and the mixture was stirred at 90 °C until consumption of starting material (2-16 h). After cooling to rt, the reaction mixture was concentrated under reduced pressure to afford the corresponding crude enaminone, which was used in the next step reaction without further purification.

General procedure D: pyrazole formation. A solution of the corresponding enaminone (1.0 eq) in absolute ethanol (0.20 M) was treated with hydrazine monohydrate (65%, 2.4 eq) and the reaction was refluxed until the reaction was completed (0.5-1 h). After cooling to rt, the mixture was concentrated under vacuum, dissolved with ethyl acetate, and washed with brine. The organic layer was dried over Na_2SO_4, filtered and concentrated under reduced pressure. The residue was purified by flash chromatography to obtain the corresponding pyrazole.

General procedure E: THP ether deprotection. To a solution of the corresponding THP ether (1.0 eq) in THF (0.66 M), 3 M HCl (4.0 eq) was added and the reaction was stirred at rt for 1 h. Then, the mixture was treated with $NaHCO_3$ saturated solution until pH 5-6 and extracted with DCM. The organic phase was dried with Na_2SO_4, filtered and

concentrated under reduced pressure to yield the desired alcohol, which was used in the next reaction without further purification.

General procedure F: alkylation of 1-(4-hydroxyphenyl)ethanone derivatives. To a solution of the corresponding 1-(4-hydroxyphenyl)ethanone (1.0 eq) in anhydrous DMF (1.0 M), K_2CO_3 (2.0 eq) was added and the reaction mixture was stirred at rt for 30 min. Then, the appropriate haloalkane (3.5 eq) was added and the mixture was heated at 130 °C for 15 min under MW irradiation. After cooling to rt, the reaction mixture was diluted with EtOAc and washed (3x) with a 1:1 mixture of water/brine. The organic layer was dried over Na_2SO_4, filtered and concentrated under reduced pressure to obtain the corresponding ether, which was used in the next reaction without further purification.

4.1.2. Synthesis of final compound 1

***tert*-Butyl (3,5-dimethyl-1*H*-pyrazol-4-yl) carbonate, 2.** To a solution of 3,5-dimethyl-1*H*-pyrazol-4-ol (1.0 eq, 1.34 mmol, 150 mg) and triethylamine (1.1 eq, 1.47 mmol, 0.21 mL) in anhydrous DCM (1.2 M), di-*tert*-butyl dicarbonate (1.1 eq, 1.47 mmol, 321 mg) was added and the reaction mixture was stirred at rt for 1 h. Then, the solvent was removed under reduced pressure and the resulting residue was purified by flash chromatography (hexane/EtOAc 8:2 to 2:8) to afford compound **2** as a white solid (235 mg, 84%).

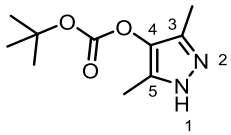

Mp: 98 °C. **R_f**: 0.83 (hexane/EtOAc 2:8). **IR (ATR, cm^{-1})**: ν 2982 (N-H, C-H), 1761 (C=O), 1277 (C-O), 1150 (C-O). **^{1}H-NMR (Acetone-d_6, 300 MHz)**: δ 1.51 (s, 9H, $C(CH_3)_3$), 2.08 (s, 6H, $2CH_3$), 11.33 (br s, 1H, NH). **^{13}C-NMR (Acetone-d_6, 75 MHz)**: δ 8.7 ($2CH_3$), 27.7 ($C(\underline{C}H_3)_3$), 83.3 ($\underline{C}(CH_3)_3$), 132.2 (C_3, C_5), 152.5 (C=O), C4 was not observed. **HPLC (t_R, min)**: 11.9. **MS (ESI, *m/z*)**: 213.1 $[M+H]^+$.

1-Benzyl-3,5-dimethyl-1*H*-pyrazol-4-yl *tert*-butyl carbonate, 3. To a solution of compound **2** (1.0 eq, 0.47 mmol, 100 mg) in anhydrous DMSO (0.7 M), potassium hydroxide (1.5 eq, 0.71 mmol, 40 mg) was added and the reaction was stirred at 80 °C for 1 h. The mixture was then cooled to rt, benzyl chloride (1.0 eq, 0.47 mmol, 54 µL) was added and the reaction was stirred at rt for additional 2 h. The mixture was then poured into water and extracted with chloroform (2x). The combined organic phases were dried

over Na_2SO_4, filtered and concentrated under reduced pressure. Then, the residue was purified by flash chromatography (hexane to hexane/EtOAc 6:4) to yield the corresponding pyrazole **3** as a white solid (78 mg, 55%).

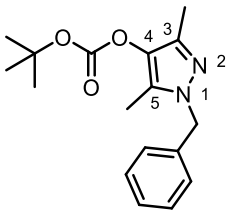

R_f: 0.48 (hexane/EtOAc 7:3). **^{1}H-NMR ($CDCl_3$, 300 MHz)**: δ 1.63 (s, 9H, $C(CH_3)_3$), 2.16 (s, 3H, CH_3), 2.26 (s, 3H, CH_3), 4.82 (s, 2H, CH_2), 7.29-7.42 (m, 5H, CH_{Ph}). **^{13}C-NMR ($CDCl_3$, 75 MHz)**: δ 11.5 (CH_3), 11.7 (CH_3), 28.2 ($C(\underline{C}H_3)_3$), 76.8 (CH_2), 84.8 ($\underline{C}(CH_3)_3$), 128.6 (CH_{Ph}), 128.7 ($2CH_{Ph}$), 128.8 ($2CH_{Ph}$), 133.3 (C_{pyr}), 136.7 (C_{Ph}), 141.7 (C_{pyr}), 146.6 (C_{pyr}), 148.9 (C=O). **HPLC (t_R, min)**: 14.8. **MS (ESI, *m/z*)**: 303.3 $[M+H]^+$.

1-Benzyl-3,5-dimethyl-1*H*-pyrazol-4-ol, 4. To a solution of compound **3** (1.0 eq, 0.44 mmol, 134 mg) in DCM (0.2 M), TFA (15.0 eq, 6.65 mmol, 0.51 mL) was added and the reaction was stirred at rt for 1.5 h. The mixture was then diluted with DCM and washed with a saturated $NaHCO_3$ solution. The aqueous phase was extracted with DCM (2x), and the combined organic phases were dried over Na_2SO_4, filtered and evaporated under reduced pressure to give compound **4** as a white solid (90 mg, 100%), which was used without further purification.

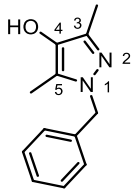

R_f: 0.16 (hexane/EtOAc 6:4 + 0.1% NH_3). **^{1}H-NMR ($CDCl_3$, 300 MHz)**: δ 2.10 (s, 6H, $2CH_3$), 4.83 (s, 2H, CH_2), 7.28-7.41 (m, 5H, CH_{Ph}). **^{13}C-NMR ($CDCl_3$, 75 MHz)**: δ 9.9 ($2CH_3$), 76.7 (CH_2), 128.3 (CH_{Ph}), 128.6 ($2CH_{Ph}$), 128.7 ($2CH_{Ph}$), 137.5 (C_{Ph}), 138.7 (C_{pyr}), $2C_{pyr}$ were not observed. **HPLC (t_R, min)**: 11.3. **MS (ESI, *m/z*)**: 203.2 $[M+H]^+$.

1-Benzyl-3,5-dimethyl-4-phenoxy-1*H*-pyrazole, 5. Following general procedure A using compound **4** (40 mg, 0.20 mmol), phenylboronic acid (20 mg, 0.17 mmol) and triethylamine (46 µL, 0.33 mmol) at rt, compound **5** was obtained as an oil (15 mg, 33%). Chromatography: hexane to hexane/EtOAc 6:4.

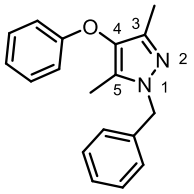

R_f: 0.59 (hexane/EtOAc 7:3). **IR (ATR, cm^{-1})**: ν 1597 (C=C), 1503 (C=C), 1366 (C-O), 1208 (C-O). **^{1}H-NMR ($CDCl_3$, 300 MHz)**: δ 2.10 (s, 3H, CH_3), 2.25 (s, 3H, CH_3), 4.90 (s, 2H, CH_2), 7.27-7.49 (m, 10H, CH_{Ph}). **^{13}C-NMR ($CDCl_3$, 75 MHz)**: δ 10.1 (CH_3), 11.1 (CH_3), 76.8 (CH_2), 124.3 ($2CH_{Ph}$), 127.1 (CH_{Ph}), 128.4 (CH_{Ph}), 128.6 ($2CH_{Ph}$), 128.7 ($2CH_{Ph}$), 129.1 ($2CH_{Ph}$), 129.9 (C_{pyr}), 137.4 (C_{Ph}), 140.3 (C_{pyr}), 140.5 (C_{Ph}), 141.5 (C_{pyr}). **HPLC (t_R, min)**: 14.9. **MS (ESI, *m/z*)**: 279.2 $[M+H]^+$.

3,5-Dimethyl-4-phenoxy-1*H*-pyrazole, 1. A solution of *N*-benzyl pyrazole **5** (1.0 eq, 0.08 mmol, 22 mg) in DMF (0.025 M) was pumped through a 10% Pd/C cartridge at 70 °C and 0.5 mL/min flow rate under atmospheric pressure (full-H_2 mode) using an H-Cube flow hydrogenation system. The resulting solution was diluted with ethyl acetate and washed with a 1:1 water/brine mixture. The organic layer was dried over Na_2SO_4, filtered and concentrated under reduced pressure. The residue was purified by flash chromatography (hexane to hexane/EtOAc 1:1.) to yield compound **1** as a yellow solid (10 mg, 67%).

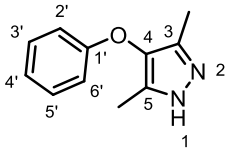

Mp: 120-122 °C. **R_f**: 0.44 (hexane/EtOAc 1:1). **IR (ATR, cm^{-1})**: ν 3300 (N-H), 1598 (C=C), 1503 (C=C), 1366 (C-O), 1210 (C-O). **^{1}H-NMR ($CDCl_3$, 300 MHz)**: δ 2.17 (s, 3H, CH_3), 2.17 (s, 3H, CH_3), 5.20 (s, 1H, NH), 7.26-7.48 (m, 5H, CH_{Ph}). **^{13}C-NMR ($CDCl_3$, 75 MHz)**: δ 9.9 (CH_3), 10.4 (CH_3), 124.3 ($C_{2'}$, $C_{6'}$), 126.5 (C_{pyr}), 127.1 ($C_{4'}$), 129.1 ($C_{3'}$, $C_{5'}$), 137.2 (C_{pyr}), 139.3 (C_{pyr}), 140.2 ($C_{1'}$). **HPLC (t_R, min)**: 10.9. **MS (ESI, *m/z*)**: 189.2 $[M+H]^+$.

4.1.3. Synthesis of intermediate ketones 25-43

2-(2-Chlorophenoxy)-1-(4-methoxyphenyl)ethan-1-one, 25. Following general procedure B using 2-chlorophenol (300 mg, 2.33 mmol) and 2-bromo-1-(4-methoxyphenyl)ethanone (535 mg, 2.33 mmol), compound **25** was obtained as a white solid (262 mg, 41%). Chromatography: hexane to hexane/EtOAc 9:1.

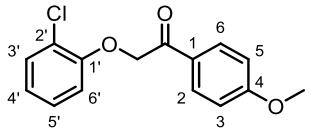

Mp: 108-110 °C. **R_f**: 0.41 (hexane/EtOAc 8:2). **IR (ATR, cm^{-1})**: ν 1720 (C=O), 1550 (C=C), 1270 (C-O), 1220 (C-O), 800 (C-Cl). **^{1}H-NMR ($CDCl_3$, 300 MHz)**: δ 3.88 (s, 3H, CH_3), 5.27 (s, 2H, CH_2), 6.86 (dd, *J*=8.2, 1.4, 1H, $H_{6'}$), 6.89-6.95 (m, 1H, $H_{4'}$), 6.96 (d, *J*=9.0, 2H, H_3, H_5), 7.16 (ddd, *J*=8.2, 7.5, 1.6, 1H, $H_{5'}$), 7.37 (dd, *J*=7.9, 1.6, 1H, $H_{3'}$), 8.03 (d, *J*=9.0, 2H, H_2, H_6). **^{13}C-NMR ($CDCl_3$, 75 MHz)**: δ 55.7 (CH_3), 72.0 (CH_2), 114.16 (C_3, C_5), 114.18 ($C_{6'}$), 122.5 ($C_{4'}$), 123.3 ($C_{2'}$), 127.6 (C_1), 127.8 ($C_{5'}$), 130.7 ($C_{3'}$), 130.9 (C_2, C_6), 153.9 ($C_{1'}$), 164.3 (C_4), 192.8 (C=O). **HPLC (t_R, min)**: 14.2. **MS (ESI, *m/z*)**: 277.1, 279.1 $[M+H]^+$.

2-(3-Chlorophenoxy)-1-(4-methoxyphenyl)ethan-1-one, 26. Following general procedure B using 3-chlorophenol (300 mg, 2.33 mmol) and 2-bromo-1-(4-methoxyphenyl)ethanone (535 mg, 2.33 mmol), compound **26** was obtained as a white solid (286 mg, 44%). Chromatography: hexane to hexane/EtOAc 8:2.

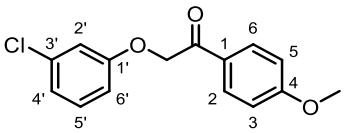

Mp: 95-98 °C. **R_f**: 0.30 (hexane/EtOAc 8:2). **IR (ATR, cm^{-1})**: ν 1694 (C=O), 1601 (C=C), 1228 (C-O), 826 (C-Cl). **^{1}H-NMR ($CDCl_3$, 300 MHz)**: δ 3.89 (s, 3H, CH_3), 5.21 (s, 2H, CH_2), 6.83 (ddd, *J*=8.4, 2.4, 0.9, 1H, $H_{6'}$), 6.92-7.01 (m, 4H, H_3, H_5, $H_{2'}$, $H_{4'}$), 7.20 (ddd, *J*=8.3, 7.8, 0.5, 1H, $H_{5'}$), 7.98 (d, *J*=9.0, 2H, H_2, H_6).**^{13}C-NMR ($CDCl_3$, 75 MHz)**: δ 55.7 (CH_3), 70.8 (CH_2), 113.3 ($C_{6'}$), 114.2 (C_3, C_5), 115.5 ($C_{2'}$), 121.9 ($C_{4'}$), 127.6 (C_1), 130.5 ($C_{5'}$), 130.7 (C_2, C_6), 135.1 ($C_{3'}$), 159.0 ($C_{1'}$), 164.3 (C_4), 192.5 (C=O). **HPLC (t_R, min)**: 14.4. **MS (ESI, *m/z*)**: 277.1, 279.1 $[M+H]^+$.

2-(4-Chlorophenoxy)-1-(4-methoxyphenyl)ethan-1-one, 27. Following general procedure B using 4-chlorophenol (500 mg, 3.89 mmol) and 2-bromo-1-(4-methoxyphenyl)ethanone (891 mg, 3.89 mmol), compound **27** was obtained as a white solid (600 mg, 56%). Chromatography: hexane to hexane/EtOAc 7:3.

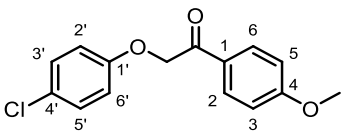

Mp: 86-88 °C. **R_f**: 0.40 (hexane/EtOAc 8:2). **IR (ATR, cm^{-1})**: ν 1750 (C=O), 1590 (C=C), 1490 (C=C), 1250 (C-O), 800 (C-Cl). **^{1}H-NMR ($CDCl_3$, 300 MHz)**: δ 3.89 (s, 3H, CH_3), 5.20 (s, 2H, CH_2), 6.87 (d, *J*=9.1, 2H, $H_{2'}$, $H_{6'}$), 6.97 (d, *J*=9.0, 2H, H_3, H_5) 7.23 (d, *J*=9.1, 2H, $H_{3'}$, $H_{5'}$), 7.98 (d, *J*=9.0, 2H, H_2, H_6). **^{13}C-NMR ($CDCl_3$, 75 MHz)**: δ 55.7 (CH_3), 70.9 (CH_2), 114.2 (C_3, C_5), 116.2 ($C_{2'}$, $C_{6'}$), 126.6 ($C_{4'}$), 127.5 (C_1), 129.6 ($C_{3'}$, $C_{5'}$), 130.6 (C_2, C_6), 156.8 ($C_{1'}$), 164.3 (C_4), 192.9 (C=O). **HPLC (t_R, min)**: 14.3. **MS (ESI, *m/z*)**: 277.1, 279.1 $[M+H]^+$.

2-(2-Fluorophenoxy)-1-(4-methoxyphenyl)ethan-1-one, 28. Following general procedure B using 2-fluorophenol (200 mg, 1.78 mmol) and 2-bromo-1-(4-methoxyphenyl)ethanone (409 mg, 1.78 mmol), compound **28** was obtained as a white solid (321 mg, 69%). Chromatography: hexane to hexane/EtOAc 8:2.

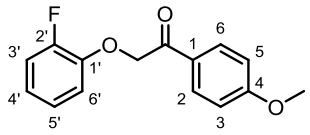

Mp: 93-95 °C. **R_f**: 0.47 (hexane/EtOAc 7:3). **IR (ATR, cm^{-1})**: ν 1690 (C=O), 1598 (C=C), 1502 (C=C), 1234 (C-O), 1170 (C-F). **^{1}H-NMR ($CDCl_3$, 300 MHz)**: δ 3.88 (s, 3H, CH_3), 5.29 (s, 2H, CH_2), 6.96 (d, *J*=9.0, 2H, H_3, H_5), 6.88-7.14 (m, 4H, $H_{3'}$-$H_{6'}$), 8.00 (d, *J*=8.9, 2H, H_2, H_6). **^{13}C-NMR ($CDCl_3$, 75 MHz)**: δ 55.7 (CH_3), 72.3 (CH_2), 114.2 (C_3, C_5), 116.3 (d, *J*=1.7, $C_{5'}$), 116.7 (d, *J*=18.3, $C_{3'}$), 122.4 (d, *J*=6.9, $C_{6'}$), 124.5 (d, *J*=4.0, $C_{4'}$), 127.6 (C_1), 130.7 (C_2, C_6), 146.3 (d, *J*=10.3, $C_{1'}$), 153.0 (d, *J*=246.1, $C_{2'}$), 164.3 (C_4), 192.8 (C=O). **HPLC (t_R, min)**: 13.6. **MS (ESI, *m/z*)**: 261.1 $[M+H]^+$.

2-(3-Fluorophenoxy)-1-(4-methoxyphenyl)ethan-1-one, 29. Following general procedure B using 3-fluorophenol (150 mg, 1.34 mmol) and 2-bromo-1-(4-methoxyphenyl)ethanone (307 mg, 1.34 mmol), compound **29** was obtained as a white solid (130 mg, 37%). Chromatography: hexane to hexane/EtOAc 8:2.

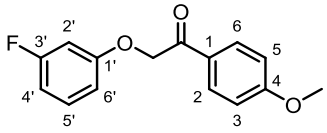

Mp: 72 °C. **R_f**: 0.55 (hexane/EtOAc 7:3). **IR (ATR, cm^{-1})**: ν 1692 (C=O), 1598 (C=C), 1235 (C-O), 1140 (C-F). **^{1}H-NMR ($CDCl_3$, 300 MHz)**: δ 3.88 (s, 3H, CH_3), 5.21 (s, 2H, CH_2), 6.60-6.74 (m, 3H, $H_{2'}$, $H_{4'}$, $H_{6'}$), 6.96 (d, *J*=8.9, 2H, H_3, H_5), 7.16-7.26 (m, 1H, $H_{5'}$), 7.98 (d, *J*=9.0, 2H, H_2, H_6). **^{13}C-NMR ($CDCl_3$, 75 MHz)**: δ 55.7 (CH_3), 70.8 (CH_2), 102.9 (d, *J*=25.1, $C_{2'}$), 108.5 (d, *J*=21.3, $C_{4'}$), 110.5 (d, *J*=3.0, $C_{6'}$), 114.2 (C_3, C_5), 127.6 (C_1), 130.5 (d, *J*=10.0, $C_{5'}$),

130.6 (C_2, C_6), 159.5 (d, *J*=10.8, $C_{1'}$), 163.7 (d, *J*=245.6, $C_{3'}$), 164.3 (C_4), 192.5 (C=O). **HPLC (t_R, min)**: 13.7. **MS (ESI, *m/z*)**: 261.0 $[M+H]^+$.

2-(4-Fluorophenoxy)-1-(4-methoxyphenyl)ethan-1-one, 30. Following general procedure B using 4-fluorophenol (200 mg, 1.78 mmol) and 2-bromo-1-(4-methoxyphenyl)ethanone (409 mg, 1.78 mmol), compound **30** was obtained as a white solid (179 mg, 39%). Chromatography: hexane to hexane/EtOAc 8:2.

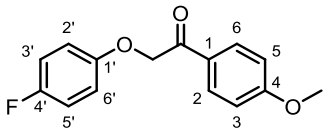

Mp: 96-98 °C. **R_f**: 0.56 (hexane/EtOAc 7:3). **IR (ATR, cm^{-1})**: ν 1689 (C=O), 1598 (C=C), 1502 (C=C), 1203 (C-O), 1170 (C-F). **^{1}H-NMR ($CDCl_3$, 300 MHz)**: δ 3.88 (s, 3H, CH_3), 5.19 (s, 2H, CH_2), 6.88 (dd, *J*=9.4, 4.4, 2H, $H_{2'}$, $H_{6'}$), 6.93-6.99 (m, 2H, $H_{3'}$, $H_{5'}$), 6.96 (d, *J*=8.9, 2H, H_3, H_5), 7.98 (d, *J*=8.9, 2H, H_2, H_6). **^{13}C-NMR ($CDCl_3$, 75 MHz)**: δ 55.7 (CH_3), 71.5 (CH_2), 114.2 (C_3, C_5), 116.1 (d, *J*=23.3, $C_{3'}$, $C_{5'}$), 116.1 (d, *J*=8.0, $C_{2'}$, $C_{6'}$), 127.7 (C_1), 130.6 (C_2, C_6), 154.4 (d, *J*=2.2, $C_{1'}$), 157.8 (d, *J*=239.2, $C_{4'}$), 164.3 (C_4), 193.1 (C=O). **HPLC (t_R, min)**: 13.6. **MS (ESI, *m/z*)**: 261.0, 262.0 $[M+H]^+$.

1-(4-Methoxyphenyl)-2-[2-(trifluoromethyl)phenoxy]ethan-1-one, 31. Following general procedure B using 2-(trifluoromethyl)phenol (150 mg, 0.93 mmol) and 2-bromo-1-(4-methoxyphenyl)ethanone (212 mg, 0.93 mmol), compound **31** was obtained as a white solid (146 mg, 51%). Chromatography: hexane to hexane/EtOAc 8:2.

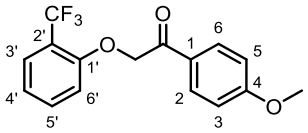

Mp: 75-76 °C. **R_f**: 0.50 (hexane/EtOAc 7:3). **IR (ATR, cm^{-1})**: ν 1692 (C=O), 1598 (C=C), 1320 (C-O), 1224 (C-O), 1111 (C-F). **^{1}H-NMR ($CDCl_3$, 300 MHz)**: δ (s, 3H, CH_3), 5.27 (s, 2H, CH_2), 6.90 (d, *J*=8.4, 1H, $H_{6'}$), 6.95 (d, *J*=9.0, 2H, H_3, H_5), 7.02 (tquint, *J*=7.6, 0.9, 1H, $H_{4'}$), 7.43 (ddd, *J*=8.3, 7.6, 0.7, 1H, $H_{5'}$), 7.58 (dd, *J*=7.7, 0.8, 1H, $H_{3'}$), 8.02 (d, *J*=9.0, 2H, H_2, H_6).**^{13}C-NMR ($CDCl_3$, 75 MHz)**: δ 55.7 (CH_3), 71.7 (CH_2), 113.1 ($C_{6'}$), 114.1 (C_3, C_5), 119.2 (q, *J*=30.9, $C_{2'}$), 121.0 ($C_{5'}$), 123.7 (q, *J*=272.5, CF_3), 127.4 (q, *J*=5.3, $C_{3'}$), 127.44 (C_1), 131.1 (C_2, C_6), 133.4 ($C_{4'}$), 156.1 (q, *J*=1.8, $C_{1'}$), 164.4 (C_4), 193.0 (C=O). **HPLC (t_R, min)**: 14.5. **MS (ESI, *m/z*)**: 311.2 $[M+H]^+$.

1-(4-Methoxyphenyl)-2-[3-(trifluoromethyl)phenoxy]ethan-1-one, 32. Following general procedure B using 3-(trifluoromethyl)phenol (150 mg, 0.93 mmol) and 2-bromo-1-(4-methoxyphenyl)ethanone (212 mg, 0.93 mmol), compound **32** was obtained as a white solid (154 mg, 54%). Chromatography: hexane to hexane/EtOAc 9:1.

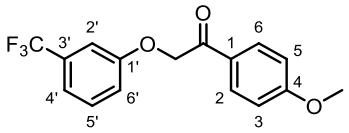

Mp: 98-100 °C. **R_f**: 0.54 (hexane/EtOAc 7:3). **IR (ATR, cm^{-1})**: ν 1696 (C=O), 1601 (C=C), 1172 (C-O), 1126 (C-F). **^{1}H-NMR ($CDCl_3$, 300 MHz)**: δ 3.89 (s, 3H, CH_3), 5.27 (s, 2H, CH_2), 6.98 (d, *J*=8.9, 2H, H_3, H_5), 7.10 (br dd, *J*=8.2, 2.7, 1H, $H_{6'}$), 7.18 (br s, 1H, $H_{2'}$), 7.24 (br d, *J*=7.7, 1H, $H_{4'}$), 7.39 (t, *J*=8.0, 1H, $H_{5'}$), 7.99 (d, *J*=8.9, 2H, H_2, H_6).**^{13}C-NMR ($CDCl_3$, 75 MHz)**: δ 55.7 (CH_3), 70.7 (CH_2), 112.0 (q, *J*=3.8, $C_{2'}$), 114.3 (C_3, C_5), 118.2 ($C_{5'}$), 118.4 (q, *J*=3.8, $C_{4'}$), 124.0 (q, *J*=272.3, CF_3) 127.5 (C_1), 130.3 ($C_{6'}$), 130.6 (C_2, C_6), 132.1 (q, *J*=32.5, $C_{3'}$), 158.4 ($C_{1'}$), 164.4 (C_4), 192.3 (C=O). **HPLC (t_R, min)**: 14.5. **MS (ESI, *m/z*)**: 311.2 $[M+H]^+$.

1-(4-Methoxyphenyl)-2-[4-(trifluoromethyl)phenoxy]ethan-1-one, 33. Following general procedure B using 4-(trifluoromethyl)phenol (150 mg, 0.93 mmol) and 2-bromo-1-(4-methoxyphenyl)ethanone (212 mg, 0.93 mmol), compound **33** was obtained as a white solid (95 mg, 33%). Chromatography: hexane to hexane/EtOAc 9:1.

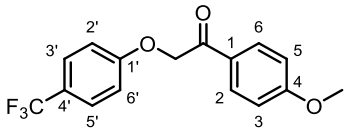

Mp: 108 °C. **R_f**: 0.50 (hexane/EtOAc 7:3). **IR (ATR, cm^{-1})**: ν 1689 (C=O), 1334 (C-O), 1170 (C-O), 1108 (C-F). **^{1}H-NMR ($CDCl_3$, 300 MHz)**: δ 3.89 (s, 3H, CH_3), 5.28 (s, 2H, CH_2), 6.98 (d, *J*=8.9, 2H, H_3, H_5), 6.99 (br d, *J*=8.5, 2H, $H_{2'}$, $H_{6'}$), 7.54 (br d, *J*=8.5, 2H, $H_{3'}$, $H_{5'}$), 7.99 (d, *J*=8.9, 2H, H_2, H_6).**^{13}C-NMR ($CDCl_3$, 75 MHz)**: δ 55.7 (CH_3), 70.6 (CH_2), 114.3 (C_3, C_5), 114.9 ($C_{2'}$, $C_{6'}$), 123.9 (d, *J*=32.9, $C_{4'}$), 124.4 (d, *J*=271.3, CF_3), 127.2 (q, *J*=3.8, $C_{3'}$, $C_{5'}$), 127.5 (C_1), 130.6 (C_2, C_6), 160.6 (q, *J*=1.2, $C_{1'}$), 164.4 (C_4), 192.3 (C=O). **HPLC (t_R, min)**: 14.5. **MS (ESI, *m/z*)**: 311.2 $[M+H]^+$.

1-(4-Methoxyphenyl)-2-(2-methylphenoxy)ethan-1-one, 34. Following general procedure B using 2-methylphenol (150 mg, 1.39 mmol) and 2-bromo-1-(4-methoxyphenyl)ethanone (318 mg, 1.39 mmol), compound **34** was obtained as a white solid (131 mg, 37%). Chromatography: hexane to hexane/EtOAc 8:2.

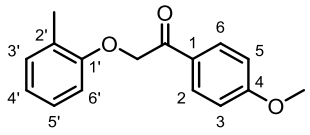

Mp: 77 °C. **R_f**: 0.48 (hexane/EtOAc 8:2). **IR (ATR, cm^{-1})**: ν 1691 (C=O), 1597 (C=C), 1220 (C-O), 1168 (C-O). **^{1}H-NMR ($CDCl_3$, 300 MHz)**: δ 2.30 (s, 3H, CH_3), 3.88 (s, 3H, OCH_3), 5.20 (s, 2H, CH_2), 6.75 (dd, *J*=8.4, 1.1, 1H, $H_{6'}$), 6.89 (td, *J*=7.4, 1.1, 1H, $H_{4'}$), 6.96 (d, *J*=9.0, 2H, H_3, H_5), 7.06-7.18 (m, 2H, $H_{3'}$, $H_{5'}$), 8.02 (d, *J*=9.0, 2H, H_2, H_6).**^{13}C-NMR ($CDCl_3$, 75 MHz)**: δ 16.5 (CH_3), 55.6 (OCH_3), 71.2 (CH_2), 111.5 ($C_{6'}$), 114.1 (C_3, C_5), 121.4 ($C_{4'}$), 126.9 ($C_{5'}$), 127.3 ($C_{2'}$), 127.9 (C_1), 130.8 (C_2, C_6), 131.1 ($C_{3'}$), 156.4 ($C_{1'}$), 164.1 (C_4), 193.7 (C=O). **HPLC (t_R, min)**: 14.6. MS (ESI, *m/z*): 257.2 $[M+H]^+$.

1-(4-Methoxyphenyl)-2-(3-methylphenoxy)ethan-1-one, 35. Following general procedure B using 3-methylphenol (150 mg, 1.39 mmol) and 2-bromo-1-(4-methoxyphenyl)ethanone (318 mg, 1.39 mmol), compound **35** was obtained as an oil (150 mg, 42%). Chromatography: hexane to hexane/EtOAc 8:2.

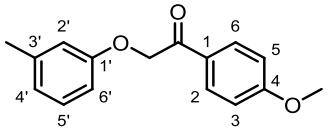

R_f: 0.49 (hexane/EtOAc 7:3). **IR (ATR, cm^{-1})**: ν 1681 (C=O), 1598 (C=C), 1231 (C-O), 1157 (C-O). **^{1}H-NMR ($CDCl_3$, 300 MHz)**: δ 2.32 (s, 3H, CH_3), 3.88 (s, 3H, OCH_3), 5.19 (s, 2H, CH_2), 6.70-6.84 (m, 3H, $H_{2'}$, $H_{4'}$, $H_{6'}$), 6.96 (d, *J*=8.9, 2H, H_3, H_5), 7.16 (t, *J*=7.9, 1H, $H_{5'}$), 8.01 (d, *J*=8.9, 2H, H_2, H_6).**^{13}C-NMR ($CDCl_3$, 75 MHz)**: δ 21.7 (CH_3), 55.7 (OCH_3), 70.9 (CH_2), 111.7 ($C_{6'}$), 114.1 (C_3, C_5), 115.8 ($C_{2'}$), 122.6 ($C_{4'}$), 127.9 (C_1), 129.4 ($C_{5'}$), 130.7 (C_2, C_6), 139.8 ($C_{3'}$), 158.3 ($C_{1'}$), 164.2 (C_4), 193.4 (C=O). **HPLC (t_R, min)**: 14.3. **MS (ESI, *m/z*)**: 257.2 $[M+H]^+$.

1-(4-Methoxyphenyl)-2-(4-methylphenoxy)ethan-1-one, 36. Following general procedure B using 4-methylphenol (150 mg, 1.39 mmol) and 2-bromo-1-(4-methoxyphenyl)ethanone (318 mg, 1.39 mmol), compound **36** was obtained as a white solid (111 mg, 31%). Chromatography: hexane to hexane/EtOAc 8:2.

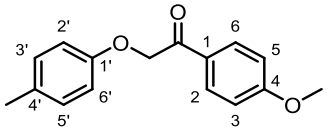

Mp: 85-87 °C. **R_f**: 0.39 (hexane/EtOAc 8:2). **IR (ATR, cm^{-1})**: ν 1691 (C=O), 1598 (C=C), 1508 (C=C), 1217 (C-O), 1169 (C-O). **^{1}H-NMR ($CDCl_3$, 300 MHz)**: δ 2.28 (s, 3H, CH_3), 3.88 (s, 3H, OCH_3), 5.18 (s, 2H, CH_2), 6.84 (d, *J*=8.6, 2H, $H_{2'}$, $H_{6'}$), 6.96 (d, *J*=8.9, 2H, H_3, H_5), 7.07 (d, *J*=8.8, 2H, $H_{3'}$, $H_{5'}$), 8.00 (d, *J*=9.0, 2H, H_2, H_6).**^{13}C-NMR ($CDCl_3$, 75 MHz)**: δ 20.6 (CH_3), 55.7 (OCH_3), 71.1 (CH_2), 114.1 (C_3, C_5), 114.8 ($C_{2'}$, $C_{6'}$), 127.9 (C_1), 130.1 ($C_{3'}$, $C_{5'}$), 130.7 (C_2, C_6), 131.0 ($C_{4'}$), 156.2 ($C_{1'}$), 164.1 (C_4), 193.5 (C=O). **HPLC (t_R, min)**: 14.3. **MS (ESI, *m/z*)**: 257.2 $[M+H]^+$.

2-(2-Methoxyphenoxy)-1-(4-methoxyphenyl)ethan-1-one, 37. Following general procedure B using 2-methoxyphenol (200 mg, 1.61 mmol) and 2-bromo-1-(4-methoxyphenyl)ethanone (369 mg, 1.61 mmol), compound **37** was obtained as a white solid (300 mg, 68%). Chromatography: hexane to hexane/EtOAc 7:3.

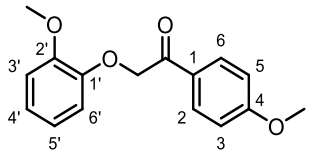

Mp: 95 °C. **R_f**: 0.40 (hexane/EtOAc 7:3). **IR (ATR, cm^{-1})**: ν 1690 (C=O), 1597 (C=C), 1502 (C=C), 1250 (C-O), 1169 (C-O). **^{1}H-NMR ($CDCl_3$, 300 MHz)**: δ 3.83 (s, 3H, CH_3), 3.85 (s, 3H, CH_3), 5.26 (s, 2H, CH_2), 6.79-6.97 (m, 4H, $H_{3'}$-$H_{6'}$), 6.92 (d, *J*=9.0, 2H, H_3, H_5), 7.99 (d, *J*=9.0, 2H, H_2, H_6). **^{13}C-NMR ($CDCl_3$, 75 MHz)**: δ 55.5 (CH_3), 55.9 (CH_3), 71.9 (CH_2), 112.2 ($C_{3'}$/$C_{6'}$), 113.9 (C_3, C_5), 114.7 ($C_{3'}$/$C_{6'}$), 120.8, 122.3 ($C_{4'}$, $C_{5'}$), 127.7 (C_1), 130.5 (C_2, C_6), 147.6, 149.7 ($C_{1'}$, $C_{2'}$), 163.9 (C_4), 193.1 (C=O). **HPLC (t_R, min)**: 13.3. **MS (ESI, *m/z*)**: 273.1 $[M+H]^+$.

2-(3-Methoxyphenoxy)-1-(4-methoxyphenyl)ethan-1-one, 38. Following general procedure B using 3-methoxyphenol (200 mg, 1.61 mmol) and 2-bromo-1-(4-methoxyphenyl)ethanone (369 mg, 1.61 mmol), compound **38** was obtained as a white solid (130 mg, 30%). Chromatography: hexane to hexane/EtOAc 7:3.

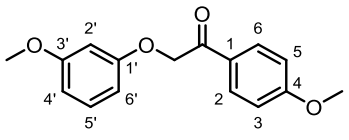

Mp: 78 °C. **R_f**: 0.41 (hexane/EtOAc 7:3). **IR (ATR, cm^{-1})**: ν 1693 (C=O), 1600 (C=C), 1237 (C-O), 1154 (C-O). **^{1}H-NMR ($CDCl_3$, 300 MHz)**: δ 3.77 (s, 3H, CH_3), 3.87 (s, 3H, CH_3), 5.19 (s, 2H, CH_2), 6.44-6.62 (m, 3H, $H_{2'}$, $H_{4'}$, $H_{6'}$), 6.96 (d, *J*=8.7, 2H, H_3, H_5), 7.17 (dd, *J*=8.9, 7.7, 1H, $H_{5'}$), 7.99 (d, *J*=8.8, 2H, H_2, H_6). **^{13}C-NMR ($CDCl_3$, 75 MHz)**: δ 55.4 (CH_3), 55.6 (CH_3),

70.8 (CH_2), 101.6, 106.7, 107.4 ($C_{2'}$, $C_{4'}$, $C_{6'}$), 114.1 (C_3, C_5), 127.8 (C_1), 130.1 ($C_{5'}$), 130.7 (C_2, C_6), 159.4, 161.0 ($C_{1'}$, $C_{3'}$), 164.2 (C_4), 193.0 (C=O). **HPLC (t_R, min)**: 13.6. **MS (ESI, *m/z*)**: 273.1 $[M+H]^+$.

2-(4-Methoxyphenoxy)-1-(4-methoxyphenyl)ethan-1-one, 39. Following general procedure B using 4-methoxyphenol (600 mg, 4.83 mmol) and 2-bromo-1-(4-methoxyphenyl)ethanone (1.11 g, 4.83 mmol), compound **39** was obtained as an off-white solid (1.00 g, 76%). Chromatography: hexane to hexane/EtOAc 7:3.

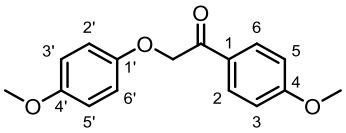

Mp: 86-89 °C. **R_f**: 0.41 (hexane/EtOAc 7:3). **IR (ATR, cm^{-1})**: ν 1690 (C=O), 1598 (C=C), 1503 (C=C), 1211 (C-O), 1169 (C-O). **^{1}H-NMR ($CDCl_3$, 300 MHz)**: δ 3.76 (s, 3H, CH_3), 3.88 (s, 3H, CH_3), 5.16 (s, 2H, CH_2), 6.77-6.94 (m, 4H, $H_{2'}$, $H_{3'}$, $H_{5'}$, $H_{6'}$), 6.96 (d, *J*=8.9, 2H, H_3, H_5), 8.00 (d, *J*=8.9, 2H, H_2, H_6). **^{13}C-NMR ($CDCl_3$, 75 MHz)**: δ 55.7 (CH_3), 55.8 (CH_3), 71.8 (CH_2), 114.1 (C_3, C_5), 114.8, 116.1 ($C_{2'}$, $C_{3'}$, $C_{5'}$, $C_{6'}$), 127.9 (C_1), 130.7 (C_2, C_6), 152.5 ($C_{1'}$), 154.6 ($C_{4'}$), 164.2 (C_4), 193.6 (C=O). **HPLC (t_R, min)**: 13.5. **MS (ESI, *m/z*)**: 273.1 $[M+H]^+$.

2-(3-(Dimethylamino)phenoxy)-1-(4-methoxyphenyl)ethan-1-one, 40. Following general procedure B using 3-(dimethylamino)phenol (200 mg, 1.46 mmol) and 2-bromo-1-(4-methoxyphenyl)ethanone (334 mg, 1.46 mmol), compound **40** was obtained as an off-white solid (200 mg, 48%). Chromatography: hexane to hexane/EtOAc 7:3.

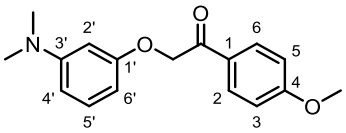

Mp: 90 °C. **R_f**: 0.40 (hexane/EtOAc 7:3). **IR (ATR, cm^{-1})**: ν 1692 (C=O), 1599 (C=C), 1232 (C-O), 1171 (C-O). **^{1}H-NMR ($CDCl_3$, 300 MHz)**: δ 2.92 (s, 6H, $N(CH_3)_2$), 3.88 (s, 3H, OCH_3), 5.18 (s, 2H, CH_2), 6.27 (ddd, *J*=8.1, 2.2, 1.0, 1H, $H_{6'}$), 6.35-6.44 (m, 2H, $H_{2'}$, $H_{4'}$), 6.95 (d, *J*=8.9, 2H, H_3, H_5), 7.08-7.16 (m, 1H, $H_{5'}$), 8.00 (d, *J*=8.9, 2H, H_2, H_6).**^{13}C-NMR ($CDCl_3$, 75 MHz)**: δ 40.7 ($N(CH_3)_2$), 55.6 (OCH_3), 71.0 (CH_2), 100.3 ($C_{2'}$), 101.9 ($C_{6'}$), 106.6 ($C_{4'}$), 114.1 (C_3, C_5), 128.0 (C_1), 129.9 ($C_{5'}$), 130.7 (C_2, C_6), 152.1 ($C_{3'}$), 159.3 ($C_{1'}$), 164.1 (C_4), 193.6 (C=O). **HPLC (t_R, min)**: 12.8. **MS (ESI, *m/z*)**: 286.1 $[M+H]^+$.

2-(4-(Dimethylamino)phenoxy)-1-(4-methoxyphenyl)ethan-1-one, 41. Following general procedure B using 4-(dimethylamino)phenol (200 mg, 1.46 mmol) and 2-bromo-1-(4-methoxyphenyl)ethanone (334 mg, 1.46 mmol), compound **41** was obtained as an off-white solid (142 mg, 34%). Chromatography: hexane to hexane/EtOAc 1:1.

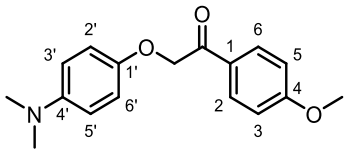

Mp: 60-62 °C. **R_f**: 0.53 (hexane/EtOAc 1:1). **IR (ATR, cm^{-1})**: ν 1690 (C=O), 1600 (C=C), 1512 (C=C), 1254 (C-O), 1168 (C-O). **^{1}H-NMR ($CDCl_3$, 300 MHz)**: δ 2.86 (s, 6H, $N(CH_3)_2$), 3.87 (s, 3H, OCH_3), 5.14 (s, 2H, CH_2), 6.72 (d, *J*=9.1, 2H, $H_{3'}$, $H_{5'}$), 6.90 (d, *J*=9.1, 2H, $H_{2'}$, $H_{6'}$), 6.95 (d, *J*=8.9, 2H, H_3, H_5), 8.00 (d, *J*=8.9, 2H, H_2, H_6).**^{13}C-NMR ($CDCl_3$, 75 MHz)**: δ 41.8 ($N(CH_3)_2$), 55.6 (OCH_3), 71.9 (CH_2), 114.0 (C_3, C_5), 114.9 ($C_{3'}$, $C_{5'}$), 116.1 ($C_{2'}$, $C_{6'}$), 127.9 (C_1), 130.7 (C_2, C_6), 146.4 ($C_{4'}$), 150.6 ($C_{1'}$), 164.0 (C_4), 194.0 (C=O).

***N*-(2-(2-(4-Methoxyphenyl)-2-oxoethoxy)phenyl)acetamide, 42.** Following general procedure B using 2-acetamidophenol (200 mg, 1.32 mmol) and 2-bromo-1-(4-methoxyphenyl)ethanone (303 mg, 1.32 mmol), compound **42** was obtained as an off-white solid (321 mg, 81%). Chromatography: hexane/EtOAc 2:8 to EtOAc.

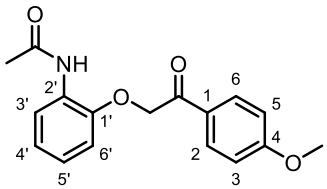

Mp: 93 °C. **R_f**: 0.64 (EtOAc). **IR (ATR, cm^{-1})**: ν 3300 (N-H), 1679 (C=O), 1599 (C=O), 1529 (C=C), 1453 (C-N), 1236 (C-O), 1173 (C-O). **^{1}H-NMR ($CDCl_3$, 300 MHz)**: δ 2.27 (s, 3H, CH_3), 3.88 (s, 3H, OCH_3), 5.34 (s, 2H, CH_2), 6.88-7.08 (m, 3H, $H_{4'}$, $H_{5'}$, $H_{6'}$), 6.97 (d, *J*=9.0, 2H, H_3, H_5), 7.92 (d, *J*=9.0, 2H, H_2, H_6), 8.30-8.40 (m, 1H, $H_{3'}$), 8.91 (s, 1H, NH). **^{13}C-NMR ($CDCl_3$, 75 MHz)**: δ 25.0 (CH_3), 55.7 (OCH_3), 73.4 (CH_2), 114.3 (C_3, C_5), 115.1 ($C_{6'}$), 120.8 ($C_{3'}$), 123.3, 123.8 ($C_{4'}$, $C_{5'}$), 127.1 (C_1), 130.0 ($C_{2'}$), 130.2 (C_2, C_6), 147.8 ($C_{1'}$), 164.5 (C_4), 168.8 (CONH), 193.3 (C=O). **HPLC (t_R, min)**: 12.4. **MS (ESI, *m/z*)**: 300.1 $[M+H]^+$.

***N*-(3-(2-(4-Methoxyphenyl)-2-oxoethoxy)phenyl)acetamide, 43.** Following general procedure B using 3-acetamidophenol (200 mg, 1.32 mmol) and 2-bromo-1-(4-

methoxyphenyl)ethanone (303 mg, 1.32 mmol), compound **43** was obtained as an off-white solid (137 mg, 35%). Chromatography: hexane/EtOAc 7:3 to 2:8

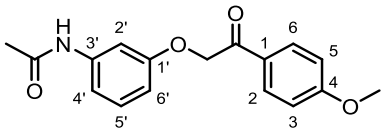

Mp: 108-110 °C. **R_f**: 0.55 (EtOAc). **IR (ATR, cm^{-1})**: ν 3300 (N-H), 1668 (C=O), 1598 (C=O), 1236 (C-O), 1160 (C-O). **^{1}H-NMR ($CDCl_3$, 300 MHz)**: δ 2.14 (s, 3H, CH_3), 3.88 (s, 3H, OCH_3), 5.21 (s, 2H, CH_2), 6.70 (dd, *J*=8.1, 2.5, 1H, $H_{6'}$), 6.95 (d, *J*=8.9, 2H, H_3, H_5), 7.02 (d, *J*=8.0, 1H, $H_{4'}$), 7.19 (t, *J*=8.1, 1H, $H_{5'}$), 7.23-7.38 (m, 2H, $H_{2'}$, NH), 7.99 (d, *J*=8.9, 2H, H_2, H_6). **^{13}C-NMR ($CDCl_3$, 75 MHz)**: δ 24.8 (CH_3), 55.7 (OCH_3), 70.8 (CH_2), 106.5 ($C_{2'}$), 111.0 ($C_{6'}$), 112.9 ($C_{4'}$), 114.2 (C_3, C_5), 127.7 (C_1), 130.0 ($C_{5'}$), 130.7 (C_2, C_6), 139.3 ($C_{3'}$), 158.8 ($C_{1'}$), 164.2 (C_4), 169.2 (CONH), 193.1 (C=O). **HPLC (t_R, min)**: 11.9. **MS (ESI, *m/z*)**: 300.1 $[M+H]^+$.

4.1.4. Synthesis of intermediate enaminones 44-62

2-(2-Chlorophenoxy)-3-(dimethylamino)-1-(4-methoxyphenyl)but-2-en-1-one, 44. Following general procedure C using compound **25** (227 mg, 0.82 mmol), crude compound **44** was obtained as an oil (304 mg, 92% crude yield).

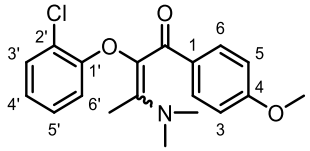

R_f: 0.33 (EtOAc). **^{1}H-NMR ($CDCl_3$, 300 MHz)**: δ Mixture of isomers A:B (1:0.7): 2.06 (s, 3H, CH_{3A}), 2.41 (s, 3H, CH_{3B}), 3.00 (s, 6H, $N(CH_3)_{2B}$), 3.02 (s, 6H, $N(CH_3)_{2A}$), 3.76 (s, 3H, OCH_{3AB}), 6.70-6.80 (m, 3H, H_{3AB}, H_{5AB}, $H_{6'AB}$), 6.86 (td, *J*=8.5, 1.5, 1H, $H_{4'AB}$), 6.99-7.06 (m, 1H, $H_{5'AB}$), 7.18 (dd, *J*=7.9, 1.6, 1H, $H_{3'B}$), 7.19 (dd, *J*=7.9, 1.6, 1H, $H_{3'A}$), 7.76 (d, *J*=8.8, 2H, H_{2B}, H_{6B}), 7.80 (d, *J*=8.8, 2H, H_{2A}, H_{6A}).

2-(3-Chlorophenoxy)-3-(dimethylamino)-1-(4-methoxyphenyl)but-2-en-1-one, 45. Following general procedure C using compound **26** (250 mg, 0.90 mmol), crude compound **45** was obtained as an oil (310 mg, 99% crude yield).

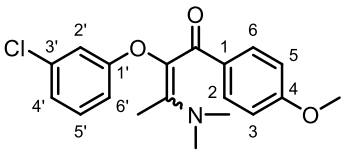

R_f: 0.41 (EtOAc). **^{1}H-NMR ($CDCl_3$, 300 MHz)**: δ Mixture of isomers A:B (1:0.7): 2.04 (s, 3H, CH_{3A}), 2.38 (s, 3H, CH_{3B}), 2.98 (s, 6H, $N(CH_3)_{2B}$), 3.02 (s, 6H, $N(CH_3)_{2A}$), 3.78 (s, 3H, OCH_{3AB}), 6.65-6.74 (m, 1H, $H_{6'AB}$), 6.76 (d, *J*=8.9, 2H, H_{3AB}, H_{5AB}), 6.79-6.85 (m, 2H, $H_{2'AB}$, $H_{4'AB}$), 6.99-7.11 (m, 1H, $H_{5'AB}$), 7.66 (d, *J*=8.8, 2H, H_{2B}, H_{6B}), 7.69 (d, *J*=8.8, 2H, H_{2A}, H_{6A}).

2-(4-Chlorophenoxy)-3-(dimethylamino)-1-(4-methoxyphenyl)but-2-en-1-one, 46. Following general procedure C using compound **27** (300 mg, 1.08 mmol), crude compound **46** was obtained as an oil (370 mg, 99% crude yield).

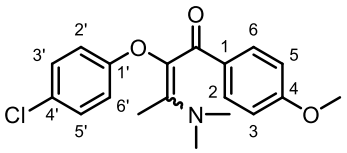

R_f: 0.31 (EtOAc). **^{1}H-NMR ($CDCl_3$, 300 MHz)**: δ Mixture of isomers A:B (1:0.7): 2.04 (s, 3H, CH_{3A}), 2.38 (s, 3H, CH_{3B}), 2.97 (s, 6H, $N(CH_3)_{2B}$), 3.02 (s, 6H, $N(CH_3)_{2A}$), 3.78 (s, 3H, OCH_{3AB}), 6.70-6.85 (m, 4H, H_{3AB}, H_{5AB}, $H_{2'AB}$, $H_{6'AB}$), 7.08 (d, *J*=9.1, 2H, $H_{3'A}$, $H_{5'A}$), 7.09 (d, *J*=9.1, 2H, $H_{3'B}$, $H_{5'B}$), 7.66 (d, *J*=9.0, 2H, H_{2B}, H_{6B}), 7.69 (d, *J*=9.0, 2H, H_{2A}, H_{6A}).

2-(2-Fluorophenoxy)-3-(dimethylamino)-1-(4-methoxyphenyl)but-2-en-1-one, 47. Following general procedure C using compound **28** (150 mg, 0.58 mmol), crude compound **47** was obtained as an oil (190 mg, 99% crude yield).

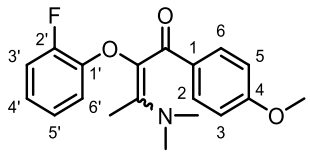

R_f: 0.36 (EtOAc). **^{1}H-NMR ($CDCl_3$, 300 MHz)**: δ Mixture of isomers A:B (1:0.7): 2.09 (s, 3H, CH_{3A}), 2.39 (s, 3H, CH_{3B}), 3.01 (s, 6H, $N(CH_3)_{2B}$), 3.02 (s, 6H, $N(CH_3)_{2A}$), 3.77 (s, 3H, OCH_{3AB}), 6.68-6.81 (m, 3H, H_{3AB}, H_{5AB}, $H_{6'AB}$), 6.83-6.98 (m, 3H, $H_{3'AB}$, $H_{4'AB}$, $H_{5'AB}$,), 7.73 (d, *J*=8.7, 2H, H_{2B}, H_{6B}), 7.76 (d, *J*=8.7, 2H, H_{2A}, H_{6A}).

2-(3-Fluorophenoxy)-3-(dimethylamino)-1-(4-methoxyphenyl)but-2-en-1-one, 48. Following general procedure C using compound **29** (123 mg, 0.47 mmol), crude compound **48** was obtained as an oil (155 mg, 99% crude yield).

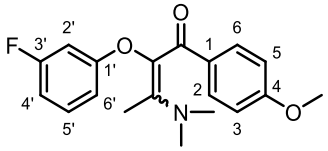

R_f: 0.17 (hexane/EtOAc 1:1). **^{1}H-NMR ($CDCl_3$, 300 MHz)**: δ Mixture of isomers A:B (1:0.7): 2.05 (s, 3H, CH_{3A}), 2.38 (s, 3H, CH_{3B}), 2.98 (s, 6H, $N(CH_3)_{2B}$), 3.02 (s, 6H, $N(CH_3)_{2A}$), 3.77 (s, 3H, OCH_{3AB}), 6.49-6.63 (m, 3H, $H_{2'AB}$, $H_{4'AB}$, $H_{6'AB}$), 6.76 (d, *J*=8.8, 2H, H_{3AB}, H_{5AB}), 7.04-7.12 (m, 1H, $H_{5'AB}$), 7.66 (d, *J*=8.9, 2H, H_{2B}, H_{6B}), 7.69 (d, *J*=8.9, 2H, H_{2A}, H_{6A}).

2-(4-Fluorophenoxy)-3-(dimethylamino)-1-(4-methoxyphenyl)but-2-en-1-one, 49. Following general procedure C using compound **30** (140 mg, 0.54 mmol), crude compound **49** was obtained as an oil (165 mg, 93% crude yield).

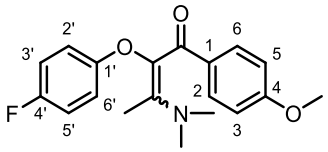

R_f: 0.30 (EtOAc). **^{1}H-NMR ($CDCl_3$, 300 MHz)**: δ Mixture of isomers A:B (1:0.7): 2.06 (s, 3H, CH_{3A}), 2.37 (s, 3H, CH_{3B}), 2.98 (s, 6H, $N(CH_3)_{2B}$), 3.01 (s, 6H, $N(CH_3)_{2A}$), 3.77 (s, 3H, OCH_{3A}), 3.78 (s, 3H, OCH_{3B}), 6.69-6.84 (m, 6H, H_{3AB}, H_{5AB}, $H_{2'AB}$, $H_{3'AB}$, $H_{5'AB}$, $H_{6'AB}$), 7.66 (d, *J*=9.0, 2H, H_{2B}, H_{6B}), 7.69 (d, *J*=9.0, 2H, H_{2A}, H_{6A}).

3-(Dimethylamino)-1-(4-methoxyphenyl)-2-(2-(trifluoromethyl)phenoxy)but-2-en-1-one, 50. Following general procedure C using compound **31** (120 mg, 0.39 mmol), crude compound **50** was obtained as an oil (135 mg, 92% crude yield).

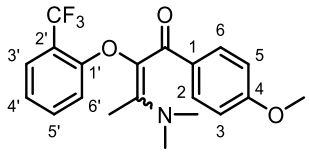

R_f: 0.16 (hexane/EtOAc 1:1). **^{1}H-NMR ($CDCl_3$, 300 MHz)**: δ Mixture of isomers A:B (1:0.5): 2.08 (s, 3H, CH_{3A}), 2.38 (s, 3H, CH_{3B}), 3.00 (s, 6H, $N(CH_3)_{2A}$), 3.02 (s, 6H, $N(CH_3)_{2B}$), 3.75 (s, 3H, OCH_{3AB}), 6.70-6.80 (m, 3H, H_{3AB}, H_{5AB}, $H_{6'AB}$), 6.82-6.89 (m, 1H, $H_{4'AB}$), 6.96-7.03 (m, 1H, $H_{5'AB}$), 7.40-7.47 (m, 1H, $H_{3'AB}$), 7.62-7.68 (m, 2H, H_{2AB}, H_{6AB}).

3-(Dimethylamino)-1-(4-methoxyphenyl)-2-(3-(trifluoromethyl)phenoxy)but-2-en-1-one, 51. Following general procedure C using compound **32** (100 mg, 0.32 mmol), crude compound **51** was obtained as an oil (93 mg, 76% crude yield).

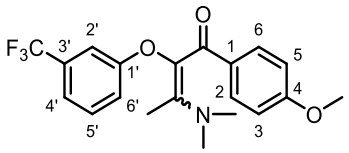

R_f: 0.12 (hexane/EtOAc 1:1). **^{1}H-NMR ($CDCl_3$, 300 MHz)**: δ Mixture of isomers A:B (1:0.7): 2.05 (s, 3H, CH_{3A}), 2.39 (s, 3H, CH_{3B}), 2.98 (s, 6H, $N(CH_3)_{2B}$), 3.02 (s, 6H, $N(CH_3)_{2A}$), 3.77 (s, 3H, OCH_{3A}), 3.78 (s, 3H, OCH_{3B}), 6.75 (d, *J*=8.9, 2H, H_{3A}, H_{5A}), 6.76 (d, *J*=8.9, 2H, H_{3B}, H_{5B}), 6.94-7.25 (m, 4H, $H_{2'AB}$, $H_{4'AB}$, $H_{5'AB}$, $H_{6'AB}$,), 7.64 (d, *J*=8.9, 2H, H_{2B}, H_{6B}), 7.67 (d, *J*=8.8, 2H, H_{2A}, H_{6A}).

3-(Dimethylamino)-1-(4-methoxyphenyl)-2-(4-(trifluoromethyl)phenoxy)but-2-en-1-one, 52. Following general procedure C using compound **33** (74 mg, 0.24 mmol), crude compound **52** was obtained as an oil (78 mg, 86% crude yield).

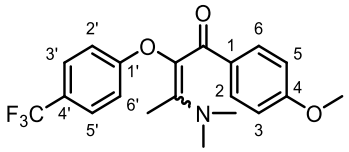

R_f: 0.13 (hexane/EtOAc 1:1). **^{1}H-NMR ($CDCl_3$, 300 MHz)**: δ Mixture of isomers A:B (1:0.7): 2.04 (s, 3H, CH_{3A}), 2.38 (s, 3H, CH_{3B}), 2.98 (s, 6H, $N(CH_3)_{2B}$), 3.02 (s, 6H, $N(CH_3)_{2A}$), 3.77 (s, 3H, OCH_{3A}), 3.78 (s, 3H, OCH_{3B}), 6.75 (d, *J*=8.9, 2H, H_{3A}, H_{5A}), 6.76 (d, *J*=8.9, 2H, H_{3B}, H_{5B}), 6.86-6.81 (m, 2H, $H_{2'AB}$, $H_{6'AB}$), 7.40 (d, *J*=9.0, 2H, $H_{3'AB}$, $H_{5'AB}$), 7.65-7.71 (m, 2H, H_{2AB}, H_{6AB}).

3-(Dimethylamino)-1-(4-methoxyphenyl)-2-(*o*-tolyloxy)but-2-en-1-one, 53. Following general procedure C using compound **34** (92 mg, 0.36 mmol), crude compound **53** was obtained as an oil (106 mg, 91% crude yield).

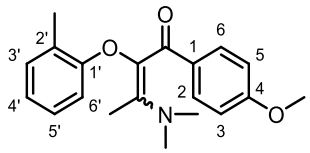

R_f: 0.35 (EtOAc). **^{1}H-NMR ($CDCl_3$, 300 MHz)**: δ Mixture of isomers A:B (1:0.8): 2.03 (s, 3H, CH_{3A}), 2.24 (s, 3H, CH_{3B}), 2.31 (s, 3H, CH_{3ArA}), 2.40 (s, 3H, CH_{3ArB}), 2.98 (s, 6H, $N(CH_3)_{2B}$),

3.03 (s, 6H, $N(CH_3)_{2A}$), 3.76 (s, 3H, OCH_{3AB}), 6.63-6.84 (m, 4H, H_{3AB}, H_{5AB}, $H_{4'AB}$, $H_{6'AB}$), 6.94-7.05 (m, 2H, $H_{3'AB}$, $H_{5'AB}$), 7.67 (d, *J*=8.9, 2H, H_{2B}, H_{6B}), 7.70 (d, *J*=8.9, 2H, H_{2A}, H_{6A}).

3-(Dimethylamino)-1-(4-methoxyphenyl)-2-(*m*-tolyloxy)but-2-en-1-one, 54. Following general procedure C using compound **35** (140 mg, 0.55 mmol), crude compound **54** was obtained as an oil (150 mg, 99% crude yield).

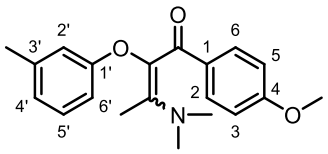

R_f: 0.13 (hexane/EtOAc 1:1). **^{1}H-NMR ($CDCl_3$, 300 MHz)**: δ Mixture of isomers A:B (1:0.7): 2.05 (s, 3H, CH_{3A}), 2.22 (s, 3H, CH_{3B}), 2.23 (s, 3H, CH_{3ArA}), 2.38 (s, 3H, CH_{3ArB}), 2.97 (s, 6H, $N(CH_3)_{2B}$), 3.02 (s, 6H, $N(CH_3)_{2A}$), 3.77 (s, 3H, OCH_{3AB}), 6.59-6.69 (m, 3H, $H_{2'AB}$, $H_{4'AB}$, $H_{6'AB}$), 6.71-6.85 (m, 2H, H_{3AB}, H_{5AB}), 6.96-7.05 (m, 1H, $H_{5'AB}$), 7.69-7.74 (m, 2H, H_{2AB}, H_{6AB}).

3-(Dimethylamino)-1-(4-methoxyphenyl)-2-(*p*-tolyloxy)but-2-en-1-one, 55. Following general procedure C using compound **36** (100 mg, 0.39 mmol), crude compound **55** was obtained as an oil (100 mg, 79% crude yield).

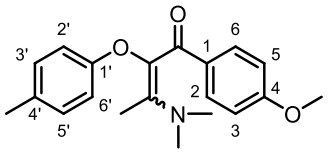

R_f: 0.29 (EtOAc). **^{1}H-NMR ($CDCl_3$, 300 MHz)**: δ Mixture of isomers A:B (1:0.7): 2.05 (s, 3H, CH_{3A}), 2.19 (s, 3H, CH_{3B}), 2.20 (s, 3H, CH_{3ArA}), 2.38 (s, 3H, CH_{3ArB}), 2.97 (s, 6H, $N(CH_3)_{2B}$), 3.02 (s, 6H, $N(CH_3)_{2A}$), 3.77 (s, 3H, OCH_{3AB}), 6.67-6.81 (m, 4H, H_{3AB}, H_{5AB}, $H_{2'AB}$, $H_{6'AB}$), 6.90-6.95 (m, 2H, $H_{3'AB}$, $H_{5'AB}$), 7.69 (d, *J*=9.0, 2H, H_{2B}, H_{6B}), 7.72 (d, *J*=8.9, 2H, H_{2A}, H_{6A}).

3-(Dimethylamino)-2-(2-methoxyphenoxy)-1-(4-methoxyphenyl)but-2-en-1-one, 56. Following general procedure C using compound **37** (200 mg, 0.73 mmol), crude compound **56** was obtained as an oil (280 mg, 99% crude yield).

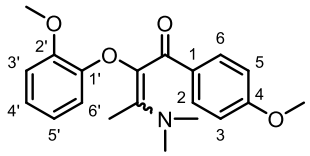

R_f: 0.11 (hexane/EtOAc 1:1). **^{1}H-NMR ($CDCl_3$, 300 MHz)**: δ Mixture of isomers A:B (1:0.7): 2.08 (s, 3H, CH_{3A}), 2.34 (s, 3H, CH_{3B}), 2.97 (s, 6H, $N(CH_3)_{2B}$), 3.01 (s, 6H, $N(CH_3)_{2A}$), 3.75 (s, 3H, $C_{2'}OCH_{3AB}$), 3.77 (s, 3H, C_4OCH_{3AB}), 6.70-6.90 (m, 6H, H_{3AB}, H_{5AB}, $H_{3'AB}$, $H_{4'AB}$, $H_{5'AB}$, $H_{6'AB}$), 7.71 (d, *J*=8.9, 2H, H_{2B}, H_{6B}), 7.75 (d, *J*=8.9, 2H, H_{2A}, H_{6A}).

3-(Dimethylamino)-2-(3-methoxyphenoxy)-1-(4-methoxyphenyl)but-2-en-1-one, 57. Following general procedure C using compound **38** (120 mg, 0.44 mmol), crude compound **57** was obtained as an oil (150 mg, 99% crude yield).

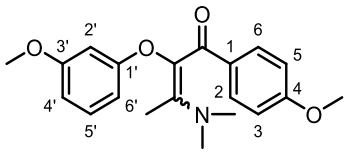

R_f: 0.10 (hexane/EtOAc 1:1). **^{1}H-NMR ($CDCl_3$, 300 MHz)**: δ Mixture of isomers A:B (1:0.6): 2.05 (s, 3H, CH_{3A}), 2.38 (s, 3H, CH_{3B}), 2.98 (s, 6H, $N(CH_3)_{2B}$), 3.03 (s, 6H, $N(CH_3)_{2A}$), 3.70 (s, 3H, $C_{3'}OCH_{3B}$), 3.71 (s, 3H, $C_{3'}OCH_{3A}$), 3.77 (s, 3H, C_4OCH_{3AB}), 6.26-6.45 (m, 3H, $H_{2'AB}$, $H_{4'AB}$, $H_{6'AB}$), 6.74 (d, *J*=8.9, 2H, H_{3B}, H_{5B}), 6.75 (d, *J*=8.9, 2H, H_{3A}, H_{5A}), 6.99-7.09 (m, 1H, $H_{5'AB}$), 7.68 (d, *J*=8.8, 2H, H_{2B}, H_{6B}), 7.70 (d, *J*=8.8, 2H, H_{2A}, H_{6A}).

3-(Dimethylamino)-2-(4-methoxyphenoxy)-1-(4-methoxyphenyl)but-2-en-1-one, 58. Following general procedure C using compound **39** (100 mg, 0.37 mmol), crude compound **58** was obtained as an oil (125 mg, 99% crude yield).

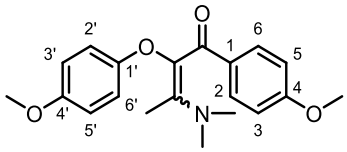

R_f: 0.24 (EtOAc). **^{1}H-NMR ($CDCl_3$, 300 MHz)**: δ Mixture of isomers A:B (1:0.7): 2.06 (s, 3H, CH_{3A}), 2.37 (s, 3H, CH_{3B}), 2.97 (s, 6H, $N(CH_3)_{2B}$), 3.01 (s, 6H, $N(CH_3)_{2A}$), 3.69 (s, 3H, $C_{4'}OCH_{3B}$), 3.70 (s, 3H, $C_{4'}OCH_{3A}$), 3.77 (s, 3H, C_4OCH_{3AB}), 6.64-6.80 (m, 6H, H_{3AB}, H_{5AB}, $H_{2'AB}$, $H_{3'AB}$, $H_{5'AB}$, $H_{6'AB}$), 7.66 (d, *J*=8.9, 2H, H_{2B}, H_{6B}), 7.69 (d, *J*=8.9, 2H, H_{2A}, H_{6A}).

3-(Dimethylamino)-2-(3-(dimethylamino)phenoxy)-1-(4-methoxyphenyl)but-2-en-1-one, 59. Following general procedure C using compound **40** (150 mg, 0.53 mmol), crude compound **59** was obtained as an oil (86 mg, 46% crude yield).

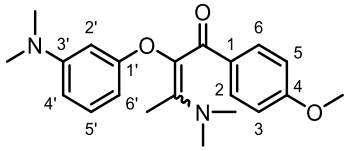

R_f: 0.22 (EtOAc). **^{1}H-NMR ($CDCl_3$, 300 MHz):** δ Mixture of isomers A:B (1:0.7): 2.06 (s, 3H, CH_{3A}), 2.38 (s, 3H, CH_{3B}), 2.85 (s, 6H, $C_{3'}N(CH_3)_{2B}$), 2.86 (s, 6H, $C_{3'}N(CH_3)_{2A}$), 2.98 (s, 6H, $N(CH_3)_{2B}$), 3.04 (s, 6H, $N(CH_3)_{2A}$), 3.77 (s, 3H, OCH_{3AB}), 6.14-6.31 (m, 3H, $H_{2'AB}$, $H_{4'AB}$, $H_{6'AB}$), 6.75 (d, *J*=9.0, 2H, H_{3B}, H_{5B}), 6.76 (d, *J*=8.9, 2H, H_{3A}, H_{5A}), 6.97-7.06 (m, 1H, $H_{5'AB}$), 7.71 (d, *J*=9.0, 2H, H_{2B}, H_{6B}), 7.73 (d, *J*=8.9, 2H, H_{2A}, H_{6A}).

3-(Dimethylamino)-2-(4-(dimethylamino)phenoxy)-1-(4-methoxyphenyl)but-2-en-1-one, 60. Following general procedure C using compound **41** (145 mg, 0.51 mmol), crude compound **60** was obtained as an oil (176 mg, 98% crude yield).

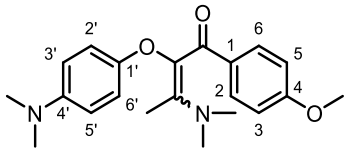

R_f: 0.22 (EtOAc). **^{1}H-NMR ($CDCl_3$, 300 MHz)**: δ Mixture of isomers A:B (1:0.7): 2.06 (s, 3H, CH_{3A}), 2.37 (s, 3H, CH_{3B}), 2.86 (s, 6H, $C_{4'}N(CH_3)_{2AB}$), 2.99 (s, 6H, $N(CH_3)_{2B}$), 3.01 (s, 6H, $N(CH_3)_{2A}$), 3.77 (s, 3H, OCH_{3AB}), 6.68-6.78 (m, 6H, H_{3AB}, H_{5AB}, $H_{2'AB}$, $H_{3'AB}$, $H_{5'AB}$, $H_{6'AB}$), 7.68-7.74 (m, 2H, H_{2AB}, H_{6AB}).

***N*-(2-((3-(Dimethylamino)-1-(4-methoxyphenyl)-1-oxobut-2-en-2-yl)oxy)phenyl) acetamide, 61.** Following general procedure C using compound **42** (172 mg, 0.58 mmol), crude compound **61** was obtained as an oil (210 mg, 99% crude yield).

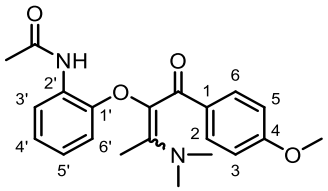

R_f: 0.31 (EtOAc). **^{1}H-NMR ($CDCl_3$, 300 MHz)**: δ Mixture of isomers A:B (1:1): 2.08 (s, 3H, CH_{3A}), 2.20 (s, 3H, $COCH_{3AB}$), 2.39 (s, 3H, CH_{3B}), 2.98 (s, 6H, $N(CH_3)_{2B}$), 3.02 (s, 6H, $N(CH_3)_{2A}$), 3.78 (s, 3H, OCH_{3AB}), 6.69-6.85 (m, 5H, H_{3AB}, H_{5AB}, $H_{4'AB}$, $H_{5'AB}$, $H_{6'AB}$), 6.48-7.57 (m, 2H, H_{2AB}, H_{6AB}), 7.64 (d, *J*=7.9, 1H, $H_{3'AB}$).

***N*-(3-((3-(Dimethylamino)-1-(4-methoxyphenyl)-1-oxobut-2-en-2-yl)oxy)phenyl) acetamide, 62.** Following general procedure C using compound **43** (133 mg, 0.44 mmol), crude compound **62** was obtained as an oil (165 mg, 99% crude yield).

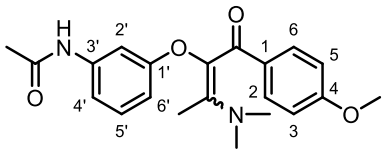

R_f: 0.31 (EtOAc). **^{1}H-NMR ($CDCl_3$, 300 MHz)**: δ Mixture of isomers A:B (1:1): 2.08 (s, 3H, CH_{3A}), 2.10 (s, 3H, $COCH_{3AB}$), 2.36 (s, 3H, CH_{3B}), 2.98 (s, 6H, $N(CH_3)_{2B}$), 3.01 (s, 6H, $N(CH_3)_{2A}$), 3.77 (s, 3H, OCH_{3AB}), 6.53-6.60 (m, 1H, $H_{6'AB}$), 6.75 (d, *J*=9.0, 2H, H_{3A}, H_{5A}), 6.76 (d, *J*=9.0, 2H, H_{3B}, H_{5B}), 6.94-7.10 (m, 3H, $H_{2'AB}$, $H_{4'AB}$, $H_{5'AB}$), 7.68 (d, *J*=9.0, 2H, H_{2B}, H_{6B}), 7.71 (d, *J*=9.0, 2H, H_{2A}, H_{6A}).

4.1.5. Synthesis of final compounds 6-24

4-(2-Chlorophenoxy)-3-(4-methoxyphenyl)-5-methyl-1*H*-pyrazole, 6. Following general procedure D using enaminone **44** (260 mg, 0.75 mmol), compound **6** was obtained as an off-white solid (155 mg, 66%). Chromatography: hexane to hexane/EtOAc 7:3.

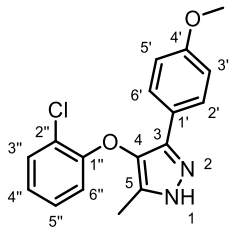

Mp: 120-122 °C. **R_f**: 0.58 (EtOAc). **IR (ATR, cm^{-1})**: ν 3115 (N-H), 1509 (C=C), 1441 (C=C), 1244 (C-O), 832 (C-Cl). **^{1}H-NMR ($CDCl_3$, 300 MHz)**: δ 2.14 (s, 3H, CH_3), 3.78 (s, 3H, OCH_3), 6.70 (dd, *J*=8.2, 1.5, 1H, $H_{6''}$), 6.85 (d, *J*=8.9, 2H, $H_{3'}$, $H_{5'}$), 6.92 (td, *J*=7.7, 1.5, 1H, $H_{4''}$), 7.02-7.10 (m, 1H, $H_{5''}$) 7.42 (dd, *J*=7.9, 1.6, 1H, $H_{3''}$), 7.66 (d, *J*=8.9, 2H, $H_{2'}$, $H_{6'}$). **^{13}C-NMR ($CDCl_3$, 75 MHz)**: δ 9.8 (CH_3), 55.4 (OCH_3), 114.4 ($C_{3',5'}$), 114.9 ($C_{6''}$), 122.4 ($C_{1'}$), 122.5 ($C_{2''}$), 122.9 ($C_{4''}$), 127.3 ($C_{2',6'}$), 127.9 ($C_{5''}$), 130.7 ($C_{3''}$), 133.1, 137.1 (C_4, C_5), 138.4 (C_3), 153.9 ($C_{1''}$), 159.7 ($C_{4'}$). **HPLC (t_R, min)**: 13.5. **MS (ESI, *m/z*)**: 315.1, 317.1 $[M+H]^+$.

4-(3-Chlorophenoxy)-3-(4-methoxyphenyl)-5-methyl-1*H*-pyrazole, 7. Following general procedure D using enaminone **45** (332 mg, 0.96 mmol), compound **7** was obtained as an off-white solid (128 mg, 42%). Chromatography: hexane to hexane/EtOAc 7:3.

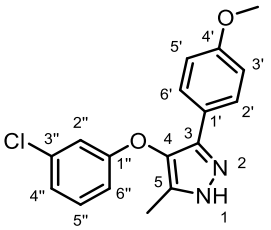

Mp: 128-130 °C. **R_f**: 0.67 (EtOAc). **IR (ATR, cm^{-1})**: ν 3125 (N-H), 1590 (C=C), 1466 (C=C), 1243 (C-O), 824 (C-Cl). **^{1}H-NMR ($CDCl_3$, 300 MHz)**: δ 2.12 (s, 3H, CH_3), 3.78 (s, 3H, OCH_3), 6.80-6.83 (m, 1H, $H_{6''}$), 6.85 (d, *J*=8.8, 2H, $H_{3'}$, $H_{5'}$), 6.93-7.00 (m, 2H, $H_{2''}$, $H_{4''}$), 7.17 (t, *J*=8.1, 1H, $H_{5''}$), 7.60 (d, *J*=8.9, 2H, $H_{2'}$, $H_{6'}$). **^{13}C-NMR ($CDCl_3$, 75 MHz)**: δ 9.9 (CH_3), 55.4 (OCH_3), 113. 6 ($C_{6''}$), 114.4 ($C_{3'}$, $C_{5'}$), 115.8 ($C_{2''}$), 122.4 ($C_{4''}$), 122.5 ($C_{1'}$), 127.3 ($C_{2'}$, $C_{6'}$), 130.6 ($C_{5''}$), 132.9 (C_4/C_5), 135.3 ($C_{3''}$), 137.3 (C_4/C_5), 138.3 (C_3), 159.2 ($C_{1''}$), 159.7 ($C_{4'}$). **HPLC (t_R, min)**: 13.8. **MS (ESI, *m/z*)**: 315.1, 317.1 $[M+H]^+$.

4-(4-Chlorophenoxy)-3-(4-methoxyphenyl)-5-methyl-1*H*-pyrazole, 8. Following general procedure D using enaminone **46** (423 mg, 1.22 mmol), compound **8** was obtained as a white solid (131 mg, 34%). Chromatography: hexane to hexane/EtOAc 6:4.

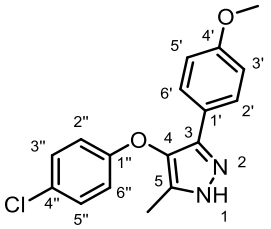

Mp: 70-72 °C. **R_f**: 0.72 (EtOAc). **IR (ATR, cm^{-1})**: ν 3129 (N-H), 1480 (C=C), 1242 (C-O), 824 (C-Cl). **^{1}H-NMR ($CDCl_3$, 300 MHz)**: δ 2.09 (s, 3H, CH_3), 3.77 (s, 3H, OCH_3), 6.83 (d, *J*=8.9, 2H, $H_{3'}$, $H_{5'}$), 6.86 (d, *J*=9.0, 2H, $H_{2''}$, $H_{6''}$), 7.19 (d, *J*=9.0, 2H, $H_{3''}$, $H_{5''}$), 7.59 (d, *J*=8.9, 2H, $H_{2'}$, $H_{6'}$). **^{13}C-NMR ($CDCl_3$, 75 MHz)**: δ 9.8 (CH_3), 55.4 (OCH_3), 114.4 ($C_{3'}$, $C_{5'}$), 116.5 ($C_{2''}$, $C_{6''}$), 122.6 ($C_{1'}$), 127.3 ($C_{2'}$, $C_{6'}$), 129.7 ($C_{3''}$, $C_{5''}$), 133.2 ($C_{4''}$), 136.8, 137.2 (C_4, C_5), 138.4 (C_3), 157.1 ($C_{1''}$), 159.6 ($C_{4'}$). **HPLC (t_R, min)**: 13.8. **MS (ESI, *m/z*)**: 315.1, 317.1 $[M+H]^+$.

4-(2-Fluorophenoxy)-3-(4-methoxyphenyl)-5-methyl-1*H*-pyrazole, 9. Following general procedure D using enaminone **47** (190 mg, 0.58 mmol), compound **9** was obtained as an oil (124 mg, 72%). Chromatography: hexane to hexane/EtOAc 6:4.

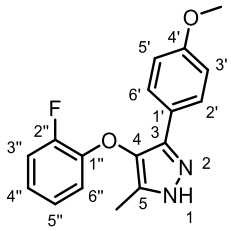

R_f: 0.47 (hexane/EtOAc 7:3). **IR (ATR, cm^{-1})**: ν 3250 (N-H), 1497 (C=C), 1253 (C-O), 1031 (C-F). **^{1}H-NMR ($CDCl_3$, 300 MHz)**: δ 2.09 (s, 3H, CH_3), 3.75 (s, 3H, OCH_3), 6.66-6.74 (m, 1H, $H_{6''}$), 6.80 (d, *J*=8.8, 2H, $H_{3'}$, $H_{5'}$), 6.86-6.94 (m, 2H, $H_{4''}$, $H_{5''}$), 7.09-7.19 (m, 1H, $H_{3''}$), 7.65 (d, *J*=8.6, 2H, $H_{2'}$, $H_{6'}$), 10.24 (br s, 1H, NH). **^{13}C-NMR ($CDCl_3$, 75 MHz)**: δ 9.7 (CH_3), 55.3 (OCH_3), 114.3 ($C_{3'}$, $C_{5'}$), 115.8 ($C_{6''}$), 116.7 (d, *J*=17.8, $C_{3''}$), 122.4 (d, *J*=6.8, $C_{4''}$), 122.6 ($C_{1'}$), 124.5 (d, *J*=4.0, $C_{5''}$), 127.4 ($C_{2'}$, $C_{6'}$), 132.9, 136.9 (C_4, C_5), 138.4 (C_3), 146.2 (d, *J*=10.6, $C_{1''}$), 152.2 (d, *J*=246.4, $C_{2''}$), 159.5 ($C_{4'}$). **HPLC (t_R, min)**: 13.2. **MS (ESI, *m/z*)**: 299.1 $[M+H]^+$.

4-(3-Fluorophenoxy)-3-(4-methoxyphenyl)-5-methyl-1*H*-pyrazole, 10. Following general procedure D using enaminone **48** (160 mg, 0.49 mmol), compound **10** was obtained as an off-white solid (70 mg, 48%). Chromatography: hexane to hexane/EtOAc 6:4.

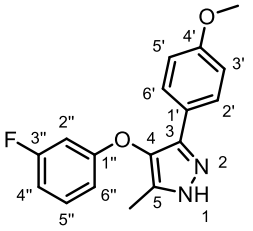

Mp: 136-139 °C. **R_f**: 0.43 (hexane/EtOAc 1:1). **IR (ATR, cm^{-1})**: ν 3250 (N-H), 1598 (C=C), 1512 (C=C), 1252 (C-O), 1120 (C-F). **^{1}H-NMR ($CDCl_3$, 300 MHz)**: δ 2.13 (s, 3H, CH_3), 3.78 (s, 3H, OCH_3), 6.65 (dt, *J*=10.3, 2.4, 1H, $H_{2''}$), 6.69-6.75 (m, 2H, $H_{4''}$, $H_{6''}$), 6.85 (d, *J*=8.7, 2H, $H_{3'}$, $H_{5'}$), 7.20 (td, *J*=8.3, 6.6, 1H, $H_{5''}$), 7.60 (d, *J*=8.9, 2H, $H_{2'}$, $H_{6'}$). **^{13}C-NMR ($CDCl_3$, 75 MHz)**: δ 9.8 (CH_3), 55.4 (OCH_3), 103.2 (d, *J*=25.6, $C_{2''}$), 109.1 (d, *J*=21.4, $C_{4''}$), 111.0 (d, *J*=3.0, $C_{6''}$), 114.4 ($C_{3'}$, $C_{5'}$), 122.5 ($C_{1'}$), 127.4 ($C_{2'}$, $C_{6'}$), 130.6 (d, *J*=9.8, $C_{5''}$), 133.0, 137.1 (C_4, C_5), 138.5 (C_3), 159.7 ($C_{4'}$), 159.8 (d, *J*=10.5, $C_{1''}$), 163.8 (d, *J*=246.1, $C_{3''}$). **HPLC (t_R, min)**: 13.4. **MS (ESI, *m/z*)**: 299.1 $[M+H]^+$.

4-(4-Fluorophenoxy)-3-(4-methoxyphenyl)-5-methyl-1*H*-pyrazole, 11. Following general procedure D using enaminone **49** (165 mg, 0.50 mmol), compound **11** was obtained as an oil (98 mg, 66%). Chromatography: hexane to hexane/EtOAc 6:4.

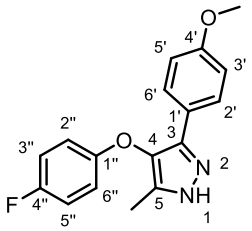

R_f: 0.38 (hexane/EtOAc 1:1). **IR (ATR, cm^{-1})**: ν 3150 (N-H), 1494 (C=C), 1248 (C-O), 1187 (C-F). **^{1}H-NMR ($CDCl_3$, 300 MHz)**: δ 2.08 (s, 3H, CH_3), 3.76 (s, 3H, OCH_3), 6.82 (d, *J*=8.9, 2H, $H_{3'}$, $H_{5'}$), 6.84-6.96 (m, 4H, $H_{2''}$, $H_{3''}$, $H_{5''}$, $H_{6''}$), 7.61 (d, *J*=8.9, 2H, $H_{2'}$, $H_{6'}$), 8.72 (br s, 1H, NH). **^{13}C-NMR ($CDCl_3$, 75 MHz)**: δ 9.8 (CH_3), 55.3 (OCH_3), 114.3 ($C_{3'}$, $C_{5'}$), 116.2 (d, *J*=23.3, $C_{3''}$, $C_{5''}$), 116.2 (d, *J*=8.2, $C_{2''}$, $C_{6''}$), 122.7 ($C_{1'}$), 127.3 ($C_{2'}$, $C_{6'}$), 133.6, 137.1 (C_4, C_5), 138.3 (C_3), 154.5 (d, *J*=2.3, $C_{1''}$), 158.0 (d, *J*=239.3, $C_{4''}$), 159.6 ($C_{4'}$). **HPLC (t_R, min)**: 13.3. **MS (ESI, *m/z*)**: 299.1 $[M+H]^+$.

3-(4-Methoxyphenyl)-5-methyl-4-(2-(trifluoromethyl)phenoxy)-1H-pyrazole, 12. Following general procedure D using enaminone **50** (135 mg, 0.36 mmol), compound **12** was obtained as an oil (16 mg, 13%). Chromatography: hexane to hexane/EtOAc 6:4.

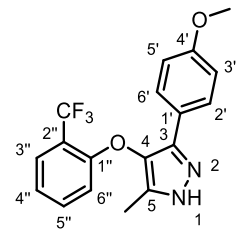

R_f: 0.32 (hexane/EtOAc 1:1). **IR (ATR, cm^{-1})**: ν 3138 (N-H), 1457 (C=C), 1244 (C-O), 1114 (C-O), 1033 (C-F). **^{1}H-NMR ($CDCl_3$, 300 MHz)**: 2.09 (s, 3H, CH_3), 3.76 (s, 3H, OCH_3), 6.74 (d, *J*=8.4, 1H, $H_{6''}$), 6.83 (d, *J*=9.0, 2H, $H_{3'}$, $H_{5'}$), 7.03 (t, *J*=7.7, 1H, $H_{4''}$), 7.27-7.33 (m, 1H, $H_{5''}$), 7.59-7.70 (m, 3H, $H_{2'}$, $H_{6'}$, $H_{3''}$). **^{13}C-NMR ($CDCl_3$, 75 MHz)**: δ 9.7 (CH_3), 55.3 (OCH_3), 114.3 ($C_{6''}$), 114.4 ($C_{3'}$, $C_{5'}$), 118.8 (q, *J*=31.4, $C_{2''}$), 121.5 ($C_{4''}$), 122.4 ($C_{1'}$), 123.8 (d, *J*=272.4, CF_3), 127.3 ($C_{2'}$, $C_{6'}$), 127.4 ($C_{3''}$), 132.3 (C_4/C_5), 133.5 ($C_{5''}$), 137.0 (C_4/C_5), 138.6 (C_3), 156.0 ($C_{1''}$), 159.7 ($C_{4'}$). **HPLC (t_R, min)**: 13.9. **MS (ESI, *m/z*)**: 349.1 $[M+H]^+$.

3-(4-Methoxyphenyl)-5-methyl-4-(3-(trifluoromethyl)phenoxy)-1H-pyrazole, 13. Following general procedure D using enaminone **51** (93 mg, 0.25 mmol), compound **13** was obtained as a white solid (21 mg, 25%). Chromatography: hexane to hexane/EtOAc 6:4.

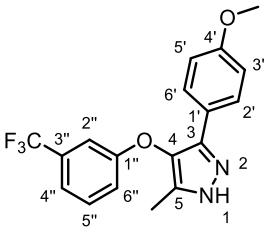

Mp: 105-108 °C. **R_f**: 0.42 (hexane/EtOAc 1:1). **IR (ATR, cm^{-1})**: ν 3136 (N-H), 1448 (C=C), 1244 (C-O), 1164 (C-O), 1119 (C-F). **^{1}H-NMR ($CDCl_3$, 300 MHz)**: 2.11 (s, 3H, CH_3), 3.77 (s, 3H, OCH_3), 6.46 (br s, 1H, NH), 6.84 (d, *J*=8.9, 2H, $H_{3'}$, $H_{5'}$), 7.07 (dd, *J*=8.2, 2.0, 1H, $H_{6''}$), 7.20-7.27 (m, 2H, $H_{2''}$, $H_{4''}$), 7.35 (t, *J*=7.9, 1H, $H_{5''}$), 7.60 (d, *J*=8.9, 2H, $H_{2'}$, $H_{6'}$). **^{13}C-NMR ($CDCl_3$, 75 MHz)**: δ 9.9 (CH_3), 55.4 (OCH_3), 112.4 (q, *J*=3.9, $C_{2''}$), 114.4 ($C_{3'}$, $C_{5'}$), 118.3 ($C_{6''}$), 119.0 (q, *J*=3.9, $C_{4''}$), 122.3 ($C_{1'}$), 123.9 (q, *J*=272.5, CF_3), 127.4 ($C_{2'}$, $C_{6'}$), 130.4 ($C_{5''}$), 132.3 (q, *J*=32.5, $C_{3''}$), 132.7, 137.0 (C_4, C_5), 138.6 (C_3), 158.6 ($C_{1''}$), 159.8 ($C_{4'}$). **HPLC (t_R, min)**: 14.0. **MS (ESI, *m/z*)**: 349.1 $[M+H]^+$.

3-(4-Methoxyphenyl)-5-methyl-4-(4-(trifluoromethyl)phenoxy)-1H-pyrazole, 14. Following general procedure D using enaminone **52** (78 mg, 0.21 mmol), compound **14** was obtained as a white solid (8 mg, 11%). Chromatography: hexane to hexane/EtOAc 6:4.

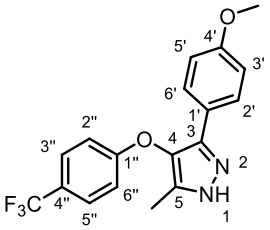

Mp: 167 °C. **R_f**: 0.54 (hexane/EtOAc 1:1). **IR (ATR, cm^{-1})**: ν 3209 (N-H), 1245 (C-O), 1103 (C-O), 1064 (C-F). **^{1}H-NMR ($CDCl_3$, 300 MHz)**: 2.12 (s, 3H, CH_3), 3.78 (s, 3H, OCH_3), 6.11 (br s, 1H, NH), 6.85 (d, *J*=8.9, 2H, $H_{3'}$, $H_{5'}$), 7.00 (d, *J*=8.4, 2H, $H_{2''}$, $H_{6''}$), 7.51 (d, *J*=8.5, 2H, $H_{3''}$, $H_{5''}$), 7.59 (d, *J*=8.9, 2H, $H_{2'}$, $H_{6'}$). **^{13}C-NMR ($CDCl_3$, 75 MHz)**: δ 9.8 (CH_3), 55.4 (OCH_3), 114.5 ($C_{3'}$, $C_{5'}$), 115.3 ($C_{2''}$, $C_{6''}$), 120.7 (q, *J*=271.1, CF_3), 122.2 ($C_{1'}$), 124.5 (q, *J*=32.7, $C_{4''}$), 127.34 ($C_{2'}$, $C_{6'}$), 127.35 (q, *J*=3.6, $C_{3''}$, $C_{5''}$), 132.7, 137.1 (C_4, C_5), 138.5 (C_3), 159.8 ($C_{4'}$), 160.9 (d, *J*=1.2, $C_{1''}$). **HPLC (t_R, min)**: 14.0. **MS (ESI, *m/z*)**: 349.1 $[M+H]^+$.

3-(4-Methoxyphenyl)-5-methyl-4-(*o*-tolyloxy)-1*H*-pyrazole, 15. Following general procedure D using enaminone **53** (106 mg, 0.33 mmol), compound **15** was obtained as an off-white solid (15 mg, 16%). Chromatography: hexane to hexane/EtOAc 6:4.

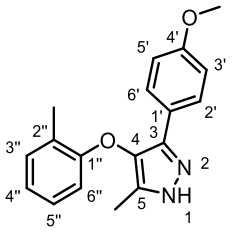

Mp: 104 °C. **R_f**: 0.34 (hexane/EtOAc 1:1). **IR (ATR, cm^{-1})**: ν 3140 (N-H), 1486 (C=C), 1242 (C-O), 1177 (C-O). **^{1}H-NMR ($CDCl_3$, 300 MHz)**: 2.09 (s, 3H, CH_{3pyr}), 2.44 (s, 3H, CH_{3Ar}), 3.77 (s, 3H, OCH_3), 6.61 (dd, *J*=8.2, 1.3, 1H, $H_{6''}$), 6.84 (d, *J*=8.8, 2H, $H_{3'}$, $H_{5'}$), 6.90 (td, *J*=7.4, 1.3, 1H, $H_{4''}$), 6.96-7.06 (m, 1H, $H_{5''}$), 7.21 (dd, *J*=7.3, 1.8, 1H, $H_{3''}$), 7.63 (d, *J*=8.9, 2H, $H_{2'}$, $H_{6'}$), 7.85 (br s, 1H, NH). **^{13}C-NMR ($CDCl_3$, 75 MHz)**: δ 9.8 (CH_{3pyr}), 16.5 (CH_{3Ar}), 55.4 (OCH_3), 112.9 ($C_{6''}$), 114.3 ($C_{3'}$, $C_{5'}$), 121.9 ($C_{4''}$), 122.7 ($C_{1'}$), 126.5 ($C_{2''}$), 127.0 ($C_{5''}$), 127.3 ($C_{2'}$, $C_{6'}$), 131.2 ($C_{3''}$), 133.3, 137.2 (C_4, C_5), 138.4 (C_3), 156.5 ($C_{1''}$), 159.6 ($C_{4'}$). **HPLC (t_R, min)**: 13.8. **MS (ESI, *m/z*)**: 295.2 $[M+H]^+$.

3-(4-Methoxyphenyl)-5-methyl-4-(*m*-tolyloxy)-1*H*-pyrazole, 16. Following general procedure D using enaminone **54** (150 mg, 0.46 mmol), compound **16** was obtained as an off-white solid (52 mg, 38%). Chromatography: hexane to hexane/EtOAc 6:4.

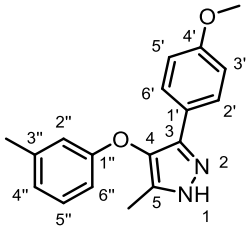

Mp: 107 °C. **R_f**: 0.38 (hexane/EtOAc 1:1). **IR (ATR, cm^{-1})**: ν 3137 (N-H), 1512 (C=C), 1250 (C-O). **^{1}H-NMR ($CDCl_3$, 300 MHz)**: 2.09 (s, 3H, CH_{3pyr}), 2.30 (s, 3H, CH_{3Ar}), 3.75 (s, 3H, OCH_3), 6.72-6.82 (m, 3H, $H_{2''}$, $H_{4''}$, $H_{6''}$), 6.81 (d, *J*=8.8, 2H, $H_{3'}$, $H_{5'}$), 7.14 (t, *J*=8.1, 1H, $H_{5''}$), 7.65 (d, *J*=8.9, 2H, $H_{2'}$, $H_{6'}$), 10.28 (br s, 1H, NH). **^{13}C-NMR ($CDCl_3$, 75 MHz)**: δ 9.8 (CH_{3pyr}), 21.6 (CH_{3Ar}), 55.3 (OCH_3), 112.1 ($C_{6''}$), 114.2 ($C_{3'}$, $C_{5'}$), 115.9 ($C_{2''}$), 122.8 ($C_{4''}$), 122.9 ($C_{1'}$), 127.4 ($C_{2'}$, $C_{6'}$), 129.5 ($C_{5''}$), 133.3, 137.1 (C_4, C_5), 138.5 (C_3), 139.9 ($C_{3''}$), 158.5 ($C_{1''}$), 159.4 ($C_{4'}$). **HPLC (t_R, min)**: 13.7. **MS (ESI, *m/z*)**: 295.2 $[M+H]^+$.

3-(4-Methoxyphenyl)-5-methyl-4-(*p*-tolyloxy)-1*H*-pyrazole, 17. Following general procedure D using enaminone **55** (100 mg, 0.31 mmol), compound **17** was obtained as an oil (22 mg, 24%). Chromatography: hexane to hexane/EtOAc 6:4.

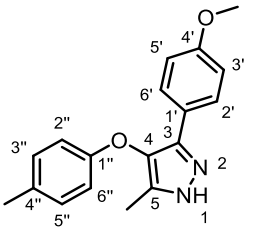

R_f: 0.33 (hexane/EtOAc 1:1). **IR (ATR, cm^{-1})**: ν 3139 (N-H), 1500 (C=C), 1243 (C-O), 1205 (C-O). **^{1}H-NMR ($CDCl_3$, 300 MHz)**: 2.09 (s, 3H, CH_{3pyr}), 2.28 (s, 3H, CH_{3Ar}), 3.76 (s, 3H, OCH_3), 6.81 (d, *J*=8.9, 2H, $H_{3'}$, $H_{5'}$), 6.83 (d, *J*=8.6, 2H, $H_{2''}$, $H_{6''}$), 7.04 (d, *J*=8.7, 2H, $H_{3''}$, $H_{5''}$), 7.64 (d, *J*=9.0, 2H, $H_{2'}$, $H_{6'}$), 9.35 (br s, 1H, NH). **^{13}C-NMR ($CDCl_3$, 75 MHz)**: δ 9.9 (CH_{3pyr}), 20.6 (CH_{3Ar}), 55.3 (OCH_3), 114.2 ($C_{3'}$, $C_{5'}$), 115.0 ($C_{2''}$, $C_{6''}$), 122.9 ($C_{1'}$), 127.4 ($C_{2'}$, $C_{6'}$), 130.2 ($C_{3''}$, $C_{5''}$), 131.3 ($C_{4''}$), 133.5, 137.1 (C_4, C_5), 138.5 (C_3), 156.5 ($C_{1''}$), 159.4 ($C_{4'}$). **HPLC (t_R, min)**: 13.8. **MS (ESI, *m/z*)**: 295.2 $[M+H]^+$.

4-(2-Methoxyphenoxy)-3-(4-methoxyphenyl)-5-methyl-1*H*-pyrazole, 18. Following general procedure D using enaminone **56** (330 mg, 0.97 mmol), compound **18** was obtained as an off-white solid (122 mg, 41%). Chromatography: hexane to hexane/EtOAc 6:4.

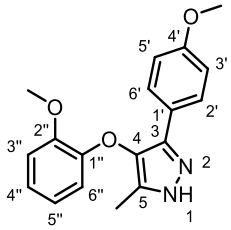

Mp: 114 °C. **R_f**: 0.24 (hexane/EtOAc 1:1). **IR (ATR, cm^{-1})**: ν 3142 (N-H), 1497 (C=C), 1243 (C-O), 1173 (C-O), 1025 (C-O). **^{1}H-NMR ($CDCl_3$, 300 MHz)**: 2.12 (s, 3H, CH_3), 3.77 (s, 3H, $C_{4'}OCH_3$), 3.98 (s, 3H, $C_{2''}OCH_3$), 6.67 (dd, *J*=7.8, 1.3, 1H, $H_{6''}$), 6.72-6.79 (m, 1H, $H_{4''}$/$H_{5''}$), 6.84 (d, *J*=8.9, 2H, $H_{3'}$, $H_{5'}$), 6.91-6.96 (m, 2H, $H_{3''}$, $H_{4''}$/$H_{5''}$), 7.65 (d, *J*=8.9, 2H, $H_{2'}$, $H_{6'}$). **^{13}C-NMR ($CDCl_3$, 75 MHz)**: δ 9.9 (CH_3), 55.4 ($C_{4'}O\underline{C}H_3$), 56.3 ($C_{2''}O\underline{C}H_3$), 112.4 ($C_{3''}$), 114.3 ($C_{3'}$, $C_{5'}$), 114.4 ($C_{6''}$), 121.0, 122.4 ($C_{4''}$, $C_{5''}$), 122.9 ($C_{1'}$), 127.2 ($C_{2'}$, $C_{6'}$), 133.6, 137.2 (C_4, C_5), 138.4 (C_3), 147.8 ($C_{1''}$), 149.1 ($C_{2''}$), 159.5 ($C_{4'}$). **HPLC (t_R, min)**: 12.6. **MS (ESI, *m/z*)**: 311.2 $[M+H]^+$.

4-(3-Methoxyphenoxy)-3-(4-methoxyphenyl)-5-methyl-1*H*-pyrazole, 19. Following general procedure D using enaminone **57** (160 mg, 0.47 mmol), compound **19** was

obtained as an off-white solid (44 mg, 30%). Chromatography: hexane to hexane/EtOAc 6:4.

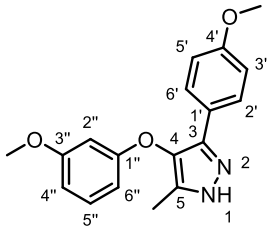

Mp: 110 °C. **R_f**: 0.28 (hexane/EtOAc 1:1). **IR (ATR, cm^{-1})**: ν 3144 (N-H), 1487 (C=C), 1242 (C-O), 1131 (C-O), 1031 (C-O). **^{1}H-NMR ($CDCl_3$, 300 MHz)**: 2.10 (s, 3H, CH_3), 3.75 (s, 3H, OCH_3), 3.76 (s, 3H, OCH_3), 6.49-6.59 (m, 3H, $H_{2''}$, $H_{4''}$, $H_{6''}$), 6.82 (d, *J*=9.1, 2H, $H_{3'}$, $H_{5'}$), 7.09-7.20 (m, 1H, $H_{5''}$), 7.62 (d, *J*=8.8, 2H, $H_{2'}$, $H_{6'}$). **^{13}C-NMR ($CDCl_3$, 75 MHz)**: δ 9.8 (CH_3), 55.3 (OCH_3), 55.4 (OCH_3), 101.7 ($C_{2''}$), 107.5 ($C_{4''}$, $C_{6''}$), 114.3 ($C_{3'}$, $C_{5'}$), 122.8 ($C_{1'}$), 127.4 ($C_{2'}$, $C_{6'}$), 130.2 ($C_{5''}$), 133.2, 137.1 (C_4, C_5), 138.5 (C_3), 159.5, 159.8 ($C_{3''}$, $C_{4'}$), 161.1 ($C_{1''}$). **HPLC (t_R, min)**: 13.3. **MS (ESI, *m/z*)**: 311.2 $[M+H]^+$.

4-(4-Methoxyphenoxy)-3-(4-methoxyphenyl)-5-methyl-1*H*-pyrazole, 20. Following general procedure D using enaminone **58** (130 mg, 0.38 mmol), compound **20** was obtained as an off-white solid (73 mg, 32%). Chromatography: hexane to hexane/EtOAc 6:4.

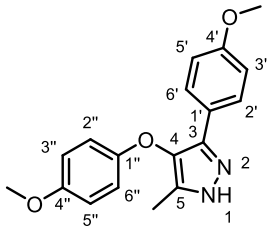

Mp: 115 °C. **R_f**: 0.26 (hexane/EtOAc 1:1). **IR (ATR, cm^{-1})**: ν 3132 (N-H), 1496 (C=C), 1234 (C-O), 1197 (C-O), 1030 (C-O). **^{1}H-NMR ($CDCl_3$, 300 MHz)**: 2.11 (s, 3H, CH_3), 3.75 (s, 3H, $C_{4''}OCH_3$), 3.78 (s, 3H, $C_{4'}OCH_3$), 6.78 (d, *J*=9.3, 2H, $H_{3''}$, $H_{5''}$), 6.86 (d, *J*=8.9, 2H, $H_{3'}$, $H_{5'}$), 6.87 (d, *J*=9.3, 2H, $H_{2''}$, $H_{6''}$), 7.64 (d, *J*=8.9, 2H, $H_{2'}$, $H_{6'}$). **^{13}C-NMR ($CDCl_3$, 75 MHz)**: δ 9.9 (CH_3), 55.4 ($C_{4'}O\underline{C}H_3$), 55.8 ($C_{4''}O\underline{C}H_3$), 114.3 ($C_{3'}$, $C_{5'}$), 114.8 ($C_{3''}$, $C_{5''}$), 116.0 ($C_{2''}$, $C_{6''}$), 122.9 ($C_{1'}$), 127.3 ($C_{2'}$, $C_{6'}$), 133.9, 137.2 (C_4, C_5), 138.3 (C_3), 152.5 ($C_{1''}$), 154.7 ($C_{4''}$), 159.6 ($C_{4'}$). **HPLC (t_R, min)**: 12.9. **MS (ESI, *m/z*)**: 311.2 $[M+H]^+$.

3-((3-(4-Methoxyphenyl)-5-methyl-1*H*-pyrazol-4-yl)oxy)-*N*,*N*-dimethylaniline, 21. Following general procedure D using enaminone **59** (86 mg, 0.24 mmol), compound **21**

was obtained as an off-white solid (20 mg, 26%). Chromatography: hexane to hexane/EtOAc 7:3.

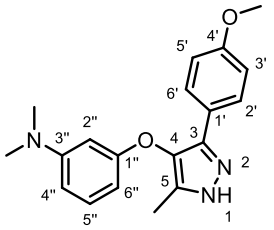

Mp: 139-141 °C. **R_f**: 0.28 (hexane/EtOAc 1:1). **IR (ATR, cm^{-1})**: ν 3200 (N-H), 1613 (C=C), 1502 (C=C), 1248 (C-O). **^{1}H-NMR ($CDCl_3$, 300 MHz)**: δ 2.14 (s, 3H, CH_3), 2.91 (s, 6H, $N(CH_3)_2$), 3.78 (s, 3H, OCH_3), 6.24 (ddd, *J*=8.1, 2.2, 0.9, 1H, $H_{6''}$), 6.34-6.41 (m, 2H, $H_{2''}$, $H_{4''}$), 6.86 (d, *J*=8.9, 2H, $H_{3'}$, $H_{5'}$), 7.09 (dd, *J*=8.9, 8.1, 1H, $H_{5''}$), 7.64 (d, *J*=8.8, 2H, $H_{2'}$, $H_{6'}$). **^{13}C-NMR ($CDCl_3$, 75 MHz)**: δ 10.0 (CH_3), 40.6 ($N(CH_3)_2$), 55.4 (OCH_3), 99.9 ($C_{2''}$), 103.0 ($C_{6''}$), 106.6 ($C_{4''}$), 114.4 ($C_{3'}$, $C_{5'}$), 122.9 ($C_{1'}$), 127.3 ($C_{2'}$, $C_{6'}$), 130.0 ($C_{5''}$), 133.5, 137.5 (C_4, C_5), 138.5 (C_3), 152.1 ($C_{3''}$), 159.5, 159.6 ($C_{1''}$, $C_{4'}$). **HPLC (t_R, min)**: 15.0. **MS (ESI, *m/z*)**: 324.3 $[M+H]^+$.

4-((3-(4-Methoxyphenyl)-5-methyl-1*H*-pyrazol-4-yl)oxy)-*N*,*N*-dimethylaniline, 22. Following general procedure D using enaminone **60** (176 mg, 0.50 mmol), compound **22** was obtained as an oil (20 mg, 13%). Chromatography: hexane to hexane/EtOAc 6:4.

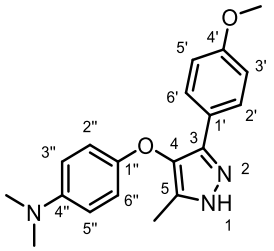

R_f: 0.24 (hexane/EtOAc 1:1). **IR (ATR, cm^{-1})**: ν 3250 (N-H), 1505 (C=C), 1245 (C-O). **^{1}H-NMR ($CDCl_3$, 300 MHz)**: δ 2.11 (s, 3H, CH_3), 2.87 (s, 6H, $N(CH_3)_2$), 3.78 (s, 3H, OCH_3), 6.70 (d, *J*=9.2, 2H, $H_{3''}$, $H_{5''}$), 6.85 (d, *J*=9.3, 2H, $H_{2''}$, $H_{6''}$), 6.86 (d, *J*=8.9, 2H, $H_{3'}$, $H_{5'}$), 7.66 (d, *J*=8.9, 2H, $H_{2'}$, $H_{6'}$). **^{13}C-NMR ($CDCl_3$, 75 MHz)**: δ 10.0 (CH_3), 41.8 ($N(CH_3)_2$), 55.4 (OCH_3), 114.3 ($C_{3'}$, $C_{5'}$), 114.7 ($C_{3''}$, $C_{5''}$), 115.9 ($C_{2''}$, $C_{6''}$), 122.9 ($C_{1'}$), 127.3 ($C_{2'}$, $C_{6'}$), 134.2, 137.3 (C_4, C_5), 138.2 (C_3), 146.3 ($C_{4''}$), 150.8 ($C_{1''}$), 159.5 ($C_{4'}$). **HPLC (t_R, min)**: 10.0. **MS (ESI, *m/z*)**: 324.3 $[M+H]^+$.

***N*-(2-((3-(4-Methoxyphenyl)-5-methyl-1*H*-pyrazol-4-yl)oxy)phenyl)acetamide, 23.** Following general procedure D using enaminone **61** (210 mg, 0.57 mmol), compound **23** was obtained as an off-white solid (90 mg, 47%). Chromatography: hexane to hexane/EtOAc 7:3.

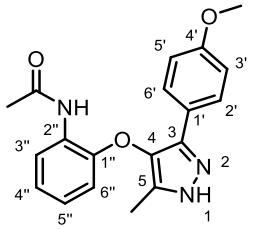

Mp: 223-225 °C. **R_f**: 0.55 (EtOAc). **IR (ATR, cm^{-1})**: ν 3226 (N-H), 1668 (C=O), 1604 (C=C), 1530 (C=C), 1449 (C-N), 1248 (C-O). **^{1}H-NMR (DMSO-*d*$_6$, 300 MHz)**: δ 2.00 (br s, 3H, CH_{3pyr}), 2.16 (s, 3H, CH_3CO), 3.72 (s, 3H, OCH_3), 6.52-6.59 (m, 1H, $H_{6''}$), 6.80-7.02 (m, 4H, $2H_{Ar}$, $H_{3'}$, $H_{5'}$, $H_{4''}$, $H_{5''}$), 7.65 (br s, 2H, $H_{2'}$, $H_{6'}$), 8.00 (br s, 1H, $H_{3''}$), 9.61 (s, 1H, NHCO), 12.65 (s, 1H, NH_{pyr}). **^{13}C-NMR (DMSO-*d*$_6$, 75 MHz)**: δ 9.0 (CH_{3pyr}), 23.8 ($\underline{C}H_3CO$), 55.1 (OCH_3), 112.9 ($C_{6''}$), 113.9 (br s, $C_{3'}$, $C_{5'}$), 121.6 ($C_{4''}$/$C_{5''}$), 123.1 ($C_{3''}$), 124.3 ($C_{4''}$/$C_{5''}$), 125.0 ($C_{1'}$), 126.5 (br s, $C_{2'}$, $C_{6'}$), 127.6 ($C_{2''}$), 132.1, 134.0, 137.9 (C_3, C_4, C_5), 158.6, 158.9 ($C_{1''}$, $C_{4'}$), 168.8 (C=O). **HPLC (t_R, min)**: 11.5. **MS (ESI, *m/z*)**: 338.2 $[M+H]^+$.

***N*-(3-((3-(4-Methoxyphenyl)-5-methyl-1*H*-pyrazol-4-yl)oxy)phenyl)acetamide, 24.** Following general procedure D using enaminone **62** (165 mg, 0.45 mmol), compound **24** was obtained as a white solid (80 mg, 53%). Chromatography: hexane to hexane/EtOAc 6:4.

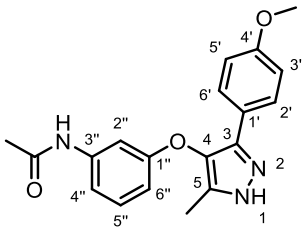

Mp: 223-225 °C. **R_f**: 0.23 (EtOAc). **IR (ATR, cm^{-1})**: ν 3300 (N-H), 1668 (C=O), 1602 (C=C), 1487 (C-N), 1252 (C-O). **^{1}H-NMR (methanol-*d*$_4$, 300 MHz)**: δ 2.06 (s, 3H, CH_3CO), 2.10 (s, 3H, CH_{3pyr}), 3.76 (s, 3H, OCH_3), 6.65 (dt, *J*=7.0, 2.5, 1H, $H_{6''}$), 6.88 (d, *J*=8.9, 2H, $H_{3'}$, $H_{5'}$), 7.14-7.25 (m, 3H, $H_{2''}$, $H_{4''}$, $H_{5''}$), 7.61 (d, *J*=8.9, 2H, $H_{2'}$, $H_{6'}$), 7.90 (s, 1H, NHCO). **^{13}C-NMR (methanol-*d*$_4$, 75 MHz)**: δ 9.5 (CH_{3pyr}), 23.8 ($\underline{C}H_3CO$), 55.7 (OCH_3), 107.7 ($C_{4''}$), 111.6 ($C_{6''}$), 114.6 ($C_{2''}$), 115.1 ($C_{3'}$, $C_{5'}$), 123.6 ($C_{1'}$), 128.3 ($C_{2'}$, $C_{6'}$), 130.9 ($C_{5''}$), 134.0, 137.9 (C_4,

C_5), 141.4 ($C_{3''}$), 160.2 ($C_{1''}$), 161.0 ($C_{4'}$), 171.7 (C=O), C_3 was not observed. **HPLC (t_R, min)**: 11.5. **MS (ESI, *m/z*)**: 338.2 $[M+H]^+$.

4.1.6. Synthesis of intermediate ketones 69-74

2-(2,4-Dichlorophenoxy)-1-(4-methoxyphenyl)ethan-1-one, 69. Following general procedure B using 2,4-dichlorophenol (1.00 g, 6.13 mmol) and 2-bromo-1-(4-methoxyphenyl)ethanone (1.40 g, 6.13 mmol), compound **69** was obtained as a white solid (1.53 g, 80%). Chromatography: hexane to hexane/EtOAc 8:2.

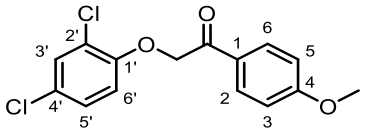

Mp: 110-112 °C. **R_f**: 0.40 (hexane/EtOAc 8:2). **IR (ATR, cm^{-1})**: ν 1691 (C=O), 1231 (C-O). **^{1}H-NMR ($CDCl_3$, 300 MHz)**: δ 3.88 (s, 3H, CH_3), 5.27 (s, 2H, CH_2), 6.77 (d, *J*=8.8, 1H, $H_{6'}$), 6.96 (d, *J*=9.0, 2H, H_3, H_5), 7.12 (dd, *J*=8.8, 2.5, 1H, $H_{5'}$), 7.37 (d, *J*=2.5, 1H, $H_{3'}$), 7.99 (d, *J*=9.0, 2H, H_2, H_6). **^{13}C-NMR ($CDCl_3$, 75 MHz)**: δ 55.7 (CH_3), 72.0 (CH_2), 114.2 (C_3, C_5), 115.0 ($C_{6'}$), 124.2 ($C_{2'}$), 126.9 ($C_{4'}$), 127.4 (C_1), 127.7 ($C_{5'}$), 130.4 ($C_{3'}$), 130.8 (C_2, C_6), 152.8 ($C_{1'}$), 164.4 (C_4), 192.3 (C=O). **HPLC (t_R, min)**: 15.4. **MS (ESI, *m/z*)**: 311.1, 313.0, 315.1 $[M+H]^+$.

2-(3,5-Dichlorophenoxy)-1-(4-methoxyphenyl)ethan-1-one, 70. Following general procedure B using 3,5-dichlorophenol (250 mg, 1.53 mmol) and 2-bromo-1-(4-methoxyphenyl)ethanone (351 mg, 1.53 mmol), compound **70** was obtained as a white solid (324 mg, 68%). Chromatography: hexane to hexane/EtOAc 9:1.

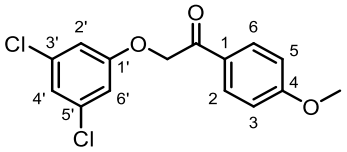

Mp: 96-98 °C. **R_f**: 0.38 (hexane/EtOAc 8:2). **IR (ATR, cm^{-1})**: ν 1700 (C=O), 1550 (C=C), 1290 (C-O), 780 (C-Cl). **^{1}H-NMR ($CDCl_3$, 300 MHz)**: δ 3.90 (s, 3H, CH_3), 5.22 (s, 2H, CH_2), 6.83 (d, *J*=1.8, 2H, $H_{2'}$, $H_{6'}$), 6.94-7.02 (m, 2H, H_3, H_5, $H_{4'}$) 7.97 (d, *J*=9.0, 2H, H_2, H_6). **^{13}C-NMR ($CDCl_3$, 75 MHz)**: δ 55.7 (CH_3), 70.8 (CH_2), 114.1 ($C_{2'}$, $C_{6'}$), 114.3 (C_3, C_5), 122.1 ($C_{4'}$), 127.3 (C_1), 130.6 (C_2, C_6), 135.6 ($C_{3'}$, $C_{5'}$), 159.3 ($C_{1'}$), 164.4 (C_4), 191.7 (C=O). **HPLC (t_R, min)**: 15.4. **MS (ESI, *m/z*)**: 311.1, 313.1, 315.1 $[M+H]^+$.

2-(3,4-Dichlorophenoxy)-1-(4-methoxyphenyl)ethan-1-one, 71. Following general procedure B using 3,4-dichlorophenol (150 mg, 0.92 mmol) and 2-bromo-1-(4-methoxyphenyl)ethanone (211 mg, 0.92 mmol), compound **71** was obtained as a white solid (134 mg, 47%). Chromatography: hexane to hexane/EtOAc 8:2.

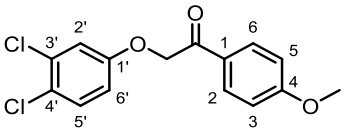

Mp: 102-104 °C. $\mathbf{R_f}$: 0.51 (hexane/EtOAc 7:3). **IR (ATR, cm^{-1})**: ν 1686 (C=O), 1598 (C=C), 1470 (C=C), 1219 (C-O), 832 (C-Cl). **^{1}H-NMR ($CDCl_3$, 300 MHz)**: δ 3.89 (s, 3H, CH_3), 5.21 (s, 2H, CH_2), 6.80 (dd, *J*=8.9, 2.9, 1H, $H_{6'}$), 6.98 (d, *J*=9.0, 2H, H_3, H_5), 7.03 (d, *J*=2.9, 1H, $H_{2'}$), 7.32 (d, *J*=8.9, 1H, $H_{5'}$), 7.97 (d, *J*=9.0, 2H, H_2, H_6).**^{13}C-NMR ($CDCl_3$, 75 MHz)**: δ 55.7 (CH_3), 70.9 (CH_2), 114.3 (C_3, C_5), 114.8 ($C_{6'}$), 117.0 ($C_{2'}$), 125.1 ($C_{4'}$), 127.4 (C_1), 130.6 (C_2, C_6), 130.9 ($C_{5'}$), 133.1 ($C_{3'}$), 157.3 ($C_{1'}$), 164.4 (C_4), 192.2 (C=O). **HPLC (t_R, min)**: 15.0. **MS (ESI, *m/z*)**: 311.1, 313.1, 315.1 $[M+H]^+$.

2-(2,5-Dichlorophenoxy)-1-(4-methoxyphenyl)ethan-1-one, 72. Following general procedure B using 2,5-dichlorophenol (200 mg, 1.23 mmol) and 2-bromo-1-(4-methoxyphenyl)ethanone (281 mg, 1.23 mmol), compound **72** was obtained as a white solid (220 mg, 58%). Chromatography: hexane to hexane/EtOAc 9:1.

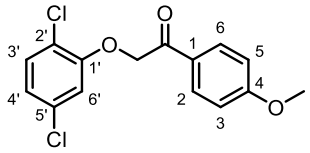

Mp: 120-123 °C. $\mathbf{R_f}$: 0.6 (hexane/EtOAc 7:3). **IR (ATR, cm^{-1})**: ν 1687(C=O), 1599 (C=C), 1478 (C=C), 1230 (C-O), 1172 (C-O). **^{1}H-NMR ($CDCl_3$, 300 MHz)**: δ 3.89 (s, 3H, CH_3), 5.29 (s, 2H, CH_2), 6.83 (d, *J*=2.3, 1H, $H_{6'}$), 6.91 (dd, *J*=8.5, 2.2, 1H, $H_{4'}$), 6.97 (d, *J*=9.0, 2H, H_3, H_5), 7.30 (d, *J*=8.5, 1H, $H_{3'}$), 8.00 (d, *J*=9.0, 2H, H_2, H_6). **^{13}C-NMR ($CDCl_3$, 75 MHz)**: δ 55.7 (CH_3), 71.7 (CH_2), 114.3 (C_3, C_5), 114.6 ($C_{6'}$), 121.8 ($C_{2'}$), 122.5 ($C_{4'}$), 127.4 (C_1), 130.8 (C_2, C_6), 131.2 ($C_{3'}$), 133.2 ($C_{5'}$), 154.4 ($C_{1'}$), 164.4 (C_4), 191.8 (C=O). **HPLC (t_R, min)**: 15.0. **MS (ESI, *m/z*)**: 311.1, 313.1, 315.1 $[M+H]^+$.

2-(2,4-Difluorophenoxy)-1-(4-methoxyphenyl)ethan-1-one, 73. Following general procedure B using 2,4-difluorophenol (1.00 g, 7.70 mmol) and 2-bromo-1-(4-

methoxyphenyl)ethanone (1.76 g, 7.70 mmol), compound **73** was obtained as a white solid (560 mg, 26%). Chromatography: hexane/EtOAc 9:1 to 8:2.

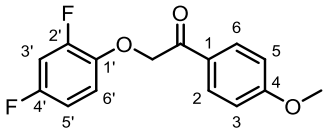

Mp: 151-153 °C. **R_f**: 0.79 (hexane/EtOAc 7:3). **IR (ATR, cm^{-1})**: ν 1631 (C=O), 1230 (C-O). **^{1}H-NMR ($CDCl_3$, 300 MHz)**: δ 3.88 (s, 3H, CH_3), 5.26 (s, 2H, CH_2), 6.75 (dddd, *J*=9.2, 7.8, 3.0, 1.7, 1H, $H_{5'}$), 6.81-6.94 (m, 2H, $H_{3'}$, $H_{6'}$), 6.96 (d, *J*=9.0, 2H, H_3, H_5), 7.97 (d, *J*=9.0, 2H, H_2, H_6). **^{13}C-NMR ($CDCl_3$, 75 MHz)**: δ 55.7 (CH_3), 73.0 (CH_2), 105.3 (dd, *J*=26.9, 22.2, $C_{3'}$), 110.5 (dd, *J*=22.6, 4.0, $C_{5'}$), 114.2 (C_3, C_5), 117.5 (dd, *J*=9.6, 2.7, $C_{6'}$), 127.5 (C_1), 130.6 (C_2, C_6), 142.9 (dd, *J*=10.6, 3.5, $C_{1'}$), 153.0 (dd, *J*=249.8, 12.3, $C_{2'}$), 157.3 (dd, *J*=242.8, 10.7, $C_{4'}$), 164.3 (C_4), 192.6 (C=O). **HPLC (t_R, min)**: 13.9. **MS (ESI, *m/z*)**: 279.0 $[M+H]^+$.

2-(3,4-Difluorophenoxy)-1-(4-methoxyphenyl)ethan-1-one, 74. Following general procedure B using 3,4-difluorophenol (200 mg, 1.54 mmol) and 2-bromo-1-(4-methoxyphenyl)ethanone (352 mg, 1.54 mmol), compound **74** was obtained as an off-white solid (247 mg, 58%). Chromatography: hexane to hexane/EtOAc 7:3.

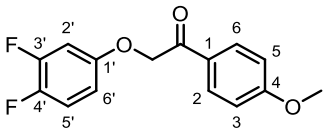

Mp: 92-93 °C. **R_f**: 0.43 (hexane/EtOAc 7:3). **IR (ATR, cm^{-1})**: ν 1689 (C=O), 1599 (C=C), 1511 (C=C), 1237 (C-O), 1159 (C-F). **^{1}H-NMR ($CDCl_3$, 300 MHz)**: 3.89 (s, 3H, CH_3), 5.19 (s, 2H, CH_2), 6.63 (dtd, *J*=9.1, 3.2, 1.7, 1H, $H_{6'}$), 6.77 (ddd, *J*=11.7, 6.5, 3.0, 1H, $H_{2'}$), 6.97 (d, *J*=9.0, 2H, H_3, H_5), 7.05 (dt, *J*=10.0, 9.0, 1H, $H_{5'}$), 7.97 (d, *J*=9.0, 2H, H_2, H_6). **^{13}C-NMR ($CDCl_3$, 75 MHz)**: δ 55.7 (CH_3), 71.3 (CH_2), 109.9 (d, *J*=20.5, $C_{2'}$), 110.2 (dd, *J*=5.9, 3.5, $C_{6'}$), 114.3 (C_3, C_5), 117.4 (dd, *J*=18.7, 1.6, $C_{5'}$), 127.5 (C_1), 130.6 (C_2, C_6), 145.9 (dd, *J*=241.8, 12.8, $C_{3'}$/$C_{4'}$), 150.7 (dd, *J*=248.6, 14.0, $C_{3'}$/$C_{4'}$), 154.6 ($C_{1'}$), 164.4 (C_4), 195.5 (C=O). **HPLC (t_R, min)**: 13.9. **MS (ESI, *m/z*)**: 279.0 $[M+H]^+$.

4.1.7. Synthesis of intermediate enaminones 75-80

4-(2,4-Dichlorophenoxy)-3-(4-methoxyphenyl)-5-methyl-1H-pyrazole, 75.
Following general procedure C using compound **69** (263 mg, 0.85 mmol), crude compound **75** was obtained as an oil (168 mg, 52% crude yield).

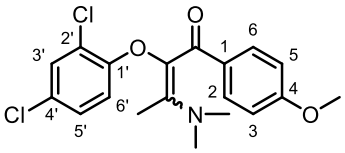

R_f: 0.30 (EtOAc). **^{1}H-NMR ($CDCl_3$, 300 MHz)**: δ Mixture of isomers A:B (1:1): 2.04 (s, 3H, CH_{3A}), 2.40 (s, 3H, CH_{3B}), 2.99 (s, 6H, $N(CH_3)_{2B}$), 3.02 (s, 6H, $N(CH_3)_{2A}$), 3.78 (s, 3H, OCH_{3AB}), 6.74-6.77 (m, 3H, H_{3AB}, H_{5AB}, $H_{6'B}$), 6.80 (d, *J*=9.0, 1H, $H_{6'A}$), 6.99 (dd, *J*=8.9, 2.5, 1H, $H_{5'A}$), 7.00 (dd, *J*=8.9, 2.5, 1H, $H_{5'B}$), 7.17-7.20 (m, 1H, $H_{3'AB}$), 7.73 (d, *J*=8.9, 2H, H_{2B}, H_{6B}), 7.77 (d, *J*=8.9, 2H, H_{2A}, H_{6A}).

2-(3,5-Dichlorophenoxy)-3-(dimethylamino)-1-(4-methoxyphenyl)but-2-en-1-one, 76. Following general procedure C using compound **70** (156 mg, 0.50 mmol), crude compound **76** was obtained as an oil (188 mg, 99% crude yield).

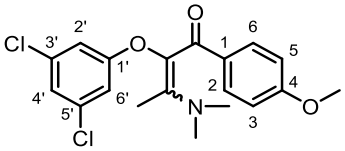

R_f: 0.54 (EtOAc). **^{1}H-NMR ($CDCl_3$, 300 MHz)**: δ Mixture of isomers A:B (1:0.8): 2.06 (s, 3H, CH_{3A}), 2.38 (s, 3H, CH_{3B}), 2.99 (s, 6H, $N(CH_3)_{2B}$), 3.02 (s, 6H, $N(CH_3)_{2A}$), 3.79 (s, 3H, OCH_{3AB}), 6.70 (d, *J*=1.8, 2H, $H_{2'B}$, $H_{6'B}$), 6.73 (d, *J*=1.8, 3H, $H_{2'A}$, $H_{6'A}$), 6.76-6.81 (m, 2H, H_{3AB}, H_{5AB}), 6.83-6.85 (m, 1H, $H_{4'AB}$), 7.64 (d, *J*=8.9, 2H, H_{2B}, H_{6B}), 7.68 (d, *J*=9.0, 2H, H_{2A}, H_{6A}).

2-(3,4-Dichlorophenoxy)-3-(dimethylamino)-1-(4-methoxyphenyl)but-2-en-1-one, 77. Following general procedure C using compound **71** (400 mg, 1.29 mmol), crude compound **77** was obtained as an oil (500 mg, 99% crude yield).

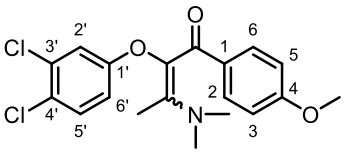

R_f: 0.41 (EtOAc). **^{1}H-NMR ($CDCl_3$, 300 MHz)**: δ Mixture of isomers A:B (1:0.7): 2.03 (s, 3H, CH_{3A}), 2.38 (s, 3H, CH_{3B}), 2.98 (s, 6H, $N(CH_3)_{2B}$), 3.01 (s, 6H, $N(CH_3)_{2A}$), 3.79 (s, 3H, OCH_{3AB}), 6.65 (dd, *J*=8.9, 2.9, $H_{6'B}$), 6.68 (dd, *J*=8.9, 2.9, 1H, $H_{6'A}$), 6.77 (d, *J*=9.0, 2H, H_{3AB}, H_{5AB}), 6.90 (d, *J*=2.9, 1H, $H_{2'B}$), 6.93 (d, *J*=2.8, 1H, $H_{2'A}$), 7.17 (d, *J*=8.9, 1H, $H_{5'A}$), 7.18 (d, *J*=8.8, 1H, $H_{5'B}$), 7.65 (d, *J*=9.1, 2H, H_{2B}, H_{6B}), 7.68 (d, *J*=8.9, 2H, H_{2A}, H_{6A}).

2-(2,5-Dichlorophenoxy)-3-(dimethylamino)-1-(4-methoxyphenyl)but-2-en-1-one, 78. Following general procedure C using compound **72** (195 mg, 0.63 mmol), crude compound **78** was obtained as an oil (220 mg, 92% crude yield).

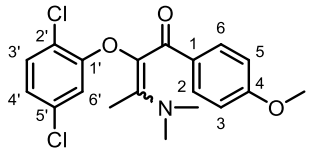

R_f: 0.25 (hexane/EtOAc 1:1). **^{1}H-NMR ($CDCl_3$, 300 MHz)**: δ Mixture of isomers A:B: (1:0.7) 2.06 (s, 3H, CH_{3A}), 2.42 (s, 3H, CH_{3B}), 3.01 (s, 6H, $N(CH_3)_{2A}$), 3.03 (s, 6H, $N(CH_3)_{2B}$), 3.78 (s, 3H, OCH_{3AB}), 6.76 (d, *J*=9.0, 2H, H_{3B}, H_{5B}), 6.77 (d, *J*=9.0, 2H, H_{3A}, H_{5A}), 6.83 (d, *J*=2.4, 1H, $H_{6'AB}$), 6.86-6.91 (m, 2H, $H_{3'AB}$, $H_{4'AB}$), 7.74 (d, *J*=8.9, 2H, H_{2B}, H_{6B}), 7.77 (d, *J*=8.9, 2H, H_{2A}, H_{6A}).

4-(2,4-Difluorophenoxy)-3-(4-methoxyphenyl)-5-methyl-1H-pyrazole, 79. Following general procedure C using compound **73** (200 mg, 0.72 mmol), crude compound **79** was obtained as an oil (100 mg, 40% crude yield).

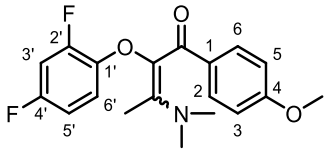

R_f: 0.17 (hexane/EtOAc 4:6). **^{1}H-NMR ($CDCl_3$, 300 MHz)**: δ Mixture of isomers A:B (1:0.7): 2.08 (s, 3H, CH_{3A}), 2.37 (s, 3H, CH_{3B}), 3.01 (s, 6H, $N(CH_3)_{2AB}$), 3.78 (s, 3H, OCH_{3AB}), 6.55-6.87 (m, 3H, $H_{3'AB}$, $H_{5'AB}$, $H_{6'AB}$), 6.76 (d, *J*=8.8, 2H, H_{3AB}, H_{5AB}), 7.69-7.75 (m, 2H, H_{2AB}, H_{6AB}).

2-(3,4-Difluorophenoxy)-3-(dimethylamino)-1-(4-methoxyphenyl)but-2-en-1-one, 80. Following general procedure C using compound **74** (200 mg, 0.72 mmol), crude compound **80** was obtained as an oil (250 mg, 99% crude yield).

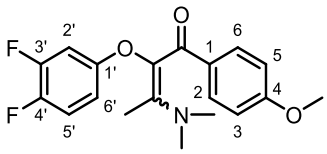

R_f: 0.12 (hexane/EtOAc 1:1). **^{1}H-NMR ($CDCl_3$, 300 MHz)**: δ Mixture of isomers A:B (1:0.7): 2.05 (s, 3H, CH_{3A}), 2.37 (s, 3H, CH_{3B}), 2.99 (s, 6H, $N(CH_3)_{2B}$), 3.01 (s, 6H, $N(CH_3)_{2A}$),

3.78 (s, 3H, OCH_{3AB}), 6.43-6.57 (m, 1H, $H_{6'AB}$), 6.56-6.69 (m, 1H, $H_{2'AB}$), 6.76 (d, *J*=8.9, 2H, H_{3AB}, H_{5AB}), 6.85-6.97 (m, 1H, $H_{5'AB}$), 7.64 (d, *J*=8.8, 2H, H_{2B}, H_{6B}), 7.67 (d, *J*=8.8, 2H, H_{2A}, H_{6A}).

4.1.8. Synthesis of final compounds 63-68

4-(2,4-Dichlorophenoxy)-3-(4-methoxyphenyl)-5-methyl-1*H*-pyrazole, 63.
Following general procedure D using enaminone **75** (154 mg, 0.41 mmol), compound **63** was obtained as an oil (63 mg, 44%). Chromatography: hexane to hexane/EtOAc 7:3.

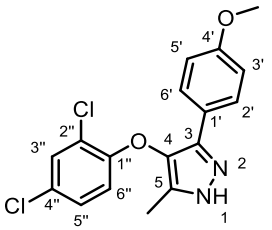

R_f: 0.16 (hexane/EtOAc 1:1). **IR (ATR, cm^{-1})**: ν 3133 (N-H), 1251 (C-O). **^{1}H-NMR ($CDCl_3$, 300 MHz)**: δ 2.13 (s, 3H, CH_3), 3.79 (s, 3H, OCH_3), 6.60 (d, *J*=8.9, 1H, $H_{6''}$), 6.86 (d, *J*=9.0, 2H, $H_{3'}$, $H_{5'}$), 7.00 (dd, *J*=8.9, 2.5, 1H, $H_{5''}$), 7.42 (d, *J*=2.5, 1H, $H_{3''}$), 7.62 (d, *J*=9.0, 2H, $H_{2'}$, $H_{6'}$). **^{13}C-NMR ($CDCl_3$, 75 MHz)**: δ 9.7 (CH_3), 55.4 (OCH_3), 114.5 ($C_{3'}$, $C_{5'}$), 115.6 ($C_{6''}$), 122.1 ($C_{1'}$), 123.3 ($C_{2''}$), 127.26 ($C_{2'}$, $C_{6'}$), 127.32 ($C_{4''}$), 127.9 ($C_{5''}$), 130.4 ($C_{3''}$), 132.9, 137.0 (C_4, C_5), 138.3 (C_3), 152.7 ($C_{1''}$), 159.9 ($C_{4'}$). **HPLC (t_R, min)**: 15.0. **MS (ESI, *m/z*)**: 349.1, 351.0, 353.0 $[M+H]^+$.

4-(3,5-Dichlorophenoxy)-3-(4-methoxyphenyl)-5-methyl-1*H*-pyrazole, 64.
Following general procedure D using enaminone **76** (184 mg, 0.48 mmol), compound **64** was obtained as a white solid (46 mg, 27%). Chromatography: hexane to hexane/EtOAc 7:3.

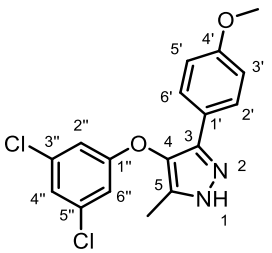

Mp: 171-173 °C. **R_f**: 0.76 (EtOAc). **IR (ATR, cm^{-1})**: ν 3117 (N-H), 1574 (C=C), 1244 (C-O), 831 (C-Cl). **^{1}H-NMR ($CDCl_3$, 300 MHz)**: δ 2.15 (s, 3H, CH_3), 3.81 (s, 3H, OCH_3), 6.84 (d, *J*=1.8, 2H, $H_{2''}$, $H_{6''}$), 6.90 (d, *J*=9.0, 2H, $H_{3'}$, $H_{5'}$), 7.00 (t, *J*=1.8, 1H, $H_{4''}$), 7.57 (d, *J*=9.0, 2H,

$H_{2'}$, $H_{6'}$). **^{13}C-NMR ($CDCl_3$, 75 MHz)**: δ 9.9 (CH_3), 55.4 (OCH_3), 114.3 ($C_{2''}$, $C_{6''}$), 114.5 ($C_{3'}$, $C_{5'}$), 122.3 ($C_{1'}$), 122.7 ($C_{4''}$), 127.3 ($C_{2'}$, $C_{6'}$), 132.5 (C_4/C_5), 135.9 ($C_{3''}$, $C_{5''}$), 136.9 (C_4/C_5), 138.5 (C_3), 159.5 ($C_{1''}$), 159.8 ($C_{4'}$). **HPLC (t_R, min)**: 15.0. **MS (ESI, *m/z*)**: 349.1, 351.0, 353.0 $[M+H]^+$.

4-(3,4-Dichlorophenoxy)-3-(4-methoxyphenyl)-5-methyl-1*H*-pyrazole, 65 (UCM-22018). Following general procedure D using enaminone **77** (260 mg, 0.68 mmol), compound **65** was obtained as a white solid (99 mg, 42%). Chromatography: hexane to hexane/EtOAc 6:4.

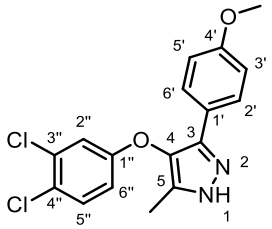

Mp: 152 °C. **R_f**: 0.33 (hexane/EtOAc 1:1). **IR (ATR, cm^{-1})**: ν 3146 (N-H), 1463 (C=C), 1249 (C-O), 1118 (C-O), 833 (C-Cl). **^{1}H-NMR ($CDCl_3$, 300 MHz)**: δ 2.13 (s, 3H, CH_3), 3.79 (s, 3H, OCH_3), 6.79 (dd, *J*=8.9, 2.9, 1H, $H_{6''}$), 6.87 (d, *J*=8.9, 2H, $H_{3'}$, $H_{5'}$), 7.04 (d, *J*=2.9, 1H, $H_{2''}$), 7.30 (d, *J*=8.9, 1H, $H_{5''}$), 7.58 (d, *J*=8.9, 2H, $H_{2'}$, $H_{6'}$). **^{13}C-NMR ($CDCl_3$, 75 MHz)**: δ 9.8 (CH_3), 55.4 (OCH_3), 114.5 ($C_{3'}$, $C_{5'}$), 114.9 ($C_{6''}$), 117.3 ($C_{2''}$), 122.2 ($C_{1'}$), 125.6 ($C_{4''}$), 127.3 ($C_{2'}$, $C_{6'}$), 131.1 ($C_{5''}$), 132.8 (C_4/C_5), 133.4 ($C_{3''}$), 136.9 (C_4/C_5), 138.5 (C_3), 157.4 ($C_{1''}$), 159.8 ($C_{4'}$). **HPLC (t_R, min)**: 15.1. **MS (ESI, *m/z*)**: 349.0, 351.0, 353.0 $[M+H]^+$. **HRMS (ESI, *m/z*)**: calculated for $C_{17}H_{14}Cl_2N_2O_2$ [M-H]: 348.0432, found 349.0437.

4-(2,5-Dichlorophenoxy)-3-(4-methoxyphenyl)-5-methyl-1*H*-pyrazole, 66.
Following general procedure D using enaminone **78** (220 mg, 0.58 mmol), compound **66** was obtained as a white solid (35 mg, 17%). Chromatography: hexane to hexane/EtOAc 6:4.

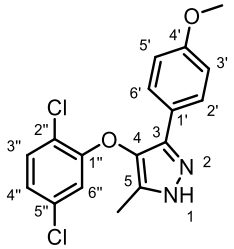

Mp: 150 °C. **R_f**: 0.46 (hexane/EtOAc 1:1). **IR (ATR, cm^{-1})**: ν 3141 (N-H), 1580 (C=C), 1512 (C=C), 1471, 1250 (C-O), 834 (C-Cl). **^{1}H-NMR ($CDCl_3$, 300 MHz)**: δ 2.12 (s, 3H, CH_3), 3.77 (s, 3H, OCH_3), 6.70 (d, *J*=2.3, 1H, $H_{6''}$), 6.84 (d, *J*=8.9, 2H, $H_{3'}$, $H_{5'}$), 6.90 (dd, *J*=8.5, 2.3, 1H, $H_{4''}$), 7.33 (d, *J*=8.5, 1H, $H_{3''}$), 7.63 (d, *J*=8.9, 2H, $H_{2'}$, $H_{6'}$). **^{13}C-NMR ($CDCl_3$, 75 MHz)**: δ 9.7 (CH_3), 55.3 (OCH_3), 114.4 ($C_{3'}$, $C_{5'}$), 115.2 ($C_{6''}$), 121.0 ($C_{2''}$), 122.3 ($C_{1'}$), 123.0 ($C_{4''}$), 127.4 ($C_{2'}$, $C_{6'}$), 131.2 ($C_{3''}$), 132.6 (C_4/C_5), 133.4 ($C_{5''}$), 136.8 (C_4/C_5), 138.5 (C_3), 154.4 ($C_{1''}$), 159.8 ($C_{4'}$). **HPLC (t_R, min)**: 14.7. **MS (ESI, *m/z*)**: 349.0, 351.0, 353.0 $[M+H]^+$.

4-(2,4-Difluorophenoxy)-3-(4-methoxyphenyl)-5-methyl-1*H*-pyrazole, 67.

Following general procedure D using enaminone **79** (135 mg, 0.39 mmol), compound **67** was obtained as an oil (95 mg, 77%). Chromatography: hexane to hexane/EtOAc 7:3.

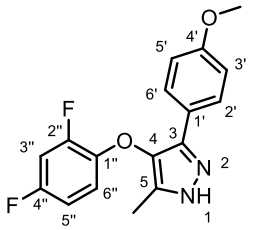

R_f: 0.35 (hexane/EtOAc 1:1). **IR (ATR, cm^{-1})**: ν 3139 (N-H), 1250 (C-O). **^{1}H-NMR ($CDCl_3$, 300 MHz)**: δ 2.13 (s, 3H, CH_3), 3.79 (s, 3H, OCH_3), 5.97 (s, 1H, NH), 6.60-6.68 (m, 2H, $H_{5''}$, $H_{6''}$), 6.86 (d, *J*=8.8, 2H, $H_{3'}$, $H_{5'}$), 6.89-6.93 (m, 1H, $H_{3''}$), 7.63 (d, *J*=8.8, 2H, $H_{2'}$, $H_{6'}$). **^{13}C-NMR ($CDCl_3$, 75 MHz)**: δ 9.7 (CH_3), 55.4 (OCH_3), 105.3 (dd, *J*=27.0, 21.6, $C_{3''}$), 110.7 (dd, *J*=22.7, 3.9, $C_{5''}$), 114.4 ($C_{3'}$, $C_{5'}$), 116.1 (dd, *J*=9.4, 1.9, $C_{6''}$), 122.3 ($C_{1'}$), 127.4 ($C_{2'}$, $C_{6'}$), 133.3, 137.0 (C_4, C_5), 138.4 (C_3), 142.7 (dd, *J*=10.7, 3.6, $C_{1''}$), 151.8 (dd, *J*=249.9, 12.1, $C_{2''}$), 157.1 (dd, *J*=243.0, 10.0, $C_{4''}$), 159.8 ($C_{4'}$). **HPLC (t_R, min)**: 13.6. **MS (ESI, *m/z*)**: 317.1 $[M+H]^+$.

4-(3,4-Difluorophenoxy)-3-(4-methoxyphenyl)-5-methyl-1*H*-pyrazole, 68.

Following general procedure D using enaminone **80** (280 mg, 0.81 mmol), compound **68** was obtained as an off-white solid (89 mg, 35%). Chromatography: hexane to hexane/EtOAc 6:4.

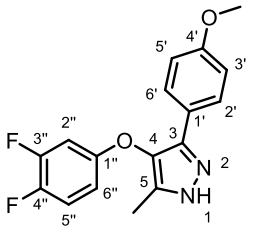

Mp: 128 °C. **R_f**: 0.27 (hexane/EtOAc 1:1). **IR (ATR, cm^{-1})**: ν 3200 (N-H), 1508 (C=C), 1249 (C-O), 1033 (C-F). **^{1}H-NMR ($CDCl_3$, 300 MHz)**: 2.10 (s, 3H, CH_3), 3.89 (s, 3H, OCH_3), 6.63 (dtd, *J*=8.8, 3.2, 1.6, 1H, $H_{6''}$), 6.76 (ddd, *J*=11.5, 6.5, 3.0, 1H, $H_{2''}$), 6.83 (d, *J*=9.0, 2H, $H_{3'}$, $H_{5'}$), 7.02 (q, *J*=9.2, 1H, $H_{5''}$), 7.58 (d, *J*=8.8, 2H, $H_{2'}$, $H_{6'}$). **^{13}C-NMR ($CDCl_3$, 75 MHz)**: δ 9.8 (CH_3), 55.4 (OCH_3), 104.9 (d, *J*=21.0, $C_{2''}$), 110.5 (dd, *J*=5.9, 3.6, $C_{6''}$), 114.4 ($C_{3'}$, $C_{5'}$), 117.6 (dd, *J*=18.6, 1.4, $C_{5''}$), 122.5 ($C_{1'}$), 127.3 ($C_{2'}$, $C_{6'}$), 133.1, 137.2 (C_4, C_5), 138.2 (C_3), 145.9 (dd, *J*=241.8, 12.8, $C_{3''}$/$C_{4''}$), 150.7 (dd, *J*=248.6, 14.0, $C_{3''}$/$C_{4''}$), 154.6 (dd, *J*=8.1, 2.1, $C_{1''}$), 159.7 ($C_{4'}$). **HPLC (t_R, min)**: 13.7. **MS (ESI, *m/z*)**: 317.1 $[M+H]^+$.

4.1.9. Synthesis of intermediate ketones 84-86

2-(3,4-Dichlorophenoxy)-1-phenylethan-1-one, 84. Following general procedure B using 3,4-dichlorophenol (200 mg, 1.23 mmol) and 2-bromoacetophenone (244 mg, 1.23 mmol), compound **84** was obtained as a white solid (175 mg, 51%). Chromatography: hexane to hexane/EtOAc 8:2.

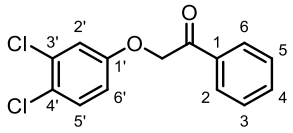

Mp: 101-103 °C. **R_f**: 0.58 (hexane/EtOAc 8:2). **IR (ATR, cm^{-1})**: ν 1697 (C=O), 1470 (C=C), 1220 (C-O), 755 (C-Cl). **^{1}H-NMR ($CDCl_3$, 300 MHz)**: δ 5.28 (s, 2H, CH_2), 6.80 (dd, *J*=8.9, 2.9, 1H, $H_{6'}$), 7.04 (d, *J*=2.9, 1H, $H_{2'}$), 7.33 (d, *J*=8.9, 1H, $H_{5'}$), 7.49-7.55 (m, 2H, H_3, H_5), 7.62-7.68 (m, 1H, H_4), 7.96-8.00 (m, 2H, H_2, H_6).**^{13}C-NMR ($CDCl_3$, 75 MHz)**: δ 70.9 (CH_2), 114.7 ($C_{6'}$), 116.9 ($C_{2'}$), 125.1 ($C_{4'}$), 128.1 (C_2, C_6), 129.0 (C_3, C_5), 130.8 ($C_{5'}$), 133.1 ($C_{3'}$), 134.2 (C_4), 134.2 (C_1), 157.0 ($C_{1'}$), 193.6 (C=O). **HPLC (t_R, min)**: 14.9. **MS (ESI, *m/z*)**: 281.0, 283.0, 285.0 $[M+H]^+$.

2-(3,4-Dichlorophenoxy)-1-(2-methoxyphenyl)ethan-1-one, 85. Following general procedure B using 3,4-dichlorophenol (200 mg, 1.23 mmol) and 2-bromo-1-(2-methoxyphenyl)ethanone (281 mg, 1.23 mmol), compound **85** was obtained as a white solid (202 mg, 53%). Chromatography: hexane to hexane/EtOAc 8:2.

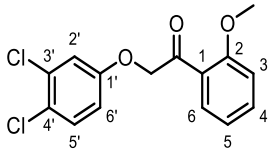

Mp: 74-76 °C. **R_f**: 0.58 (hexane/EtOAc 7:3). **IR (ATR, cm^{-1})**: ν 1682 (C=O), 1593 (C=C), 1471 (C=C), 1284 (C-O), 973 (C-Cl). **^{1}H-NMR ($CDCl_3$, 300 MHz)**: δ 3.98 (s, 3H, CH_3), 5.23 (s, 2H, CH_2), 6.77 (dd, *J*=8.9, 2.9, 1H, $H_{6'}$), 6.99 (d, *J*=2.9, 1H, $H_{2'}$), 7.01-7.12 (m, 2H, H_3, H_5), 7.31 (d, *J*=8.9, 1H, $H_{5'}$), 7.56 (ddd, *J*=8.4, 7.3, 1.9, 1H, H_4), 7.93 (dd, *J*=7.8, 1.8, 1H, H_6). **^{13}C-NMR ($CDCl_3$, 75 MHz)**: δ 55.9 (CH_3), 74.6 (CH_2), 111.7 (C_3), 115.0 ($C_{6'}$), 116.9 ($C_{2'}$), 121.4 (C_5), 124.6 ($C_{4'}$), 124.7 (C_1), 130.8 ($C_{5'}$), 131.2 (C_6), 133.0 ($C_{3'}$), 135.2 (C_4), 157.6 ($C_{1'}$), 159.5 (C_2), 194.7 (C=O). **HPLC (t_R, min)**: 15.3. **MS (ESI, *m/z*)**: 311.0, 313.0, 315.0 $[M+H]^+$.

2-(3,4-Dichlorophenoxy)-1-(3-methoxyphenyl)ethan-1-one, 86. Following general procedure B using 3,4-dichlorophenol (200 mg, 1.23 mmol) and 2-bromo-1-(3-methoxyphenyl)ethanone (281 mg, 1.23 mmol), compound **86** was obtained as a white solid (140 mg, 37%). Chromatography: hexane to hexane/EtOAc 8:2.

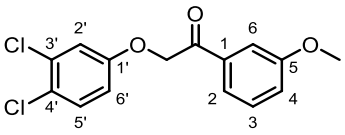

Mp: 106-108 °C. **R_f**: 0.59 (hexane/EtOAc 7:3). **IR (ATR, cm^{-1})**: ν 1701 (C=O), 1585 (C=C), 1472 (C=C), 1261 (C-O), 778 (C-Cl). **^{1}H-NMR ($CDCl_3$, 300 MHz)**: δ 3.85 (s, 3H, CH_3), 5.25 (s, 2H, CH_2), 6.78 (dd, *J*=8.9, 2.9, 1H, $H_{6'}$), 7.01 (d, *J*=2.9, 1H, $H_{2'}$), 7.16 (ddd, *J*=8.2, 2.6, 1.0, 1H, H_4), 7.30 (d, *J*=8.9, 1H, $H_{5'}$), 7.34-7.44 (m, 1H, H_3), 7.55-7.46 (m, 2H, H_2, H_6). **^{13}C-NMR ($CDCl_3$, 75 MHz)**: δ 55.6 (CH_3), 71.0 (CH_2), 112.5 (C_2), 114.8 ($C_{6'}$), 116.9 ($C_{2'}$), 120.5 (C_6), 120.6 (C_4), 125.0 ($C_{4'}$), 130.1 (C_3), 130.9 ($C_{5'}$), 133.1 ($C_{3'}$), 135.5 (C_1), 157.1 ($C_{1'}$), 160.1 (C_5), 193.3 (C=O). **HPLC (t_R, min)**: 15.0. **MS (ESI, *m/z*)**: 311.0, 313.0, 315.0 $[M+H]^+$.

4.1.10. Synthesis of intermediate enaminones 87-89

2-(3,4-Dichlorophenoxy)-3-(dimethylamino)-1-phenylbut-2-en-1-one, 87. Following general procedure C using compound **84** (150 mg, 0.53 mmol), crude compound **87** was obtained as an oil (170 mg, 91% crude yield).

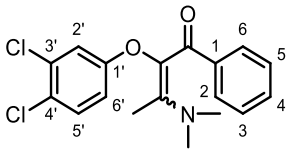

R_f: 0.15 (hexane/EtOAc 1:1). **^{1}H-NMR ($CDCl_3$, 300 MHz)**: δ Mixture of isomers A:B (1:0.8): 2.05 (s, 3H, CH_{3A}), 2.43 (s, 3H, CH_{3B}), 3.00 (s, 6H, $N(CH_3)_{2B}$), 3.06 (s, 6H, $N(CH_3)_{2A}$), 6.61 (dd, *J*=8.9, 2.9, 1H, $H_{6'B}$), 6.65 (dd, *J*=8.9, 2.9, 1H, $H_{6'A}$), 6.86 (d, *J*=2.9, 1H, $H_{2'B}$), 6.90

(d, *J*=2.8, 1H, $H_{2'A}$), 7.17 (d, *J*=8.9, 1H, $H_{5'AB}$), 7.22-7.35 (m, 3H, H_{3AB}, H_{4AB}, H_{5AB}), 7.55-7.65 (m, 2H, H_{2AB}, H_{6AB}).

2-(3,4-Dichlorophenoxy)-3-(dimethylamino)-1-(2-methoxyphenyl)but-2-en-1-one, 88. Following general procedure C using compound **85** (175 mg, 0.56 mmol), crude compound **88** was obtained as an oil (260 mg, 99% crude yield).

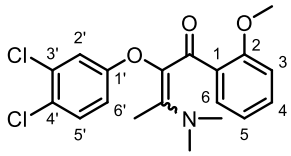

R_f: 0.23 (hexane/EtOAc 1:1). **^{1}H-NMR ($CDCl_3$, 300 MHz)**: δ Mixture of isomers A:B (1:0.7): 2.08 (s, 3H, CH_{3A}), 2.40 (s, 3H, CH_{3B}), 2.97 (s, 6H, $N(CH_3)_{2B}$), 3.01 (s, 6H, $N(CH_3)_{2A}$), 3.79 (s, 3H, OCH_{3AB}), 6.51-7.58 (m, 1H, $H_{6'AB}$), 6.74-7.92 (m, 3H, H_{3AB}, H_{5AB}, $H_{2'AB}$), 7.09 (d, *J*=8.9, 1H, $H_{5'AB}$), 7.10-7.21 (m, 2H, H_{4AB}, H_{6AB}).

2-(3,4-Dichlorophenoxy)-3-(dimethylamino)-1-(3-methoxyphenyl)but-2-en-1-one, 89. Following general procedure C using compound **86** (130 mg, 0.42 mmol), crude compound **89** was obtained as an oil (160 mg, 99% crude yield).

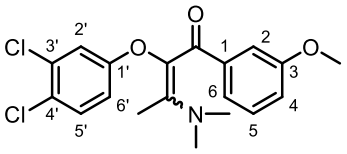

R_f: 0.17 (hexane/EtOAc 1:1). **^{1}H-NMR ($CDCl_3$, 300 MHz)**: δ Mixture of isomers A:B (1:0.7): 2.05 (s, 3H, CH_{3A}), 2.42 (s, 3H, CH_{3B}), 3.00 (s, 6H, $N(CH_3)_{2B}$), 3.07 (s, 6H, $N(CH_3)_{2A}$), 3.73 (s, 3H, OCH_{3A}), 3.74 (s, 3H, OCH_{3B}), 6.64 (dd, *J*=8.9, 2.9, 1H, $H_{6'B}$), 6.67 (dd, *J*=8.9, 2.9, 1H, $H_{6'A}$), 6.84-6.90 (m, 1H, H_{4AB}), 6.88 (d, *J*=2.9, 1H, $H_{2'B}$), 6.92 (d, *J*=2.8, 1H, $H_{2'A}$), 7.09-7.24 (m, 4H, H_{2AB}, H_{5AB}, H_{6AB}, $H_{5'AB}$).

4.1.11. Synthesis of final compounds 81-83

4-(3,4-Dichlorophenoxy)-5-methyl-3-phenyl-1*H*-pyrazole, 81. Following general procedure D using enaminone **87** (170 mg, 0.49 mmol), compound **81** was obtained as an off-white solid (72 mg, 47%). Chromatography: hexane to hexane/EtOAc 6:4.

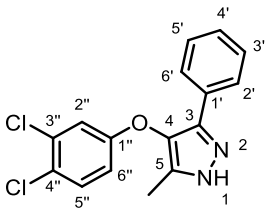

Mp: 77 °C. **R_f**: 0.53 (hexane/EtOAc 1:1). **IR (ATR, cm^{-1})**: ν 3133 (N-H), 1586 (C=C), 1465 (C=C), 1254 (C-O), 1120 (C-O), 909 (C-Cl). **^{1}H-NMR ($CDCl_3$, 300 MHz)**: δ 2.12 (s, 3H, CH_3), 6.80 (dd, *J*=8.9, 2.9, 1H, $H_{6''}$), 7.05 (d, *J*=2.9, 1H, $H_{2''}$), 7.30 (d, *J*=8.9, 1H, $H_{5''}$),7.30-7.37 (m, 3H, $H_{3'}$, $H_{4'}$, $H_{5'}$), 7.64-7.68 (m, 2H, $H_{2'}$, $H_{6'}$). **^{13}C-NMR ($CDCl_3$, 75 MHz)**: δ 9.8 (CH_3), 114.9 ($C_{6''}$), 117.3 ($C_{2''}$), 125.7 ($C_{4''}$), 126.0 ($C_{2'}$, $C_{6'}$), 128.5 ($C_{4'}$), 129.0 ($C_{3'}$, $C_{5'}$), 129.8 ($C_{1'}$), 131.1 ($C_{5''}$), 133.3 (C_4/C_5), 133.4 ($C_{3''}$), 136.8 (C_4/C_5), 138.9 (C_3), 157.4 ($C_{1''}$). **HPLC (t_R, min)**: 15.3. **MS (ESI, *m/z*)**: 319.1, 321.1, 323.1 $[M+H]^+$.

4-(3,4-Dichlorophenoxy)-3-(2-methoxyphenyl)-5-methyl-1*H*-pyrazole, 82.

Following general procedure D using enaminone **88** (285 mg, 0.75 mmol), compound **82** was obtained as an off-white solid (22 mg, 8%). Chromatography: hexane to hexane/EtOAc 6:4.

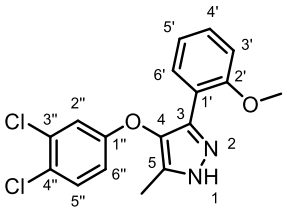

Mp: 134 °C. **R_f**: 0.31 (hexane/EtOAc 1:1). **IR (ATR, cm^{-1})**: ν 3150 (N-H), 1466 (C=C), 1253 (C-O), 753 (C-Cl). **^{1}H-NMR ($CDCl_3$, 300 MHz)**: δ 2.11 (s, 3H, CH_3), 3.98 (s, 3H, OCH_3), 6.83 (dd, *J*=8.9, 2.9, 1H, $H_{6''}$), 6.95 (ddd, *J*=7.7, 7.3, 1.1, 1H, $H_{5'}$), 7.00 (dd, *J*=8.4, 1.1, 1H, $H_{3'}$), 7.06 (d, *J*=2.9, 1H, $H_{2''}$), 7.22-7.31 (m, 1H, $H_{4'}$), 7.31 (d, *J*=8.8, 1H, $H_{5''}$), 7.76 (dd, *J*=7.8, 1.7, 1H, $H_{6'}$). **^{13}C-NMR ($CDCl_3$, 75 MHz)**: δ 10.9 (CH_3), 55.9 (OCH_3), 111.5 ($C_{3'}$), 115.0 ($C_{6''}$), 116.6 ($C_{1'}$), 117.4 ($C_{2''}$), 121.8 ($C_{5'}$), 125.6 ($C_{4''}$), 127.5 ($C_{6'}$), 129.5 ($C_{4'}$), 130.6 (C_3), 131.1 ($C_{5''}$), 133.4 ($C_{3''}$), 133.4, 141.2 (C_4, C_5), 155.8 ($C_{2'}$), 157.1 ($C_{1''}$). **HPLC (t_R, min)**: 15.5. **MS (ESI, *m/z*)**: 349.0, 351.0, 353.0 $[M+H]^+$.

4-(3,4-Dichlorophenoxy)-3-(3-methoxyphenyl)-5-methyl-1*H*-pyrazole, 83.

Following general procedure D using enaminone **89** (165 mg, 0.43 mmol), compound **83** was obtained as an off-white solid (83 mg, 55%). Chromatography: hexane to hexane/EtOAc 6:4.

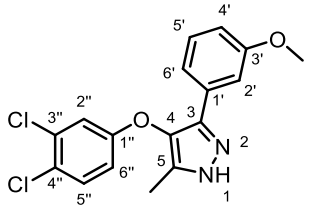

Mp: 136 °C. **R_f**: 0.38 (hexane/EtOAc 1:1). **IR (ATR, cm^{-1})**: ν 3200 (N-H), 1587 (C=C), 1464 (C=C), 1256 (C-O), 1224 (C-O), 855 (C-Cl). **^{1}H-NMR ($CDCl_3$, 300 MHz)**: δ 2.11 (s, 3H, CH_3), 3.72 (s, 3H, OCH_3), 6.79 (dd, *J*=8.9, 2.9, 1H, $H_{6''}$), 6.81-6.86 (m, 1H, $H_{4'}$), 7.04 (d, *J*=2.9, 1H, $H_{2''}$), 7.21-7.27 (m, 3H, $H_{2'}$, $H_{5'}$, $H_{6'}$), 7.29 (d, *J*=8.8, 1H, $H_{5''}$), 7.85 (br s, 1H, NH). **^{13}C-NMR ($CDCl_3$, 75 MHz)**: δ 9.7 (CH_3), 55.3 (OCH_3), 111.3 ($C_{2'}$), 114.4 ($C_{4'}$), 114.9 ($C_{6''}$), 117.2 ($C_{2''}$), 118.4 ($C_{6'}$), 125.7 ($C_{4''}$), 130.1 ($C_{5'}$), 131.0 ($C_{1'}$), 131.1 ($C_{5''}$), 133.3 (C_4/C_5), 133.4 ($C_{3''}$), 136.7 (C_4/C_5), 138.8 (C_3), 157.4 ($C_{1''}$), 160.0 ($C_{3'}$). **HPLC (t_R, min)**: 15.1. **MS (ESI, *m/z*)**: 349.0, 351.0, 353.0 $[M+H]^+$.

4.1.12. Synthesis of intermediate ketones 96-101, 107, 109

2-Bromo-1-(4-((tetrahydro-2*H*-pyran-2-yl)oxy)phenyl)ethan-1-one, 96. To a solution of 2-bromo-1-(4-hydroxyphenyl)ethanone (1.0 eq, 2.37 mmol, 510 mg) in anhydrous DCM (0.5 M), 3,4-dihydro-2*H*-pyran (1.5 eq, 3.56 mmol, 0.33 mL) and pyridinium *p*-toluenesulfonate (0.05 eq, 0.12 mmol, 30 mg) were added and the reaction mixture was stirred at rt for 3 h. After this time, a saturated $NaHCO_3$ solution was added, and the mixture was extracted with DCM (x2). The combined organic phases were dried with Na_2SO_4, filtered and concentrated under reduced pressure to obtain compound **96** as a red solid (621 mg, 88%), which was used without further purification.

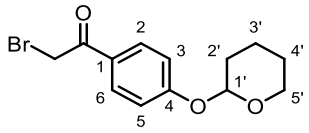

Mp: 106-109 °C. **R_f**: 0.74 (hexane/EtOAc 6:4). **IR (ATR, cm^{-1})**: ν 1671 (C=O), 1597 (C=C), 1245 (C-O), 1169 (C-O), 950 (C-Br). **^{1}H-NMR ($CDCl_3$, 300 MHz)**: δ 1.57-2.12 (m, 6H, $2H_{2'}$, $2H_{3'}$, $2H_{4'}$), 3.63 (dtd, *J*=11.3, 4.0, 1.6, 1H, $H_{5'}$), 3.84 (ddd, *J*=11.3, 9.8, 3.1, 1H, $H_{5'}$), 4.40 (s, 2H, CH_2), 5.53 (t, *J*=3.1, 1H, $H_{1'}$), 7.11 (d, *J*=8.9, 2H, H_3, H_5), 7.95 (d, *J*=8.9, 2H, H_2, H_6). **^{13}C-NMR ($CDCl_3$, 75 MHz)**: δ 18.5 ($C_{3'}$), 25.1 ($C_{4'}$), 30.1 ($C_{2'}$), 30.9 (CH_2), 62.1 ($C_{5'}$), 96.2 ($C_{1'}$), 116.3 (C_3, C_5), 127.5 (C_1), 131.3 (C_2, C_6), 161.8 (C_4), 190.1 (C=O). **HPLC (t_R, min)**: 14.5. **MS (ESI, *m/z*)**: 215.1, 217.1 $[(M\text{-THP})+H]^+$. The spectroscopic data are consistent with those reported in the bibliography.[147]

2-(3,4-Dichlorophenoxy)-1-(4-((tetrahydro-2*H*-pyran-2-yl)oxy)phenyl)ethan-1-one, 97. To a solution of 3,4-dichlorophenol (1.0 eq, 1.67 mmol, 272 mg) and K_2CO_3 (4.2 eq, 7.02 mmol, 970 mg) in anhydrous DMF (0.38 M), compound **96** (1.0 eq, 1.67 mmol, 500 mg) was added and the mixture was heated at 80 °C for 30 min under MW irradiation. After cooling to rt, the reaction mixture was diluted with EtOAc and washed with a 1:1 mixture of water/brine. The organic layer was dried over Na_2SO_4, filtered and concentrated under reduced pressure. The residue was purified by flash chromatography (hexane to hexane/EtOAc 7:3) to obtain compound **97** as a white solid (380 mg, 60%).

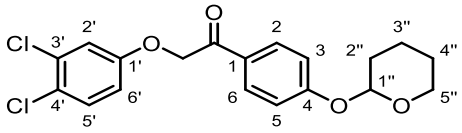

Mp: 132-134 °C. **R_f**: 0.46 (hexane/AcOEt, 8:2). **IR (ATR, cm^{-1})**: ν 1694 (C=O), 1600 (C=C), 1509 (C=C), 1224 (C-O), 954 (C-Cl). **^{1}H-NMR (CDCl$_3$, 300 MHz)**: δ1.58-2.06 (m, 6H, 2H$_{2''}$, 2H$_{3''}$, 2H$_{4''}$), 3.63 (dtd, *J*=11.4, 3.8, 1.5, 1H, H$_{5''}$), 3.84 (ddd, *J*=11.3, 9.8, 3.2, 1H, H$_{5''}$), 5.21 (s, 2H, CH$_2$), 5.54 (t, *J*=2.9, 1H, H$_{1''}$), 6.80 (dd, *J*=8.9, 2.9, 1H, H$_{6'}$), 7.03 (d, *J*=2.9, 1H, H$_{2'}$), 7.13 (d, *J*=9.0, 2H, H$_3$, H$_5$), 7.32 (d, *J*=8.9, 1H, H$_{5'}$), 7.95 (d, *J*=9.0, 2H, H$_2$, H$_6$). **^{13}C-NMR (CDCl$_3$, 75 MHz)**: δ 18.5 (C$_{3''}$), 25.2 (C$_{4''}$), 30.2 (C$_{2''}$), 62.2 (C$_{5''}$), 70.9 (CH$_2$), 96.2 (C$_{1''}$), 114.9 (C$_{6'}$), 116.5 (C$_3$, C$_5$), 117.0 (C$_{2'}$), 125.1 (C$_{4'}$), 127.9 (C$_1$), 130.4 (C$_2$, C$_6$), 130.9 (C$_{5'}$), 133.1 (C$_{3'}$), 157.3 (C$_{1'}$), 162.0 (C$_4$), 192.2. (C=O). **HPLC (t$_R$, min)**: 16.5. **MS (ESI, *m/z*)**: 297.1, 299.1, 301.1 [(M-THP)+H]$^+$.

2-(3,4-Dichlorophenoxy)-1-(4-hydroxyphenyl)ethan-1-one, 98. Following general procedure E using compound **97** (700 mg, 0.34 mmol) and 3 M HCl (2.5 mL, 7.44 mmol), compound **98** was obtained as a white solid (375 mg, 69%).

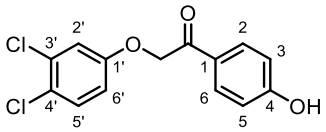

Mp: 220-223 °C. **R_f**: 0.12 (hexane/AcOEt, 8:2). **IR (ATR, cm^{-1})**: ν 3154 (O-H), 1664 (C=O), 1572 (C=C), 1473 (C=C), 1246 (C-O), 1216 (C-O), 990 (C-Cl). **^{1}H-NMR (DMSO-*d*$_6$, 300 MHz)**: δ 5.55 (s, 2H, CH$_2$), 6.89 (d, *J*=8.8, 2H, H$_3$, H$_5$), 6.98 (dd, *J*=9.0, 2.9, 1H, H$_{6'}$), 7.29 (d, *J*=2.9, 1H, H$_{2'}$), 7.50 (d, *J*=9.0, 1H, H$_{5'}$), 7.89 (d, *J*=8.8, 2H, H$_2$, H$_6$), 10.49 (s, 1H, OH).**^{13}C-NMR (DMSO-*d*$_6$, 75 MHz)**: δ 70.2 (CH$_2$), 115.4 (C$_3$, C$_5$), 115.7 (C$_{6'}$), 116.5 (C$_{2'}$), 122.6 (C$_{4'}$), 125.8 (C$_1$), 130.5 (C$_2$, C$_6$), 130.8 (C$_{5'}$), 131.5 (C$_{3'}$), 157.7 (C$_{1'}$), 162.7 (C$_4$), 191.8 (C=O). **HPLC (t$_R$, min)**: 13.6. **MS (ESI, *m/z*)**: 297.1, 299.0, 301.1 [M+H]$^+$.

2-(3,4-Dichlorophenoxy)-1-(4-ethoxyphenyl)ethan-1-one, 99. Following general procedure F using compound **98** (100 mg, 0.34 mmol) and iodoethane (184 mg, 1.18 mmol), compound **99** was obtained as an off-white solid (95 mg, 87%).

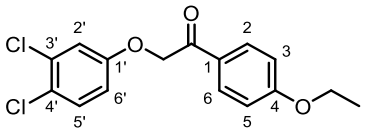

Mp: 100-102 °C. **R_f**: 0.43 (hexane/AcOEt, 8:2). **IR (ATR, cm^{-1})**: ν 1687 (C=O), 1599 (C=C), 1474 (C=C), 1224 (C-O), 1173 (C-O), 973 (C-Cl). **^{1}H-NMR ($CDCl_3$, 300 MHz)**: δ 1.46 (t, *J*=7.0, 3H, CH_3), 4.12 (q, *J*=7.0, 2H, $C\underline{H}_2CH_3$), 5.21 (s, 2H, CH_2CO), 6.80 (dd, *J*=8.9, 2.9, 1H, $H_{6'}$), 6.96 (d, *J*=9.0, 2H, H_3, H_5), 7.03 (d, *J*=2.9, 1H, $H_{2'}$), 7.32 (d, *J*=8.9, 1H, $H_{5'}$), 7.95 (d, *J*=9.0, 2H, H_2, H_6).**^{13}C-NMR ($CDCl_3$, 75 MHz)**: δ 14.8 (CH_3), 64.1 ($\underline{C}H_2CH_3$), 70.9 ($\underline{C}H_2CO$), 114.7 (C_3, C_5), 114.9 ($C_{6'}$), 117.0 ($C_{2'}$), 125.05 ($C_{4'}$), 127.2 (C_1), 130.6 (C_2, C_6), 130.9 ($C_{5'}$), 133.13 ($C_{3'}$), 157.3 ($C_{1'}$), 163.9 (C_4), 192.1 (C=O). **HPLC (t_R, min)**: 15.7. **MS (ESI, *m/z*)**: 325.2, 327.1, 329.1 $[M+H]^+$.

2-(3,4-Dichlorophenoxy)-1-{4-[(propan-2-yl)oxy]phenyl}ethan-1-one, 100.
Following general procedure F compound **98** (150 mg, 0.51 mmol) and 2-bromopropane (217 mg, 1.77 mmol), compound **100** was obtained as a white solid (143 mg, 84%).

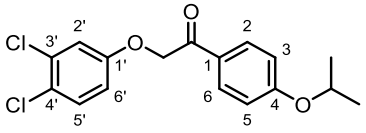

Mp: 113 °C. **R_f**: 0.61 (hexane/AcOEt, 7:3). **IR (ATR, cm^{-1})**: ν 1684 (C=O), 1602 (C=C), 1221 (C-O), 862 (C-Cl). **^{1}H-NMR ($CDCl_3$, 300 MHz)**: δ 1.38 (d, *J*=6.0, 6H, $2(CH_3)_2$), 4.67 (hept, *J*=6.0, 1H, CH), 5.21 (s, 2H, CH_2), 6.80 (dd, *J*=8.9, 2.9, 1H, $H_{6'}$), 6.94 (d, *J*=8.9, 2H, H_3, H_5), 7.03 (d, *J*=2.9, 1H, $H_{2'}$), 7.32 (d, *J*=8.9, 1H, $H_{5'}$), 7.94 (d, *J*=9.0, 2H, H_2, H_6).**^{13}C-NMR ($CDCl_3$, 75 MHz)**: δ 22.0 ($2(CH_3)_2$), 70.5 (CH), 70.9 (CH_2), 114.9 ($C_{6'}$), 115.6 (C_3, C_5), 117.0 ($C_{2'}$), 125.0 ($C_{4'}$), 126.9 (C_1), 130.6 (C_2, C_6), 130.9 ($C_{5'}$), 133.1 ($C_{3'}$), 157.3 ($C_{1'}$), 163.0 (C_4), 192.0 (C=O). **HPLC (t_R, min)**: 16.2. **MS (ESI, *m/z*)**: 339.1, 341.1, 343.1 $[M+H]^+$.

1-[4-(Cyclopropylmethoxy)phenyl]-2-(3,4-dichlorophenoxy)ethan-1-one, 101.
Following general procedure F using compound **98** (140 mg, 0.47 mmol) and (iodomethyl)cyclopropane (300 mg, 1.65 mmol), compound **101** was obtained as a white solid (142 mg, 86%).

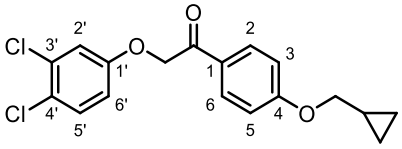

Mp: 113 °C. **R_f**: 0.61 (hexane/AcOEt, 7:3). **IR (ATR, cm^{-1})**: ν 1684 (C=O), 1602 (C=C), 1221 (C-O), 826 (C-Cl). **^{1}H-NMR ($CDCl_3$, 300 MHz)**: δ 0.38 (m, 2H, $CH_{2cyclop}$), 0.69 (m, 2H, $CH_{2cyclop}$), 1.28 (m, 1H, CH), 3.89 (d, *J*=7.0, 2H, CH_2CH), 5.21 (s, 2H, CH_2CO) 6.80 (dd, *J*=8.9, 2.9, 1H, $H_{6'}$), 6.96 (d, *J*=8.9, 2H, H_3, H_5), 7.03 (d, *J*=2.9, 1H, $H_{2'}$), 7.32 (d, *J*=8.9, 1H, $H_{5'}$), 7.95 (d, *J*=8.9, 2H, H_2, H_6).**^{13}C-NMR ($CDCl_3$, 75 MHz)**: δ 3.4 ($2CH_{2cyclop}$), 10.2 (CH), 70.9 (CH_2CO), 73.2 (CH_2CH), 114.8 (C_3, C_5), 114.9 ($C_{6'}$), 117.0 ($C_{2'}$), 125.0 ($C_{4'}$), 127.2 (C_1), 130.6 (C_2, C_6), 130.9 ($C_{5'}$), 133.1 ($C_{3'}$), 157.3 ($C_{1'}$), 163.9 (C_4), 192.1 (C=O). **HPLC (t_R, min)**: 16.1. **MS (ESI, *m/z*)**: 351.1, 353.1, 355.2 $[M+H]^+$.

2-(3,4-Dichlorophenoxy)-1-(4-(trifluoromethyl)phenyl)ethan-1-one, 107. To a solution of 3,4-dichlorophenol (1.0 eq, 0.92 mmol, 150 mg) and DBU (1.2 eq, 1.10 mmol, 0.17 mL) in anhydrous DMF (0.38 M), 2-bromo-1-(4-(trifluoromethyl)phenyl)ethan-1-one (1.0 eq, 0.92 mmol, 246 mg) was added and the reaction was stirred at rt for 1 min. Then, the mixture was diluted with EtOAc and washed with a 1:1 water/brine mixture. The organic layer was dried over Na_2SO_4, filtered and concentrated under reduced pressure. The residue was purified by flash chromatography (hexane to hexane/EtOAc 8:2) to yield compound **107** as a white solid (184 mg, 57%).

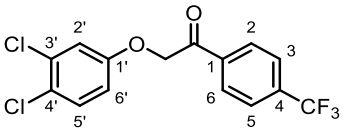

Mp: 100-102 °C. **R_f**: 0.46 (hexane/AcOEt, 9:1). **IR (ATR, cm^{-1})**: ν 1709 (C=O), 1474 (C=C), 1326 (C-O), 1128 (C-O), 1066 (C-F), 975 (C-Cl). **^{1}H-NMR ($CDCl_3$, 300 MHz)**: δ 5.26 (s, 2H, CH_2), 6.79 (dd, *J*=8.9, 2.9, 1H, $H_{6'}$), 7.03 (d, *J*=2.9, 1H, $H_{2'}$), 7.32 (d, *J*=8.9, 1H, $H_{5'}$), 7.78 (d, *J*=8.1, 2H, H_3, H_5), 8.09 (d, *J*=8.1, 2H, H_2, H_6).**^{13}C-NMR ($CDCl_3$, 75 MHz)**: δ 71.2 (CH_2), 114.8 ($C_{6'}$), 117.0 ($C_{2'}$), 123.5 (q, *J*=272.9, CF_3), 125.5 ($C_{4'}$), 126.1 (q, *J*=3.8, C_3, C_5), 128.7 (C_2, C_6), 131.1 ($C_{5'}$), 133.3 ($C_{3'}$), 135.3 (q, *J*=32.9, C_4), 137.0 (C_1), 156.9 ($C_{1'}$), 193.1 (C=O). **HPLC (t_R, min)**: 13.8. **MS (ESI, *m/z*)**: 347.0, 349.0 $[M-H]^-$.

2-(3,4-Dichlorophenoxy)-1-(4-nitrophenyl)ethan-1-one, 109. To a mixture of 3,4-dichlorophenol (1.0 eq, 2.45 mmol, 400 mg) and K_2CO_3 (2.0 eq, 4.91 mmol, 678 mg) in anhydrous DMF (0.38 M), 2-bromo-4-nitroacetophenone (2.0 eq, 4.91 mmol, 1.20 g) was

added and the reaction was stirred at rt for 16 h. After this time, the mixture was diluted with EtOAc and washed with a 1:1 water/brine mixture. The organic layer was dried over Na_2SO_4, filtered and concentrated under reduced pressure. The residue was purified by flash chromatography (hexane to hexane/EtOAc 8:2) to yield compound **109** as a yellow solid (390 mg, 49%).

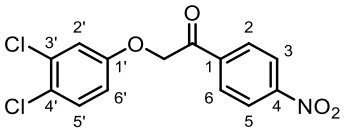

Mp: 169-171 °C. **R_f**: 0.64 (hexane/EtOAc 7:3). **IR (ATR, cm^{-1})**: ν 1713 (C=O), 1664 (C=C), 1522 (NO_2), 1475 (C=C), 1345 (NO_2), 1219 (C-O), 987 (C-Cl). **^{1}H-NMR ($CDCl_3$, 300 MHz)**: δ 5.25 (s, 2H, CH_2), 6.80 (dd, *J*=8.9, 2.9, 1H, $H_{6'}$), 7.03 (d, *J*=2.9, 1H, $H_{2'}$), 7.35 (d, *J*=8.9, 1H, $H_{5'}$), 8.15 (d, *J*=9.0, 2H, H_2, H_6), 8.36 (d, *J*=9.0, 2H, H_3, H_5). **^{13}C-NMR ($CDCl_3$, 75 MHz)**: δ 71.5 (CH_2), 114.8 ($C_{6'}$), 117.0 ($C_{2'}$), 124.3 (C_3, C_5), 125.8 ($C_{4'}$), 129.6 (C_2, C_6), 131.1 ($C_{5'}$), 133.4 ($C_{3'}$), 138.8 (C_4), 151.0 (C_1), 156.7 ($C_{1'}$), 192.9 (C=O). **HPLC (t_R, min)**: 14.7 (compound does not ionize; only detected by UV absorption).

4.1.13. Synthesis of intermediate enaminones 102-105, 108, 110

2-(3,4-Dichlorophenoxy)-3-(dimethylamino)-1-(4-ethoxyphenyl)but-2-en-1-one, 102. Following general procedure C using compound **99** (120 mg, 0.37 mmol), crude compound **102** was obtained as an oil (146 mg, 99% crude yield).

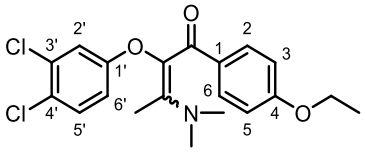

R_f: 0.13 (hexane/EtOAc 6:4). **^{1}H-NMR ($CDCl_3$, 300 MHz)**: δ Mixture of isomers A:B (1:0.7): 1.36-1.42 (m, 3H, $CH_2C\underline{H}_{3AB}$), 2.03 (s, 3H, CH_{3A}), 2.37 (s, 3H, CH_{3B}), 2.98 (s, 6H, $N(CH_3)_{2B}$), 3.01 (s, 6H, $N(CH_3)_{2A}$), 3.97-4.06 (m, 2H, CH_{2AB}), 6.65 (dd, *J*=9.0, 2.8, 1H, $H_{6'B}$), 6.67 (dd, *J*=8.9, 2.9, 1H, $H_{6'A}$), 6.72-6.78 (m, 2H, H_{3AB}, H_{5AB}), 6.90 (d, *J*=2.9, 1H, $H_{2'B}$), 6.93 (d, *J*=2.8, 1H, $H_{2'A}$), 7.17 (d, *J*=8.9, 1H, $H_{5'A}$), 7.18 (d, *J*=8.8, 1H, $H_{5'B}$), 7.64 (d, *J*=9.0, 2H, H_{2B}, H_{6B}), 7.67 (d, *J*=8.9, 2H, H_{2A}, H_{6A}).

2-(3,4-Dichlorophenoxy)-3-(dimethylamino)-1-(4-isopropoxyphenyl)but-2-en-1-one, 103. Following general procedure C using compound **100** (120 mg, 0.35 mmol), crude compound **103** was obtained as an oil (145 mg, 99% crude yield).

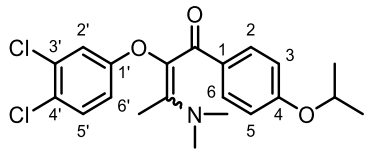

R_f: 0.12 (hexane/AcOEt, 6:4). **^{1}H-NMR ($CDCl_3$, 300 MHz)**: δ Mixture of isomers A:B (1:0.7): 1.30 (d, *J*=6.0, 6H, $CH(C\underline{H}_3)_{2A}$), 1.31 (d, *J*=6.0, 6H, $CH(C\underline{H}_3)_{2B}$), 2.03 (s, 3H, CH_{3A}), 2.36 (s, 3H, CH_{3B}), 2.98 (s, 6H, $N(CH_3)_{2B}$), 3.01 (s, 6H, $N(CH_3)_{2A}$), 4.46-4.72 (m, 1H, CH_{AB}), 6.65 (dd, *J*=9.0, 2.9, 1H, $H_{6'B}$), 6.67 (dd, *J*=8.9, 2.9, 1H, $H_{6'A}$), 6.72-6.78 (m, 2H, H_{3AB}, H_{5AB}), 6.90 (d, *J*=2.9, 1H, $H_{2'B}$), 6.93 (d, *J*=2.9, 1H, $H_{2'A}$), 7.17 (d, *J*=8.9, 1H, $H_{5'A}$), 7.18 (d, *J*=8.8, 1H, $H_{5'B}$), 7.64 (d, *J*=9.0, 2H, H_{2B}, H_{6B}), 7.67 (d, *J*=8.9, 2H, H_{2A}, H_{6A}).

1-(4-(Cyclopropylmethoxy)phenyl)-2-(3,4-dichlorophenoxy)-3-(dimethylamino) but-2-en-1-one, 104. Following general procedure C using compound **101** (120 mg, 0.34 mmol), crude compound **104** was obtained as an oil (144 mg, 99% crude yield).

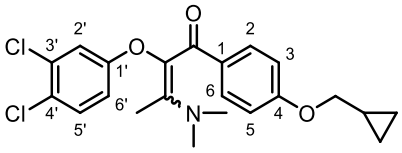

R_f: 0.13 (hexane/AcOEt, 6:4). **^{1}H-NMR ($CDCl_3$, 300 MHz)**: δ Mixture of isomers A:B (1:0.7): 0.24-0.40 (m, 2H, $CH_{2cyclopAB}$), 0.53-0.71 (m, 2H, $CH_{2cyclopAB}$), 1.16-1.33 (m, 1H, CH_{AB}), 2.03 (s, 3H, CH_{3A}), 2.40 (s, 3H, CH_{3B}), 2.98 (s, 6H, $N(CH_3)_{2B}$), 3.01 (s, 6H, $N(CH_3)_{2A}$), 3.73-3.81 (m, 2H, OCH_{2AB}), 6.65 (dd, *J*=9.0, 2.8, 1H, $H_{6'B}$), 6.67 (dd, *J*=8.9, 2.9, 1H, $H_{6'A}$), 6.72-6.78 (m, 2H, H_{3AB}, H_{5AB}), 6.90 (d, *J*=2.9, 1H, $H_{2'B}$), 6.93 (d, *J*=2.8, 1H, $H_{2'A}$), 7.17 (d, *J*=8.9, 1H, $H_{5'A}$), 7.18 (d, *J*=8.8, 1H, $H_{5'B}$), 7.64 (d, *J*=9.0, 2H, H_{2B}, H_{6B}), 7.67 (d, *J*=8.9, 2H, H_{2A}, H_{6A}).

2-(3,4-Dichlorophenoxy)-3-(dimethylamino)-1-(4-((tetrahydro-2*H*-pyran-2-yl)oxy) phenyl)but-2-en-1-one, 105. Following general procedure C using compound **97** (100 mg, 0.26 mmol) for 2 h, crude compound **105** was obtained as an oil (110 mg, 93% crude yield).

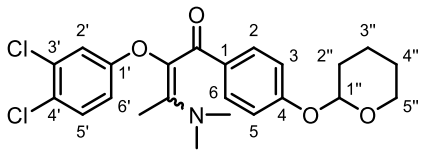

R_f: 0.12 (hexane/AcOEt, 1:1). **^{1}H-NMR ($CDCl_3$, 300 MHz)**: δ Mixture of isomers A:B (1:0.6): 1.55-2.02 (m, 6H, $2H_{2''AB}$, $2H_{3''AB}$, $2H_{4''AB}$), 2.03 (s, 3H, CH_{3A}), 2.40 (s, 3H, CH_{3B}), 2.98 (s, 6H, $N(CH_3)_{2B}$), 3.01 (s, 6H, $N(CH_3)_{2A}$), 3.50-3.70 (m, 1H, $H_{5''AB}$), 3.77-3.96 (m, 1H, $H_{5''AB}$),

5.50 (t, *J*=3.2, 1H, $H_{1''AB}$), 6.65 (dd, *J*=9.0, 2.8, 1H, $H_{6'B}$), 6.67 (dd, *J*=8.9, 2.9, 1H, $H_{6'A}$), 6.90 (d, *J*=8.7, 2H, H_{3AB}, H_{5AB}), 6.92 (d, *J*=2.9, 1H, $H_{2'B}$), 6.93 (d, *J*=2.8, 1H, $H_{2'A}$), 7.17 (d, *J*=8.9, 1H, $H_{5'A}$), 7.18 (d, *J*=8.9, 1H, $H_{5'B}$), 7.62 (d, *J*=8.8, 2H, H_{2B}, H_{6B}), 7.66 (d, *J*=8.8, 2H, H_{2A}, H_{6A}).

2-(3,4-Dichlorophenoxy)-3-(dimethylamino)-1-(4-(trifluoromethyl)phenyl)but-2-en-1-one, 108. Following general procedure C using compound **107** (100 mg, 0.29 mmol) at 60 °C, crude compound **108** was obtained as an oil (100 mg, 84% crude yield).

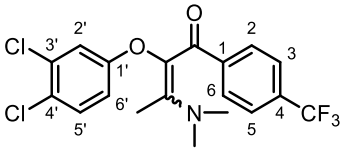

R_f: 0.18 (hexane/AcOEt, 8:2). **^{1}H-NMR ($CDCl_3$, 300 MHz)**: δ Mixture of isomers A:B (1:0.7): 2.06 (s, 3H, CH_{3A}), 2.53 (s, 3H, CH_{3B}), 3.03 (s, 6H, $N(CH_3)_{2B}$), 3.12 (s, 6H, $N(CH_3)_{2A}$), 6.57 (dd, *J*=8.9, 2.9, 1H, $H_{6'B}$), 6.64 (dd, *J*=8.9, 2.9, 1H, $H_{6'A}$), 6.82 (d, *J*=2.9, 1H, $H_{2'B}$), 6.89 (d, *J*=2.9, 1H, $H_{2'A}$), 7.19 (d, *J*=8.9, 1H, $H_{5'B}$), 7.20 (d, *J*=8.9, 1H, $H_{5'A}$), 7.50-7.53 (m, 2H, H_{3AB}, H_{5AB}), 7.68-7.72 (m, 2H, H_{2AB}, H_{6AB}).

2-(3,4-Dichlorophenoxy)-3-(dimethylamino)-1-(4-nitrophenyl)but-2-en-1-one, 110. Following general procedure C using compound **109** (100 mg, 0.29 mmol) at 50 °C, crude compound **110** was obtained as an oil (325 mg, 97% crude yield).

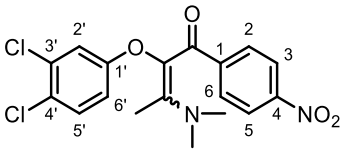

R_f: 0.22 (AcOEt). **^{1}H-NMR ($CDCl_3$, 300 MHz)**: δ Mixture of isomers A:B (1:0.7): 2.08 (s, 3H, CH_{3A}), 2.44 (s, 3H, CH_{3B}), 3.01 (s, 6H, $N(CH_3)_{2B}$), 3.16 (s, 6H, $N(CH_3)_{2A}$), 6.56 (dd, *J*=8.8, 2.9, 1H, $H_{6'B}$), 6.63 (dd, *J*=8.9, 2.9, 1H, $H_{6'A}$), 6.81 (d, *J*=2.9, 1H, $H_{2'B}$), 6.88 (d, *J*=2.8, 1H, $H_{2'A}$), 7.17-7.23 (m, 1H, $H_{5'AB}$), 7.64 (d, *J*=8.8, 2H, H_{2B}, H_{6B}), 7.73 (d, *J*=8.8, 2H, H_{2A}, H_{6A}), 8.06-8.13 (m, 2H, H_{3AB}, H_{5AB}).

4.1.14. Synthesis of intermediate pyrazoles 106, 111, 112

4-(3,4-Dichlorophenoxy)-5-methyl-3-(4-((tetrahydro-2*H*-pyran-2-yl)oxy)phenyl)-1*H*-pyrazole, 106. Following general procedure D using enaminone **105** (110 mg, 0.24

mmol), compound **106** was obtained as a white solid (17 mg, 17%). Chromatography: hexane to hexane/EtOAc 6:4.

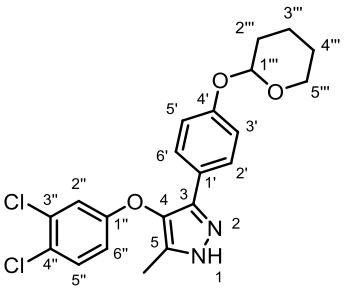

R_f: 0.44 (hexane/AcOEt, 1:1). **^{1}H-NMR ($CDCl_3$, 300 MHz)**: δ1.54-2.03 (m, 6H, $2H_{2'''}$, $2H_{3'''}$, $2H_{4'''}$), 2.08 (s, 3H, CH_3), 3.52-3.64 (m, 1H, $H_{5'''}$), 3.86 (ddd, *J*=12.1, 9.3, 3.1, 1H, $H_{5'''}$), 5.39 (t, *J*=3.3, 1H, $H_{1'''}$), 6.76 (dd, *J*=8.9, 2.9, 1H, $H_{6''}$), 6.99 (d, *J*=8.8, 2H, $H_{3'}$, $H_{5'}$), 7.04 (d, *J*=2.9, 1H, $H_{2''}$), 7.27 (d, *J*=8.9, 1H, $H_{5''}$), 7.56 (d, *J*=8.8, 2H, $H_{2'}$, $H_{6'}$).

4-(3,4-Dichlorophenoxy)-5-methyl-3-(4-nitrophenyl)-1*H*-pyrazole, 111. Following general procedure D using enaminone **110** (325 mg, 0.82 mmol) at rt, compound **111** was obtained as a yellow solid (100 mg, 33%). Chromatography: hexane to hexane/EtOAc 6:4.

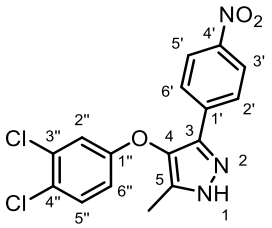

Mp: 210°C. **R_f**: 0.45 (hexane/EtOAc 1:1). **IR (ATR, cm^{-1})**: ν 3190 (N-H), 1602 (C=C), 1516 (NO_2), 1466 (C=C), 1345 (NO_2), 1255 (C-O), 855 (C-Cl). **^{1}H-NMR ($CDCl_3$, 300 MHz)**: δ 2.16 (s, 3H, CH_3), 6.80 (dd, *J*=8.9, 2.9, 1H, $H_{6''}$), 7.01 (d, *J*=2.9, 1H, $H_{2''}$), 7.32 (d, *J*=8.9, 1H, $H_{5''}$), 7.91 (d, *J*=8.9, 2H, $H_{2'}$, $H_{6'}$), 8.19 (d, *J*=8.9, 2H, $H_{3'}$, $H_{5'}$). **^{13}C-NMR ($CDCl_3$, 75 MHz)**: δ 9.0 (CH_3), 114.8 ($C_{6''}$), 117.1 ($C_{2''}$), 124.3 ($C_{3'}$, $C_{5'}$), 126.2 ($C_{4''}$), 126.4 ($C_{2'}$, $C_{6'}$), 131.3 ($C_{5''}$), 133.6 ($C_{3''}$), 134.0, 134.1 (C_4, C_5), 137.3 (C_3), 147.2 ($C_{1'}$), 149.9 ($C_{4'}$), 157 ($C_{1''}$).

4-(4-(3,4-Dichlorophenoxy)-5-methyl-1*H*-pyrazol-3-yl)aniline, 112. A solution of compound **111** (20 mg, 0.06 mmol) in DCM (0.05 M) was pumped through a 10% Pd/C cartridge at rt and 0.5 mL/min flow rate under atmospheric pressure (full-H_2 mode) using an H-Cube continuous flow hydrogenation reactor. The resulting solution was

concentrated under reduced pressure to afford compound **112** as a white solid (17 mg, 93%), which was used without further purification.

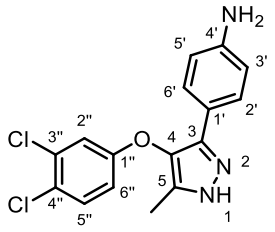

Mp: 100-102 °C. **R_f**: 0.26 (hexane/EtOAc 3:7). **IR (ATR, cm^{-1})**: ν 3230 (N-H), 1621 (C=C), 1511 (C=C), 1466 (C=C), 1252 (C-N), 1120 (C-O), 833 (C-Cl). **^{1}H-NMR ($CDCl_3$, 300 MHz)**: δ 2.10 (s, 3H, CH_3), 4.51 (br s, 2H, NH_2), 6.63 (d, *J*=8.6, 2H, $H_{3'}$, $H_{5'}$), 6.79 (dd, *J*=8.9, 2.9, 1H, $H_{6''}$), 7.04 (d, *J*=2.9, 1H, $H_{2''}$), 7.29 (d, *J*=8.9, 1H, $H_{5''}$), 7.42 (d, *J*=8.6, 2H, $H_{2'}$, $H_{6'}$). **^{13}C-NMR ($CDCl_3$, 75 MHz)**: δ 10.0 (CH_3), 114.9 ($C_{6''}$), 115.3 ($C_{3'}$, $C_{5'}$), 117.3 ($C_{2''}$), 119.7 ($C_{1'}$), 125.5 ($C_{4''}$), 127.1 ($C_{2'}$, $C_{6'}$), 131.1 ($C_{5''}$), 132.4 (C_4/C_5), 133.3 ($C_{3''}$), 137.8 (C_4/C_5), 138.0 (C_3), 146.8 ($C_{4'}$), 157.6 ($C_{1''}$).

4.1.15. Synthesis of final compounds 90-95

4-(3,4-Dichlorophenoxy)-3-(4-ethoxyphenyl)-5-methyl-1*H*-pyrazole, 90. Following general procedure D using enaminone **102** (150 mg, 0.38 mmol), compound **90** was obtained as a white solid (42 mg, 31%). Chromatography: hexane to hexane/EtOAc 6:4.

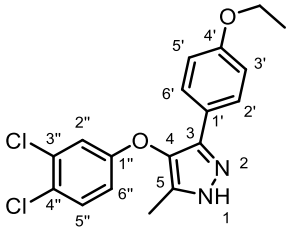

Mp: 161 °C. **R_f**: 0.23 (hexane/EtOAc 6:4). **IR (ATR, cm^{-1})**: ν 3135 (N-H), 1466 (C=C), 1252 (C-O), 1119 (C-O), 837 (C-Cl). **^{1}H-NMR ($CDCl_3$, 300 MHz)**: δ 1.40 (t, *J*=7.0, 3H, $CH_2\underline{CH}_3$), 2.14 (s, 3H, CH_{3pyr}) 4.02 (q, *J*=7.0, 2H, CH_2), 6.80 (dd, *J*=8.9, 2.9, 1H, $H_{6''}$), 6.87 (d, *J*=8.9, 2H, $H_{3'}$, $H_{5'}$), 7.04 (d, *J*=2.9, 1H, $H_{2''}$), 7.30 (d, *J*=8.9, 1H, $H_{5''}$), 7.55 (d, *J*=8.9, 2H, $H_{2'}$, $H_{6'}$). **^{13}C-NMR ($CDCl_3$, 75 MHz)**: δ 9.9 (CH_{3pyr}), 14.9 ($CH_2\underline{C}H_3$), 63.6 (CH_2), 114.9 ($C_{6''}$), 115.0 ($C_{3'}$, $C_{5'}$), 117.3 ($C_{2''}$), 122.1 ($C_{1'}$), 125.6 ($C_{4''}$), 127.3 ($C_{2'}$, $C_{6'}$), 131.1 ($C_{5''}$), 132.8 (C_4/C_5), 133.4 ($C_{3''}$), 136.9 (C_4/C_5), 138.5 (C_3), 157.5 ($C_{1''}$), 159.2 ($C_{4'}$). **HPLC (t_R, min)**: 15.5. **MS (ESI, *m/z*)**: 363.0, 365.0, 367.0 $[M+H]^+$.

4-(3,4-Dichlorophenoxy)-3-(4-isopropoxyphenyl)-5-methyl-1*H*-pyrazole, 91. Following general procedure D using enaminone **103** (148 mg, 0.36 mmol), compound **91** was obtained as an off-white solid (35 mg, 26%). Chromatography: hexane to hexane/EtOAc 6:4.

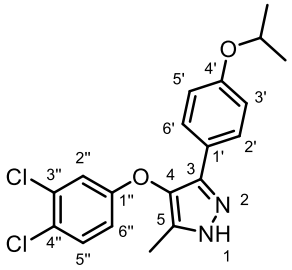

Mp: 100-102 °C. **R_f**: 0.30 (hexane/EtOAc 6:4). **IR (ATR, cm^{-1})**: ν 3132 (N-H), 1465 (C=C), 1249 (C-O), 1119 (C-O), 835 (C-Cl). **^{1}H-NMR ($CDCl_3$, 300 MHz)**: δ 1.30 (d, *J*=6.0, 6H, $CH(C\underline{H}_3)_2$), 2.08 (s, 3H, CH_{3pyr}) 4.51 (hept, *J*=6.1, 1H, CH), 6.80 (dd, *J*=8.8, 2.9, 1H, $H_{6''}$), 6.86 (d, *J*=8.9, 2H, $H_{3'}$, $H_{5'}$), 7.04 (d, *J*=2.9, 1H, $H_{2''}$), 7.30 (d, *J*=8.8, 1H, $H_{5''}$), 7.55 (d, *J*=8.8, 2H, $H_{2'}$, $H_{6'}$). **^{13}C-NMR ($CDCl_3$, 75 MHz)**: δ 10.0 (CH_{3pyr}), 21.2 ($CH(\underline{C}H_3)_2$), 70.1 (CH), 114.9 ($C_{6''}$), 116.3 ($C_{3'}$, $C_{5'}$), 117.3 ($C_{2''}$), 122.2 ($C_{1'}$), 125.6 ($C_{4''}$), 127.2 ($C_{2'}$, $C_{6'}$), 131.1 ($C_{5''}$), 132.8 (C_4/C_5), 133.4 ($C_{3''}$), 136.9 (C_4/C_5), 138.5 (C_3), 157.5 ($C_{1''}$), 158.2 ($C_{4'}$). **HPLC (t_R, min)**: 16.0. **MS (ESI, *m/z*)**: 377.1, 379.1, 381.1 $[M+H]^+$.

3-(4-(Cyclopropylmethoxy)phenyl)-4-(3,4-dichlorophenoxy)-5-methyl-1*H*-pyrazole, 92. Following general procedure D using enaminone **104** (150 mg, 0.36 mmol), compound **92** was obtained as an off-white solid (28 mg, 20%). Chromatography: hexane to hexane/EtOAc 6:4.

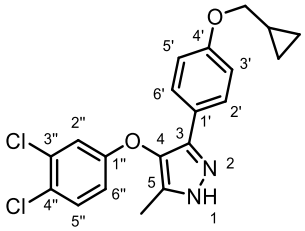

Mp: 85 °C. **R_f**: 0.32 (hexane/EtOAc 6:4). **IR (ATR, cm^{-1})**: ν 3137 (N-H), 1465 (C=C), 1250 (C-O), 1119 (C-O), 1025 (C-O), 833 (C-Cl). **^{1}H-NMR ($CDCl_3$, 300 MHz)**: δ 0.34 (m, 2H, $CH_{2cyclop}$), 0.62 (m, 2H, $CH_{2cyclop}$), 1.25 (m, 1H, CH), 2.12 (s, 3H, CH_3), 3.77 (d, *J*=7.0, 2H, OCH_2), 6.79 (dd, *J*=8.9, 2.8, 1H, $H_{6''}$), 6.86 (d, *J*=8.8, 2H, $H_{3'}$, $H_{5'}$), 7.05 (d, *J*=2.8, 1H, $H_{2''}$), 7.29 (d, *J*=8.9, 1H, $H_{5''}$), 7.55 (d, *J*=8.7, 2H, $H_{2'}$, $H_{6'}$). **^{13}C-NMR ($CDCl_3$, 75 MHz)**: δ 3.3 (2 $CH_{2cyclop}$), 9.9 (CH_3), 10.3 (CH), 72.9 (OCH_2), 114.9 ($C_{6''}$), 115.1 ($C_{3'}$, $C_{5'}$), 117.3 ($C_{2''}$), 122.2

($C_{1'}$), 125.6 ($C_{4''}$), 127.2 ($C_{2'}$, $C_{6'}$), 131.1 ($C_{5''}$), 132.8 (C_4/C_5), 133.4 ($C_{3''}$), 136.9 (C_4/C_5), 138.5 (C_3), 157.5 ($C_{1''}$), 159.3 ($C_{4'}$). **HPLC (t_R, min)**: 15.9. **MS (ESI, *m/z*)**: 389.0, 391.1, 393.0 $[M+H]^+$.

4-(4-(3,4-Dichlorophenoxy)-5-methyl-1*H*-pyrazol-3-yl)phenol, 93. Following general procedure E using compound **106** (17 mg, 0.04 mmol), compound **93** was obtained as an off-white solid (8 mg, 60%).

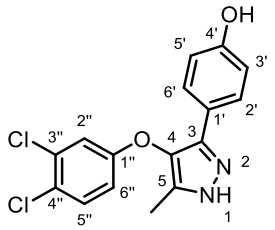

Mp: 130-132 °C. **R_f**: 0.30 (hexane/EtOAc 6:4). **IR (ATR, cm^{-1})**: ν 3253 (N-H, O-H), 1464 (C=C), 1229 (C-O), 1118 (C-O), 836 (C-Cl). **^{1}H-NMR ($CDCl_3$, 300 MHz)**: δ 2.11 (s, 3H, CH_3), 6.76 (m, 3H, $H_{6''}$, $H_{3'}$, $H_{5'}$), 7.02 (d, *J*=2.9, 1H, $H_{2''}$), 7.28 (d, *J*=8.9, 1H, $H_{5''}$), 7.46 (d, *J*=8.6, 2H, $H_{2'}$, $H_{6'}$), 7.70 (br s, 1H, OH). **^{13}C-NMR ($CDCl_3$, 75 MHz)**: δ 9.8 (CH_3), 114.9 ($C_{6''}$), 116.1 ($C_{3'}$, $C_{5'}$), 117.3 ($C_{2''}$), 121.8 ($C_{1'}$), 125.7 ($C_{4''}$), 127.7 ($C_{2'}$, $C_{6'}$), 131.1 ($C_{5''}$), 132.7 (C_4/C_5), 133.4 ($C_{3''}$), 137.2 (C_4/C_5), 138.6 (C_3), 156.5 ($C_{4'}$), 157.4 ($C_{1''}$). **HPLC (t_R, min)**: 13.0. **MS (ESI, *m/z*)**: 335.1, 337.0, 339.0 $[M+H]^+$.

4-(3,4-Dichlorophenoxy)-5-methyl-3-(4-(trifluoromethyl)phenyl)-1*H*-pyrazole, 94. Following general procedure D using enaminone **108** (100 mg, 0.24 mmol), compound **94** was obtained as an oil (16 mg, 17%). Chromatography: DCM to DCM/EtOAc 7:3.

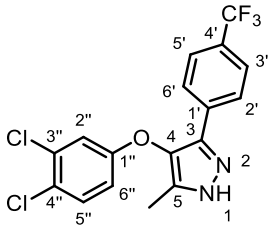

R_f: 0.11 (hexane/EtOAc 8:2). **IR (ATR, cm^{-1})**: ν 3200 (N-H), 1466 (C=C), 1325 (C-O), 1121 (C-F), 846 (C-Cl). **^{1}H-NMR ($CDCl_3$, 500 MHz)**: δ 2.18 (s, 3H, CH_3), 6.80 (dd, *J*=8.9, 2.9, 1H, $H_{6''}$), 7.03 (d, *J*=2.9, 1H, $H_{2''}$), 7.33 (d, *J*=8.9, 1H, $H_{5''}$), 7.60 (d, *J*=8.2, 2H, $H_{3'}$, $H_{5'}$), 7.85 (d, *J*=8.2, 2H, $H_{2'}$, $H_{6'}$).**^{13}C-NMR ($CDCl_3$, 125 MHz)**: δ 9.3 (CH_3), 114.8 ($C_{6''}$), 117.2 ($C_{2''}$), 124.2 (q, *J*=272.1, CF_3), 125.9 (q, *J*=3.8, $C_{3'}$, $C_{5'}$), 126.0 ($C_{4''}$), 126.1 ($C_{2'}$, $C_{6'}$), 130.2 (q, *J*=32.6, $C_{4'}$),

131.3 ($C_{5''}$), 132.1 (C_4/C_5), 133.6 ($C_{3''}$), 133.9 ($C_{1'}$), 134.2 (C_4/C_5), 139.9 (C_3), 157.2 ($C_{1''}$). **HPLC (t_R, min)**: 17.2. **MS (ESI, *m/z*, %)**: 387.0, 389.1, 391.0 $[M+H]^+$.

***N*-(4-(4-(3,4-Dichlorophenoxy)-5-methyl-1*H*-pyrazol-3-yl)phenyl)acetamide, 95.** To a solution of compound **112** (1.0 eq, 0.12 mmol, 40 mg) in a 3:1 DCM/pyridine mixture (0.04 M), acetic anhydride (1.2 eq, 0.14 mmol, 14 µL) was added at 0 °C. The reaction was stirred for 1 h at 0 °C and at rt for an additional 4 h. Then, the mixture was concentrated under reduced pressure and the residue was diluted with DCM and washed with a saturated $NaHCO_3$ solution. The organic layer was dried over Na_2SO_4, filtered and concentrated. The residue was purified by flash chromatography (hexane to hexane/EtOAc 1:1) to yield the *N*,*N*-diacetyl derivative (20 mg), which was dissolved in a 3:2 THF/MeOH mixture and treated with a 10% NaOH aq solution (10 µL) for 1 h at rt. After solvent removal, the crude was diluted in EtOAc, washed with water, dried over Na_2SO_4, filtered and concentrated to obtain compound **95** (10.4 mg, 23%) as a white solid.

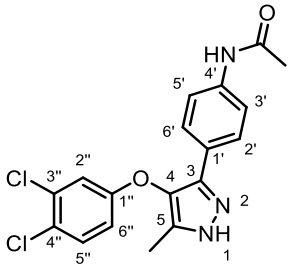

Mp: 100-102 °C. **R_f**: 0.13 (hexane/EtOAc 3:7). **IR (ATR, cm^{-1})**: ν 3229 (N-H), 1670 (C=O), 1538 (C=C), 1466 (C=C), 1255 (C-O), 1120 (C-O). **^{1}H-NMR ($CDCl_3$, 300 MHz)**: δ 2.14 (s, 3H, CH_{3pyr}), 2.17 (s, 3H, $COCH_3$), 6.78 (dd, *J*=8.9, 2.9, 1H, $H_{6''}$), 7.02 (d, *J*=2.9, 1H, $H_{2''}$), 7.30 (d, *J*=8.8, 1H, $H_{5''}$), 7.38 (s, 1H, CONH), 7.46 (d, *J*=8.4, 2H, $H_{3'}$, $H_{5'}$), 7.59 (d, *J*=8.3, 2H, $H_{2'}$, $H_{6'}$). **^{13}C-NMR ($CDCl_3$, 75 MHz)**: δ 9.7 (CH_{3pyr}), 24.8 ($CO\underline{C}H_3$), 114.9 ($C_{6''}$), 117.3 ($C_{2''}$), 120.3 ($C_{3'}$, $C_{5'}$), 125.7 ($C_{4''}$), 125.8 ($C_{1'}$), 126.7 ($C_{2'}$, $C_{6'}$), 131.2 ($C_{5''}$), 133.1 (C_4/C_5), 133.4 ($C_{3''}$), 136.7 (C_4/C_5), 138.1 ($C_{4'}$), 138.5 (C_3), 157.3 ($C_{1''}$), 168.6 (C=O). **HPLC (t_R, min)**: 12.8. **MS (ESI, *m/z*)**: 376.1, 378.1, 380.2 $[M+H]^+$.

4.1.16. Synthesis of intermediate compounds 118 and 119

2-(3,4-Dichlorophenoxy)-3-(dimethylamino)-1-(4-methoxyphenyl)prop-2-en-1-one, 118. Compound **71** (1.0 eq, 0.32 mmol, 100 mg) and *N*,*N*-dimethylformamide dimethyl acetal (DMFDMA) (2.0 eq, 0.64 mmol, 85 µL) were dissolved in anhydrous DMF (0.2 M) in a MW vial and the reaction mixture was heated to 80 °C for 75 minutes under

MW irradiation. The mixture was then concentrated to dryness to yield compound **118** (one isomer) as an off-white solid (110 mg, 94% crude yield), which was used in next step without further purification.

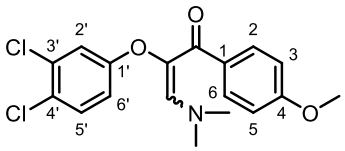

Mp: 159 °C. **R_f**: 0.30 (hexane/EtOAc 1:1). **IR (ATR, cm^{-1})**: ν 1649 (C=O), 1586 (C=C), 1466 (C=C), 1322 (C-N), 1253 (C-O), 1117 (C-O), 974 (C-Cl). **^{1}H-NMR ($CDCl_3$, 300 MHz)**: δ 3.04 (s, 6H, $N(CH_3)_2$), 3.82 (s, 3H, OCH_3), 6.81 (dd, *J*=8.9, 2.9, 1H, $H_{6'}$), 6.86 (d, *J*=8.6, 2H, H_3, H_5), 7.04 (d, *J*=2.8, 1H, $H_{2'}$), 7.15 (s, 1H, C=CH), 7.26 (d, *J*=8.9, 1H, $H_{5'}$), 7.66 (d, *J*=8.8, 2H, H_2, H_6).**^{13}C-NMR ($CDCl_3$, 75 MHz)**: δ 34.9 ($N(CH_3)_2$), 55.5 (OCH_3), 113.5 (C_3, C_5), 115.0 ($C_{6'}$), 117.2 ($C_{2'}$), 124.9 ($C_{4'}$), 126.7 (C_1), 130.7 (C_2, C_6), 131.0 ($C_{5'}$), 131.7 (C=CH), 133.2 ($C_{3'}$), 144.2 (C=CH), 158.0 ($C_{1'}$), 161.8 (C_4), 187.9 (C=O). **HPLC (t_R, min)**: 14.0. **MS (ESI, *m/z*)**: 366.0, 368.0, 370.0 $[M+H]^+$.

4'-Methoxy-3-methyl-[1,1'-biphenyl]-2-ol, 119. 2-Bromo-6-methylphenol (1.0 eq, 0.80 mmol, 150 mg), 4-methoxyphenylboronic acid (1.2 eq, 0.96 mmol, 146 mg), $Pd(PPh_3)_4$ (5 mol %, 0.04 mmol, 46 mg) and K_3PO_4 (4.0 eq, 3.21 mmol, 681 mg) were dissolved in a 10:2:1 mixture of toluene/ethanol/water (0.2 M) in a MW vial. The reaction mixture was heated to 160 °C for 40 min under MW irradiation. The mixture was then filtered through celite, and the filtrated was washed with brine and evaporated to dryness. The residue was purified by flash chromatography (hexane to hexane/EtOAc 8:2) to yield compound **119** as a white solid (89 mg, 52%).

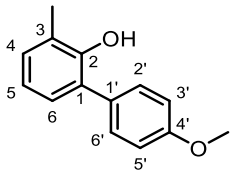

Mp: 65-66 °C. **R_f**: 0.50 (hexane/EtOAc 9:1). **IR (ATR, cm^{-1})**: ν 3454 (O-H), 1608 (C=C), 1510 (C=C), 1241 (C-O), 1084 (C-O), 1023 (C-O). **^{1}H-NMR ($CDCl_3$, 300 MHz)**: δ 2.31 (s, 3H, CH_3), 3.87 (s, 3H, OCH_3), 5.23 (s, 1H, OH), 6.88 (t, *J*=7.5, 1H, H_5), 6.99-7.07 (m, 1H, H_4/H_6), 7.02 (d, *J*=8.7, 2H, $H_{3'}$, $H_{5'}$), 7.12 (br d, *J*=6.9, 1H, H_4 /H_6), 7.38 (d, *J*=8.7, 2H, $H_{2'}$, $H_{6'}$). **^{13}C-NMR ($CDCl_3$, 75 MHz)**: δ 16.3 (CH_3), 55.5 (OCH_3), 114.9 ($C_{3'}$, $C_{5'}$), 120.3 (CH_{Ar}), 124.6 (C_{Ar}), 127.5 (C_{Ar}), 127.9 (CH_{Ar}), 129.5 (C_{Ar}), 130.3 (CH_{Ar}), 130.5 ($C_{2'}$, $C_{6'}$), 150.9 (C_2), 159.5 ($C_{4'}$). **HPLC (t_R, min)**: 13.5. **MS (ESI, *m/z*)**: 215.1, 216.2 $[M+H]^+$.

4.1.17. Synthesis of final compounds 113-117

4-(3,4-Dichlorophenoxy)-3-(4-methoxyphenyl)-1,5-dimethyl-1*H*-pyrazole, 113 and 4-(3,4-dichlorophenoxy)-5-(4-methoxyphenyl)-1,3-dimethyl-1*H*-pyrazole, 114. To a solution of compound **65** (1.0 eq, 0.26 mmol, 90 mg) in anhydrous DMF (0.07 M), NaH (60% dispersion in mineral oil, 2.0 eq, 0.52 mmol, 21 mg) was added at 0 °C and the mixture was stirred at rt for 2 h. Next, iodomethane (1.0 eq, 0.26 mmol, 37 mg) was added and the reaction was stirred overnight at rt. Then, the reaction was quenched with water, diluted with EtOAc and washed with a 1:1 mixture of water/brine. The organic fraction was combined, dried over Na_2SO_4, filtered and concentrated under reduced pressure. The crude, containing a 2:1 mixture of regioisomers, was purified by preparative chromatography (DCM/EtOAc 9:1) to isolate 1,5-dimethyl derivative **113** (26 mg, 28%) and 1,3-dimethyl derivative **114** (12 mg, 13%).

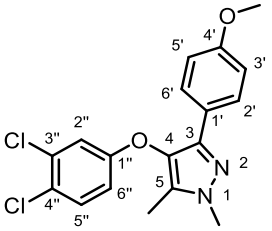

113: **Mp**: 145-148 °C. **R_f**: 0.83 (DCM/EtOAc 9:1). **IR (ATR, cm^{-1})**: ν 1536 (C=C), 1465 (C=C), 1306 (C-O), 1247 (C-O), 1119 (C-O), 836 (C-Cl). **^{1}H-NMR (CDCl$_3$, 300 MHz)**: δ 2.10 (s, 3H, CH_3), 3.78 (s, 3H, OCH_3), 3.83 (s, 3H, NCH_3), 6.80 (dd, *J*=8.9, 2.9, 1H, $H_{6''}$), 6.85 (d, *J*=8.9, 2H, $H_{3'}$, $H_{5'}$), 7.03 (d, *J*=2.9, 1H, $H_{2''}$), 7.29 (d, *J*=8.9, 1H, $H_{5''}$,), 7.67 (d, *J*=9.0, 2H, $H_{2'}$, $H_{6'}$). **^{13}C-NMR (CDCl$_3$, 75 MHz)**: δ 8.8 (CH_3), 37.1 (NCH_3), 55.3 (OCH_3), 114.1 ($C_{3'}$, $C_{5'}$), 114.9 ($C_{6''}$), 117.2 ($C_{2''}$), 124.4 ($C_{1'}$), 125.4 ($C_{4''}$), 127.3 ($C_{2'}$, $C_{6'}$), 131.1 ($C_{5''}$), 131.3 (C_5), 132.6 (C_4), 133.3 ($C_{3''}$), 141.0 (C_3), 157.7 ($C_{1''}$), 159.3 ($C_{4'}$). **HPLC (t_R, min)**: 16.2. **MS (ESI, *m/z*)**: 363.2, 365.1, 367.1 $[M+H]^+$.

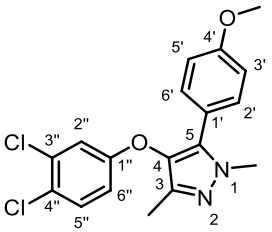

114: **Mp**: 145-148 °C. **R_f**: 0.74 (DCM/EtOAc 9:1). **IR (ATR, cm^{-1})**: ν 1508 (C=C), 1466 (C=C), 1301 (C-O), 1250 (C-O), 1119 (C-O), 831 (C-Cl). **^{1}H-NMR (CDCl$_3$, 300 MHz)**: δ 2.10 (s, 3H, CH_3), 3.81 (s, 6H, OCH_3, NCH_3), 6.74 (dd, *J*=8.8, 2.9, 1H, $H_{6''}$), 6.92 (d, *J*=8.8, 2H, $H_{3'}$, $H_{5'}$), 6.98 (d, *J*=2.8, 1H, $H_{2''}$), 7.23 (d, *J*=8.9, 2H, $H_{2'}$, $H_{6'}$), 7.27 (d, *J*=8.8, 1H, $H_{5''}$). **^{13}C-NMR (CDCl$_3$,**

75 MHz): δ 10.9 (CH_3), 37.9 (NCH_3), 55.4 (OCH_3), 114.5 ($C_{3'}$, $C_{5'}$), 114.9 ($C_{6''}$), 117.2 ($C_{2''}$), 120.2 ($C_{1'}$), 125.3 ($C_{4''}$), 130.3 ($C_{2'}$, $C_{6'}$), 130.9 ($C_{5''}$), 133.2 ($C_{3''}$), 133.4 (C_3/C_4), 134.9 (C_5), 139.6 (C_3/C_4), 157.9 ($C_{1''}$), 160.1 ($C_{4'}$). **HPLC (t_R, min)**: 16.2. **MS (ESI, *m/z*)**: 363.1, 365.1, 367.1 $[M+H]^+$.

4-(3,4-Dichlorophenoxy)-3-(4-methoxyphenyl)-1*H*-pyrazole, 115. To a solution of enaminone **118** (1.0 eq, 0.25 mmol, 90 mg) in absolute ethanol (0.1 M), hydrazine monohydrate (2.0 eq, 0.50 mmol, 40 µL) was added, followed by addition of a 4 M HCl solution in dioxane (1.1 eq, 0.27 mmol, 70 µL). The reaction was heated at 65 °C for 3 h. After cooling to rt, the mixture was concentrated under vacuum, dissolved with EtOAc, and washed with brine. The organic layers were combined, dried over Na_2SO_4, filtered and concentrated under reduced pressure to yield compound **115** as a yellow solid (53 mg, 64%). Chromatography: hexane to hexane/EtOAc 6:4.

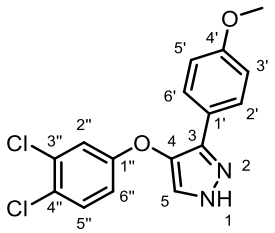

Mp: 90-92 °C. **R_f**: 0.65 (hexane/EtOAc 1:1). **IR (ATR, cm^{-1})**: ν 3150 (N-H), 1465 (C=C), 1252 (C-O), 1178 (C-O), 1120 (C-O), 834 (C-Cl). **^{1}H-NMR ($CDCl_3$, 300 MHz)**: δ 3.80 (s, 3H, OCH_3), 6.88 (m, 3H, $H_{3'}$, $H_{5'}$, $H_{6''}$), 7.11 (d, *J*=2.9, 1H, $H_{2''}$), 7.32 (d, *J*=8.9, 1H, $H_{5''}$), 7.50 (br s, 1H, H_5), 7.63 (d, *J*=8.9, 2H, $H_{2'}$, $H_{6'}$). **^{13}C-NMR ($CDCl_3$, 75 MHz)**: δ 55.4 (OCH_3), 114.5 ($C_{3'}$, $C_{5'}$), 115.5 ($C_{6''}$), 117.9 ($C_{2''}$), 121.6 ($C_{1'}$), 126.1 ($C_{4''}$), 127.6 ($C_{2'}$, $C_{6'}$), 127.8 (C_5), 131.1 ($C_{5''}$), 131.9 (C_4), 133.4 ($C_{3''}$), 137.4 (C_3), 157.8 ($C_{1''}$), 160.0 ($C_{4'}$). **HPLC (t_R, min)**: 14.5. **MS (ESI, *m/z*)**: 335.0, 337.0, 339.0 $[M+H]^+$.

4-(3,4-Dichlorophenoxy)-5-(4-methoxyphenyl)-3-methylisoxazole, 116. Enaminone **77** (1.0 eq, 0.24 mmol, 90 mg) was dissolved in a 1:1 1,2-dimethoxyethane/water mixture (0.08 M) and hydroxylamine hydrochloride (2.0 eq, 0.47 mmol, 33 mg) was added. Then, the reaction was heated at 60 °C for 25 h. After this time, the reaction was concentrated under reduced pressure and the aqueous residue was diluted with EtOAc and washed with brine. The organic phases were dried over Na_2SO_4, filtered and concentrated under reduced pressure, and the residue was purified by chromatography (hexane/EtOAc 9:1 to 1:1) to yield compound **116** as a white solid (17 mg, 23%).

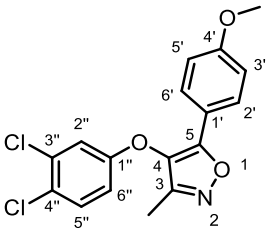

Mp: 107-109 °C. **R_f**: 0.7 (hexane/EtOAc 7:3). **IR (ATR, cm^{-1})**: ν 1465 (C=C), 1255 (C-O), 834 (C-Cl). **^{1}H-NMR ($CDCl_3$, 300 MHz)**: δ 2.15 (s, 3H, CH_3), 3.83 (s, 3H, OCH_3), 6.83 (dd, *J*=8.9, 2.9, 1H, $H_{6''}$), 6.94 (d, *J*=9.0, 2H, $H_{3'}$, $H_{5'}$), 7.10 (d, *J*=2.9, 1H, $H_{2''}$), 7.36 (d, *J*=8.9, 1H, $H_{5''}$), 7.71 (d, *J*=9.1, 2H, $H_{2'}$, $H_{6'}$). **^{13}C-NMR ($CDCl_3$, 75 MHz)**: δ 9.5 (CH_3), 55.5 (OCH_3), 114.6 ($C_{3'}$, $C_{5'}$), 114.7 ($C_{6''}$), 117.5 ($C_{2''}$), 119.1 ($C_{1'}$), 126.8 ($C_{4''}$), 127.2 ($C_{2'}$, $C_{6'}$), 129.8 (C_3/C_4), 131.4 ($C_{5''}$), 133.8 ($C_{3''}$), 156.0 (C_3/C_4), 156.2 ($C_{1''}$), 158.3 (C_5), 161.2 ($C_{4'}$). **HPLC (t_R, min)**: 16.0. **MS (ESI, *m/z*)**: 350.0, 352.0, 354.0 $[M+H]^+$.

2-(3,4-Dichlorophenoxy)-4'-methoxy-3-methyl-1,1'-biphenyl, 117. Following general procedure A using compound **119** (23 mg, 0.11 mmol), 3,4-(dichlorophenyl)boronic acid (31 mg, 0.16) and pyridine (52 µL, 0.64 mmol) at 40 °C, compound **117** was obtained as a white solid (6 mg, 16%). Chromatography: hexane to hexane/EtOAc 8:2.

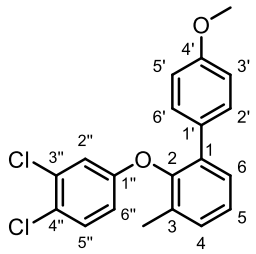

Mp: 108-109 °C. **R_f**: 0.59 (hexane/EtOAc 9:1). **IR (ATR, cm^{-1})**: ν 1467 (C=C), 1253 (C-O), 833 (C-Cl). **^{1}H-NMR (Acetone-d_6, 700 MHz)**: δ 2.18 (s, 3H, CH_3), 3.75 (s, 3H, OCH_3), 6.65 (dd, *J*=8.9, 2.9, 1H, $H_{6''}$), 6.83 (d, *J*=2.9, 1H, $H_{2''}$), 6.87 (d, *J*=8.7, 1H, $H_{3'}$, $H_{5'}$), 7.27-7.36 (m, 4H, H_4, H_5, $H_{5''}$, H_6), 7.41 (d, *J*=8.8, 2H, $H_{2'}$, $H_{6'}$). **^{13}C-NMR (Acetone-d_6, 175 MHz)**: δ 16.6 (CH_3), 55.4 (OCH_3), 114.0 ($C_{3'}$, $C_{5'}$), 116.1 ($C_{6''}$), 117.8 ($C_{2''}$), 124.7 ($C_{4''}$), 127.2 (C_6), 129.9 (C_5), 130.4 ($C_{1'}$), 130.9 ($C_{2'}$, $C_{6'}$), 131.4 (C_4), 131.9 ($C_{5''}$), 132.5 (C_3), 133.2 ($C_{3''}$), 136.0 (C_1), 149.8 (C_2), 158.0 ($C_{1''}$), 160.1 ($C_{4'}$). **HPLC (t_R, min)**: 16.5. **HRMS (ESI, *m/z*)**: calculated for $C_{20}H_{16}Cl_2O_2$ [M-H]: 358.0527, found 358.0516.

4.2. Biological experiments

4.2.1. Cell culture

RH7777 hepatoma cells stably expressing the LPA_1 receptor were kindly provided by Prof. Gabor Tigyi (University of Tennessee, Health Science Center, Memphis, USA), and B103 neuroblastoma cells stably expressing the LPA_2 or LPA_3 receptors were provided by Prof. Jerold Chun (Sanford Burnham Prebys Medical Discovery Institute, La Jolla, California, USA). All reagents were acquired from Gibco. Cells were maintained in Dulbecco's modified Eagle medium (DMEM) supplemented with 10% heat inactivated fetal bovine serum (FBS), 1% non-essential amino acids, 1% sodium pyruvate, 10 U/mL penicillin, and 10 µg/mL streptomycin. Cells were incubated in a humidified atmosphere at 37 °C in the presence of 5% CO_2. For passage, cells were rinsed with phosphate buffered saline (PBS) and incubated with 0.125% trypsin, 0.02% EDTA solution for 2 min at 37 °C. Detached cells were resuspended in growth medium, counted if necessary, and splitted onto dishes containing fresh media.

4.2.2. Evaluation of receptor activation by Ca^{2+} mobilization assay

Intracellular calcium levels changes were measured by using the fluorescent calcium sensitive dye Fluo-4NW (Invitrogen). RH7777 or B103 cells were plated on black-wall clear-bottom 96-well plates (Corning) at a density of 50000 cells/well and cultured overnight. The culture medium was then replaced with Fluo-4NW dye loading solution containing 2.5 µM of probenecid and incubated for 30 min at 37 °C followed by an additional 30 min at rt. Fluorescence changes were registered in a FluoStar Optima instrument (BMG Labtech) at 525 nm using an excitation wavelength of 494 nm. Each well was monitored for 240 s. 20 µL of the test compound from a 6x stock solution in assay buffer were added after 120 s of starting the measurement. Transient Ca^{2+} increase was quantified by calculating the difference between maximum and baseline values for each well. As positive controls, 10 µM LPA and 10 µM ionomycin were included in every experiment. At this concentration, LPA induced a response about 30-33% of the one shown by ionomycin, which agrees with previously described results.[148] The data presented are from two to four independent experiments carried out in triplicate or quadruplicate. Dose-response curves were generated and IC_{50} values calculated by nonlinear regression analysis using PRISM software version 9.

4.2.3. Parallel artificial membrane permeability assay (PAMPA)

Prior to use, the commercially available 96-well Corning Gentest pre-coated PAMPA plate system (Cultek S.L.U., Spain) was warmed to rt for 30 min. Then, 300 µL of a 20 µM solution of the compound under study (including as reference compounds propranolol and metoprolol) in 2% DMSO in PBS were added into wells in the donor plate, and 200 µL of PBS were added into wells in the acceptor plate. The acceptor plate was placed on the donor plate by slowly lowering the pre-coated PAMPA plate. The assembly was incubated at rt for 5 h, and then buffer samples were collected carefully from each plate. The final concentrations of compound in both donor and acceptor wells were analyzed by HPLC-MS using SIM mode and quantification was estimated by using the peak area integration normalized with an internal standard. Permeability values of the compound under study, and propranolol and metoprolol as reference compounds, were calculated using the following formula: $P\ (cm/s)=\{-\ln[1- C_A(t)/C_{eq}]\}/[A*(1/V_D+1/V_A)*t]$, where A=filter area (0.3 cm^2), V_D=donor well volume (0.3 mL), V_A=acceptor well volume (0.2 mL), t=incubation time (s), $C_A(t)$=compound concentration (µM) in acceptor well at time t, $C_D(t)$=compound concentration (µM) in donor well at time t, and $C_{eq}=[C_D(t)*V_D+C_A(t)*V_A]/(V_D+V_A)$.

4.2.4. Stability in human and mouse serum

An aliquot of 625 µL of a 250 µM solution of tested compound in PBS (pH 7.4) was added to 1.875 mL of mouse (Europa Bioproducts, EQSM-0100) or human (Sigma Aldrich) serum pre-warmed at 37 °C. Next, the solution was incubated at 37 °C, taking aliquots of 250 µL at times ranging from 0 to 48 hours. Each aliquot was quenched in 375 µL of cold ACN, vortexed, incubated for 10 min in ice and centrifuged at 39000*g* for 10 min. Supernatants were then analyzed by HPLC-MS using SIM mode, and quantification was estimated by using the peak area integration normalized with an internal standard.

4.2.5. Stability assays in mouse and human liver microsomes

Tested compound (1 µM) was incubated at 37 °C in PBS with NADPH (final concentration of 2 mM) and $MgCl_2$ (final concentration of 5 mM). Reactions were initiated by the addition of a suspension of MLMs (male CD-1 mice pooled, Sigma-Aldrich) or HLMs (male human pooled, Sigma-Aldrich), at a final protein concentration of 1 mg/mL. The solutions were shaken in a vortex and kept at 37 °C in a water bath open to the air. Aliquots of 100 µL were quenched at time zero and at seven points ranging to 2 h (MLM) or 8 h (HLM) by pouring into 100 µL of ice-cold ACN. Quenched samples were centrifuged

at 10000*g* for 5 min, and the supernatants were filtered through a polytetrafluoroethylene membrane syringe filter (pore size of 0.2 µm, Albet Labscience). The relative loss of parent compound over the course of the incubation was monitored by HPLC-MS using SIM mode. Concentrations were quantified by measuring the area under the peak ($[M+H]^+$) and converted to the percentage of remaining compound, using the time zero peak area value as 100%. The natural logarithm of the percentage remaining versus time data for each compound was fitted to linear regression, and the slope was used to calculate the degradation half-life time.

4.2.6. HSA binding assay

The binding of compounds to HSA was determined by incubating a fixed concentration of the compound with different concentrations of immobilized HSA, using the TRANSILXL HSA Binding Kit (TMP-0210-2096, Sovicell). An 8-well unit of the TRANSIL assay plate was used for each compound; six wells contained increasing concentrations of HSA immobilized on silica beads suspended in PBS at pH 7.4, and two wells contained buffer only and serve as references to account for nonspecific binding. The TRANSIL assay plate was thawed for 3 h at rt and centrifuged at 750*g* for 5 s. Then, 15 µL of an 80 µM stock solution of the compound in PBS (for a final concentration of 5 µM) was added to each well of the 8-well unit, and the plate was incubated on a plate shaker at 1000 rpm for 12 min at rt. After this time, the plate was centrifuged at 750*g* for 10 min, and 50 µL of the supernatants were transferred for analytical quantification by HPLC-MS using selected ion monitoring as acquisition method. The binding percentage was calculated from the remaining free compound concentration in the supernatant of each well, using the spreadsheet and algorithms supplied with the kit.

4.2.7. MTT cytotoxicity assay

AF3 or IMR-90 cells were seeded in 96-well plates (10^4 cells per well) in DMEM with 10% FBS for 24 h prior to treatments. The medium was then replaced by fresh medium containing tested compound or the equivalent volume of DMSO as vehicle. After the corresponding time, the medium was replaced by fresh DMEM with 5 mg/mL of MTT (Sigma-Aldrich), and the cells were incubated for 4 h at 37 °C in the dark. The supernatants were removed, formazan crystals were dissolved in DMSO (100 µL/well), and the absorbance was measured at 570 nm (OD570-630) using an Asys UVM 340 microplate reader (Biochrom Ltd., Cambridge, UK). The background absorbance of blank wells

containing only medium with compound or vehicle were subtracted from each test well. The results were reported as cell viability percentage for tested compound relative to vehicle, obtained from at least two experiments performed in triplicate.

4.2.8. Determination of the *in vivo* levels of compound 65

Compound **65** was administered intraperitoneally (25 mg/kg) in adult female 12-16 weeks old C57Bl/6J mice. At different time points after drug administration (0.5, 1, 2, 4 and 6 h), mice were sacrificed and brain, spinal cord, and blood samples were obtained. Brain and spinal cord were immediately frozen and kept at -80 °C until analysis. Blood was allowed to clot at rt for 30 min and centrifuged at 4 °C for 10 min at 16000*g*. Serum was transferred to a clean polypropylene tube and stored at -80 °C until analysis. For analysis, a volume of cold acetonitrile was added to the serum, brain and spinal cord samples, which were then incubated in an ice bath for 10 min and centrifuged at 4 °C for 10 min at 16000*g*. The resulting organic layers were filtered through a PTFE filter (0.2 µm, 13 mm diameter, Fisher Scientific) and 20 µL of each sample were analysed by LC-MS/MS at the UCM's Mass Spectrometry CAI.

4.2.9. Evaluation of the *in vivo* efficacy of compound 65

Complete Freund's adjuvant was administered to the paw of C57Bl/6J mice (10−12 weeks old). Then, mice were treated daily with compound **65** (25 mg/kg, i.p.) starting at 1 h following lesion and for 14 consecutive days, and inflammation was assessed. These experiments were done in collaboration with Professor Rubèn López Vales from Universidad Autónoma de Barcelona.

5. REFERENCES

5. REFERENCES

(1) Liebisch, G.; Fahy, E.; Aoki, J.; Dennis, E. A.; Durand, T.; Ejsing, C. S.; Fedorova, M.; Feussner, I.; Griffiths, W. J.; Köfeler, H.; Merrill, A. H., Jr.; Murphy, R. C.; O'Donnell, V. B.; Oskolkova, O.; Subramaniam, S.; Wakelam, M. J. O.; Spener, F. Update on LIPID MAPS classification, nomenclature, and shorthand notation for MS-derived lipid structures. *J. Lipid. Res.* **2020**, *61*, 1539-1555.

(2) Doktorova, M.; Symons, J. L.; Levental, I. Structural and functional consequences of reversible lipid asymmetry in living membranes. *Nat. Chem. Biol.* **2020**, *16*, 1321-1330.

(3) Horn, A.; Jaiswal, J. K. Structural and signaling role of lipids in plasma membrane repair. *Curr. Top. Membr.* **2019**, *84*, 67-98.

(4) Levental, I.; Lyman, E. Regulation of membrane protein structure and function by their lipid nano-environment. *Nat. Rev. Mol. Cell. Biol.* **2023**, *24*, 107-122.

(5) Vogel, F. C. E.; Chaves-Filho, A. B.; Schulze, A. Lipids as mediators of cancer progression and metastasis. *Nat. Cancer* **2024**, *5*, 16-29.

(6) Lim, S. A.; Su, W.; Chapman, N. M.; Chi, H. Lipid metabolism in T cell signaling and function. *Nat. Chem. Biol.* **2022**, *18*, 470-481.

(7) Martin-Perez, M.; Urdiroz-Urricelqui, U.; Bigas, C.; Benitah, S. A. The role of lipids in cancer progression and metastasis. *Cell Metab.* **2022**, *34*, 1675-1699.

(8) Welte, M. A.; Gould, A. P. Lipid droplet functions beyond energy storage. *Biochim. Biophys. Acta.* **2017**, *1862*, 1260-1272.

(9) Zadoorian, A.; Du, X.; Yang, H. Lipid droplet biogenesis and functions in health and disease. *Nat. Rev. Endocrinol.* **2023**, *19*, 443-459.

(10) Bieberich, E. It's a lipid's world: bioactive lipid metabolism and signaling in neural stem cell differentiation. *Neurochem. Res.* **2012**, *37*, 1208-1229.

(11) van Jaarsveld, M. T.; Houthuijzen, J. M.; Voest, E. E. Molecular mechanisms of target recognition by lipid GPCRs: relevance for cancer. *Oncogene* **2016**, *35*, 4021-4035.

(12) Leuti, A.; Fazio, D.; Fava, M.; Piccoli, A.; Oddi, S.; Maccarrone, M. Bioactive lipids, inflammation and chronic diseases. *Adv. Drug Deliv. Rev.* **2020**, *159*, 133-169.

(13) Samovski, D.; Jacome-Sosa, M.; Abumrad, N. A. Fatty acid transport and signaling: mechanisms and physiological implications. *Annu. Rev. Physiol.* **2023**, *85*, 317-337.

(14) Dennis, E. A.; Norris, P. C. Eicosanoid storm in infection and inflammation. *Nat. Rev. Immunol.* **2015**, *15*, 511-523.

(15) Maccarrone, M.; Di Marzo, V.; Gertsch, J.; Grether, U.; Howlett, A. C.; Hua, T.; Makriyannis, A.; Piomelli, D.; Ueda, N.; van der Stelt, M. Goods and bads of the endocannabinoid system as a therapeutic target: lessons learned after 30 years. *Pharmacol. Rev.* **2023**, *75*, 885-958.

(16) Tan, S. T.; Ramesh, T.; Toh, X. R.; Nguyen, L. N. Emerging roles of lysophospholipids in health and disease. *Prog. Lipid. Res.* **2020**, *80*, 101068-101082.

(17) Kano, K.; Aoki, J.; Hla, T. Lysophospholipid mediators in health and disease. *Annu. Rev. Pathol.* **2022**, *17*, 459-483.

(18) Bravo, G.; Cedeño, R. R.; Casadevall, M. P.; Ramió-Torrentà, L. Sphingosine-1-phosphate (S1P) and S1P signaling pathway modulators, from current insights to future perspectives. *Cells* **2022**, *11*, 2058-2073.

(19) Yanagida, K.; Shimizu, T. Lysophosphatidic acid, a simple phospholipid with myriad functions. *Pharmacol. Ther.* **2023**, *246*, 108421-108437.

(20) Meduri, B.; Pujar, G. V.; Durai Ananda Kumar, T.; Akshatha, H. S.; Sethu, A. K.; Singh, M.; Kanagarla, A.; Mathew, B. Lysophosphatidic acid (LPA) receptor modulators: structural features and recent development. *Eur. J. Med. Chem.* **2021**, *222*, 113574-113600.

(21) Baker, D. L.; Desiderio, D. M.; Miller, D. D.; Tolley, B.; Tigyi, G. J. Direct quantitative analysis of lysophosphatidic acid molecular species by stable isotope dilution electrospray ionization liquid chromatography-mass spectrometry. *Anal. Biochem.* **2001**, *292*, 287-295.

(22) Moolenaar, W. H.; van Meeteren, L. A.; Giepmans, B. N. The ins and outs of lysophosphatidic acid signaling. *Bioessays* **2004**, *26*, 870-881.

(23) Tokumura, A. Metabolic pathways and physiological and pathological significances of lysolipid phosphate mediators. *J. Cell Biochem.* **2004**, *92*, 869-881.

(24) Geraldo, L. H. M.; Spohr, T.; Amaral, R. F. D.; Fonseca, A.; Garcia, C.; Mendes, F. A.; Freitas, C.; dosSantos, M. F.; Lima, F. R. S. Role of lysophosphatidic acid and its receptors

in health and disease: novel therapeutic strategies. *Sig. Transduct. Target. Ther.* **2021**, *6*, 45-63.

(25) Yung, Y. C.; Stoddard, N. C.; Mirendil, H.; Chun, J. Lysophosphatidic acid signaling in the nervous system. *Neuron* **2015**, *85*, 669-682.

(26) Xiang, H.; Lu, Y.; Shao, M.; Wu, T. Lysophosphatidic acid receptors: biochemical and clinical implications in different diseases. *J. Cancer* **2020**, *11*, 3519-3535.

(27) van Meeteren, L. A.; Moolenaar, W. H. Regulation and biological activities of the autotaxin-LPA axis. *Prog. Lipid. Res.* **2007**, *46*, 145-160.

(28) Sheng, X.; Yung, Y. C.; Chen, A.; Chun, J. Lysophosphatidic acid signalling in development. *Development* **2015**, *142*, 1390-1395.

(29) Kremer, K. N.; Buser, A.; Thumkeo, D.; Narumiya, S.; Jacobelli, J.; Pelanda, R.; Torres, R. M. LPA suppresses T cell function by altering the cytoskeleton and disrupting immune synapse formation. *Proc. Natl. Acad. Sci. U. S. A.* **2022**, *119*, e2118816119.

(30) Stoddard, N. C.; Chun, J. Promising pharmacological directions in the world of lysophosphatidic acid signaling. *Biomol. Ther.* **2015**, *23*, 1-11.

(31) López-Serrano, C.; Santos-Nogueira, E.; Francos-Quijorna, I.; Coll-Miró, M.; Chun, J.; López-Vales, R. Lysophosphatidic acid receptor type 2 activation contributes to secondary damage after spinal cord injury in mice. *Brain. Behav. Immun.* **2019**, *76*, 258-267.

(32) Yanagida, K.; Valentine, W. J. Druggable lysophospholipid signaling pathways. *Adv. Exp. Med. Biol.* **2020**, *1274*, 137-176.

(33) Lin, Y.-H.; Lin, Y.-C.; Chen, C.-C. Lysophosphatidic acid receptor antagonists and cancer: the current trends, clinical implications, and trials. *Cells* **2021**, *10*, 1629-1645.

(34) Balijepalli, P.; Sitton, C. C.; Meier, K. E. Lysophosphatidic acid signaling in cancer cells: what makes LPA so special? *Cells* **2021**, *10*, 2059-2079.

(35) Rivera-Lopez, C. M.; Tucker, A. L.; Lynch, K. R. Lysophosphatidic acid (LPA) and angiogenesis. *Angiogenesis* **2008**, *11*, 301-310.

(36) Nakamura, Y.; Shimizu, Y. Cellular and molecular control of lipid metabolism in idiopathic pulmonary fibrosis: clinical application of the lysophosphatidic acid pathway. *Cells* **2023**, *12*, 548-572.

(37) Kano, K.; Matsumoto, H.; Inoue, A.; Yukiura, H.; Kanai, M.; Chun, J.; Ishii, S.; Shimizu, T.; Aoki, J. Molecular mechanism of lysophosphatidic acid-induced hypertensive response. *Sci. Rep.* **2019**, *9*, 2662-2674.

(38) Zhou, Z.; Subramanian, P.; Sevilmis, G.; Globke, B.; Soehnlein, O.; Karshovska, E.; Megens, R.; Heyll, K.; Chun, J.; Saulnier-Blache, J. S.; Reinholz, M.; van Zandvoort, M.;

Weber, C.; Schober, A. Lipoprotein-derived lysophosphatidic acid promotes atherosclerosis by releasing CXCL1 from the endothelium. *Cell Metab.* **2011**, *13*, 592-600.

(39) Kim, D.; Li, H. Y.; Lee, J. H.; Oh, Y. S.; Jun, H.-S. Lysophosphatidic acid increases mesangial cell proliferation in models of diabetic nephropathy via Rac1/MAPK/KLF5 signaling. *Exp. Mol. Med.* **2019**, *51*, 1-10.

(40) Zhao, Y.; Hasse, S.; Zhao, C.; Bourgoin, S. G. Targeting the autotaxin-lysophosphatidic acid receptor axis in cardiovascular diseases. *Biochem. Pharmacol.* **2019**, *164*, 74-81.

(41) Jose, A.; Kienesberger, P. C. Autotaxin-LPA-LPP3 axis in energy metabolism and metabolic disease. *Int. J. Mol. Sci.* **2021**, *22*, 9575-9590.

(42) Okudaira, S.; Yukiura, H.; Aoki, J. Biological roles of lysophosphatidic acid signaling through its production by autotaxin. *Biochimie* **2010**, *92*, 698-706.

(43) Pagès, C.; Simon, M. F.; Valet, P.; Saulnier-Blache, J. S. Lysophosphatidic acid synthesis and release. *Prostag. Oth. Lipid M.* **2001**, *64*, 1-10.

(44) Aoki, J.; Inoue, A.; Okudaira, S. Two pathways for lysophosphatidic acid production. *Biochim. Biophys. Acta.* **2008**, *1781*, 513-518.

(45) González-Gil, I.; Zian, D.; Vázquez-Villa, H.; Ortega-Gutiérrez, S.; López-Rodríguez, M. L. The status of the lysophosphatidic acid receptor type 1 (LPA1R). *MedChemComm* **2015**, *6*, 13-23.

(46) Yung, Y. C.; Stoddard, N. C.; Chun, J. LPA receptor signaling: pharmacology, physiology, and pathophysiology. *J. Lipid. Res.* **2014**, *55*, 1192-1214.

(47) Meduri, B.; Pujar, G. V.; Durai Ananda Kumar, T.; Akshatha, H. S.; Sethu, A. K.; Singh, M.; Kanagarla, A.; Mathew, B. Lysophosphatidic acid (LPA) receptor modulators: structural features and recent development. *Eur. J. Med. Chem.* **2021**, *222*, 113574.

(48) Yang, D.; Zhou, Q.; Labroska, V.; Qin, S.; Darbalaei, S.; Wu, Y.; Yuliantie, E.; Xie, L.; Tao, H.; Cheng, J.; Liu, Q.; Zhao, S.; Shui, W.; Jiang, Y.; Wang, M. W. G protein-coupled receptors: structure- and function-based drug discovery. *Signal. Transduct. Target. Ther.* **2021**, *6*, 7-34.

(49) Smith, S. O. Deconstructing the transmembrane core of class A G protein-coupled receptors. *Trends. Biochem. Sci.* **2021**, *46*, 1017-1029.

(50) Li, J.; Ge, Y.; Huang, J. X.; Strømgaard, K.; Zhang, X.; Xiong, X. F. Heterotrimeric G proteins as therapeutic targets in drug discovery. *J. Med. Chem.* **2020**, *63*, 5013-5030.

(51) Hecht, J. H.; Weiner, J. A.; Post, S. R.; Chun, J. Ventricular zone gene-1 (vzg-1) encodes a lysophosphatidic acid receptor expressed in neurogenic regions of the developing cerebral cortex. *J. Cell Biol.* **1996**, *135*, 1071-1083.

(52) Chrencik, J. E.; Roth, C. B.; Terakado, M.; Kurata, H.; Omi, R.; Kihara, Y.; Warshaviak, D.; Nakade, S.; Asmar-Rovira, G.; Mileni, M.; Mizuno, H.; Griffith, M. T.; Rodgers, C.; Han, G. W.; Velasquez, J.; Chun, J.; Stevens, R. C.; Hanson, M. A. Crystal structure of antagonist bound human lysophosphatidic acid receptor 1. *Cell* **2015**, *161*, 1633-1643.

(53) Taniguchi, R.; Inoue, A.; Sayama, M.; Uwamizu, A.; Yamashita, K.; Hirata, K.; Yoshida, M.; Tanaka, Y.; Kato, H. E.; Nakada-Nakura, Y.; Otani, Y.; Nishizawa, T.; Doi, T.; Ohwada, T.; Ishitani, R.; Aoki, J.; Nureki, O. Structural insights into ligand recognition by the lysophosphatidic acid receptor LPA(6). *Nature* **2017**, *548*, 356-360.

(54) Chun, J.; Hla, T.; Lynch, K. R.; Spiegel, S.; Moolenaar, W. H. International Union of Basic and Clinical Pharmacology. LXXVIII. Lysophospholipid receptor nomenclature. *Pharmacol. Rev.* **2010**, *62*, 579-587.

(55) Davenport, A. P.; Alexander, S. P.; Sharman, J. L.; Pawson, A. J.; Benson, H. E.; Monaghan, A. E.; Liew, W. C.; Mpamhanga, C. P.; Bonner, T. I.; Neubig, R. R.; Pin, J. P.; Spedding, M.; Harmar, A. J. International Union of Basic and Clinical Pharmacology. LXXXVIII. G protein-coupled receptor list: recommendations for new pairings with cognate ligands. *Pharmacol. Rev.* **2013**, *65*, 967-986.

(56) Lescop, C.; Brotschi, C.; Williams, J. T.; Sager, C. P.; Birker, M.; Morrison, K.; Froidevaux, S.; Delahaye, S.; Nayler, O.; Bolli, M. H. Discovery of a novel orally active, selective LPA receptor type 1 antagonist, 4-(4-(2-Isopropylphenyl)-4-((2-methoxy-4-methylphenyl)carbamoyl)piperidin-1-yl)-4-oxobutanoic acid, with a distinct molecular scaffold. *J. Med. Chem.* **2024**, *67*, 2379-2396.

(57) González-Gil, I.; Zian, D.; Vázquez-Villa, H.; Hernández-Torres, G.; Martínez, R. F.; Khiar-Fernández, N.; Rivera, R.; Kihara, Y.; Devesa, I.; Mathivanan, S.; del Valle, C. R.; Zambrana-Infantes, E.; Puigdomenech, M.; Cincilla, G.; Sanchez-Martinez, M.; Rodríguez de Fonseca, F.; Ferrer-Montiel, A. V.; Chun, J.; López-Vales, R.; López-Rodríguez, M. L.; Ortega-Gutiérrez, S. A novel agonist of the type 1 lysophosphatidic acid receptor (LPA1), UCM-05194, shows efficacy in neuropathic pain amelioration. *J. Med. Chem.* **2020**, *63*, 2372-2390.

(58) An, S.; Bleu, T.; Hallmark, O. G.; Goetzl, E. J. Characterization of a novel subtype of human G protein-coupled receptor for lysophosphatidic acid. *J. Biol. Chem.* **1998**, *273*, 7906-7910.

(59) Ishii, I.; Fukushima, N.; Ye, X.; Chun, J. Lysophospholipid receptors: signaling and biology. *Annu. Rev. Biochem.* **2004**, *73*, 321-354.

(60) Weiner, J. A.; Fukushima, N.; Contos, J. J.; Scherer, S. S.; Chun, J. Regulation of Schwann cell morphology and adhesion by receptor-mediated lysophosphatidic acid signaling. *J. Neurosci.* **2001**, *21*, 7069-7078.

(61) Shano, S.; Moriyama, R.; Chun, J.; Fukushima, N. Lysophosphatidic acid stimulates astrocyte proliferation through LPA1. *Neurochem. Int.* **2008**, *52*, 216-220.

(62) Matas-Rico, E.; García-Diaz, B.; Llebrez-Zayas, P.; López-Barroso, D.; Santín, L.; Pedraza, C.; Smith-Fernández, A.; Fernández-Llebrez, P.; Tellez, T.; Redondo, M.; Chun, J.; De Fonseca, F. R.; Estivill-Torrús, G. Deletion of lysophosphatidic acid receptor LPA1 reduces neurogenesis in the mouse dentate gyrus. *Mol. Cell Neurosci.* **2008**, *39*, 342-355.

(63) Contos, J. J.; Chun, J. Genomic characterization of the lysophosphatidic acid receptor gene, lp(A2)/Edg4, and identification of a frameshift mutation in a previously characterized cDNA. *Genomics* **2000**, *64*, 155-169.

(64) Yung, Yun C.; Stoddard, Nicole C.; Mirendil, H.; Chun, J. Lysophosphatidic acid signaling in the nervous system. *Neuron* **2015**, *85*, 669-682.

(65) Tigyi, G. J.; Johnson, L. R.; Lee, S. C.; Norman, D. D.; Szabo, E.; Balogh, A.; Thompson, K.; Boler, A.; McCool, W. S. Lysophosphatidic acid type 2 receptor agonists in targeted drug development offer broad therapeutic potential. *J. Lipid. Res.* **2019**, *60*, 464-474.

(66) Im, D. S.; Heise, C. E.; Harding, M. A.; George, S. R.; O'Dowd, B. F.; Theodorescu, D.; Lynch, K. R. Molecular cloning and characterization of a lysophosphatidic acid receptor, Edg-7, expressed in prostate. *Mol. Pharmacol.* **2000**, *57*, 753-759.

(67) Bandoh, K.; Aoki, J.; Hosono, H.; Kobayashi, S.; Kobayashi, T.; Murakami-Murofushi, K.; Tsujimoto, M.; Arai, H.; Inoue, K. Molecular cloning and characterization of a novel human G-protein-coupled receptor, EDG7, for lysophosphatidic acid. *J. Biol. Chem.* **1999**, *274*, 27776-27785.

(68) Choi, J. W.; Herr, D. R.; Noguchi, K.; Yung, Y. C.; Lee, C. W.; Mutoh, T.; Lin, M. E.; Teo, S. T.; Park, K. E.; Mosley, A. N.; Chun, J. LPA receptors: subtypes and biological actions. *Annu. Rev. Pharmacol. Toxicol.* **2010**, *50*, 157-186.

(69) Aikawa, S.; Kano, K.; Inoue, A.; Wang, J.; Saigusa, D.; Nagamatsu, T.; Hirota, Y.; Fujii, T.; Tsuchiya, S.; Taketomi, Y.; Sugimoto, Y.; Murakami, M.; Arita, M.; Kurano, M.; Ikeda, H.; Yatomi, Y.; Chun, J.; Aoki, J. Autotaxin-lysophosphatidic acid-LPA(3) signaling at the embryo-epithelial boundary controls decidualization pathways. *EMBO J.* **2017**, *36*, 2146-2160.

(70) Ye, X. Lysophospholipid signaling in the function and pathology of the reproductive system. *Hum. Reprod. Update.* **2008**, *14*, 519-536.

(71) Hama, K.; Aoki, J.; Bandoh, K.; Inoue, A.; Endo, T.; Amano, T.; Suzuki, H.; Arai, H. Lysophosphatidic receptor, LPA3, is positively and negatively regulated by progesterone and estrogen in the mouse uterus. *Life. Sci.* **2006**, *79*, 1736-1740.

(72) Ye, X.; Hama, K.; Contos, J. J.; Anliker, B.; Inoue, A.; Skinner, M. K.; Suzuki, H.; Amano, T.; Kennedy, G.; Arai, H.; Aoki, J.; Chun, J. LPA3-mediated lysophosphatidic acid signalling in embryo implantation and spacing. *Nature* **2005**, *435*, 104-108.

(73) Lai, S. L.; Yao, W. L.; Tsao, K. C.; Houben, A. J.; Albers, H. M.; Ovaa, H.; Moolenaar, W. H.; Lee, S. J. Autotaxin/Lpar3 signaling regulates Kupffer's vesicle formation and left-right asymmetry in zebrafish. *Development* **2012**, *139*, 4439-4448.

(74) Noguchi, K.; Ishii, S.; Shimizu, T. Identification of p2y9/GPR23 as a novel G protein-coupled receptor for lysophosphatidic acid, structurally distant from the Edg family. *J. Biol. Chem.* **2003**, *278*, 25600-25606.

(75) Xie, Y.; Wang, X.; Wu, X.; Tian, L.; Zhou, J.; Li, X.; Wang, B. Lysophosphatidic acid receptor 4 regulates osteogenic and adipogenic differentiation of progenitor cells via inactivation of RhoA/ROCK1/β-catenin signaling. *Stem Cells* **2020**, *38*, 451-463.

(76) Yanagida, K.; Ishii, S.; Hamano, F.; Noguchi, K.; Shimizu, T. LPA4/p2y9/GPR23 mediates rho-dependent morphological changes in a rat neuronal cell line. *J. Biol. Chem.* **2007**, *282*, 5814-5824.

(77) Lee, C. W.; Rivera, R.; Dubin, A. E.; Chun, J. LPA(4)/GPR23 is a lysophosphatidic acid (LPA) receptor utilizing G(s)-, G(q)/G(i)-mediated calcium signaling and G(12/13)-mediated Rho activation. *J. Biol. Chem.* **2007**, *282*, 4310-4317.

(78) Sumida, H.; Noguchi, K.; Kihara, Y.; Abe, M.; Yanagida, K.; Hamano, F.; Sato, S.; Tamaki, K.; Morishita, Y.; Kano, M. R.; Iwata, C.; Miyazono, K.; Sakimura, K.; Shimizu, T.; Ishii, S. LPA4 regulates blood and lymphatic vessel formation during mouse embryogenesis. *Blood* **2010**, *116*, 5060-5070.

(79) Rhee, H. J.; Nam, J. S.; Sun, Y.; Kim, M. J.; Choi, H. K.; Han, D. H.; Kim, N. H.; Huh, S. O. Lysophosphatidic acid stimulates cAMP accumulation and cAMP response element-binding protein phosphorylation in immortalized hippocampal progenitor cells. *Neuroreport* **2006**, *17*, 523-526.

(80) Takahashi, K.; Fukushima, K.; Onishi, Y.; Inui, K.; Node, Y.; Fukushima, N.; Honoki, K.; Tsujiuchi, T. Lysophosphatidic acid (LPA) signaling via LPA(4) and LPA(6) negatively regulates cell motile activities of colon cancer cells. *Biochem. Biophys. Res. Commun.* **2017**, *483*, 652-657.

(81) Lee, Z.; Cheng, C. T.; Zhang, H.; Subler, M. A.; Wu, J.; Mukherjee, A.; Windle, J. J.; Chen, C. K.; Fang, X. Role of LPA4/p2y9/GPR23 in negative regulation of cell motility. *Mol. Biol. Cell* **2008**, *19*, 5435-5445.

(82) Lee, C. W.; Rivera, R.; Gardell, S.; Dubin, A. E.; Chun, J. GPR92 as a new G12/13- and Gq-coupled lysophosphatidic acid receptor that increases cAMP, LPA5. *J. Biol. Chem.* **2006**, *281*, 23589-23597.

(83) Kotarsky, K.; Boketoft, A.; Bristulf, J.; Nilsson, N. E.; Norberg, A.; Hansson, S.; Owman, C.; Sillard, R.; Leeb-Lundberg, L. M.; Olde, B. Lysophosphatidic acid binds to and activates GPR92, a G protein-coupled receptor highly expressed in gastrointestinal lymphocytes. *J. Pharmacol. Exp. Ther.* **2006**, *318*, 619-628.

(84) Murai, N.; Hiyama, H.; Kiso, T.; Sekizawa, T.; Watabiki, T.; Oka, H.; Aoki, T. Analgesic effects of novel lysophosphatidic acid receptor 5 antagonist AS2717638 in rodents. *Neuropharmacology* **2017**, *126*, 97-107.

(85) Lin, S.; Yeruva, S.; He, P.; Singh, A. K.; Zhang, H.; Chen, M.; Lamprecht, G.; de Jonge, H. R.; Tse, M.; Donowitz, M.; Hogema, B. M.; Chun, J.; Seidler, U.; Yun, C. C. Lysophosphatidic acid stimulates the intestinal brush border Na(+)/H(+) exchanger 3 and fluid absorption via LPA(5) and NHERF2. *Gastroenterology* **2010**, *138*, 649-658.

(86) Jenkin, K. A.; He, P.; Yun, C. C. Expression of lysophosphatidic acid receptor 5 is necessary for the regulation of intestinal Na(+)/H(+) exchanger 3 by lysophosphatidic acid in vivo. *Am. J. Physiol. Gastrointest. Liver Physiol.* **2018**, *315*, G433-G442.

(87) Mathew, D.; Kremer, K. N.; Strauch, P.; Tigyi, G.; Pelanda, R.; Torres, R. M. LPA(5) is an inhibitory receptor that suppresses CD8 T-cell cytotoxic function via disruption of early TCR signaling. *Front. Immunol.* **2019**, *10*, 1159-1175.

(88) Jongsma, M.; Matas-Rico, E.; Rzadkowski, A.; Jalink, K.; Moolenaar, W. H. LPA is a chemorepellent for B16 melanoma cells: action through the cAMP-elevating LPA5 receptor. *PLoS One* **2011**, *6*, e29260.

(89) Pasternack, S. M.; von Kügelgen, I.; Al Aboud, K.; Lee, Y. A.; Rüschendorf, F.; Voss, K.; Hillmer, A. M.; Molderings, G. J.; Franz, T.; Ramirez, A.; Nürnberg, P.; Nöthen, M. M.; Betz, R. C. G protein-coupled receptor P2Y5 and its ligand LPA are involved in maintenance of human hair growth. *Nat. Genet.* **2008**, *40*, 329-334.

(90) Raza, S. I.; Muhammad, D.; Jan, A.; Ali, R. H.; Hassan, M.; Ahmad, W.; Rashid, S. In silico analysis of missense mutations in LPAR6 reveals abnormal phospholipid signaling pathway leading to hypotrichosis. *PLoS One* **2014**, *9*, e104756.

(91) Yukiura, H.; Kano, K.; Kise, R.; Inoue, A.; Aoki, J. LPP3 localizes LPA6 signalling to non-contact sites in endothelial cells. *J. Cell Sci.* **2015**, *128*, 3871-3877.

(92) Kihara, Y.; Mizuno, H.; Chun, J. Lysophospholipid receptors in drug discovery. *Exp. Cell Res.* **2015**, *333*, 171-177.

(93) Hata, E.; Sasaki, N.; Takeda, A.; Tohya, K.; Umemoto, E.; Akahoshi, N.; Ishii, S.; Bando, K.; Abe, T.; Kano, K.; Aoki, J.; Hayasaka, H.; Miyasaka, M. Lysophosphatidic acid receptors LPA4 and LPA6 differentially promote lymphocyte transmigration across high endothelial venules in lymph nodes. *Int. Immunol.* **2016**, *28*, 283-292.

(94) Tabata, K.; Baba, K.; Shiraishi, A.; Ito, M.; Fujita, N. The orphan GPCR GPR87 was deorphanized and shown to be a lysophosphatidic acid receptor. *Biochem. Biophys. Res. Commun.* **2007**, *363*, 861-866.

(95) Murakami, M.; Shiraishi, A.; Tabata, K.; Fujita, N. Identification of the orphan GPCR, P2Y(10) receptor as the sphingosine-1-phosphate and lysophosphatidic acid receptor. *Biochem. Biophys. Res. Commun.* **2008**, *371*, 707-712.

(96) Morales-Lázaro, S. L.; Serrano-Flores, B.; Llorente, I.; Hernández-García, E.; González-Ramírez, R.; Banerjee, S.; Miller, D.; Gududuru, V.; Fells, J.; Norman, D.; Tigyi, G.; Escalante-Alcalde, D.; Rosenbaum, T. Structural determinants of the transient receptor potential 1 (TRPV1) channel activation by phospholipid analogs. *J. Biol. Chem.* **2014**, *289*, 24079-24090.

(97) McIntyre, T. M.; Pontsler, A. V.; Silva, A. R.; St Hilaire, A.; Xu, Y.; Hinshaw, J. C.; Zimmerman, G. A.; Hama, K.; Aoki, J.; Arai, H.; Prestwich, G. D. Identification of an intracellular receptor for lysophosphatidic acid (LPA): LPA is a transcellular PPARgamma agonist. *Proc. Natl. Acad. Sci. U. S. A.* **2003**, *100*, 131-136.

(98) Valentine, W. J.; Fells, J. I.; Perygin, D. H.; Mujahid, S.; Yokoyama, K.; Fujiwara, Y.; Tsukahara, R.; Van Brocklyn, J. R.; Parrill, A. L.; Tigyi, G. Subtype-specific residues involved in ligand activation of the endothelial differentiation gene family lysophosphatidic acid receptors. *J. Biol. Chem.* **2008**, *283*, 12175-12187.

(99) Lin, F. T.; Lai, Y. J. Regulation of the LPA2 receptor signaling through the carboxyl-terminal tail-mediated protein-protein interactions. *Biochim. Biophys. Acta.* **2008**, *1781*, 558-562.

(100) Lee, S. J.; Ritter, S. L.; Zhang, H.; Shim, H.; Hall, R. A.; Yun, C. C. MAGI-3 competes with NHERF-2 to negatively regulate LPA2 receptor signaling in colon cancer cells. *Gastroenterology* **2011**, *140*, 924-934.

(101) Lin, F. T.; Lai, Y. J.; Makarova, N.; Tigyi, G.; Lin, W. C. The lysophosphatidic acid 2 receptor mediates down-regulation of Siva-1 to promote cell survival. *J. Biol. Chem.* **2007**, *282*, 37759-37769.

(102) Jumper, J.; Evans, R.; Pritzel, A.; Green, T.; Figurnov, M.; Ronneberger, O.; Tunyasuvunakool, K.; Bates, R.; Žídek, A.; Potapenko, A.; Bridgland, A.; Meyer, C.; Kohl, S. A. A.; Ballard, A. J.; Cowie, A.; Romera-Paredes, B.; Nikolov, S.; Jain, R.; Adler, J.; Back, T.; Petersen, S.; Reiman, D.; Clancy, E.; Zielinski, M.; Steinegger, M.; Pacholska, M.; Berghammer, T.; Bodenstein, S.; Silver, D.; Vinyals, O.; Senior, A. W.; Kavukcuoglu, K.; Kohli, P.; Hassabis, D. Highly accurate protein structure prediction with AlphaFold. *Nature* **2021**, *596*, 583-589.

(103) Bai, Z.; Cai, L.; Umemoto, E.; Takeda, A.; Tohya, K.; Komai, Y.; Veeraveedu, P. T.; Hata, E.; Sugiura, Y.; Kubo, A.; Suematsu, M.; Hayasaka, H.; Okudaira, S.; Aoki, J.; Tanaka, T.; Albers, H. M.; Ovaa, H.; Miyasaka, M. Constitutive lymphocyte transmigration across the basal lamina of high endothelial venules is regulated by the autotaxin/lysophosphatidic acid axis. *J. Immunol.* **2013**, *190*, 2036-2048.

(104) Contos, J. J.; Ishii, I.; Fukushima, N.; Kingsbury, M. A.; Ye, X.; Kawamura, S.; Brown, J. H.; Chun, J. Characterization of lpa(2) (Edg4) and lpa(1)/lpa(2) (Edg2/Edg4) lysophosphatidic acid receptor knockout mice: signaling deficits without obvious phenotypic abnormality attributable to lpa(2). *Mol. Cell. Biol.* **2002**, *22*, 6921-6929.

(105) Solís, K. H.; Romero-Ávila, M. T.; Guzmán-Silva, A.; García-Sáinz, J. A. The LPA(3) receptor: regulation and activation of signaling pathways. *Int. J. Mol. Sci.* **2021**, *22*, 6704-6722.

(106) Digby, G. J.; Lober, R. M.; Sethi, P. R.; Lambert, N. A. Some G protein heterotrimers physically dissociate in living cells. *Proc. Natl. Acad. Sci. U. S. A.* **2006**, *103*, 17789-17794.

(107) Lin, Y. H.; Lin, Y. C.; Chen, C. C. Lysophosphatidic acid receptor antagonists and cancer: the current trends, clinical implications, and trials. *Cells* **2021**, *10*, 1629-1645.

(108) Tigyi, G. J.; Yue, J.; Norman, D. D.; Szabo, E.; Balogh, A.; Balazs, L.; Zhao, G.; Lee, S. C. Regulation of tumor cell-microenvironment interaction by the autotaxin-lysophosphatidic acid receptor axis. *Adv. Biol. Regul.* **2019**, *71*, 183-193.

(109) Mills, G. B.; Moolenaar, W. H. The emerging role of lysophosphatidic acid in cancer. *Nat. Rev. Cancer.* **2003**, *3*, 582-591.

(110) Yu, S.; Murph, M. M.; Lu, Y.; Liu, S.; Hall, H. S.; Liu, J.; Stephens, C.; Fang, X.; Mills, G. B. Lysophosphatidic acid receptors determine tumorigenicity and aggressiveness of ovarian cancer cells. *J. Natl. Cancer. Inst.* **2008**, *100*, 1630-1642.

(111) Li, M.; Xiao, D.; Zhang, J.; Qu, H.; Yang, Y.; Yan, Y.; Liu, X.; Wang, J.; Liu, L.; Wang, J.; Duan, X. Expression of LPA2 is associated with poor prognosis in human breast cancer and regulates HIF-1α expression and breast cancer cell growth. *Oncol. Rep.* **2016**, *36*, 3479-3487.

(112) Deng, W.; Wang, D. A.; Gosmanova, E.; Johnson, L. R.; Tigyi, G. LPA protects intestinal epithelial cells from apoptosis by inhibiting the mitochondrial pathway. *Am. J. Physiol. Gastrointest. Liver. Physiol.* **2003**, *284*, G821-G829.

(113) Geng, H.; Lan, R.; Singha, P. K.; Gilchrist, A.; Weinreb, P. H.; Violette, S. M.; Weinberg, J. M.; Saikumar, P.; Venkatachalam, M. A. Lysophosphatidic acid increases proximal tubule cell secretion of profibrotic cytokines PDGF-B and CTGF through LPA2- and Gαq-mediated Rho and αvβ6 integrin-dependent activation of TGF-β. *Am. J. Pathol.* **2012**, *181*, 1236-1249.

(114) Huang, L. S.; Fu, P.; Patel, P.; Harijith, A.; Sun, T.; Zhao, Y.; Garcia, J. G.; Chun, J.; Natarajan, V. Lysophosphatidic acid receptor-2 deficiency confers protection against bleomycin-induced lung injury and fibrosis in mice. *Am. J. Respir. Cell Mol. Biol.* **2013**, *49*, 912-922.

(115) Leng, F.; Edison, P. Neuroinflammation and microglial activation in Alzheimer disease: where do we go from here? *Nat. Rev. Neurol.* **2021**, *17*, 157-172.

(116) Araújo, B.; Caridade-Silva, R.; Soares-Guedes, C.; Martins-Macedo, J.; Gomes, E. D.; Monteiro, S.; Teixeira, F. G. Neuroinflammation and Parkinson's disease-From neurodegeneration to therapeutic opportunities. *Cells* **2022**, *11*, 2908-2948.

(117) Puigdomenech-Poch, M.; Martínez-Muriana, A.; Andrés-Benito, P.; Ferrer, I.; Chun, J.; López-Vales, R. Dual role of lysophosphatidic acid receptor 2 (LPA(2)) in Amyotrophic Lateral Sclerosis. *Front. Cell Neurosci.* **2021**, *15*, 600872-600886.

(118) Weng, H.-R.; Taing, K.; Chen, L.; Penney, A. EZH2 methyltransferase regulates neuroinflammation and neuropathic pain. *Cells* **2023**, *12*, 1058-1076.

(119) Vergne-Salle, P.; Bertin, P. Chronic pain and neuroinflammation. *Joint Bone Spine* **2021**, *88*, 105222-105229.

(120) Wang, H.; Xu, C. A novel progress: glial cells and inflammatory pain. *ACS Chem. Neurosci.* **2022**, *13*, 288-295.

(121) Fuggle, N. R.; Howe, F. A.; Allen, R. L.; Sofat, N. New insights into the impact of neuro-inflammation in rheumatoid arthritis. *Front. Neurosci.* **2014**, *8*, 357-368.

(122) Berg, K. A.; Clarke, W. P. Making sense of pharmacology: inverse agonism and functional selectivity. *Int. J. Neuropsychopharmacol.* **2018**, *21*, 962-977.

(123) Shonberg, J.; Lopez, L.; Scammells, P. J.; Christopoulos, A.; Capuano, B.; Lane, J. R. Biased agonism at G protein-coupled receptors: the promise and the challenges-a medicinal chemistry perspective. *Med. Res. Rev.* **2014**, *34*, 1286-1330.

(124) Zhang, M.; Chen, T.; Lu, X.; Lan, X.; Chen, Z.; Lu, S. G protein-coupled receptors (GPCRs): advances in structures, mechanisms, and drug discovery. *Sig. Transduct. Target. Ther.* **2024**, *9*, 88.

(125) Liu, W.; Hopkins, A. M.; Hou, J. The development of modulators for lysophosphatidic acid receptors: A comprehensive review. *Bioorg. Chem.* **2021**, *117*, 105386-105404.

(126) Virag, T.; Elrod, D. B.; Liliom, K.; Sardar, V. M.; Parrill, A. L.; Yokoyama, K.; Durgam, G.; Deng, W.; Miller, D. D.; Tigyi, G. Fatty alcohol phosphates are subtype-selective agonists and antagonists of lysophosphatidic acid receptors. *Mol. Pharmacol.* **2003**, *63*, 1032-1042.

(127) Durgam, G. G.; Virag, T.; Walker, M. D.; Tsukahara, R.; Yasuda, S.; Liliom, K.; van Meeteren, L. A.; Moolenaar, W. H.; Wilke, N.; Siess, W.; Tigyi, G.; Miller, D. D. Synthesis, structure-activity relationships, and biological evaluation of fatty alcohol phosphates as lysophosphatidic acid receptor ligands, activators of PPARgamma, and inhibitors of autotaxin. *J. Med. Chem.* **2005**, *48*, 4919-4930.

(128) Kano, K.; Arima, N.; Ohgami, M.; Aoki, J. LPA and its analogs-attractive tools for elucidation of LPA biology and drug development. *Curr. Med. Chem.* **2008**, *15*, 2122-2131.

(129) Gajewiak, J.; Tsukahara, R.; Tsukahara, T.; Fujiwara, Y.; Yu, S.; Lu, Y.; Murph, M.; Mills, G. B.; Tigyi, G.; Prestwich, G. D. Alkoxymethylenephosphonate analogues of (Lyso) phosphatidic acid stimulate signaling networks coupled to the LPA2 receptor. *ChemMedChem* **2007**, *2*, 1789-1798.

(130) Kiss, G. N.; Fells, J. I.; Gupte, R.; Lee, S. C.; Liu, J.; Nusser, N.; Lim, K. G.; Ray, R. M.; Lin, F. T.; Parrill, A. L.; Sümegi, B.; Miller, D. D.; Tigyi, G. Virtual screening for LPA2-specific agonists identifies a nonlipid compound with antiapoptotic actions. *Mol. Pharmacol.* **2012**, *82*, 1162-1173.

(131) Knowlden, S. A.; Hillman, S. E.; Chapman, T. J.; Patil, R.; Miller, D. D.; Tigyi, G.; Georas, S. N. Novel inhibitory effect of a lysophosphatidic acid 2 agonist on allergen-driven airway inflammation. *Am. J. Respir. Cell Mol. Biol.* **2016**, *54*, 402-409.

(132) Patil, R.; Fells, J. I.; Szabó, E.; Lim, K. G.; Norman, D. D.; Balogh, A.; Patil, S.; Strobos, J.; Miller, D. D.; Tigyi, G. J. Design and synthesis of sulfamoyl benzoic acid analogues with subnanomolar agonist activity specific to the LPA2 receptor. *J. Med. Chem.* **2014**, *57*, 7136-7140.

(133) Zhang, H.; Xu, X.; Gajewiak, J.; Tsukahara, R.; Fujiwara, Y.; Liu, J.; Fells, J. I.; Perygin, D.; Parrill, A. L.; Tigyi, G.; Prestwich, G. D. Dual activity lysophosphatidic acid receptor pan-antagonist/autotaxin inhibitor reduces breast cancer cell migration in vitro and causes tumor regression in vivo. *Cancer Res.* **2009**, *69*, 5441-5449.

(134) Ohta, H.; Sato, K.; Murata, N.; Damirin, A.; Malchinkhuu, E.; Kon, J.; Kimura, T.; Tobo, M.; Yamazaki, Y.; Watanabe, T.; Yagi, M.; Sato, M.; Suzuki, R.; Murooka, H.; Sakai, T.; Nishitoba, T.; Im, D. S.; Nochi, H.; Tamoto, K.; Tomura, H.; Okajima, F. Ki16425, a subtype-selective antagonist for EDG-family lysophosphatidic acid receptors. *Mol. Pharmacol.* **2003**, *64*, 994-1005.

(135) Beck, H. P.; Kohn, T.; Rubenstein, S.; Hedberg, C.; Schwandner, R.; Hasslinger, K.; Dai, K.; Li, C.; Liang, L.; Wesche, H.; Frank, B.; An, S.; Wickramasinghe, D.; Jaen, J.; Medina, J.; Hungate, R.; Shen, W. Discovery of potent LPA2 (EDG4) antagonists as potential anticancer agents. *Bioorg. Med. Chem. Lett.* **2008**, *18*, 1037-1041.

(136) Fells, J. I.; Tsukahara, R.; Liu, J.; Tigyi, G.; Parrill, A. L. Structure-based drug design identifies novel LPA3 antagonists. *Bioorg. Med. Chem.* **2009**, *17*, 7457-7464.

(137) Fells, J. I.; Tsukahara, R.; Fujiwara, Y.; Liu, J.; Perygin, D. H.; Osborne, D. A.; Tigyi, G.; Parrill, A. L. Identification of non-lipid LPA3 antagonists by virtual screening. *Bioorg. Med. Chem.* **2008**, *16*, 6207-6217.

(138) Khiar-Fernández, N.; Zian, D.; Vázquez-Villa, H.; Martínez, R. F.; Escobar-Peña, A.; Foronda-Sainz, R.; Ray, M.; Puigdomenech-Poch, M.; Cincilla, G.; Sánchez-Martínez, M.; Kihara, Y.; Chun, J.; López-Vales, R.; López-Rodríguez, M. L.; Ortega-Gutiérrez, S. Novel antagonist of the type 2 lysophosphatidic acid receptor (LPA2), UCM-14216, ameliorates spinal cord injury in mice. *J. Med. Chem.* **2022**, *65*, 10956-10974.

(139) Armani, E.; Rizzi, A.; Iotti, N.; Saccani, F.; Di Lascia, M. R.; Tigli, L.; Pappani, A.; Marchini, G.; Murgo, A.; Capelli, A. M.; Delcanale, M.; Puccini, P.; Villetti, G.; Civelli, M.; Beato, C.; Giuliani, M.; Mundi, C.; Murarolli, F.; Pagano, M.; Raveglia, L. F.; Remelli, R.; Amari, G. Discovery of a potent, selective, and orally bioavailable tool compound for

probing the role of lysophosphatidic acid type 2 receptor antagonists in fibrotic disorders. *J. Med. Chem.* **2023**, *66*, 5622-5656.

(140) Prek, B.; Bezenšek, J.; Kasunič, M.; Grošelj, U.; Svete, J.; Stanovnik, B. Reactions of enaminones and related compounds with *N,N*-dimethylacetamide dimethyl acetal. A simple one-pot metal-free synthesis of polysubstituted benzene derivatives. *Tetrahedron* **2014**, *70*, 2359-2369.

(141) Henary, E.; Casa, S.; Dost, T. L.; Sloop, J. C.; Henary, M. The role of small molecules containing fluorine atoms in medicine and imaging applications. *Pharmaceuticals* **2024**, *17*, 281-306.

(142) Kadu, B. S. Suzuki–Miyaura cross coupling reaction: recent advancements in catalysis and organic synthesis. *Catal. Sci. Technol.* **2021**, *11*, 1186-1221.

(143) Qiao, J. X.; Lam, P. Y. S. Copper-promoted carbon-heteroatom bond cross-coupling with boronic acids and derivatives. *Synthesis* **2011**, *2011*, 829-856.

(144) Kammer, M. N.; Kussrow, A. K.; Olmsted, I. R.; Bornhop, D. J. A highly compensated interferometer for biochemical analysis. *ACS Sens.* **2018**, *3*, 1546-1552.

(145) Ray, M.; Nagai, K.; Kihara, Y.; Kussrow, A.; Kammer, M. N.; Frantz, A.; Bornhop, D. J.; Chun, J. Unlabeled lysophosphatidic acid receptor binding in free solution as determined by a compensated interferometric reader. *J. Lipid. Res.* **2020**, *61*, 1244-1251.

(146) Mizuno, H.; Kihara, Y.; Kussrow, A.; Chen, A.; Ray, M.; Rivera, R.; Bornhop, D. J.; Chun, J. Lysophospholipid G protein-coupled receptor binding parameters as determined by backscattering interferometry. *J. Lipid. Res.* **2019**, *60*, 212-217.

(147) Tissot, M.; Phipps, R. J.; Lucas, C.; Leon, R. M.; Pace, R. D.; Ngouansavanh, T.; Gaunt, M. J. Gram-scale enantioselective formal synthesis of morphine through an ortho-para oxidative phenolic coupling strategy. *Angew. Chem.* **2014**, *53*, 13498-13501.

(148) Hopper, D. W.; Ragan, S. P.; Hooks, S. B.; Lynch, K. R.; Macdonald, T. L. Structure-activity relationships of lysophosphatidic acid: conformationally restricted backbone mimetics. *J. Med. Chem.* **1999**, *42*, 963-970.